THE UNIVERSITY OF QUEENSLAND

AUSTRALIA

DNA methylation and chromatin dynamics during postnatal cardiomyocyte maturation

Ms Sim Choon Boon

B.Eng, M.Sc (Genetics)

A thesis submitted for the degree of Doctor of Philosophy at

The University of Queensland in 2017

School of Biomedical Sciences.

Abstract

Background: The neonatal mammalian heart has a transient capacity for regeneration, which is lost shortly after birth. A series of critical developmental transitions including a switch from hyperplastic to hypertrophic growth occur during this postnatal regenerative window, preparing the heart for the increased contractile demands of postnatal life. Postnatal cardiomyocyte maturation and loss of regenerative capacity are associated with expression alterations of thousands of genes embedded within tightly controlled transcriptional networks, which remain poorly understood. Interestingly, although mitogenic stimulation of neonatal cardiomyocytes results in proliferation, the same stimuli induce hypertrophy in adult cardiomyocytes by activating different transcriptional pathways, indicating that cardiomyocyte maturation may result from epigenetic modifications during development. Notably, DNA methylation and chromatin compaction are both important epigenetic modifications associated with a decrease in transcription factor (TF) accessibility to DNA. However, the role of both DNA methylation and chromatin compaction during postnatal cardiac maturation remain largely unknown.

Hypothesis: Postnatal changes in DNA methylation and chromatin compaction silence transcriptional networks required for cardiomyocyte proliferation during postnatal heart development.

Aims: This PhD Thesis focuses on characterising the role of DNA methylation and chromatin dynamics during postnatal cardiac development and maturation using *in vitro* and *in vivo* model systems. Three major Aims are addressed:

- Aim 1: To characterize transcription and DNA methylation dynamics during postnatal rodent cardiac development (Chapter 3).

- Aim 2: To determine the role of DNA methylation in regulating the expression of cell cycle related genes in mouse and human cardiomyocytes (Chapter 4).

- Aim 3: To understand the relationship between chromatin accessibility and transcription during mouse and human cardiomyocyte development (Chapter 5).

Results: In Aim 1, global DNA methylation changes were characterized during postnatal development. Marked changes in the expression levels of key DNA methylation enzymes were observed during the first month of postnatal heart development. Postnatal inhibition of DNA methylation using 5-aza-2'-deoxycytidine (5aza-dC; 1mg/kg/day) reduced global DNA methylation levels in the heart *in vivo* and was associated with a marked increase in cardiomyocyte proliferation (~3-fold) and ~50% reduction in binucleated cardiomyocytes compared to saline-treated controls, suggesting DNA methylation is required for postnatal cardiomyocyte cell cycle arrest. Next-generation mRNA sequencing (RNA-seq) and genome-wide sequencing of methylated DNA (methyl-CpG binding domain enrichment and sequencing (MBD-seq)) identified dynamic changes in the cardiac methylome during postnatal development (2545 differentially methylated regions (DMRs) from postnatal day (P) 1 to P14 in the mouse). ~80% of DMRs were hypermethylated and these DMRs were associated with transcriptional shut down of important developmental signalling pathways.

In Aim 2, a specific subset of cell cycle genes displaying differentially regulated gene expression and DNA methylation patterns were profiled to understand how DNA methylation is involved in regulating cardiomyocyte proliferation. Gene expression profiling of these cell cycle genes during development and following 5aza-dC treatment in mouse hearts, as well as 3D human cardiac organoids (hCOs), verified that DNA methylation was required for transcriptional regulation of a small group of cell cycle genes. Interestingly, 5aza-dC (10μM) also induced ~2-fold increase in cardiomyocyte proliferation in hCOs. These findings suggest that DNA methylation has a direct role in the regulation of a subset of genes required for cardiomyocyte proliferation in both mice and humans.

Chromatin accessibility results from the integrated action of multiple epigenetic marks. In Aim 3, cardiomyocyte nuclei were isolated from both human and mouse developmental heart samples for RNA-seq and for transposase-accessible chromatin with high-throughput sequencing (ATAC-seq) to profile changes in transcription and chromatin accessibility during cardiomyocyte development in mice (P1 to P56) and humans (foetal (14-19 weeks (wks)), 0-10 years (yrs), 10-30 yrs and 30+ yrs). RNA-seq confirmed that cardiomyocyte cell cycle arrest occurs between P1 and P14 in the mouse. Moreover, ATAC-seq identified open chromatin signatures at various genomic features, including CG islands, transcription start sites (TSSs), enhancers, TF binding sites and protein coding regions, while intergenic regions were associated with compact chromatin. Integration of RNA-seq and ATAC-seq data demonstrated a strong correlation between transcription and chromatin accessibility at the different stages of cardiomyocyte development. TF motif analysis

identified E2F transcription factor 4 (E2f4) and Forkhead box M1 (Foxm1) sites as being transcriptionally repressed and undergoing chromatin compaction from P1 to P56. E2f4 and Foxm1 are well known TFs that regulate cell cycle, thus suggesting that cell cycle genes are epigenetically silenced during cardiomyocyte maturation.

Conclusion: This PhD Thesis provides novel evidence for widespread alterations in DNA methylation during postnatal heart maturation and suggests that cardiomyocyte cell cycle arrest during the neonatal period is subject to regulation by DNA methylation and chromatin compaction. Together, this PhD Thesis provides new insights into the role of DNA methylation and chromatin dynamics during cardiac development. This Thesis provides a new framework for the epigenetic regulation of transcription during postnatal cardiomyocyte maturation and points towards an epigenetic mechanism for cardiomyocyte terminal differentiation during the neonatal period.

Declaration

This thesis is composed of my original work, and contains no material previously published or written by another person except where due reference has been made in the text. I have clearly stated the contribution by others to jointly-authored works that I have included in my thesis.

I have clearly stated the contribution of others to my thesis as a whole, including statistical assistance, survey design, data analysis, significant technical procedures, professional editorial advice, and any other original research work used or reported in my thesis. The content of my thesis is the result of work I have carried out since the commencement of my research higher degree candidature and does not include a substantial part of work that has been submitted to qualify for the award of any other degree or diploma in any university or other tertiary institution. I have clearly stated which parts of my thesis, if any, have been submitted to qualify for another award.

I acknowledge that an electronic copy of my thesis must be lodged with the University Library and, subject to the policy and procedures of The University of Queensland, the thesis be made available for research and study in accordance with the Copyright Act 1968 unless a period of embargo has been approved by the Dean of the Graduate School.

I acknowledge that copyright of all material contained in my thesis resides with the copyright holder(s) of that material. Where appropriate I have obtained copyright permission from the copyright holder to reproduce material in this thesis.

Publications during Candidature

Publications arising from this thesis

1. **Sim CB**, Ziemann M, Kaspi A, Harikrishnan KN, Ooi J, Khurana I, Chang L, Hudson JE, El-Osta A, Porrello ER. Dynamic changes in the cardiac methylome during postnatal development. The FASEB Journal, 2015 Apr;29(4):1329-43. (impact factor: 5.48).
2. **Sim CB**, Quaife-Ryan GA, Porrello ER, Hudson JE. Resetting the epigenome for heart regeneration. Seminar in Cell and Developmental Biology, 2016 Jan 7. (impact factor: 6.27).

Presentations arising from this thesis

1. **Sim CB**, Lal S, Dos Remedios C, Hudson JE and Porrello ER. **Isolation of cardiomyocyte nuclei from archived human heart samples.** 4th Meeting of the Australian Network of Cardiac and Vascular Developmental Biologists (ANCVDB). (Adelaide, Australia, 2015).
2. **Sim CB**, Lal S, Dos Remedios C, Hudson JE and Porrello ER. **Isolation of cardiomyocyte nuclei from archived human heart samples.** 6th International Postgraduate Symposium in Biomedical Sciences. (Brisbane, Australia, 2015).
3. **Sim CB**, Ziemann M, Kaspi A, Harikrishnan KN, Ooi J, Khurana I, Chang L, Hudson JE, El-Osta A and Porrello ER. **Dynamic changes in the cardiac methylome during postnatal development.** 2nd Annual Awards Seminar of the Queensland Physiology Interest Group (QPIG). (Brisbane, Australia, 2014).
4. **Sim CB**, Ziemann M, Kaspi A, Harikrishnan KN, Ooi J, Khurana I, Chang L, Hudson JE, El-Osta A and Porrello ER. **Postnatal DNA methylation dynamics during heart development.** 3rd Meeting of the Australian Network of Cardiac and Vascular Developmental Biologists (ANCVDB). (Melbourne, Australia, 2014)
5. **Sim CB**, Ziemann M, Kaspi A, Harikrishnan KN, Ooi J, Khurana I, Chang L, Hudson JE, El-Osta A and Porrello ER. **Dynamic changes in the cardiac methylome during postnatal development.** 2014 Australian Physiological Society symposium (AuPS). (Brisbane, Australia, 2014).
6. **Sim CB**, Ziemann M, Kaspi A, Harikrishnan KN, Ooi J, Khurana I, Chang L, Hudson JE, El-Osta A and Porrello ER. **Dynamic changes in the cardiac methylome during postnatal development.** 5th International Postgraduate Symposium in Biomedical Sciences. (Brisbane, Australia, 2014).

7. **Sim CB**, Ziemann M, Kaspi A, Harikrishnan KN, Ooi J, Khurana I, Chang L, Hudson JE, El-Osta A and Porrello ER. **Dynamic changes in the cardiac methylome during postnatal development.** 2014 Brisbane Cell and Developmental Biology Meeting. (Brisbane, Australia, 2014).
8. **Sim CB**, Ooi J, Harikrishnan KN, Ziemann M, Kaspi A, Chang L, Khurana I, El-Osta A and Porrello E.R. **Role of DNA methylation during postnatal cardiomyocyte maturation.** 2nd Meeting of the Australian Network of Cardiac and Vascular Developmental Biologists (ANCVDB). (Gold Coast, Australia, 2013).
9. **Sim CB**, Ooi J, Harikrishnan KN, Ziemann M, Kaspi A, Chang L, Khurana I, El-Osta A and Porrello ER. **Role of DNA methylation during postnatal cardiomyocyte maturation.** 4th International Postgraduate Symposium in Biomedical Sciences. (Brisbane, Australia, 2013).

Publications included in this thesis

1. **Sim CB**, Quaife-Ryan GA, Porrello ER, Hudson JE. Resetting the epigenome for heart regeneration. Seminar in Cell and Developmental Biology, 2016 Jan 7. (impact factor: 6.27) – incorporated as Chapter 1.

Contributor	Statement of contribution
Author: Sim CB (Candidate)	Wrote the paper (50%)
Author: Quaife-Ryan GA	Wrote the paper (50%)
Author: Porrello ER (supervisor)	Edited the paper (50%)
Author: Hudson JE (supervisor)	Edited the paper (50%)

2. **Sim CB**, Ziemann M, Kaspi A, Harikrishnan KN, Ooi J, Khurana I, Chang L, Hudson JE, El-Osta A, Porrello ER. Dynamic changes in the cardiac methylome during postnatal development. The FASEB Journal, 2015 Apr;29(4):1329-43. (impact factor: 5.48) – incorporated as Chapter 3.

Contributor	Statement of contribution
Author: Sim CB (Candidate)	Designed experiments (45%) Wrote the paper (80%) Generated data for all figures except figures mentioned below (70%)
Author: Ziemann M	Wrote the paper (20%) Bioinformatics analyses and generated data for Figures 3.4A, B, 3.5, 3.7, 3.8, 3.12 and Table 3.1, 3.2, 3.3 (20%).
Author: Kaspi A	Consultant of bioinformatics analyses
Author: Harikrishnan KN	Performed pull-down experiment for MBD-seq

	(5%)
Author: Ooi J	Assisted Ziemann M for bioinformatics analyses
Author: Khurana I	Performed pull-down experiment for MBD-seq (5%)
Author: Chang L	Assisted Ziemann M for bioinformatics analyses
Author: Hudson JE (supervisor)	Designed experiments (10%) Edited the paper (33.33%)
Author: El-Osta A	Conceived the project (50%) Edited the paper (33.33%)
Author: Porrello ER (supervisor)	Conceived the project (50%) Designed experiments (45%) Edited the paper (33.33%)

Contributions by others to the thesis

All of the work presented in this Thesis is my own work except the following:

1. Sample collection for Figure 3.3 was performed with assistance of Ms Sindhu Igoor (previous research assistant in the lab).
2. Pull-down experiment of MBD-seq for Figure 3.5 was performed by Dr Harikrishnan Kaipananickal (postdoc of Baker IDI Heart and Diabetes Institute).
3. Bioinformatics analyses for Figures 3.4A, B, 3.5, 3.7, 3.8, 3.12 and Table 3.1, 3.2, 3.3 were performed by Dr Mark Ziemann (postdoc of Baker IDI Heart and Diabetes Institute). The data have been published in the FASEB Journal with both of us as co-first author.
4. Figure 4.5A and B are kindly provided by the postdoc, Dr Richard Mills in the lab. The 3D human organoid tissues for Figure 4.5 C-E were provided by Dr Mills and his PhD student Holly Voges. I did the subsequent drug treatment on the organoids as well as data collection.
5. Experiments to generate results for Table 5.3, 5.4, 5.5 were performed under the guidance of Dr Mark Ziemann (postdoc of Baker IDI Heart and Diabetes Institute).
6. Bioinformatics analysis (including primary and secondary analysis of RNA-seq and ATAC-seq datasets to generate counted-read matrix as well as tertiary analysis, such as MDS plots, heatmaps, GSEA analyses, genome features, and datasets integration) for Figure 5.5-11, 5.13, 5.14 and Table 5.2, 5.6, 5.7, 5.8, 5.9 were generated by me under the supervision of Dr Mark Ziemann, Dr Haloom Rafehi and Dr Antony Kaspi.

Statement of parts of the thesis submitted to qualify for the award of another degree

None.

Acknowledgements

A PhD is a long journey. It is as long as undergraduate study but requires more dedication and focus. It is the end of one's education path but the beginning of one's research career. It takes dedication, persistence and honesty to conquer the "PhD Mountain" and enthusiasm to excel.

I am very lucky to pursue my PhD training in the Thudorrello lab under 3 great supervisors, Dr Enzo Porrello, Dr James Hudson and Prof Wally Thomas. Three equally decent and respectable men as well as great scientists, who have given me invaluable guidance in scientific training and have taught me important lessons for life. To Enzo, thank you for taking me on board 4 years ago. Like I always say, it changed my life. Thank you for always being there when I needed you and always pointing me in the right direction when I was in doubt. You have shown me many important virtues to be a good scientist: hardworking, always be on top of the game, critical thinking, impartial and be kind to others. But the most important lesson you gave me is to always have great passion in what you do so there will be no regret in life. Thank you Enzo for being such a great mentor. To James, being an engineer you pursue the same question from a different perspective than a typical biologist and have shown me the importance of quality control, standardized pipelines and protocols. Thank you for the encouragement for never giving up and having persistence in what I am doing as well as your critical comments. To Wally, thank you for being so caring and helpful all the time even when you are incredibly busy. Thank you for being such a great model of how to succeed and be happy in one's career while genuinely helping others to achieve their full potential. I remember what you once told me, "just focus on the important scientific question and approach it with integrity as 100 years from now, people will not remember what kind of person you are but they will remember your research outcomes". Thank you to the 3 of you for creating such a positive, helpful and encouraging environment for your fellows.

I would also like to express my gratitude to Prof Assam El-Osta for offering a warm welcome to me to work in your lab at the Baker IDI Heart and Diabetes Institute. Thanks for creating such a dynamic and friendly scientific environment. To Dr Mark Ziemann, Dr Haloom Rafehi and Mr Antony Kaspi, thank you for all for your patient guidance during the steep learning track to the bioinformatics world. I could not achieve so much without your help. To Dr Kiymet Bozaoglu, Dr Harikrishnan Kaipananickal, Mr Ishant Khurana, Ms Hanah Rodriguez, Dr Abdul Waheed Khan, Dr Natasha Tuano and the rest of the team, thank you for your friendly help in scientific questions and participation in life when I was in Melbourne by myself.

A journey in PhD and science would be difficult without the important insightful discussions and technical support from others. To Dr David Simmons, Dr Geoff Osborne, Dr Neville Butcher, Dr Richard Gordon, Dr Sean Lal, Dr Jose Polo, Dr Mirana Ramialison, Prof Chen Chen, Dr Xin Li Zhang, Dr Jason Lynch, Dr Ken Loh, Dr Shu Ngo, Dr Frederik Steyn, Ms Barb Arnts, Mr Gerard Pattison, Ms Kym French and Dr David Pennisi, thank you all for helping me throughout various difficulties I met during the course of my PhD.

To members of the Thudorrello lab: Dr Celine Vivien, Sindhu Igoor, Dr Zhibin Ma, Gregory Quaife-Ryan, Dr Richard Mills, Shannon O'Brien, Holly Voges, Dr Melissa Reichelt, Dr Simon Foster, Dr Zhen Wang, Dr Brooke Purdue, Dr Drew Titmarsh, Dr Vikram Ratnu, Ms Ngari Teakle and all members, thank you for offering me your great support in science and day to day company. This lab is great because of you all. Together with all of the Macgregor Level 5 members, thank you for these 4 years of great times.

Of course, this PhD would not be possible without generous funding support. Thanks to The University of Queensland for the UQ International scholarship that supported me over the last 3.5 years as well as the generous financial support from Enzo and James over the last 6 months. Also, a big great thanks to the following personnel and departments: Ms Marrianne Hamlet, Mr James Mather, Ms Fiona Gilloway, Mr Nigel Deeming, Mr Adam Beauchamp, Dr Darryl Whitehead, Dr Shaun Walter, Ms Rebecca Gao, Mr Gabriel de Godoy, Ms Donna Callaghan, Ms Deborah McCamley, Mr Don Weerheim, Ms Virginia Nink, AIBN and Otto Animal Facility and the IT group. Thank you for covering administration, facility service, financial and IT support to make my life easier. I would also like to thank the QFAB Bioinformatics facility for the great assistance and for provision of all bioinformatics analysis and software support.

Last but not least, thanks to Dr Kirsty Short, Pauline Monnot, Danielle Edwards, Dr Jereme Spiers, Zhe Zhang, Emily Dorey, Dr Alice McGovern, Dr James Cuffe, Dr Cortina Chen, Lachlan Harris and all my dearest friends around the world. Your friendship and our sharing of the ups and downs of scientific life built the precious memories of the last 4 years. Thanks for being there. Also, thank you Nicole Spykie, I would not be here without your advice.

Finally, my greatest thanks to my fantastic family. Thank you for being there, for your support, for always believing in me even when I lost faith. Thanks for standing by me.

They say it takes a village to raise a child. To me, it takes all of you to achieve this PhD degree.

Keywords

heart development, cardiomyocyte maturation, cardiomyocyte proliferation, epigenetics, cardiac regeneration, dna methylation, chromatin landscape, rna-seq, mbd-seq, atac-seq

Australian and New Zealand Standard Research Classifications (ANZSRC)

ANZSRC code: 060102, Bioinformatics, 35%

ANZSRC code: 060103, Cell Development, Proliferation and Death, 55%

ANZSRC code: 060111, Signal Transduction, 10%

Fields of Research (FoR) Classification

FoR code: 0601, Biochemistry and Cell Biology, 100%

To Dad.

Summary of Table of Contents

Table of Contents

List of Figures

List of Tables

Abbreviations and Definitions

Abbreviation	Definition
5aza	5-azacytidine
5aza-dC	5-aza-2’-deoxycytidine
5-mC	5-methylcytosine
Ac	acetylation
Actn	α-actinin
Adora2a	adenosine A2a receptor
AMPK	5’ adenosine monophosphate-activated protein kinase
ATAC-seq	transposase-accessible chromatin with high-throughput sequencing
ATRX	α-thalassemia mental retardation syndrome X-linked
BMCs	bone marrow cells
BMP	bone morphogenetic protein
BrdU	bromodeoxyuridine
CBP	CREB binding protein
Ccn	cyclin
Cdc2	cell division cycle 2 kinase
Cdk	cyclin-dependent kinase
Cdkn	cyclin dependent kinase inhibitor
CDS	coding DNA sequences
CFU-Fs	colony-forming units - fibroblasts
CGI	CpG island
CGS	CpG shore
CHD	coronary heart disease
ChIP-seq	chromatin immunoprecipitation sequencing

CHTF18	chromosome transmission fidelity factor 18
CIT	citron rho-interacting serine/threonine kinase
CM	cardiomyocytes
cmlc-2	cardiac-specific cardiac myosin light chain 2
Col1a1, Col3a1	collagen type 1 or 3 alpha 1 chain
CPCs	cardiac progenitor cells
CpG	cytosine-guanine dinucleotide
CreER	Cre recombinase
CRs	chromatin remodellers
CSCs	cardiac stem cells
Ctcf	CCTC binding factor
CTDP1	carboxy-terminal domain phosphatase subunit 1
cTnnI/ cTnI	cardiac troponin I
cTnnT/ cTnT	cardiac troponin T
CVD	cardiovascular disease
Ddr2	discoidin domain receptor tyrosine kinase 2
Dmd	dystrophin
DMRs	differentially methylated regions
DNase-seq	DNase I hypersensitive site sequencing
Dnmts	DNA methyltransferases
DOT1L	disruptor of telomeric silencing-1
dpci	days post cryoinjury
dpi	days post injection
DTA	diphtheria toxin A chain
E2f4	E2F transcription factor 4
ECG	Electrocardiograms
EdU	5-ethynyl-2’deoxyuriding

EGFR	epidermal growth factor receptor
EMs	epigenetic modifiers
ENCODE	Encyclopedia of DNA Elements
eRNAs	enhancer RNAs
ESCs	embryonic stem cells
FACS	Fluorescence-activate cell sorting
FAIRE-seq	formaldehyde-assisted isolation of regulatory elements
Fbn1	fibrillin 1
FDR	false discovery rate
FGF	fibroblast growth factor
FOX	Forkhead box
FSC	forward scatter
Gadd45	Growth Arrest and DNA Damage 45
GFP	Green fluorescent protein
GPSM2	G-protein signalling modulator 2
GSEA	Gene Set Enrichment Analysis
H3K27	histone 3, lysine 27
HATs	histone acetyl transferases
Hccs	Holocytochrome c synthase
hCOs	human cardiac organoids
HDACs	histone deacetylases
hESCs	human embryonic stem cells
hiPSCs	human induced pluripotent cells
HMTs	histone methyltransferases
HW/BW	heart weight to body weight ratio
IGF2	Insulin-like growth factor 2
IGF2BP2	Insulin-like growth factor 2 binding protein 2

Igf2bp3	Insulin-like growth factor 2 binding protein 3
INSC	Inscuteable homolog
iPSCs	induced pluripotent stem cells
ISWI	imitation SWI
Itgam	integrin subunit alpha M
Jmj	Jumonji
JMJD3	Jumonji domain-containing protein 3
kbp	kilobase pair
KDM	histone lysine demethylase
KDM2B	Lysine demethylase 2B
KLF9	Kruppel-like factor 9
KMT2D	Lysine methyltransferase 2D
LAD	left anterior descending
lncRNAs	long non-coding RNAs
Ly75	lymphocyte antigen 75
Mapk	mitogen activated protein kinase
MBD-seq	methyl-CpG binding domain enrichment and sequencing
MDS	multidimensional scaling
me3	trimethylation
MeDIP-seq	methylated DNA immunoprecipitation
MI	myocardial infarction
miRNAs/ miR	microRNAs
Mlc2a	atrial myosin light chain
Myh6/ αMhc	myosin heavy chain 6 or alpha myosin heavy chain
Myh7/ βMhc	myosin heavy chain 7 or beta myosin heavy chain
NAD	nicotinamide adenine dinucleotide
Neat1	nuclear paraspeckle assembly transcript 1

non-CM	non-cardiomyocytes
Nrg1	neuregulin 1
Nrsf	neuron-restrictive silencer factor
P	postnatal day
PAK4	p21 (RAC1) activated kinase 4
PCM1	pericentriolar material 1
PCNA	proliferating cell nuclear antigen
pH3	phosphorylated-histone H3
PI3K	phosphoinositide 3-kinase
POLD2	DNA polymerase delta 2, accessory subunit
PRIM2	Primase (DNA) subunit 2
PSCs	pluripotent stem cells
PTM	post-translational modification
PTP	protein tyrosine phosphatase
PTPRR	Protein tyrosine phosphatase receptor type R
qPCR	quantitative PCR
RA	retinoic acid
raldh2	retinaldehyde dehydrogenase 2
Rb	retinoblastoma
RNA-seq	next-generation mRNA sequencing
RT	reverse transcription
SAH	S-adenosylhomocysteine
SAM	S-adenosylmethionine
SH3PXD2B	SH3 and PX domains 2B
SMs	skeletal myoblasts
SMYD1	SET and MYND domain containing 1
Srf	serum response factor

SSC	side scatter
SWI/SNF	switch/sucrose non-fermentable
TCA	tricarboxylic acid
Tcf3	transcription factor 3
TDG	thymine DNA glycosylase
TET	ten-eleven translocation
TF	transcription factor
TGF β	transforming growth factor β
Tnnc1	slow skeletal and cardiac type troponin C1
Tnni1	slow skeletal type troponin I1
Tnni3	cardiac type troponin I3
Tnnt2	cardiac type troponin T2
TSSs	transcription start sites
UBE2C	Ubiquitin conjugating enzyme E2 C
UTX	ubiquitously transcribed tetratricopeptide repeat, X chromosome
VEGF	vascular endothelial growth factor
Vwf	von Willebrand factor
wks	weeks
Yap1	yes associated protein 1
yrs	years

Chapter 1

A Review of the Literature

The voyages of Science:

To boldly go where no man has gone before.

Adapted from Star Trek.

Chapter 1. A Review of the Literature

In contrast to adults, recent evidence suggests that neonatal mice are able to regenerate following cardiac injury. This regenerative capacity is reliant on robust induction of cardiomyocyte proliferation, which is required for faithful regeneration of the heart following injury. However, cardiac regenerative potential is lost as cardiomyocytes mature and permanently withdraw from the cell cycle shortly after birth. Recently, a handful of factors responsible for the regenerative disparity between the adult and neonatal heart have been identified, but the proliferative response of adult cardiomyocytes following modulation of these factors rarely reaches neonatal levels. The inefficient re-induction of proliferation in adult cardiomyocytes may be due to the epigenetic landscape, which drastically changes during cardiac development and maturation. This review provides an overview of heart development, maturation and the role of epigenetic modifiers in developmental processes related to cardiac regeneration. An epigenetic framework is proposed for heart regeneration whereby adult cardiomyocyte identity requires resetting to a neonatal-like state to facilitate cell cycle re-entry and regeneration following cardiac injury.

1.1. Cardiac diseases and the need for regeneration therapy

More than 15 million people die from cardiovascular disease (CVD) each year, which contributes to 30% of the overall mortality rate and is anticipated to grow to more than 23 million by 2030 (Mathers and Loncar, 2006; World Health Organization., 2011). Among all CVD cases each year, more than half are attributed to coronary heart disease (CHD), also known as ischemic heart disease. CHD is one of the most important causes of coronary events, such as acute myocardial infarction (MI, also known as heart attack). MI is caused by insufficient blood flow to the heart, which can lead to up to 25% loss of cardiomyocytes within a few hours (Laflamme and Murry, 2011). After suffering from MI and massive cell death, the heart, as a post-mitotic organ, instead of repairing and regenerating the impaired tissue, forms a fibrotic scar with no contractile ability at the site of injury. Although a scar might be a sufficient temporary fix, the lack of regenerative capacity causes the surviving cardiomyocytes to become hypertrophic in order to compensate for the loss of functional cardiomyocytes. This process may lead to contractile dysfunction, arrhythmia and often culminates in heart failure or sudden cardiac death (Olson, 2004). Therefore, there is a need for regenerative therapies for ischemic heart disease. This section will focus on introducing the therapeutic approaches that are currently used in the clinic, as well as current research efforts towards the development of regenerative therapeutics for heart disease (**Figure 1.1**).

1.1.1. Current clinical therapeutic approaches

The current clinical therapeutic approaches for patients suffering a heart attack include pharmacological treatments, medical procedures or mechanical support devices (Canseco et al., 2015; Gerbin and Murry, 2015; Olson, 2004). Pharmacological treatments such as statins, ACE inhibitors and beta blockers reduce blood pressure and hypertrophic signalling (Canseco et al., 2015; Gerbin and Murry, 2015; Olson, 2004). Medical procedures, such as percutaneous coronary intervention and coronary artery bypass grafting can restore perfusion to the heart to improve cardiac function (Canseco et al., 2015; Gerbin and Murry, 2015; Olson, 2004). Mechanical support with left ventricular assist devices (LVAD) mechanically assists the failing left ventricle (Canseco et al., 2015; Gerbin and Murry, 2015; Olson, 2004). However, none of these treatments target the underlying problem, which is the loss of contractile units – cardiomyocytes. Therefore, these treatments cannot prevent the progression to end stage heart failure in many patients for which the only treatment option is heart transplantation (Tousoulis et al., 2008). With the scarcity of histocompatible donors for heart transplantation, the restoration of functional cardiomyocytes following injury through regeneration of cardiomyocytes remains a central goal in cardiology.

1.1.2. Cell therapy

Given the limitation of current clinical therapeutic tactics, various approaches to improve heart function have been investigated over the decades. This includes gene therapy, direct cell reprogramming, cell therapy and delivery of engineered tissues (**Figure 1.1**). As the adult heart is a post-mitotic organ and lacks robust regenerative capacity, cell therapies have become one of the most popular methods for induction of tissue regeneration. A considerable amount of mammalian cardiac regenerative and cell transplantation processes have been illuminated by the work of developmental biologists, stem cell biologists and cardiologists over the past decade (Choi and Poss, 2012; Gerbin and Murry, 2015; Xin et al., 2013b). Several cell types including cardiac progenitor cells (CPCs), cardiac stem cells (CSCs), embryonic stem cells (ESCs), skeletal myoblasts (SMs) and bone marrow cells (BMCs) have been used in transplantation studies for their potential myocardial regenerative ability (Choi and Poss, 2012; Gerbin and Murry, 2015; Mazhari and Hare, 2007; Tousoulis et al., 2008). Current approaches for cell therapy will be discussed in this section.

Non-cardiac cells Non-cardiac cells such as SMs and BMCs were the initial objects of interest for cardiac cell therapy studies. SMs were one of the earliest choices for cardiac cell therapy studies. While SMs were shown to improve ventricular function post-MI, the mechanism remains unclear (Hagege et al., 2003; Leobon et al., 2003; Seidel et al., 2009). Moreover, subsequent Phase I

clinical trials of SMs in humans failed on efficacy and were also associated with increased risk of cardiac arrhythmias (Menasche et al., 2008), which subsequently refocused efforts in the field on alternative approaches and other cell types (Garbern and Lee, 2013).

Some of the earliest studies of BMCs were performed by transplanting green fluorescent protein-labelled BMCs into the border region of the infarcted heart (Orlic et al., 2001). Up to 50% of the newly formed myocardium was green fluorescent protein (GFP) labelled, suggesting a transdifferentiation of transplanted BMCs into cardiomyocytes that facilitated functional regeneration of the rodent heart after MI. However, subsequent studies using cardiac-specific reporters to track the fate of transplanted BMCs contradicted the theory of transdifferentiation, despite the ability of BMCs to exert some functional benefits even though transplanted cells died after 1-2 weeks (Murry et al., 2004). Intriguingly, several related lineage tracing studies also showed that the injection of bone marrow derived cells promoted endogenous cardiomyocyte proliferation following injury, suggesting that functional improvements occur through beneficial paracrine effects (Garbern and Lee, 2013; Hatzistergos et al., 2010; Mirotsou et al., 2007). Also, while two clinical trials BOOST and REPAIR-AMI showed that injection of BMCs promotes cardiac function of patients presenting with ST-segment elevation MI, subsequent larger and more well-controlled double-blinded clinical trials such as FOCUS-CCTRN, TIME and LateTIME did not replicate the encouraging results from previous clinical trials, further questioning the efficacy of BMCs (Assmus et al., 2002; Leistner et al., 2011; Perin et al., 2012; Schachinger et al., 2004; Schachinger et al., 2006a; Schachinger et al., 2006b; Traverse et al., 2012; Traverse et al., 2010; Wollert et al., 2004).

CPCs and CSCs Several methodologies have been used to identify resident cardiac stem cell populations in the adult heart, and the expression of specific cell surface markers is one of the most popular methods. Through well-developed stem cell studies, several cell surface expression markers have been characterized such as c-kit, Sca1 and Abcg2 and, also, TFs such as Nkx2.5, Gata4, Islet1 and Wt1 which have been used to identify CPCs and stem cells from different developmental stages (embryonic, neonatal and adult) (Arceci et al., 1993; Beltrami et al., 2003; Laflamme et al., 2007; Laugwitz et al., 2008; Martin et al., 2004; Oh et al., 2003; Zhou et al., 2008). A more recent study identified adult cardiac-resident colony-forming units – fibroblasts (CFU-Fs) stem-like populations that are essential for cardiac development throughout adulthood (Chong et al., 2011). These identified progenitor cell populations exist during different developmental time frames, in low abundance and are capable of differentiating into cardiomyocytes, smooth muscle cells or endothelial cells when cultured *in vitro*.

c-kit positive cells are one of the most intensively studied and controversial cardiac progenitor cell populations. A recent study by Ellison et al stated that c-kit$^+$ cells regenerated lost cardiomyocytes in an acute cardiac failure model (Ellison et al., 2013). By using transgenic ablation of c-kit$^+$ cells, regenerative capacity and functional repair of the rodent heart was eradicated. Importantly, the c-kit$^+$ cells were also sufficient to restore the regenerative potential of the heart. Also, previous studies reported that isolated human c-kit$^+$ cardiac cells formed functional myocardium *in vivo* and facilitated the recovery of infarcted rodent hearts when injected into the injured area (Bearzi et al., 2007). Conversely, Tallini et al discovered that c-kit$^+$ cardiac cells did not contribute to cardiac myogenesis in the injured adult heart (Tallini et al., 2009). Also, Li et al showed that c-kit functions during cardiomyocyte terminal differentiation and is not an exclusive stem cell marker (Li et al., 2008). Furthermore, Kubin et al demonstrated that the inflammatory cytokine oncostatin M (OSM) induced the re-expression of c-kit in de-differentiating cardiomyocytes, challenging the credibility c-Kit as cardiac progenitor marker (Kubin et al., 2011; Li et al., 2008). This result is further supported by two quantitative genetic fate-mapping studies, which indicate that c-kit$^+$ cells are not functionally critical for cardiogenesis and do not provide a meaningful contribution to cardiomyocyte formation during development or following MI (Sultana et al., 2015; van Berlo et al., 2014).

Despite the abovementioned controversial results on the identity of CPCs, two recent clinical trials, SCIPIO and CADUCEUS, have nevertheless shown that injection of CSCs into patients post infarction enhanced cardiac function and reduced infarct size, but the cellular mechanisms for these benefits are still unclear (Bolli et al., 2011; Makkar et al., 2012). Taken together, although a number of cardiac stem cell populations have been identified in the adult heart, these controversial research outcomes have clouded the future clinical use of adult progenitor cells for cardiac regeneration.

ESCs and induced pluripotent stem cells (iPSCs) The first successful case of differentiation of human ESCs (hESCs) into cardiomyocytes was achieved in 2001 (Kehat et al., 2001). Since then, more defined protocols have been optimized to obtain more mature differentiated cardiomyocytes (Laflamme et al., 2007). It has been shown that the engraftment of hESCs derived cardiomyocytes enhanced cardiac function in the infarcted rat heart (Laflamme et al., 2007). Shiba et al also showed an electrical coupling of injected hESC derived cardiomyocytes in the infarcted guinea-pig heart with a reduction in cardiac arrhythmias (Shiba et al., 2012; Shiba et al., 2014). A more recent study by Chong et al exhibited that injection of 1 billion hESC derived cardiomyocytes to the infarcted myocardial wall of macaque monkeys (*Macaca nemestrina* - non-human primate) led to remuscularization and electrical coupling of myocardial tissue in the infarcted region (Chong et al.,

2014). However, non-fatal arrhythmias were observed in this non-human primate cardiac injury model, which was not previously observed in small rodent models, demonstrating a potential biological difference between small and large animal models (**Table 1.1**). As many previous studies were conducted using small animal models, further studies in large animal models, in particular large animals that have similar heart rates to humans, such as pigs, sheep and primates, may be necessary to understand the function, efficacy and safety of these hESC or iPSC derived cardiomyocytes before clinical application.

Collectively, ESC therapies for heart disease have shown enormous promise and future potential. However, major challenges remain as the use of human ESCs is still controversial and there is a need for immunosuppression. The different biological effects and safety concerns in primate models will need to be resolved prior to clinical translation. On the other hand, iPSCs overcome many of the moral and immunosuppression predicaments of human ESCs. Zhang et al have successfully differentiated nodal-, atrial-, and ventricular-like cardiomyocytes from human iPSCs (hiPSCs) (Zhang et al., 2009). Moreover, recent studies have demonstrated that hiPSCs can differentiate into cardiomyocytes, engraft with the injured area and improve cardiac function when injected following MI in mice (Citro et al., 2014; Funakoshi et al., 2016). However, the methods for induced-reprogramming are currently costly, lengthy and potentially carcinogenic, raising concerns regarding their potential use in this future therapeutic area (Gerbin and Murry, 2015).

Engineered heart tissue Similar to previously discussed ESC or iPSC-derived cardiomyocytes, engineered cardiac tissues could be considered as a logical extension of the cell-based therapy approach. Instead of injecting ESC or iPSC-derived cardiomyocytes to the injured heart, researchers have generated 2D or 3D myocardial tissues for transplantation into the injured heart. The recapitulation of native tissue architecture using tissue-engineering strategies holds enormous promise for regenerative medicine applications including cardiac regeneration.

In 1997, Eschenhagen and colleagues created the first successful engineered cardiac tissue by culturing neonatal rat cardiomyocytes in a collagen matrix (Eschenhagen et al., 1997). A subsequent study by Li et al transplanted engineered cardiac tissue generated from foetal rat ventricular cells and a gelatine mesh to the adult rat heart following cryoinjury. This study showed that the transplanted graft survived and maintained its function following surgery, suggesting a potential therapeutic capacity of engineered heart tissue (Li et al., 1999). A subsequent large-scale systematic study by Zimmermann et al further validated the engineered heart tissues and demonstrated that they were capable of improving cardiac function in a rat heart failure model

(Zimmermann et al., 2006). Numerous independent studies have subsequently supported these results and confirmed that transplantation of engineered heart tissue improves cardiac function following MI (Sekine et al., 2008; Stevens et al., 2009; Tulloch et al., 2011). Tissue engineering remains a research hotspot in cardiology with current research efforts focusing on the generation of 3D human cardiac tissues using ESC or iPSC derived cardiomyocytes.

Current limitations of cardiac tissue engineering include the high cost of tissue production, labour-intensive protocols required for tissue production including multiple manual handling steps, limited size due to oxygen diffusion limitations, lack of tissue vascularisation, and time taken for mechanical and electrical coupling to host myocardium (Coulombe et al., 2014; Hirt et al., 2014). Numerous studies have been targeted at addressing these issues. More cost effective and efficient protocols for producing tissues are being developed (Hansen et al., 2010), and may help facilitate a reduction in cost and labour in the future. In addition, although blood vessels infiltrate the implanted tissues at 1 mm/day following implantation (Shimizu et al., 2006), this infiltration rate may not be sufficient for larger sized patches and is associated with some necrosis (Shimizu et al., 2006). In order to address this problem, blood vessels may be pre-formed in the tissues which link to the host vasculature and become perfused (Hirt et al., 2014; Tulloch and Murry, 2013). Electro-mechanical coupling also remains a major concern due to the potential induction of arrhythmias prior to coupling, however, over time the tissues do become coupled (Riegler et al., 2015). Therefore, strategies that can enhance this process may overcome the issue in the future.

Overall, while cell therapies hold enormous potential for cardiac regenerative applications in the clinic, many limitations still need to be resolved. These include the delivery of consistent research outcomes and demonstrations of efficacy, as well as reducing the cost of tissue production and immunological rejection of stem cells. Therefore, alternative approaches that bypass the use of cells are also a major focus of current research efforts in the field and these will be discussed in the next section.

1.1.3. Cell-free therapy

Given the limitations of cell therapy, various studies have been conducted to exclude the introduction of foreign cells and investigate the stimulation of endogenous regenerations. However, given that cardiomyocytes undergo rapid cell cycle shutdown shortly after birth, two of the major strategies under investigation for induction of endogenous regeneration are the re-induction of cardiomyocyte proliferation and direct reprogramming of resident non-cardiac cell types into

cardiomyocytes. This section will focus on the current trend of cell-free therapy and direct cell reprogramming research.

Cell-free therapy As mentioned, cardiomyocytes exit cell cycle shortly postnatally. The roles of several cell cycle regulators and cellular signalling pathways have been investigated regarding their ability to induce cell cycle re-entry in cardiomyocyte during development and regeneration. Several studies have demonstrated that overexpression of core cell cycle regulatory proteins enhanced cardiomyocyte proliferation *in vitro* (Bicknell et al., 2004; Chaudhry et al., 2004; Di Stefano et al., 2011). Bicknell et al demonstrated that the overexpression of the developmentally regulated G2/M regulatory complex, cyclin (Ccn) B1- cell division cycle 2 kinase (Cdc2) promoted adult cardiomyocyte proliferation *in vitro* (Bicknell et al., 2004). Similarly, overexpression of Ccna2 promotes neonatal and adult cardiomyocyte proliferation *in vitro* (Chaudhry et al., 2004). Furthermore, *in vitro* inhibition of cyclin-dependent kinase (Cdk) inhibitors, p21, p27 and p57 promotes adult cardiomyocyte proliferation (Di Stefano et al., 2011). However, the rates of cardiomyocyte proliferation observed *in vivo* are much lower. In 1997, Soonpaa et al showed that cardiac-specific overexpression of Ccnd1 increased DNA synthesis and caused multinucleation of adult cardiomyocytes in transgenic mice (Soonpaa et al., 1997). A subsequent study from the same group further showed that cardiomyocyte-specific overexpression of Ccnd2 but not Ccnd1 or Ccnd3 promoted cardiomyocyte proliferation and reduced infarct size in the adult mouse heart following MI injury (Pasumarthi et al., 2005), suggesting that cell cycle activation through manipulation of the core cell cycle machinery could be used for cardiac regeneration. Moreover, overexpression of Ccna2 promotes cardiomyocyte mitosis and improves cardiac function in infracted adult rat and porcine hearts (Shapiro et al., 2014; Woo et al., 2006). The cell cycle TF, E2F2 has also been reported to increase cardiomyocyte proliferation *in vivo* via the promotion of cyclin A and cyclin E transcription (Ebelt et al., 2008). Sdek et al also exhibited that double knockout of retinoblastoma (Rb) and p130 re-activated the expression of cell cycle genes and promoted cardiomyocyte proliferation in adult hearts that underwent trans-aortic constriction injury (Sdek et al., 2011). Together, these studies demonstrate the important role of cell cycle genes in stimulating cell cycle re-entry of terminally differentiated cardiomyocytes.

While direct modulation of cell cycle regulators has shown encouraging results with regard to stimulating adult cardiomyocyte proliferation, the effects remain modest. Also, many have used transgenic promoters to drive overexpression of pro-proliferative genes during development but these effects could be due to immature cardiomyocyte proliferation rather than adult myocyte cell cycle re-entry (Ahuja et al., 2007). Therefore, several signalling pathways have also been

investigated with regards to their ability to control cardiomyocyte proliferation during development and regeneration in adult zebrafish and rodents. An important signalling pathway that regulates zebrafish cardiomyocyte proliferation and regeneration is retinoic acid (RA) signalling (Kikuchi et al., 2011). Kikuchi et al observed a significant up-regulation of retinaldehyde dehydrogenase 2 (raldh2, an enzyme required for RA synthesis) in the epicardium and endocardium following apical resection injury in zebrafish. Genetic inhibition of RA receptor (dn-zrar) or overexpression of RA-degrading enzyme (Cyp26) decreased cardiac proliferation and regeneration of the heart (Kikuchi et al., 2011). Insulin-like growth factor (Igf) signalling, which is required for embryonic rodent heart development, also plays an important role in zebrafish regeneration capacity (Huang et al., 2013). Inhibition of Igf signalling through expression of a dominant negative form of the Igf1 receptor (dn-Ig1r) or Igf1r inhibitor impaired cardiac proliferation and regeneration (Huang et al., 2013). In rodents, p38 mitogen activated protein kinase (Mapk) inhibitor therapy in the presence of Fgf1 improved adult murine cardiac function after injury and was associated with a low rate of cardiomyocyte cell cycle re-entry (Engel et al., 2006). Furthermore, overexpression of tyrosine kinase receptor Erbb4 (receptor for the growth factor neuregulin 1 (Nrg1)) led to ~22.6%±8.5% bromodeoxyuridine positive ($BrdU^+$, proliferation marker) mononucleated cardiomyocytes compared to ~7.2%±5.3% in control at P14. Similarly, injection of recombinant Nrg1 in adult mouse detected ~14.3%±6.5% $BrdU^+$ mononucleated cardiomyocytes compared to non-detectable $BrdU^+$ in the adult control with improvement of cardiac function following MI (Bersell et al., 2009). However, a subsequent study showed that Nrg1 did not promote adult cardiomyocyte cell cycle re-entry in either healthy or infarcted adult mice (Reuter et al., 2014). This is further supported by another study where they showed that Nrg1 lost its ability to promote cardiomyocyte proliferation after P7, concomitant with the postnatal down-regulation of its receptor Erbb2 (D'Uva et al., 2015). Interestingly, overexpression of constitutively active Erbb2 promoted neonatal and adult cardiomyocyte proliferation as well as adult cardiac function following MI (D'Uva et al., 2015). More recently, the Hippo signalling pathway, a major regulator of organ size, has been identified as another pathway involved in regulating cardiac proliferation (Heallen et al., 2011; von Gise et al., 2012; Xin et al., 2013a). An initial study has shown that Hippo signalling negatively regulated Wnt/β-catenin signals to control cardiomyocyte proliferation (Heallen et al., 2011). Subsequently, Gise et al used gain- and loss-of-function studies to demonstrate that the activation of yes associated protein 1 (Yap1), the nuclear effecter of Hippo signalling pathway, is capable of inducing postnatal cardiomyocyte proliferation without influencing their physiological hypertrophic growth (von Gise et al., 2012). Moreover, a recent study by Xin et al reported that *in vivo* Yap1 gain of function induced cardiomyocyte proliferation in both foetal (~40% 5-ethynyl-2'deoxyuriding positive (EdU^+,

proliferative marker) cardiomyocyte) and adult (~1.5% EdU^+ cardiomyocyte) heart (Xin et al., 2013a; Xin et al., 2013b).

Beside these well-characterized growth factor signalling pathways, subsets of microRNAs (miRNAs) have also been reported to play a role in cardiomyocyte proliferation and cardiac regeneration (Eulalio et al., 2012; Porrello et al., 2011a; Porrello et al., 2013). A study by Porrello et al has revealed that inhibition of the miR-15 family during postnatal development promoted myocyte proliferation and improved ventricular systolic function following MI in adult mice (Porrello et al., 2013). Subsequent studies have showed that miR17~92 promoted cardiac proliferation in foetal, embryonic and adult hearts (Chen et al., 2013; Wang et al., 2010). Also, the overexpression of miR17~92 was capable of protecting the adult heart from MI. Furthermore, through high-content functional screening of miRNAs *in vitro*, Eulalio et al identified 40 miRNAs that promoted cell cycle activity in neonatal and adult rodent cardiomyocytes (Eulalio et al., 2012). Overexpression of two of the targeted miRNAs, hsa-miR-590 and hsa-miR-199a, promoted neonatal (~25-35% EdU^+ cardiomyocytes) and adult (~6-9% EdU^+ cardiomyocytes) cardiomyocyte proliferation and induced regeneration of the adult heart following MI.

All of these research outcomes support the idea that induction of adult cardiomyocyte proliferation facilitates endogenous cardiac regeneration. However, various factors that induce potent cardiomyocyte proliferation in foetal or neonatal cardiomyocytes fail to induce the same degree of cardiomyocyte proliferation in adulthood. This critical observation suggests a potential epigenetic barrier to cardiomyocyte cell cycle re-entry, which may be established during postnatal development. Further studies to interrogate this question would help provide a better understanding of the biological processes governing postnatal cardiomyocyte maturation.

Direct cell reprogramming In 1958, John Gurdon established the concept of reprogramming when he discovered that transplantation of somatic cell nuclei into enucleated oocytes was sufficient to “reprogram” cells into a pluripotent state (Gurdon et al., 1958). It was subsequently demonstrated that delivery of a single myogenic TF, MyoD, could reprogram fibroblasts into a SM without reverting to a pluripotent state, in a process now referred to as direct reprogramming (Davis et al., 1987).

As fibroblasts and myofibroblasts are largely responsible for maintenance of the infarct scar after MI, transdifferentiation of these cell types into cardiomyocytes represents a potentially useful regenerative strategy. Previous studies showed that members of the core cardiogenic gene program

Gata4, Mef2c, Tbx5 (and Hand2) reprogrammed cardiac fibroblasts into spontaneously contracting cardiac-like myocytes *in vitro* (Ieda et al., 2010) and *in vivo* (Song et al., 2012). Recapitulation of these studies in human fibroblasts showed that GATA4, TBX5, HAND2 and two MEF2C-regulated miRNAs, miR-133 and miR-1, up-regulated the expression of cardiac troponin T (cTnnT) and tropomyosin (markers of cardiomyocytes) and created a small subset of spontaneously beating cardiomyocytes (Nam et al., 2013).

Cumulatively, these studies suggest fibroblasts, or indeed other cells types within and surrounding the infarct, could represent a viable target for cardiomyogenesis. However, current reprogramming of cell identity, in both pluripotency and direct reprogramming approaches, is an inefficient process and current strategies result in off-target effects in other cell types within and outside the heart (Ieda et al., 2010; Islas et al., 2012; Jayawardena et al., 2012; Nam et al., 2013; Polo et al., 2012). Potentially, overcoming the epigenetic roadblock could be an essential improvement for reprogramming efficiency and controlling the maturation of reprogrammed cells.

1.2. Endogenous cardiac regeneration

Clearly, the impact of the abovementioned therapies for regeneration of the infarcted heart is promising. However, some controversial outcomes require further investigation before clinical use. Also, further examination regarding cell fate and the mechanisms underlying their functional benefits need to be conducted before proposing long term benefit. Moreover, outcomes from cell-free therapy reveal the importance of endogenous cardiomyocyte proliferation during cardiac regeneration. As another avenue for replenishment of cardiomyocytes after injury, it is important to consider the mechanisms of activation of endogenous cardiac regenerative capability. In fact, heart regeneration has been investigated in depth in the past 50 years in several amphibian, teleost and mammalian species (Carvalho and de Carvalho, 2010; Laflamme and Murry, 2011; Uygur and Lee, 2016). In higher vertebrates, compared to highly regenerative organs such as liver, bone, skeletal muscle or skin, the heart is one of the least regenerative organs. Conversely, lower vertebrates possess a higher regenerative capacity compared to mammals (Oberpriller and Oberpriller, 1974; Poss et al., 2002) (**Figure 1.2**). However, several recent studies reported that 1-day old neonatal rodent heart is capable of regenerating cardiomyocytes to compensate the lost myocardium in various cardiac injury models, including apical resection, genetic ablation, cryoinjury and MI, suggesting that mammals might retain significant cardiac regenerative potential during early postnatal life (Darehzereshki et al., 2015; Haubner et al., 2012; Porrello et al., 2011b; Porrello et al., 2013; Strungs et al., 2013; Sturzu et al., 2015). This also indicates that the ability of the heart to

regenerate may not be due to inherent species differences that confer regenerative capacity, but rather due to the developmental maturation of cardiomyocytes and postnatal shutdown of regenerative capacity in mammals. In this section, endogenous cardiac regeneration in several organisms will be discussed.

1.2.1. Cardiac regeneration in urodele and anurans amphibian

Urodele and anurans are both members of the amphibian order, where urodele amphibians retain their tail throughout life (such as salamanders and newts) whereas anurans undergo morphogenesis to lose their tail and acquire limbs in adulthood (including frogs and toads). The earliest study of newt cardiac regeneration capacity was conducted by Oberpriller et al in 1974 (Oberpriller and Oberpriller, 1974). Research provided evidence for DNA synthesis and mitosis in adult newt cardiomyocytes after ventricular apical resection injury. Repair of cardiac injury started at ten days post-injury and involved the formation of blood clot, necrosis, macrophagic activity and regeneration of heart muscle, however, only a partial regeneration was observed. Recently, Witman et al observed a full regeneration in the adult newt heart following apical resection of a small portion of the cardiac ventricles, suggesting the newt heart can recover completely following injury under certain experimental conditions (Witman et al., 2011). A parallel experiment in axolotl also reported a full recovery of the injured heart within 90 days (Flink, 2002). Interestingly, studies reported that matrix deposition acted as the imminent response following injury to provide support at the injured site (Piatkowski et al., 2013). However, the deposited matrix started to be removed after 50 days and was replaced with cardiomyocytes (Piatkowski et al., 2013; Witman et al., 2011). Overall, it is now well accepted that urodele amphibian hearts are capable of regeneration following injury.

In 1973, Rumyantsev and colleagues studied the regenerative capacity of the anuran heart (Rumyantsev, 1973). Unlike the urodele amphibians discussed in the previous section, adult anuran amphibians exhibited a different regenerative response (Rumyantsev, 1973; Uygur and Lee, 2016). Studies observed cardiomyocyte dedifferentiation and cell cycle reactivation following injury in the adult frog heart (Rumyantsev, 1973). Using ^{3}H-thymidine (^{3}HTdr) tracing study, Rumyantsev et al observed up to 13% of myocytes entered into mitosis within the first two weeks after local injury in the adult frog heart, with these mitotic events peaking at 3 weeks after injury (Rumyantsev, 1973). However, the adult frog heart failed to undergo full regeneration, leaving a partially regenerated and partially scarred heart tissue (Rumyantsev, 1973; Uygur and Lee, 2016).

1.2.2. Cardiac regeneration in zebrafish

Apical resection Poss et al subsequently used similar techniques to investigate whether zebrafish possess cardiac regenerative capacity (Poss et al., 2002). Heart tissue structure and function was fully restored within two months after 20% of ventricular myocardium was excised in 1-2 year old adult zebrafish. Cardiomyocyte proliferation was histologically observed by staining $BrdU^+$ cells at 7 days after the resection. Similar to amphibians, a blood clot was formed after tissue resection to prevent blood loss. Two to four days after amputation, fibrin deposits replaced the erythrocytes. However, unlike amphibians, which had a large area of fibrin deposition, zebrafish suffered only a small extent of fibrosis and they were capable of overcoming the fibrotic response in 60 days to achieve a 100% restoration of myocardial function (Poss et al., 2002). Interestingly, sarcomeric structural re-organization was observed during the restoration of the myocardium. Notably, cell fate tracking studies established that cardiac regeneration was accompanied with the dedifferentiation and division of pre-existing cardiomyocytes (Jopling et al., 2010; Kikuchi et al., 2010). The source of regenerated cardiomyocytes will be further discussed in the upcoming section.

Cryoinjury Using cardiac resection, which involves removal of a large portion of tissue, may not be the optimal model for studying cardiac regeneration, because MI involves localized cardiomyocyte cell death and inflammation. Interestingly, several groups have established cryoinjury models, which are believed to be a closer model to MI (Chablais et al., 2011; Gonzalez-Rosa et al., 2011). Research groups have used liquid nitrogen pre-cooled stainless cryoprobes to injure the adult zebrafish myocardium, which leads to mortality of 25% of the cardiac tissue in the injured area. Using transgenic fish with cardiac-specific cardiac myosin light chain 2 (cmlc2) promoter driven GFP protein or nuclear DsRed 2, the whole reparative process following cryoinjury was observed (Chablais et al., 2011). Similar to apical resection, cryoinjury also triggered an instant blood clot formation followed by fibrin deposition at 4 days post cryoinjury (dpci), collagen network introduction at 7 dpci to form a fibrotic scar and recovery beginning at 14 dpci. By the time of 60 dpci, the injured area was almost completely replenished with nascent cardiomyocytes. Electrocardiograms (ECG) showed the functional recovery of original electrical properties, proving that newly formed myocardium functionally integrated with the pre-existing myocardium (Chablais et al., 2011). Remarkably, although a massive fibrotic scar was formed after cryoinjury in zebrafish, which is similar to the response of mammalian heart after suffering from infarction, zebrafish managed to overcome the obstacles and replaced the scar with regenerated cardiac tissue, suggesting that scar formation after injury is compatible with cardiac regeneration in zebrafish (Gonzalez-Rosa et al., 2011).

Genetic ablation A recent study conducted by Wang et al using genetic ablation removed more than 60% of ventricular myocardium, which caused acute heart failure in zebrafish (Wang et al., 2011). By crossing cmlc-2 promoter controlled tamoxifen inducible Cre recombinase (CreER) transgenic fish line with myocyte specific β-actin 2 driven cytotoxic diptheria toxin A chain (DTA) expression in transgenic fish line, Wang et al managed to induce cardiomyocyte specific cell death after 5-7 days of tamoxifen injections. Regeneration started rapidly at 7 days post injection (dpi). By 14 dpi, close to 50% of the ablated tissue was replaced by proliferating myocytes and at 30 dpi heart muscularisation was completed. Although the massive cardiac cell death decreased exercise tolerance and increased mortality following heat stress, it did not influence fish survival, demonstrating that the major selective loss of cardiac muscle cells was enough to activate cardiac regeneration. This non-surgical, targeted genetic ablation model, which triggered massive cardiomyocyte cell death without any surgical intervention, creates a closer approximation to MI and provides a more stable platform to study injury and proliferation in other cell types or animals (Wang et al., 2011).

Source of cardiomyocytes Heart regeneration studies in zebrafish show that lower vertebrates maintain a greater regenerative capacity compared to higher vertebrates. Presently, an issue of intense interest is whether pre-existing cardiomyocytes, non-myocytes or CSCs are the contributory cell population in myocardial regeneration. In 2006, Lepilina et al used cardiac specific fluorescent reporters and reported that newly regenerated cardiomyocytes were derived from an undifferentiated epicardial progenitor cell population (Lepilina et al., 2006). However, a more recent study by the same group and Jopling et al showed a converse outcome (Jopling et al., 2010; Kikuchi et al., 2010). Using the Cre/lox genetic fate-mapping system, they revealed that de-differentiation and proliferation of pre-existing cardiomyocytes after amputation was the predominant mechanism driving cardiomyocyte regeneration following injury. Similarly, Wang et al observed the phenomenon of massive sarcomere disorganization in existing cardiomyocytes concomitant with cardiac regeneration at 7 and 14 dpi in the genetic ablation injury model (Wang et al., 2011). Kikuchi et al reported apical resection of zebrafish initiated cardiac specific expression of the TF gata4 in the subepicardial ventricular layer within 7 dpa and gata4^{+} cells subsequently migrated into the injury sites (Kikuchi et al., 2010). gata4^{+} cells were co-labelled with BrdU at edges of the wound and inside of the injury site at 7 and 14 dpa, respectively, suggesting DNA synthesis in gata4^{+} cells contributes to heart regeneration. In fact, gata4 is an embryonic cardiogenesis gene, which is necessary for embryonic cardiac development and vascularisation (Choi and Poss, 2012). The re-expression of gata4 in subepicardial cells proposed a re-activation of the embryonic gene program in adult cardiomyocytes. Together, current research suggests that the

regeneration of zebrafish heart following injury is accomplished by pre-existing cardiomyocytes through de-differentiation and cell cycle re-entry.

1.2.3. Cardiac regeneration in embryonic and neonatal rodents

Genetic knockout Compared to the high regenerative capacity of lower vertebrates, adult mammalian hearts possess a remarkably low rate of cardiac regeneration. However, a study by Drenckhahn et al reported that the foetal mouse heart retains some regenerative capacity (Drenckhahn et al., 2008). The mitochondrial enzyme Holocytochrome c synthase (Hccs) is involved in generating energy for cells. Cardiac specific knockout of the X-linked gene encoding Hccs caused 50% deficient cells in female embryonic hearts during mid-gestation. Unlike the embryonic lethality in males, heterozygous females survived until birth with no significant morbidity, with only 10% of cells appearing diseased, suggesting that regeneration of diseased cells compensated for this genetic deficiency during embryonic foetal heart development. This research outcome suggested a potential for regeneration in the embryonic mammalian heart.

Apical resection In order to determine whether cardiac regenerative capacity extends into the early neonatal period, Porrello et al repeated the zebrafish apical resection model in neonatal mice (Porrello et al., 2011b). While P1 mice were capable of regenerating after trauma, the regenerative capacity was lost in 7-day old mice. The results implicated a developmental window for regeneration arrest within 7 days after birth in mice, which coincides with the timing of cell cycle arrest during rodent cardiac development (Li et al., 1996). Similar to the zebrafish injury model, the rodent heart showed a large blood clot shortly after resection followed by a significant inflammatory response. Full restoration of the resected area occurred within 21 days with normal systolic function evidenced by echocardiogram examination. Neonatal heart regeneration was associated with proliferation of cardiomyocytes and a full integration of newly formed cardiac muscle cells with the existing myocardium.

MI Following the observation of cardiac regeneration in neonatal mice after apical resection, another study was conducted by the same group using MI model (Porrello et al., 2013). Through inducing ischemic MI in P1 mice by left anterior descending (LAD) coronary artery ligation, they created a necrotic and severely inflammatory environment in the neonatal heart that is more similar to MI in adult humans. Similar to the apical resection results, a full functional recovery was accomplished by 21 days post-MI in neonatal mice. In contrast to the robust regeneration activity in 1-day old mice, 7-day and 14-day old mice failed to recover following LAD ligation and instead

formed large fibrotic scars, implying a loss of regenerative capacity within a week after birth. Very similar results were also obtained in an independent study performed by Haubner et al (Haubner et al., 2012).

Source of cardiomyocytes The fact that rodents possess a regenerative capacity shortly after birth opens up the possibility of reactivation of cardiac regeneration mechanisms in adulthood. The origin of the regenerated cardiomyocytes, again, becomes a very important issue. In both of the apical resection and MI studies of neonatal mice, by using tamoxifen-induced CreER controlled by alpha myosin heavy chain (aka myosin heavy chain 6, αMHC/ Myh6) to track the cardiomyocyte lineage, Porrello et al detailed that the newly formed cardiac muscle cells were originated from pre-existing cardiomyocytes (Porrello et al., 2011b; Porrello et al., 2013). Haubner et al also reported that the pre-existing cardiomyocyte population contributed to the cardiac regeneration in the 1-day old MI mouse heart (Haubner et al., 2012). These research outcomes are similar to the previously reported regeneration event in the zebrafish (Jopling et al., 2010; Kikuchi et al., 2010). Interestingly, as previously mentioned about the importance of Hippo signalling, Yap cardiac-specific inhibition in neonatal mice replaced the cardiac regenerative response with a fibrotic response, demonstrating a requirement for this signalling pathway in neonatal heart regeneration (**Figure 1.3**) (Xin et al., 2013a; Xin et al., 2013b).

1.2.4. Cardiac regeneration in adult rodents

Unlike the high regeneration capacity of mammalian foetal or neonatal cardiomyocytes, the regeneration capacity of adult myocytes is debatable. Previous studies using apical resection and induced MI already showed that following development, adult mouse failed to regenerate following injury (Porrello et al., 2011b) (Porrello et al., 2013) (Haubner et al., 2012). It is important to notice that, while sharing the similar biological processes with neonatal mouse hearts following injury which involves initial formation of blood clot, infiltration of immune cells as well as deposition of extracellular matrix at the injured region, adult mouse hearts fail to activate the cardiomyocyte proliferation to compensate the loss of cardiac tissue, ending with extensive scar formation (Uygur and Lee, 2016), suggesting a developmental modification that regulates cardiomyocyte proliferation capacity after birth (**Figure 1.2**).

Recently, Senyo et al used stable isotope labelling (^{15}N) for genetic mapping in the mouse, which showed a small regeneration rate (0.76% per year) from pre-existing cardiomyocytes (Senyo et al., 2013). This study debates the previous study from the same group by Hsieh et al that a stem cell

population was responsible for the substitution of adult mammalian cardiomyocytes after injury but not during normal aging (Hsieh et al., 2007). Moreover, two genetic fate mapping studies suggested that CPCs such as c-kit$^+$ are not required for cardiogenesis (Sultana et al., 2015; van Berlo et al., 2014). Kimura et al also identified a rare cycling cardiomyocyte population in the adult heart through hypoxia cell fate mapping (Kimura et al., 2015). Notably, 2 recent studies have performed detailed characterization on the cardiomyocyte cycling during development. While Naqvi et al demonstrated a proliferative burst of cardiomyocytes at P15 which contributed to an increase in cardiomyocyte number by 40% postnatally (Naqvi et al., 2014), Alkass et al recently contested this finding and suggested that cardiomyocyte number was established within the first week after birth with no significant changes in cardiomyocyte proliferation detected after P11 (Alkass et al., 2015). Nevertheless, both studies showed no significant changes in cardiomyocyte proliferation and myocyte number in adulthood, suggesting the limited capacity of adult cardiac proliferation.

Together, the origin of nascent cardiomyocytes being generated from either stem cell populations or existing cardiomyocytes remains a contentious issue but the adult heart does appear to have measurable, yet extremely limited, capacity for cardiomyocyte replenishment.

1.2.5. Cardiac proliferation and regeneration in human

Development Like rodents, it is a well-accepted concept that adult humans have extremely low aptitude for cardiac regeneration. A previous study accomplished by Quaini et al in 2002 by tracking female transplanted hearts in male recipients using post-mortem fluorescence in situ hybridization revealed 10% Y-chromosome positive myocytes in the transplanted female heart (Quaini et al., 2002). The result showed a low but still evident proliferation rate in human cardiac cells. Interestingly, similar data reported by Bergmann et al in 2009 tracked the integration of carbon-14 into genomic DNA after the Cold War nuclear bomb testing (Bergmann et al., 2009). The study disclosed a 1% turnover rate in human heart annually, suggesting a less than 50% cardiomyocyte replacement within a whole life span. This result was further confirmed by ploidy quantification of cardiomyocyte nuclei through immunostaining of the cardiomyocyte markers cTnnT and cTnnI, as well as pericentriolar material 1 (PCM1) (Bergmann et al., 2011). While other studies have reported much higher rates of cardiomyocyte turnover in the adult human heart (complete turnover of the entire cardiomyocyte compartment up to 15 times in females (or 11 times in males) aged 20 to 100) (Kajstura et al., 2010), these findings are highly controversial (Porrello and Olson, 2010).

The developmental timing of cardiomyocyte turnover in humans is also controversial. A study by Mollova et al studied the cardiomyocyte cell cycle activity in human hearts aged 0-59 years old and showed that myocytes from early developmental stages have high cell proliferation capacity and the number of cardiomyocytes in the left ventricle increased by 3.4 fold within the first 20 years of life (Mollova et al., 2013). However, a recent study by Bergmann et al has reported a detailed characterization of cardiomyocyte proliferation during development (Bergmann et al., 2015). The study has shown that the total number of cardiomyocyte remains stable from 1 month to 73 years of age, suggesting the number of cardiomyocytes is established perinatally and remains unchanged into adulthood (Bergmann et al., 2015), similar to their findings in developing rodent hearts (Alkass et al., 2015). The study suggested that cardiomyocyte turnover rate peaked within the first 10 years of life at ~8% and decreased exponentially into adulthood, remaining less than 1% per annum in adulthood. On the other hand, endothelial cells and mesenchymal cells have a much higher turnover rate throughout adulthood of 15% and 4% per annum, respectively (Bergmann et al., 2015). Currently, the cardiomyocyte proliferation rate and the timing of cell cycle arrest in humans are still debatable. However, all of these studies showed that while the postnatal human heart can be largely considered a post-mitotic organ, it still possesses a limited ability to proliferate into adulthood.

Regeneration It is currently unclear whether humans also possess regenerative capacity during childhood and infancy but several lines of evidence point towards a similar neonatal regenerative window in humans. In 2011, Fratz et al reported a tracing study of 14 patients who underwent corrective cardiac surgery in infancy and the report showed either no scarring (28%) or minimal scaring (57%) in these patients decades after surgery (Fratz et al., 2011). Moreover, Haubner et al recently reported a case study whereby a newborn infant who suffered a severe MI completely recovered cardiac functional after 1.5 months (Haubner et al., 2016). These intriguing clinical observations suggest the neonatal human heart might also possess substantial regenerative capacity.

Together, while the actual cardiac proliferative capability of the adult human heart remains controversial, these studies suggest that cardiac regenerative potential is developmentally regulated in humans. More extensive studies are required to investigate the molecular mechanisms that regulate cardiomyocyte maturation and regenerative capacity in the neonatal period. Such studies are required to identify much needed strategies to promote or re-introduce cardiomyocyte proliferative capability in order to facilitate cardiac regeneration following MI.

1.3. Cardiac development, maturation and arrest

The heart experiences several transitions during postnatal maturation, including increased ventricular pressure, changes in hormonal signalling, alterations in metabolic substrate utilization (from glycolytic to fatty acid oxidation), switches in sarcomeric isoforms, as well as cell cycle arrest (Celine J Vivien, 2016; Girard et al., 1992; Makinde et al., 1998; Uosaki et al., 2015; Yang et al., 2014b) (**Table 1.2**). After fertilization and throughout gestational development, organs experience a hyperplastic period, which is required for growth before parturition in all mammals. Several studies indicated that murine hearts experienced a rapid transition from hyperplasia to hypertrophy shortly after birth (Katzberg et al., 1977; Li et al., 1996; Soonpaa et al., 1996). All studies showed that rodent cardiomyocytes went through a rapid growth phase during embryogenesis and the proliferation of myocytes dropped shortly before birth. Within the first 3 days after birth, myocytes still possess the proliferative ability with the capacity to fully disassemble sarcomeres in dividing cardiomyocytes (Li et al., 1996). However, rodent cardiac muscle cells undergo their last round of DNA synthesis without further cytokinesis, leaving the cells binucleated; a process that begins around 4 days after birth and is completed by 14 days-of-age. The percentage of binucleated cardiomyocytes peaked at 2 weeks postpartum at more than 90% and this level was maintained throughout the life span (Li et al., 1996). This result was subsequently supported by an extensive quantitative experiment where it was shown that the number of cardiomyocytes is established within the first postnatal week. Additionally, two subsequent waves of non-replicative DNA synthesis occur in rodents, which contribute to multinucleation and polyploidisation of cardiomyocytes in the postnatal period (Alkass et al., 2015).

On the other hand, human ventricles are comprised of 74% mononucleated, 25.5% binucleated, and 0.5% multinucleated cardiomyocytes, with no change in these percentages during aging, cardiac hypertrophy or ischemic cardiomyopathy (Bergmann et al., 2015; Mollova et al., 2013; Olivetti et al., 1996) (**Table 1.1**). Moreover, 90% of newborn human cardiomyocytes are diploid but became tetraploid by the time of adulthood with an undetectable cytokinesis rate after 20 years of age (Bergmann et al., 2015; Botting et al., 2012; Mollova et al., 2013). Conversely, the majority of fish, newt and neonatal cardiomyocytes are mononucleated and diploid, which allow the cells to maintain regenerative capacity (Alkass et al., 2015; Matz et al., 1998; Poss, 2007). Thus, it has been suggested that the percentage of mononucleated or binucleated cardiomyocytes could account for species- and developmental stage-specific differences in the ability to re-enter the cell cycle, therefore influencing regenerative capacity (Olivetti et al., 1996; Poss, 2007; Soonpaa et al., 1996).

Currently, the mechanisms that control cardiomyocyte binucleation, polyploidy and the transition from hyperplastic to hypertrophic growth remain very poorly understood. One potential mechanism for the postnatal regulation of cardiomyocyte differentiation involves epigenetic silencing of the neonatal gene expression program, which could alter the cardiomyocyte transcriptome for the lifespan of the animal. The next section will introduce the concept of epigenetics and how it regulates various biological processes through transcriptional regulation.

1.4. Introduction to epigenetics

Every cell contains the genetic blueprint for the production of all transcripts and proteins in an organism. However, transcription and translation need to be exquisitely controlled in order to give a cell its identity and function. The establishment of the cardiac gene program requires the deployment and repression of distinct subsets of genes to facilitate cardiac development and establish a robust steady-state cell identity. Control of gene expression during development is tightly regulated by both TFs and epigenetic modifications. Nucleosomes are the fundamental unit of chromatin and the condensation of nucleosomes occludes access of gene regulatory machineries to genes and distal regulatory regions to control transcription. How this process is executed relies on interplay between three central epigenetic processes: 1) the manipulation of histones and higher order chromatin structures by ATP-dependent chromatin remodelling molecules, 2) post-translational modification (PTM) by covalent labelling of histones or the exchange of canonical histones with histone variants, and 3) direct DNA cytosine methylation. PTMs of histones and DNA methylation are the basis of the so-called “epigenetic code” and to a large extent appear to program cell identity by maintaining open chromatin at cell lineage-specific gene loci and closing chromatin at others (Efroni et al., 2008; Meissner et al., 2008; Zhu et al., 2013).

The adult mammalian heart has an extremely limited capacity for renewal and regeneration. Cardiomyocytes transition from hyperplastic to hypertrophic growth during early postnatal life (Li et al., 1996), and cardiomyocyte proliferation after cardiac injury in the adult is very low (Senyo et al., 2013; Soonpaa and Field, 1997). Comparatively, neonatal hearts are capable of regenerating following cardiac injury (Haubner et al., 2012; Porrello et al., 2011b; Porrello et al., 2013), which is dependent on the proliferative competency of neonatal cardiomyocytes. The loss of this regenerative capacity during early postnatal life coincides with dramatic changes in the transcriptional and epigenetic landscape (Gilsbach et al., 2014; Preissl et al., 2015b). Therefore, epigenetics may have a decisive role in cardiac maturation and the shutdown of cardiac regenerative ability (**Figure 1.4**). The following section outlines the known epigenetic processes governing

cardiac development and maturation, a process that could be harnessed to facilitate regeneration of the adult heart following damage.

1.4.1. Histone tail modification

An expansive catalogue of histone modifications has been identified, including lysine ubiquitination, sumoylation, acetylation and methylation, as well as serine/threonine phosphorylation (Rothbart and Strahl, 2014). These histone modifications can directly affect the state of the surrounding chromatin, and can also serve as binding sites for chromatin remodelling complexes, which can influence gene transcription (please refer to (Rothbart and Strahl, 2014) for a detailed review on this topic). This literature review will focus on methylation and acetylation, as these are the most extensively studied PTMs during cardiac development. Acetyl or methyl groups can be added by histone acetyl transferases (HATs) or histone methyltransferases (HMTs), respectively. These PTMs can also be removed by histone deacetylases (HDACs) and histone demethylases.

Histone acetylation by HATs can lead to relaxed chromatin structure and transcription of genes, as acetylation removes the positive charge on the histones, which decreases the electrostatic attraction between histone proteins and negatively charged DNA (Bannister and Kouzarides, 2011). There are 5 families of HATs (Gillette and Hill, 2015), which form part of larger protein complexes, thus enabling targeting of different enhancers and promoters. Acetylation (Ac) of histone 3, lysine 27 (H3K27) is typically correlated with active enhancers (Rothbart and Strahl, 2014) (**Table 1.3**). On the other hand, HDACs erase acetylation marks on histones, which leads to a more compact heterochromatin structure and decreased gene expression (Bannister and Kouzarides, 2011).

Histone methylation is both positively and negatively correlated with gene transcription and is dependent on the particular lysine that is methylated and the extent of the methylation (mono-, bi- or trimethylation). Some of the most clearly defined methylation sites at gene promoters are H3K4, H3K9 and H3K27 (Li et al., 2007). Trimethylation (me3) of H3K4 (H3K4me3) is correlated with active promoters, whereas many transcriptionally silent promoters are enriched for H3K27me3 and H3K9me3 (**Table 1.3**) (Li et al., 2007). Some histone methylation marks can also delineate enhancer regions (H3K4me1) or actively transcribed gene bodies (H3K36me3) (Chen and Dent, 2014). Some genes can also have a “poised” status where bivalent histone modifications are present. For example, in ESCs (ESCs), the promoters of some lineage-specific TFs are labelled with both active (H3K4me3) and repressive (H3K27me3) marks, which repress their expression, but also poise them for rapid activation upon demethylation of H3K27me3 (Bernstein et al., 2006). However,

this bivalency phenomenon ideally requires single cell analysis to exclude the possibility of artefacts due to heterogeneous cell populations (Hong et al., 2011).

1.4.2. DNA methylation

DNA methylation is one of the most well characterized epigenetic modifications and is involved in multiple gene regulatory functions and developmental processes (Smith and Meissner, 2013). DNA methylation occurs at the fifth position of cytosine of DNA is one of the most mechanistically studied epigenetic regulation and is regulated via DNA methyltransferases (Dnmts). Three major DNMTs are required for DNA methylation, DNMT1, DNMT3A and DNMT3B (Smith and Meissner, 2013). DNMT1 methylates the newly synthesized DNA strand during DNA replication to ensure transfer of methylation marks during cell division (Smith and Meissner, 2013). On the other hand, DNMT3A and DNMT3B operate as the machinery for *de novo* DNA methylation (Smith and Meissner, 2013). The three Dnmts work in concert to dynamically regulate epigenetic processing of the genome.

On the other hand, DNA can also be actively demethylated by the ten-eleven translocation (TET) family of enzymes comprising TET1, TET2 and TET3. These enzymes actively remove DNA methylation marks through progressive oxidation of the methyl group together with thymine DNA glycosylase (TDG) mediated DNA base excision repair mechanisms (Kohli and Zhang, 2013).

In mammalian cells, methylation normally occurs at CpG dinucleotides. However, methylation at non-CpG sites has also been reported in pluripotent stem cells (PSCs) (Ramsahoye et al., 2000), as well as some mouse and human tissues, including brain (Lister et al., 2013). The majority (60-80%) of CpG sites in the mammalian genome are methylated. However, less than 10% of the CpG sites are present in CG rich islands in the promoters of actively transcribed genes (Smith and Meissner, 2013). In these CpG islands (CGIs), promoter methylation is typically associated with silencing of gene transcription (Chen and Dent, 2014). This evolutionarily conserved silencing mechanism is employed during multiple stages of development (Laurent et al., 2010; Lister et al., 2009). Additionally, CpGs in gene bodies can also be methylated and this may play a role in transcription or splicing regulation (Jones, 2012).

1.4.3. ATP-dependent chromatin modifications

In addition to histone and DNA modifications, the epigenetic state is also influenced by ATP-dependent chromatin remodelling complexes. These complexes can be subcategorized into five main families: switch/sucrose non-fermentable (SWI/SNF), imitation SWI (ISWI), chromodomain-

helicase DNA-binding protein, INO80 and α-thalassemia mental retardation syndrome X-linked (ATRX) (Bartholomew, 2014). Interestingly, the number of complexes in each family increases with increasing organismal complexity (Bartholomew, 2014). In more complex mammalian organisms, specific complexes are expressed in a cell-type specific manner and are essential for normal development (Lickert et al., 2004).

1.4.4. TFs

TFs are proteins that typically bind 6-12 nucleotide sites of gene promoters and distal regulatory elements to regulate transcription. In many cases, these 6-12 nucleotide sequences repeat millions of times throughout the genome and exhibit strict spatiotemporal transcriptional control. However, chromatin immunoprecipitation sequencing (ChIP-seq) experiments have revealed two different binding behaviours: 1) widespread, seemingly stochastic, binding of TFs to genomic regions that do not appear to have transcriptional activity, or 2) TFs occupying distinct suites of genes in different cell types (Cao et al., 2010; Pilon et al., 2011). There are four mechanisms that dictate the binding of TFs to DNA: the DNA consensus sequence for TF binding, epigenetics, TF complexes (e.g. co-factors) (Bouveret et al., 2015), and TF PTMs (Filtz et al., 2014). Importantly, even if the required TF complexes and PTMs are present, epigenetics can still dictate which genes are transcribed (Wohrle et al., 2007), as TFs preferentially drive the expression of genes from regions of open chromatin (Beato and Eisfeld, 1997).

Interestingly, not all TFs are limited to euchromatic regions and some “pioneering factors” can bind to DNA and activate transcription irrespective of chromatin state (Zaret and Carroll, 2011). Pioneering TFs coordinate the recruitment of chromatin modifiers and facilitate the relaxation of chromatin (Zaret and Carroll, 2011). Rewiring of the epigenetic landscape by pioneer factors then allows “signal-dependent” TFs to drive tissue specific gene networks, such as the case with the pioneering TF FOXA1 and GATA factors (Carroll et al., 2005; Stefanovic and Christoffels, 2015; Zaret and Carroll, 2011; Zhou et al., 2012). Therefore, some TFs are capable of establishing an epigenetic framework upon which signal-dependent and tissue-specific TFs work upon to consolidate gene expression signatures and program cellular identity.

1.4.5. Non-coding RNAs

One of the greatest surprises of the Human Genome Project was the finding that only 2% of the human genome codes for protein (Carninci et al., 2005; Lander et al., 2001). In recent years, next generation sequencing studies have revealed that up to 75% of the genome is actively transcribed

(Djebali et al., 2012). The majority of non-coding RNAs have unknown biological functions and comprise a number of different classes of RNA, including long non-coding RNAs (lncRNAs) and small non-coding RNAs, such as miRNAs.

LncRNAs are defined as being >200 nucleotides long, can be either polyadenylated or non-polyadenylated, exhibit mostly nuclear expression, and appear to contain functional intramolecular domains (Djebali et al., 2012; Quinn et al., 2014). LncRNA expression is often cell-type specific (Derrien et al., 2012) and their expression concords closely with cardiac developmental and disease states (Yang et al., 2014a). Although the existence of lncRNAs has been recognized since 1991 (Bartolomei et al., 1991), little is known about their functions. Globally, evolutionarily conserved lncRNAs are negatively correlated with protein-coding gene expression and it has been postulated that they largely function to suppress the expression of other lncRNAs and protein-coding genes (Necsulea et al., 2014). For the purposes of epigenetic control, however, one of the more interesting properties of lncRNAs is their ability to act as scaffolds for the chromatin modifying machinery. For example, the lncRNA HOTAIR colocalises with PRC2 components and directs PRC2-mediated transcriptional silencing at the *HOXD* locus (Rinn et al., 2007). In fact, lncRNAs have been shown to interact with not only PRC2 but also ATP-dependent chromatin remodellers (Han et al., 2011), H3K4 HMTs (Grote et al., 2013), and DNMTs (Di Ruscio et al., 2013; Wang et al., 2015).

A specific class of lncRNAs, known as enhancer RNAs (eRNAs), are transcribed from enhancer regions and are thought to denote active enhancers (Arner et al., 2015). Indeed, eRNA transcription may precede and drive H3K4 methylation at enhancer loci, thus establishing *de novo* gene networks (Kaikkonen et al., 2013; Li et al., 2013). A paradigm whereby eRNAs cement tissue-specific enhancer-promoter interactions is supported by the fact that enhancer usage transitions during development (Arner et al., 2015), enhancer usage is highly cell type-specific (Kieffer-Kwon et al., 2013), and eRNAs are involved in enhancer-promoter chromatin interactions (Lai et al., 2013) (**Figure 1.4**).

It is therefore tempting to suggest that scaffolding RNAs could have key roles in not only chromatin organization but also epigenetic patterning, by targeting diverse epigenetic modifiers to specific loci. Hence, lncRNAs are emerging as important regulators of epigenetic processes and are the focus of continuing research.

1.4.6. Nutrition and Metabolism

Many epigenetic regulators require metabolically-derived intermediates to perform their functions (Keating and El-Osta, 2015). Recent studies have shown that folate, vitamin B12, choline and other vitamin B derivatives produce S-adenosylmethionine (SAM, methyl donor in methyltranfer process) and S-adenosylhomocysteine (SAH, product inhibitor of SAM), which are critical for DNA methylation and histone methylation via 1-carbon metabolism to provide the required substrates for epigenetic modifications (Choi and Friso, 2010; Keating and El-Osta, 2015). Moreover, Acetyl-CoA is used as a substrate for HATs, α-ketoglutarate and flavin adenine dinucleotide are TET and histone lysine demethylase (KDM) co-factors, and nicotinamide adenine dinucleotide (NAD) is required for SIRT-dependent histone deacetylation (Keating and El-Osta, 2015). This suggests that nutrition and the metabolism have impact epigenetic modifications. Moreover, in skeletal muscle, satellite cells transition from fatty acid oxidation to glycolysis during activation, leading to decreased NAD+ and reduced SIRT1 deacetylase activity (Ryall et al., 2015). Furthermore, changes in H4K16ac then lead to the regulation of 100s of genes that promote differentiation of satellite cells into skeletal muscle (Ryall et al., 2015). In addition, previous studies have shown that during postnatal switching of cardiac metabolic events, the expression activity of FoxO1 is under the control of the metabolic monitor 5' adenosine monophosphate-activated protein kinase (AMPK), which modulates downstream effectors and leads to postnatal cell cycle shutdown, providing a direct transcriptional regulatory link to cellular metabolism (Evans-Anderson et al., 2008; Sengupta et al., 2013). Collectively, these studies have indicated that epigenetic modifications are intrinsically linked with nutrition and metabolism, which impact transcriptional regulation during various biological processes.

1.5. Epigenetic regulation of cardiac development

1.5.1. Dynamic changes in the epigenome during cardiomyocyte differentiation and maturation

Chromatin landscape Epigenetic marks are established during cardiac development as cells pass through distinct stages (e.g. pluripotency > mesoderm > cardiac progenitors > cardiomyocytes) (Paige et al., 2012; Wamstad et al., 2012). There is a progressive compaction of nucleic material during differentiation of ESCs (Gifford et al., 2013) and also during cardiomyocyte maturation (Sdek et al., 2011). Chromatin compaction and gene silencing are particularly prevalent at pluripotency loci and are coupled with a global shutdown of pluripotency in somatic cells (Gifford

et al., 2013). This intimates a role of chromatin in not only controlling transcriptional output by TFs, but in a wider context, in controlling cellular differentiation and cell-lineage specification.

Global epigenetic modification Epigenetic changes have been associated with many processes during cardiac development. Recent studies by the Bruneau and Murry labs have provided a comprehensive map of changes in the epigenomic landscape during cardiac lineage specification and differentiation (Paige et al., 2012; Wamstad et al., 2012). During cardiomyocyte differentiation, chromatin patterns exhibit distinct modifications in gene sets associated with similar biological functions (Wamstad et al., 2012). This is exemplified by the existence of a distinct chromatin signature around genes related to sarcomere structure, contraction or metabolism, which share a similar expression profile in differentiated cardiomyocytes (Wamstad et al., 2012). Interestingly, there is also evidence for the acquisition of repressive histone marks at the promoters of several cell cycle genes as cardiomyocytes mature from foetal to adult stages (Sdek et al., 2011). These chromatin modification patterns could provide a fine-tuning system to guarantee the coordinated regulation of functionally comparable genes in response to differentiation signals during cardiac development.

DNA methylation patterns also exhibit dynamic signatures during cardiac development and cardiomyocyte maturation. In ESCs, TF binding sites for Oct4 and Nanog are unmethylated, while cardiac TF binding sites for Gata1-4 and Mef2c are methylated (Gilsbach et al., 2014). However, this pattern switches during development as ESC TF binding sites are highly methylated in neonatal and adult cardiomyocytes but, conversely, cardiogenic TF binding sites are demethylated in neonates and adults (Gilsbach et al., 2014). Furthermore, Gilsbach *et al.* reported the transcriptional shut down of several genes encoding foetal isoforms of sarcomeric proteins during differentiation, which was associated with an acquisition of repressive histone marks and DNA methylation from embryonic life to adulthood (Gilsbach et al., 2014). In contrast, genes involved in calcium handling and contraction were demethylated from embryonic to adult stages, which was associated with transcriptional activation of these genes during cardiac development (Gilsbach et al., 2014). While some cell cycle genes are directly methylated during cardiac maturation (Gilsbach et al., 2014), this appears to be an exception, rather than a general rule, as a clear relationship between DNA methylation and cell cycle gene transcription in cardiomyocytes is yet to emerge.

These studies have identified the acquisition of an epigenetic signature during cardiomyocyte maturation, whereby some developmental genes are silenced and others have open chromatin conformations (**Figure 1.5**). There is growing interest in the potential for induction of adult

cardiomyocyte proliferation as a strategy for promoting cardiac regeneration following MI and a recent study suggests that epigenetics plays a key role in this process. Notch stimulation was shown to induce proliferation of neonatal cardiomyocytes, but not adult cardiomyocytes (Felician et al., 2014b). Felician *et al*. demonstrated that the accumulation of repressive histone marks (H3K27me3) and DNA methylation marks at the promoters of Notch-responsive signalling effectors during neonatal development prevented Notch ligands from re-inducing proliferation in adult cardiomyocytes (Felician et al., 2014b). This indicates that adult cardiomyocytes may need to be epigenetically reset for efficient cell cycle re-induction before regeneration can occur (**Figure 1.6**). The following sections will highlight the important functions of epigenetic modifiers during cardiac development with a specific focus on their known roles in cardiomyocyte differentiation, proliferation and maturation.

1.5.2. Histone acetyltransferases and deacetylases are required for cardiomyocyte proliferation

HATs HATs can promote transcription by opening chromatin and loosening DNA-histone interactions. Two of the most well characterized and extensively studied HATs are p300 and CREB binding protein (CBP), which are ubiquitously expressed and cooperate with many different TFs to regulate gene transcription in different cell types. In addition to its role in acetylation of histone tails, p300 also interacts with and directly acetylates critical cardiac TFs, including Mef2, Gata4 and serum response factor (Srf) to enhance DNA binding (Sartorelli et al., 1997; Slepak et al., 2001; Takaya et al., 2008). Genetic knockout of *p300* is embryonically lethal (Shikama et al., 2003) and results in proliferation defects, down-regulation of cardiac structural genes (beta myosin heavy chain (aka myosin heavy chain 7, *βMhc/ Myh7*), α-actinin (*Actn*)) and cardiac structural defects including reduced trabeculation (Yao et al., 1998). Cardiovascular development is also disrupted in knock-in mice harbouring a single AT-deficient allele of *p300* or *Cbp*, which leads to myocardial hypoplasia and is associated with embryonic or neonatal lethality (Shikama et al., 2003). Collectively, these studies suggest that p300/Cbp is required for cardiomyocyte proliferation during heart development. However, the effect of conditional, cardiac-specific deletion of *p300/Cbp* has not been reported and a mechanistic framework for their involvement in cardiomyocyte proliferation is currently lacking.

HDACs HDACs remove acetylation marks and repress transcription through promotion of chromatin condensation. Class I and Class III HDACs are ubiquitously expressed, however, Class II HDACs are enriched in brain, muscle and T cells (Backs and Olson, 2006). HDACs are important for cardiac development and disease. This is highlighted by a number of global and heart-specific

gene knockout studies. Global deletion of *Hdac1* is embryonic lethal at E9.5, whereas *Hdac2* deletion leads to extensive cardiac defects in the perinatal period, including cardiomyocyte hyperplasia and apoptosis (Montgomery et al., 2007). Interestingly, Hdac2 functions with a small homeodomain factor, Hopx, to deacetylate Gata4. Combined deletion of *Hdac2* and *Hopx* leads to hyperacetylation of the Gata4 protein and is associated with a marked increase in cardiomyocyte proliferation, up-regulation of Gata4 targets and perinatal lethality (Trivedi et al., 2010). Notably, cardiac-specific deletion of either *Hdac1* or *Hdac2* alone does not result in an overt phenotype, which is likely due to redundancy. Deletion of both *Hdac1* and *Hdac2* in cardiomyocytes results in neonatal lethality and severe cardiac malfunction, such as cardiac arrhythmias, dilated cardiomyopathy and increased expression of cardiac contractile and calcium handling genes (Montgomery et al., 2007). These observations indicate that HDAC1 and HDAC2 play important roles in cardiac development and cardiomyocyte proliferation. However, it is unclear whether these effects are mediated directly via deacetylation of histone proteins or via deacetylation of non-histone proteins such as the core cardiogenic TF GATA4.

Global ablation of *Hdac3* is embryonic lethal at E9.5 (Montgomery et al., 2008), but cardiac-specific deletion of *Hdac3* generates viable mice. However, cardiac-specific *Hdac3* knockout mice die by 3-4 months of age with severe cardiac hypertrophy and abnormalities in fatty acid oxidation pathways, suggesting an important role for Hdac3 in cardiomyocyte metabolism during postnatal development (Montgomery et al., 2008). Conversely, cardiac-specific overexpression of *Hdac3* leads to ventricular myocardial thickening through excessive cardiomyocyte proliferation (Trivedi et al., 2008), and is associated with inhibition of cyclin dependent kinase inhibitors, such as cyclin dependent kinase inhibitor (*Cdkn*) *1a*, *Cdkn1b*, *Cdkn1c*, *Cdkn2b*, and *Cdkn2c* (Trivedi et al., 2008). Therefore, HDAC3 is required for physiological maturation of cardiomyocytes through its effects on proliferation and metabolism.

Class II HDACs are known to regulate the nuclear localisation of key cardiac TFs, such as Mef2, which is a critical regulator of the cardiac differentiation program and is required for cardiac growth under pathological conditions (Lu et al., 2000; Sartorelli et al., 1997). Notably, double knockout of *Hdac5* and *Hdac9* is perinatally lethal with only ~30% of offspring surviving to adulthood (Chang et al., 2004). Deletion of both *Hdac5* and *Hdac9* causes growth retardation, thin-walled myocardium and severe ventricular septal defects (Chang et al., 2004). In contrast, cardiac-specific deletion of *Hdac5* or *Hdac9* causes cardiac hypertrophy through derepression of Mef2 targets and induction of the foetal hypertrophic gene program (Chang et al., 2004; Zhang et al., 2002). While it is clear that Class II HDACs play an important role in regulating the transcriptional response of the

adult heart to cardiac stress, specific functions for Class II HDACs in cardiomyocyte proliferation have not been described.

Class III HDACs comprise members of the Sirt family (SIRT1-7). SIRT1 (Cheng et al., 2003), 3 (Koentges et al., 2015; Sundaresan et al., 2009), 6 (Sundaresan et al., 2012) and 7 (Vakhrusheva et al., 2008) are crucial for cardiac development and the response of the adult heart to cardiac stress. However, no specific role of Class III HDACs has been reported with respect to cardiac proliferation or regeneration.

In summary, these results suggest that histone acetyltransferases and deacetylases play a critical role during heart development. Several HAT and HDAC mutant mice have defects in cardiomyocyte proliferation, which implies a key role for histone acetylation in the regulation of the cardiac cell cycle. However, HATs and HDACs can modify the acetylation status of both histone and non-histone proteins, including key cardiogenic TFs, and our understanding of the mechanistic link between histone acetylation and cardiomyocyte proliferation is very limited. Few studies have evaluated the genome-wide effects of HAT or HDAC deletion on the cardiac epigenome and this remains an important goal for future research.

1.5.3. Histone methyltransferases are required for cardiomyocyte proliferation

Ezh2 SET domain-containing methyltransferases are the most studied lysine methyltransferase family in the heart. EZH2 is a SET domain-containing H3K27-specific methyltransferase and a subunit of the PRC2 complex. Cardiac-specific knockout of *Ezh2* under control of the *Nkx2.5* promoter causes lethal congenital heart malformations associated with impaired cardiomyocyte proliferation and derepression of Ezh2 targets, including several TFs or genes that are essential for cardiac organogenesis (e.g. *Pax6, Isl1, Six1* and *Bmp10* (Cassano et al., 2012)) and up-regulation of the cell cycle inhibitor *Cdkn2a* and *Cdkn2b* (Cassano et al., 2012; Chen et al., 2012). In contrast, conditional deletion of *Ezh2* in anterior heart field progenitor cells does not disrupt cardiac specification and development but rather induces cardiomyocyte hypertrophy. Interestingly, these effects appear to be dependent on Six1, a cardiac progenitor cell TF that is developmentally shut down in differentiated myocytes (Delgado-Olguin et al., 2012). Six1 is normally repressed by Ezh2, which functions to stabilize cardiac gene expression upon differentiation and to maintain postnatal cardiac homeostasis (Delgado-Olguin et al., 2012; Stergachis et al., 2013). However, deletion of *Ezh2* in differentiated cardiomyocytes does not cause any overt phenotype, which could be due to functional redundancy with Ezh1 at later stages of development (Cassano et al., 2012). Lysine

methyltransferase 2D (KMT2D) has also been shown recently to regulate cell cycle activity during cardiac development through H3K4 dimethylation (Ang et al., 2016).

SMYD1 Another important member of the SET domain-containing methyltransferase family is SET and MYND domain containing 1 (SMYD1). Early studies of SMYD1 suggested that it was critical for cardiac differentiation and development. Homozygous *Smyd1* knockout mice are embryonic lethal at E10.5 and present with severe ventricular hypoplasia and defects in right ventricular formation and trabeculation, associated with transcriptional repression of right ventricular-specific TFs, including Hand2 (Gottlieb et al., 2002). Conditional deletion of *Smyd1* using the *Nkx2.5*-Cre driver resulted in defective expansion of second heart field progenitors and reduced cardiomyocyte proliferation (Rasmussen et al., 2015). *Smyd1* morpholino knockdown in zebrafish embryos also disrupted myofiber maturation (Tan et al., 2006), further suggesting SMYD1 is essential for cardiac muscle maturation.

Dot1l The disruptor of telomeric silencing-1 (DOT1L), an H3K79-specific methyltransferase, is the most extensively studied candidate of the non-SET domain containing methyltransferase family during cardiac development. Global ablation of *Dot1l* causes growth retardation, cardiac dilation and lethality between E9.5 to E10.5 (Jones et al., 2008). ESCs developed from *Dot1l*-deficient mice display abnormalities in ploidy, telomere elongation and reduced cell proliferation (Jones et al., 2008). *Dot1l*-deficient ESCs also exhibit aberrant chromatin structure characterized by a reduction in H3K79 methylation suggesting Dot1l has an essential role in guiding chromatin condensation during embryonic development (Jones et al., 2008). Cardiac-specific ablation of *Dot1l* results in viable offspring. However, these mice develop cardiac hypertrophy at 6 months of age, associated with an increase in the total percentage of proliferating cells in the heart, although specific quantification of cardiomyocyte proliferation was not performed (Nguyen et al., 2011). Dot1l also regulates cardiac structural proteins through transcriptional regulation of its downstream target Dystrophin (Dmd), which could also contribute to the cardiac functional abnormalities observed in this model (Nguyen et al., 2011).

Jumonji (Jmj) The members of the Jmj C family are some of the most well characterized KDMs during development. Homozygous knockout of *Jmj*, which demethylates H3K9me2 or H3K27me2, is embryonic lethal around E11.5 with growth retardation and cardiac defects, including hyperplasia of trabecular cardiomyocytes (Takeuchi et al., 1999). The repressive effects of Jmj on cardiomyocyte proliferation involve direct repression of *Ccnd1* (Toyoda et al., 2003) and potentiation of the repressive effects of Rb function on E2F activity and cell cycle genes (Jung et al.,

2005). However, it is unclear whether conditional deletion of *Jmj* in the adult heart is sufficient to drive cardiomyocyte cell cycle re-entry.

Ubiquitously transcribed tetratricopeptide repeat, X chromosome (Utx) The UTX and Jmj domain-containing protein 3 (JMJD3) enzymes are KDMs that specifically target H3K27me3 (Hong et al., 2007). Studies have shown that Utx histone demethylase function is directed by core cardiac specific TFs, such as Nkx2.5, Gata4 and Tbx5, to the enhancer regions of cardiac genes, which leads to the transcriptional activation of their target genes during cardiac differentiation (Lee et al., 2012). Moreover, *Utx* deletion results in failure of ESCs to differentiate into the cardiac lineage (Lee et al., 2012; Welstead et al., 2012). Similarly, *Jmjd3* knockout ESCs fail to differentiate into mesoderm and cardiac lineages (Ohtani et al., 2013). Global genetic deletion of *Utx* results in embryonic lethality by E13.5 with developmental abnormalities in cardiac chamber formation (Lee et al., 2012; Welstead et al., 2012). *Jmjd3* homozygous knockout mice die before E6.5 (Ohtani et al., 2013). Taken together, these studies support an important role for UTX/JMJD3 (and, by inference, H3K27me3) in cardiac differentiation but further studies are required to specifically dissect the role of these enzymes in the regulation of cardiac lineage decisions.

1.5.4. DNA methylation in cardiac development and diseases

Cardiac development Some of the very first genetic studies of DNA methylation in mammals showed that genetic deletion of *Dnmt1* in the mouse germ line causes embryonic lethality associated with cardiac developmental defects, including ventricular hypoplasia (Li et al., 1992). However, despite these early observations, there is a paucity of studies on DNMT1 during cardiac development and specific functions for maintenance methylation in the cardiac lineage remain largely unexplored. In contrast, global deletion of either *Dnmt3a* or *Dnmt3b* has demonstrated critical roles for these enzymes during mammalian development, but cardiac development does not appear to be overtly impacted in these animals (Okano et al., 1999). Interestingly, a recent study exhibited that Dnmt3a but not Dnmt3b is essential for the maintenance of cardiac sarcomeric structure and contractile function in an *in vitro* foetal cardiomyocyte culture system (Fang et al., 2016). While a recent study identified an important role for Dnmt3b in cardiac valve formation during embryogenesis (Chamberlain et al., 2014), another study has demonstrated that Dnmt3a/3b are dispensable for postnatal cardiomyocyte function (Nuhrenberg et al., 2015). Cardiac-specific double deletion of *Dnmt3a/b* in cardiomyocytes, in this case driven by the atrial myosin light chain (*Mlc2a*) promoter, does not result in an overt cardiac phenotype under basal conditions or in response to cardiac stress (pressure overload) (Nuhrenberg et al., 2015), despite changes in cardiac

gene expression (Gilsbach et al., 2014). Further studies are required to assess the impact of DNMT3 on other aspects of cardiac physiology and pathology but these findings suggest that *de novo* methylation is not required for maintenance of adult cardiac function.

The lack of an evident cardiac phenotype in *Dnmt3a/3b* null mice (Nuhrenberg et al., 2015) is surprising given several recent reports of dynamic changes in the cardiac methylome during development and disease (Gilsbach et al., 2014). A recent genome-wide study has identified widespread alterations in cardiac DNA methylation patterns during the transition from foetal to adult stages. In isolated neonatal cardiomyocytes, several cardiac-specific TF binding motifs, such as Gata1-4 and Mef2c, were enriched in hypomethylated regions of the genome (Gilsbach et al., 2014). Moreover, as cardiomyocytes mature and establish the adult gene program, several cardiac genes, including those involved in calcium handling (*Atp2a2*) and contraction (*Myh6*, cardiac type troponin T2 (*Tnnt2*), cardiac type troponin I3 (*Tnni3*)), become demethylated and acquire active histone marks (H3K27ac, H3K4me3 and H3K4me1) (Gilsbach et al., 2014). Interestingly, the foetal cardiac gene program (e.g. slow skeletal type troponin I1 (*Tnni1*)) is down-regulated in adult cardiomyocytes and this transition is accompanied by increased methylation and the acquisition of repressive histone marks (H3K27me3) (Gilsbach et al., 2014). This result is supported by the transcriptome and methylome profiling data of adult cardiomyocytes derived from CPCs (Zhang et al., 2015). The study suggested that following dedifferentiation of the adult cardiomyocyte, those cells displayed an increase expression level accompanied with decrease DNA methylation in cell cycle and proliferation related genes whereas cardiomyocyte structural and functional genes obtained DNA methylation marks and decrease in their expression status (Zhang et al., 2015). Therefore, DNA methylation undergoes dynamic changes during heart development and this is associated with the establishment of the adult gene program during cardiomyocyte maturation.

Cardiac diseases The changes of DNA methylation level and its mechanism during the initiation and progression of heart disease remains largely unknown. A recent clinical research showed that the global DNA methylation level of peripheral blood leukocytes is positively correlated with CVDs (MI and stroke) (Kim et al., 2010). Moreover, Udali et al recently showed that the DNA methylation levels of several genes, such as *ESR1, ESR2, ALOX15, HSD11B2, NKCC1* and *THBS1*, is correlated with atherosclerosis, hypertension and stroke (Udali et al., 2013). Furthermore, DNA hypomethylation caused by Mthfr (related to methyl donor generation) deficiency in the mouse promoted aortic fatty streak formation (Baccarelli et al., 2010). The study has reported that DNA methylation level was decreased in the heart of the atherosclerosis-prone

gene ApoE knockout mouse, as well as in a model of aorta neointimal thickening in the New Zealand white rabbit (Baccarelli et al., 2010).

In terms of cardiomyopathy, Movassagh et al has demonstrated that dynamic changes in DNA methylation levels is correlated with differential expression of at least 3 angiogenesis-related genes in cardiomyopathy patients (Movassagh et al., 2010). A subsequent study reported by the same group showed similar results with their previous study with a further *in vitro* experiment (Movassagh et al., 2011). The study has shown that siRNA knockdown of *Dux1*, a molecule that was up-regulated after cells were treated with the DNA methylation inhibitor (RG108), led to a reduction in cell viability *in vitro,* suggesting a potential regulation of cell viability through methylation of Dux1 (Movassagh et al., 2011). Moreover, profiling of left ventricular DNA methylation level of the repeat elements in human heart failure also demonstrated a significant decrease of the DNA methylation level of satellite repeat elements associated with increase of transcription in end-stage cardiomyopathy patients (Haider et al., 2012). Furthermore, differential DNA methylation changes were observed in some heart disease-related signalling pathway molecules and identified several novel genes in dilated cardiomyopathy patients (Haas et al., 2013). *In vivo* morpholino inhibition of these novel genes (adenosine A2a receptor (Adora2a) and lymphocyte antigen 75 (Ly75)) in zebrafish impaired cardiac contractility and caused heart failure, respectively (Haas et al., 2013), suggesting the change in methylation during disease targeted cardiac contractile event.

Demethylating agent 5-azacytidine (5aza) 2 hypomethylating agents, 5aza (commercial name – Vidaza) and its derivative 5aza-dC (commercial name – Decitabine or Dacogen) are clinically approved drugs for myelodysplastic syndromes and acute myeloid leukaemia. It effectively prevents DNA methylation by incorporating into DNA (Vidaza and Dacogen) or RNA (Vidaza) as the analogue of cytidine that could not be methylated (Christman, 2002). A previous study reported that 5aza-dC rescued the hypertrophic and heart failure phenotype induced by norepinephrine (Xiao et al., 2014). This result is subsequently supported by a recent study where spontaneous hypertensive rat treated with 5aza showed ameliorated effects in cardiac fibrosis and hypertrophy. Moreover, a recent study reported that the 5aza protected cardiac function (ejection fraction, contractility and relaxation indices) and attenuation of cardiac fibrosis following MI in the rats (Kim et al., 2014), via the shifting of pro-inflammatory to anti-inflammatory macrophage phenotype through regulates the sumoylation of interferon regulatory factor-1(Jeong et al., 2015; Kim et al., 2014). This suggests that DNA methylation plays a role in regulating cardiac fibrosis and hypertrophy and this effect is reversible.

Collectively, these results have displayed the deep relationship between DNA methylation and normal cardiac development as well as cardiac diseases progression. It is important for future study to tear apart the mechanism of DNA methylation in regulating cardiac development and diseases.

1.6. Hypothesis and Aims

What we know One critical concept that can be derived from the current literature review is that mammalian cardiomyocytes lose their proliferative and regenerative capacity during postnatal development. Many pro-proliferative factors that induce myocyte division during early developmental stages fail to induce adult cardiomyocyte cell cycle re-entry to the same extent. This phenomenon might be due to the existence of epigenetic roadblocks that are progressively acquired during postnatal development, especially at genomic regions involved in regulating the transcription of genes required for cardiomyocyte proliferation. Understanding this epigenetic regulation would bring important insight to the cardiac maturation mechanism.

What we do not know As one of the most important and stable epigenetic marks, DNA methylation has emerged as a powerful regulator of developmental processes but its role in postnatal cardiomyocyte maturation remains elusive. Moreover, a broader conceptual framework for understanding how the chromatin landscape shapes cardiac development and, in particular, myocyte maturation is lacking.

Hypothesis The central hypothesis underpinning this PhD thesis is that postnatal alterations in DNA methylation and the chromatin landscape establish the mature cardiomyocyte transcriptional program associated with loss of proliferative capacity.

Aims: To test the hypothesis, this PhD Thesis focuses on characterizing the role of DNA methylation and chromatin dynamics during postnatal cardiac development and maturation using *in vitro* and *in vivo* model systems (**Figure 1.7**):

Aim 1: To characterize DNA methylation dynamics and its functional role during postnatal cardiac maturation (Chapter 3).

Aim 2: To determine the role of DNA methylation in regulating the expression of cell cycle related genes in mouse and human cardiomyocytes (Chapter 4).

Aim 3: To understand the relationship between chromatin accessibility and transcription during mouse and human cardiomyocyte development (Chapter 5).

To address the abovementioned aims, a number of classic molecular biology techniques, as well as contemporary next-generation sequencing approaches have been employed. These molecular

techniques, as well as the animal models and *in vitro* culture systems they are applied to, are described in detail in the following General Methods chapter (Chapter 2).

Table 1.1. Comparison of vertebrate models of cardiac development and regeneration.

	Newt	Zebrafish	Mouse	Human
Heart rate (beats/minute)	30	120	300-600	60-90
Chamber	3 (2 atria 1 ventricle)	2 (1 atrium 1 ventricle)	4 (2 atria 2 ventricles)	4 (2 atria 2 ventricles)
Circulation	Double	Single	Double	Double
T-tubule system	-	-	Yes	Yes
Ploidy	Diploid	Diploid	Diploid	Tetraploid or higher
Nuclear of cardiomyocytes	Mononucleated	Mononucleated	Binucleated (1 week after birth)	Mononucleated
Withdraw from cell cycle	-	-	1 week after birth	Few months after birth
Regeneration ability after injured	Yes, throughout whole life (resection)	Yes, throughout whole life (resection/ cryoinjury/ genetic ablation)	Yes, within 1st week after birth (resection/ MI/ genetic ablation/ cryoinjury)	1 case of newborn after MI

Table 1.2. Changes of various cardiomyocyte properties during maturation (Shintani et al., 2014; Yang et al., 2014b).

		Foetal/ neonatal cardiomyocyte	Adult cardiomyocyte
Morphology, structural properties	Morphology	Circular shape	Rod shape
	Size	Size increase for 30 to 40 fold during maturation	
	Contractile apparatus (sarcomere)	Longer and more organized sarcomeric structure towards maturation	
		~1.95 μm	~2.2 μm
	Myofibrillar isoform	Titan N2BA, 3200-3700 kDa	Titan N2B, 3000 kDa
		Slow skeletal type troponin I1 (TNNI1)	Cardiac type troponin I3 (TNNI3)
		αMHC/ MYH6 (human)	βMHC/ MYH7 (human)
		βMHC/ MYH7 (mouse)	αMHC/ MYH6 (mouse)
	Transverse tubules	Lack in foetal, start to appear from P6-9	Symbol of maturation
	Mitochondria	Scatter distribution in cytoplasmic	Distribute in cytoplasm in

		reticular network	crystal-like lattice pattern
		Small fraction of the myocyte volume.	20-40% of myocyte volume
		No distribution of lamellar cristae in the inner membrane	Regular distribution of mature lamellar cristae in the inner membrane
	Metabolic substrate	Glycolysis (80%)	Fatty acid β-oxidation (80%)
	Connexin 43 (gap junction protein) and N-cadherin (adherens junction protein)	Circumferentially distribution	Focus on intercalated disks (at the ends of the cells)
Electrophysiology properties	Resting membrane potential	> -90 mV	~−90 mV
	Force	~nN/ cell	~μN/ cell
		unknown (human)	44 ±11.7 mN/mm2 (human)
		0.4 to 0.8 mN/mm2 (rat)	56.4 ±4.4 mN/mm2 (rat)
	Conduction velocity	unknown (human)	0.3 to 1.0 m/s (human)

		0.33 m/s (canine)	0.50 m/s (canine)
	Membrane capacitance	17.5 ±7.6 pF	~150 pF
	Upstroke velocity	~50 V/s	~250 V/s

Table 1.3. Distinct epigenetic signatures at promoter and enhancer regions.

Epigenetic signature	Active	Repressive
Promoter	H3K4me3	5mC DNA H3K9me3 H3K27me3
Enhancer	H3K27ac H3K4me1	H3K27me3

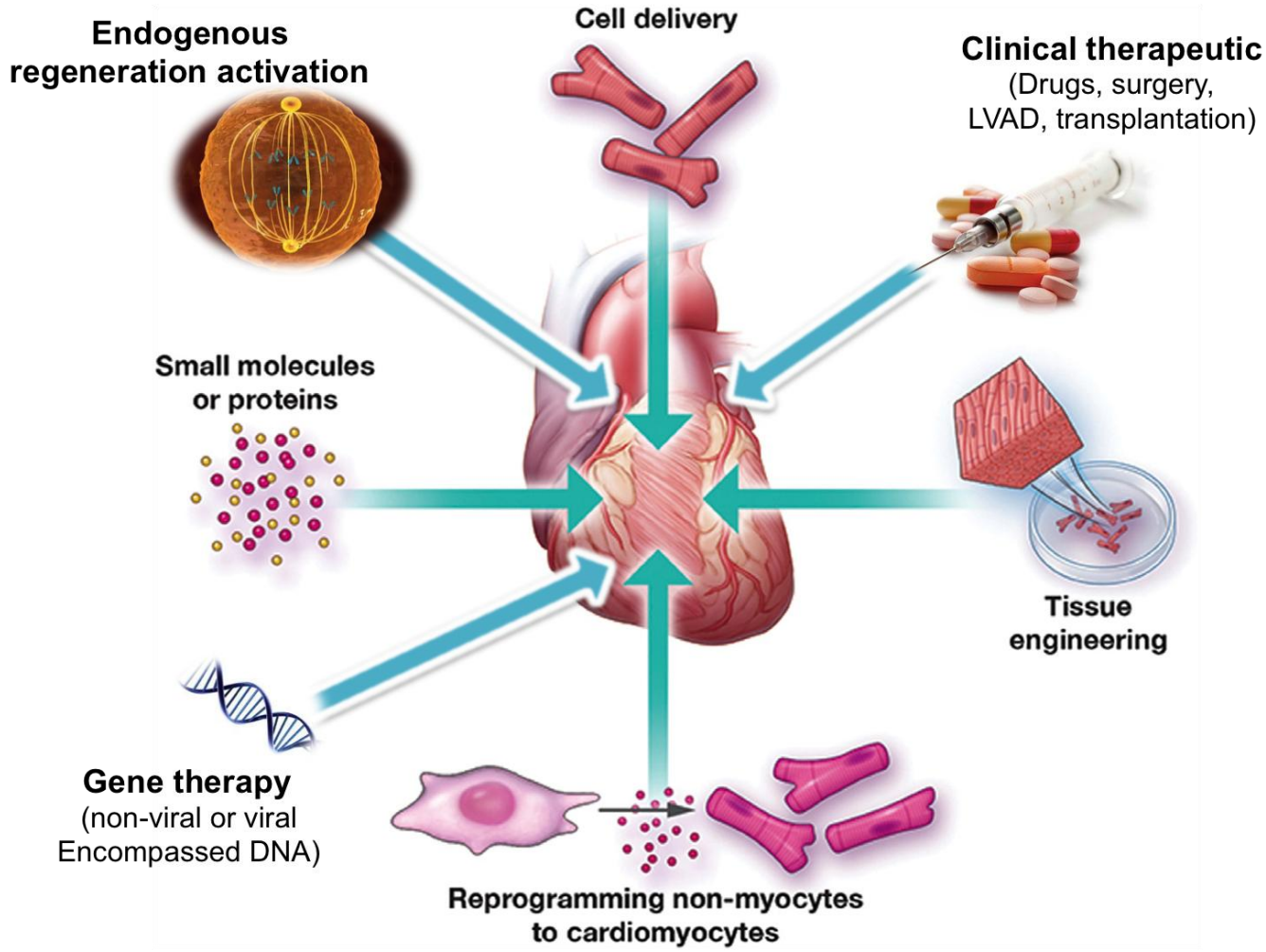

Figure 1.1. Schematic of current therapeutic approaches and research interests for cardiac pathologies (Adapted and modified from (Garbern and Lee, 2013)).

Current clinical therapeutic approaches for cardiac patients include medications, surgeries, medical assistant device and heart transplantation. Current research focuses for heart injury includes gene therapies, cell therapies, direct reprogramming of cardiomyocyte, delivery of engineered heart tissue as well as the activation of endogenous cardiomyocyte regeneration.

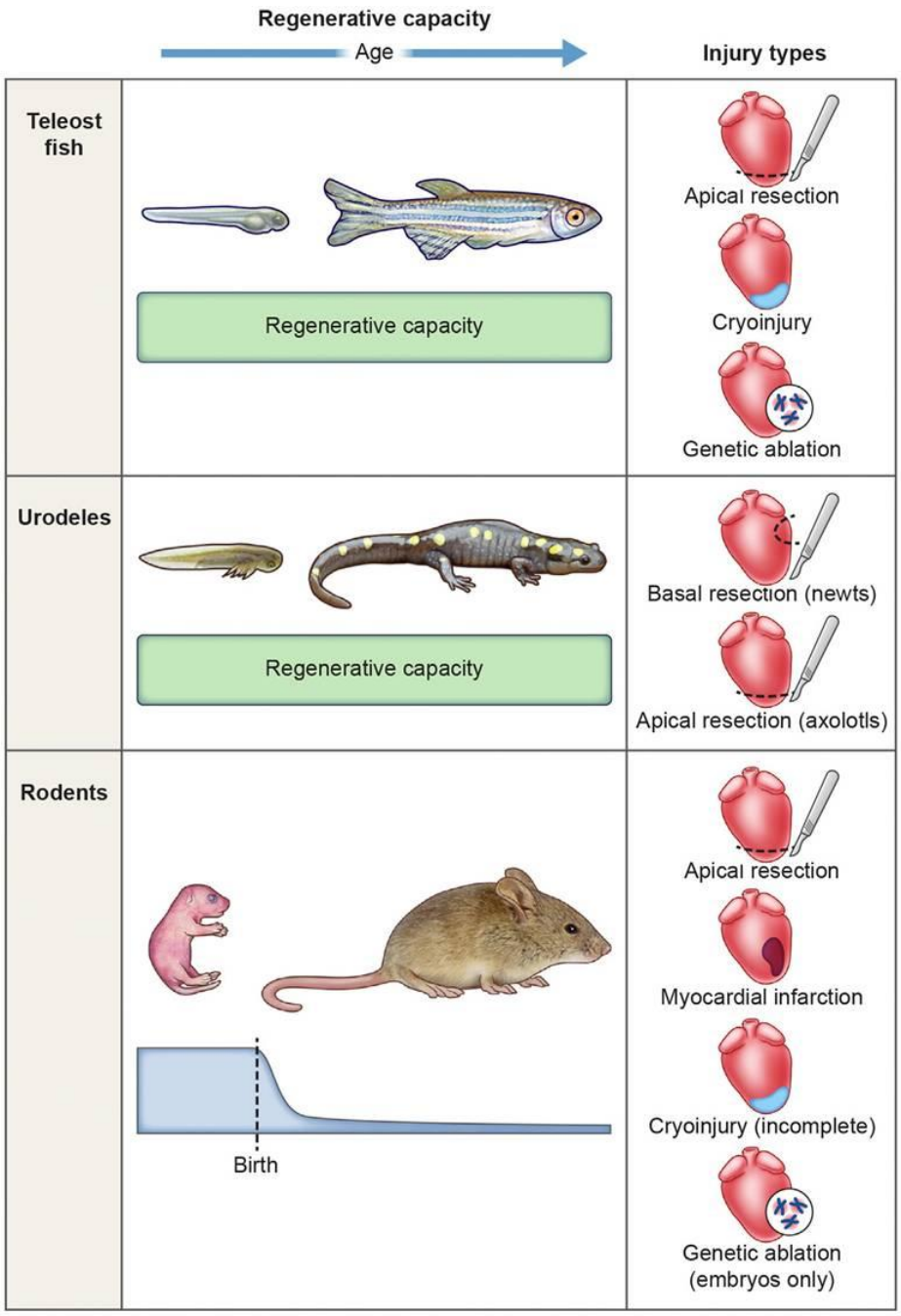

Figure 1.2. Schematic of current research models for cardiac regeneration in different species (Adapted and modified from **(Uygur and Lee, 2016)**).

The figure illustrated different tactics to induce cardiac injury including apical resection, basal resection, cryoinjury, genetic ablation and MI in teleost, amphibian and mammals (Uygur and Lee, 2016).

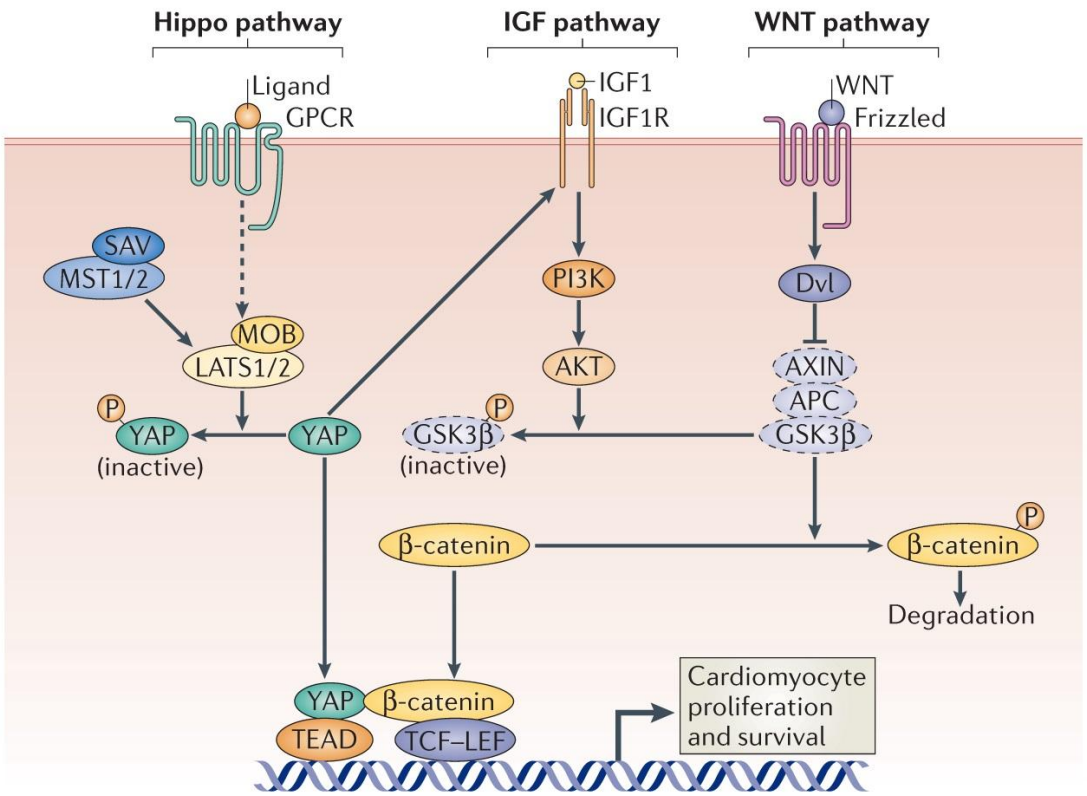

Figure 1.3. Signalling pathways involved in cardiac proliferation.

The IGF and WNT pathways activate cardiomyocyte proliferation and survival through regulating GSK3β, while the Hippo pathway inhibits cardiomyocyte proliferation via phosphorylation of the effecter protein YAP (Xin et al., 2013b).

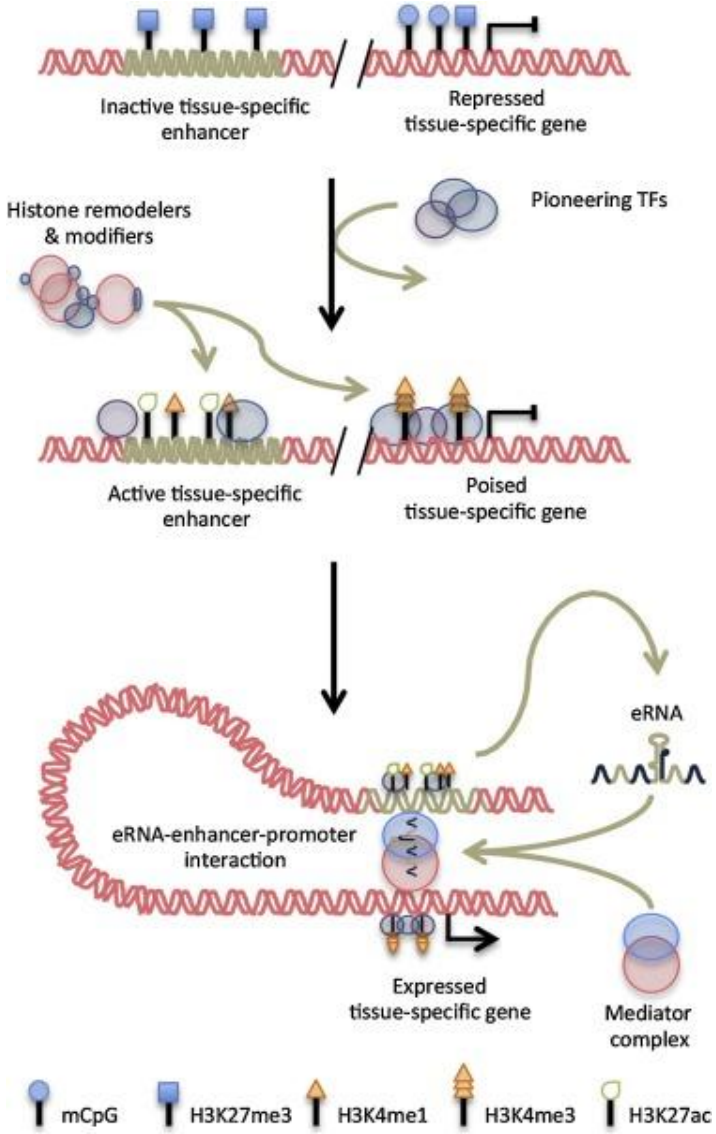

Figure 1.4. Epigenetic control of a tissue-specific gene.

Inactive enhancers and promoters are marked with inhibitory histone marks and DNA methylation. Pioneering TFs are able to bind regions of heterochromatin and initiate remodelling of the epigenetic architecture surrounding tissue-specific gene loci. Evidence also suggests that eRNAs may be expressed before the acquisition of epigenetic changes and may complex with a component of the transcription initiation complex called mediator to establish nascent enhancer-promoter transcription complexes (Kaikkonen et al., 2013; Lai et al., 2013). In this way, pioneering TFs are capable of re-awakening dormant cell-type specific enhancers to initiate cell-type specific gene expression.

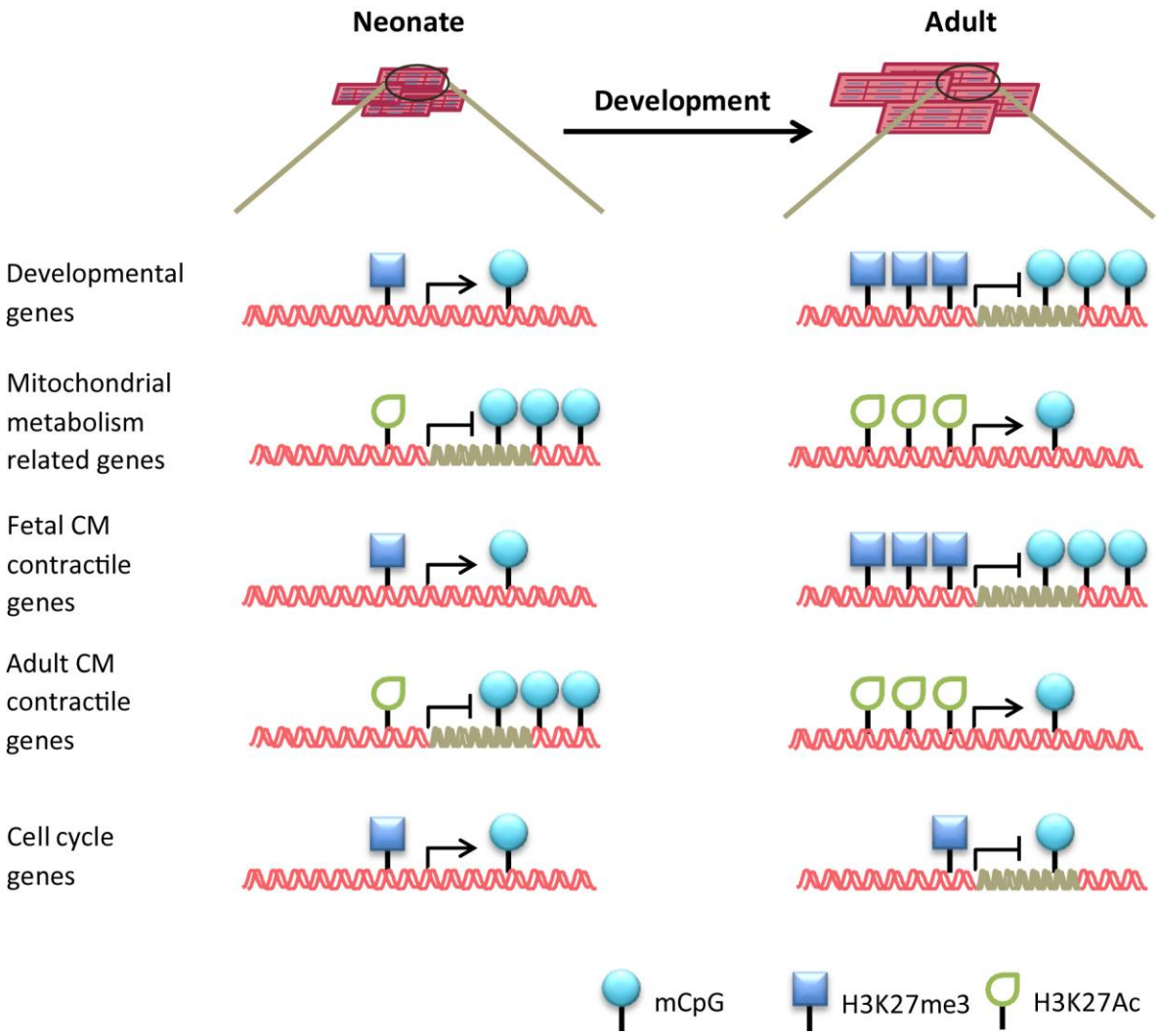

Figure 1.5. Epigenetic landscape during cardiac development and maturation.

During maturation, functionally similar gene sets are correlated with similar epigenetic marks. Developmental genes and foetal contractile genes decrease in expression level and are associated with methylation and acquisition of the repressive histone mark (H3K27me3). In contrast, mitochondrial and metabolism-related genes, as well as adult contractile genes, increase in expression and acquire active histone marks (H3K27ac) and lose gene body methylation during maturation. Cell cycle genes decrease in expression level during maturation without consistent changes in DNA methylation or the repressive histone mark (H3K27me3) (Gilsbach et al., 2014; Sim et al., 2015). It should be noted that transcription of particular genes in both foetal and adult cardiomyocytes is highly correlated with H3K4me3, H3K4me1 and H3K27ac.

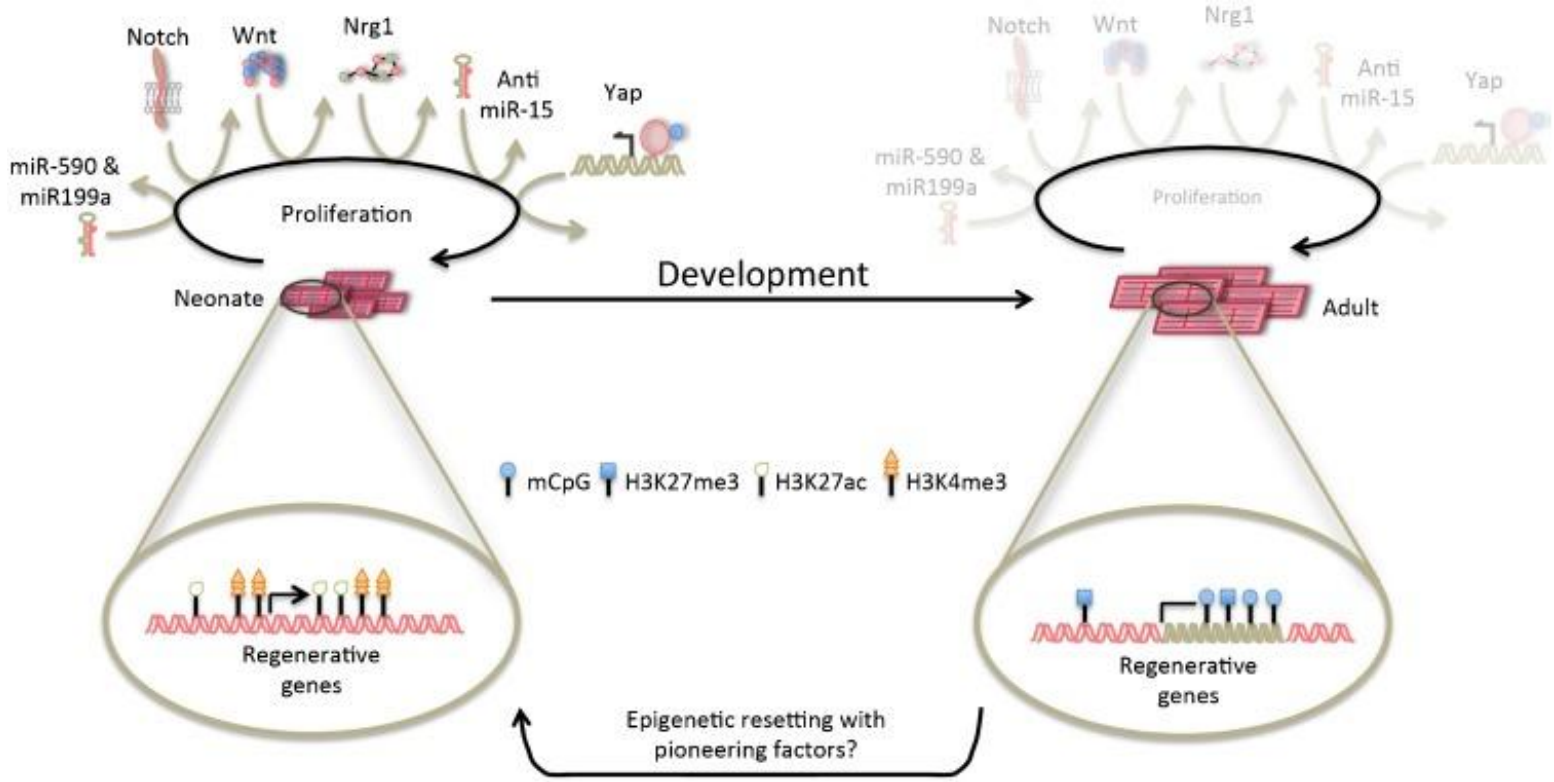

Figure 1.6. Postnatal cardiomyocyte epigenetic changes may prevent efficient cardiomyocyte cell cycle re-induction by pro-proliferative factors.

Many pro-proliferative factors such as Notch, Wnt1, NGR, YAP, miR-15 inhibition, miR-590 and miR-199a (Porrello and Olson, 2014a), potently increase neonatal cardiomyocyte proliferation but do not induce adult cardiomyocyte proliferation to the same extent. Some of the gene targets of these pro-proliferative factors may be epigenetically blocked in adult cardiomyocytes. Hence, resetting of adult epigenetic signatures to a neonatal-like state may allow re-expression of these target genes and efficient adult cardiomyocyte proliferation (Gilsbach et al., 2014).

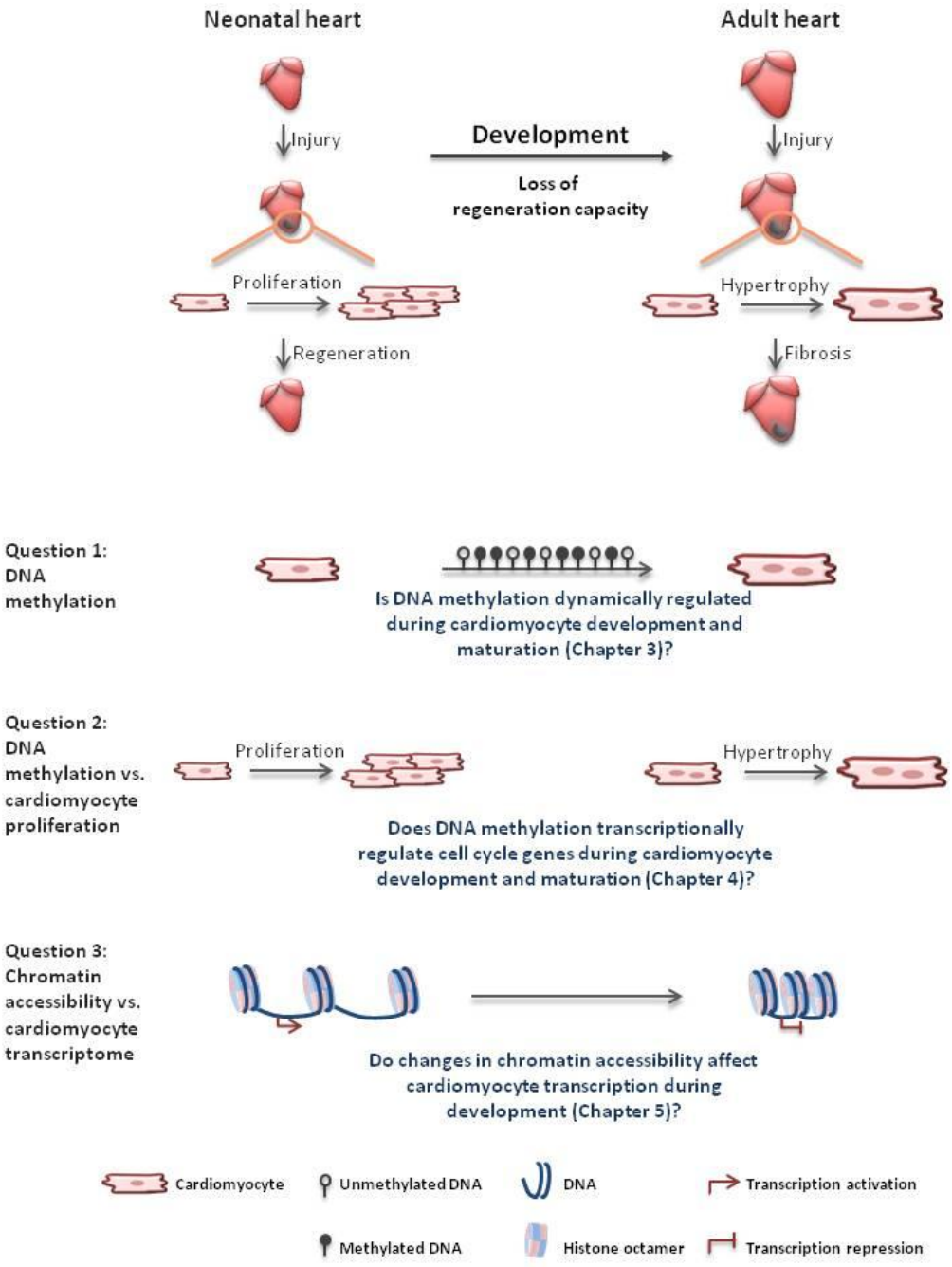

Figure 1.7. Summary of the 3 aims of this PhD Thesis in current research models.

Cardiomyocytes lose their proliferative and regenerative capacity following injury during development but the molecular mechanisms remain unclear. The current PhD Thesis is designed to investigate the 3 following questions in order to understand the developmental changes that happen during cardiomyocyte development. Question 1. Is DNA methylation dynamically regulated during cardiomyocyte development and maturation (Chapter 3)? Question 2. Does DNA methylation transcriptionally regulate cell cycle genes during cardiomyocyte development and maturation (Chapter 4)? Question 3. Do changes in chromatin accessibility affect cardiomyocyte transcription during development (Chapter 5)?

Chapter 2

General Methods

Science walks forward on two feet,

Namely theory and experiment.

But continuous progress is only made by the use of both.

Robert A. Millikan.

Chapter 2. General Methods

2.1. Experimental animals and tissue collection

All protocols were approved by The University of Queensland Animal Ethics Committees (SBMS/342/13/NHMRC and SBMS/245/13/NHMRC).

In Chapters 3 and 4, male C57BL/6 mice (The Jackson Laboratory, Bar Harbor, ME, USA) were used for global DNA methylation profiling and mRNA expression profiling during postnatal development (P1 to P84), as well as for RNA-seq and MBD-seq (P1 and P14). ICR/CD-1 mice (Charles River Laboratories, Wilmington, MA, USA) were used for neonatal 5aza-dC studies (described in Chapter 3). For DNA and RNA analysis, atrial tissues were removed from ventricles (septum intact) and ventricles were blotted and weighed before snap freezing in liquid nitrogen for storage at -80°C prior to processing.

In Chapter 5, ICR/CD-1 mice were used for the isolation of PCM1 (+) cardiomyocyte nuclei (P1, P14 and P56). Atrial tissues were removed from ventricles (septum intact) and ventricles were blotted before snap freezing in liquid nitrogen for storage at -80°C prior to processing.

2.2. DNA extraction and global analysis of DNA methylation

DNA was isolated from C57BL/6 mouse cardiac ventricles using the DNeasy Blood & Tissue Kit (Qiagen, Venlo, Limburg, Netherlands) according to the manufacturer's instructions. Briefly, 25 mg tissue was cut into ~1 mm^3/piece, placed in a 1.5 mL microcentrifuge tube and combined with 190 µL Buffer ATL. 20 µL proteinase K was added to the mixture and mixed thoroughly by vortexing. The solution was then incubated at 56 ℃ overnight in a thermomixer and combined with 4 µL of 100 mg/mL RNase A the next day. The mixture was mixed by vortexing, followed by 2 minutes incubation at room temperature. The mixture was then vortexed for 15 seconds, followed by adding 400 µL Buffer AL-ethanol (Buffer AL and 100 % ethanol are premixed in 1 volume: 1 volume ratio), and mixed thoroughly by vortexing. The mixture was then transferred into the DNeasy Mini spin column placed in a 2 mL collection tube, followed by centrifugation at 6000 x g on Microfuge 16 bench top centrifuge (Beckman Coulter, Brea, CA, USA) for 1 minute. Subsequently, the DNeasy Mini spin column was washed with 500 µL Buffer AW1, followed by centrifugation for 1 min at 6000 x g. The DNeasy Mini spin column was then washed with 500 µL Buffer AW2,

followed by centrifugation for 3 minutes at maximum speed of Microfuge 16 bench top centrifuge to dry the DNeasy membrane. For elution, 100 µL of nuclease-free water was added to the DNeasy Mini spin column, incubated at room temperature for 1 minute and then centrifuged at 6000 x g for 1 minute.

For analysis of global DNA methylation, 5-methylcytosine (5-mC) levels were measured in DNA samples (100 ng per sample) using the MethylFlash Methylated DNA Quantification Kit (Colorimetric) (Epigentek, Farmingdale, NY, USA), strictly complying with the manufacturer's instructions (detail referred to Epigentek handbook #P-1036). In this assay, DNA is bound to strip wells that are specifically treated to have a high DNA affinity. The fraction of methylated to unmethylated DNA is then quantified through an ELISA-like reaction by reading the absorbance in a microplate spectrophotometer at 450 nm.

2.3. RNA extraction, cDNA synthesis and real-time quantitative PCR (qPCR)

In Chapters 3 and 4, total RNA was extracted from mouse cardiac ventricles using TRIzol (Thermo Fisher Scientific (Ambion), Waltham, MA, USA) according to the manufacturer's recommended protocol. Briefly, up to 20 mg heart tissue was lysed in 1 mL TRIzol solution, followed by homogenization on ice until no tissue chunks were visible. The mixture was then placed at room temperature for 5 minutes and then combined with 0.2 mL of chloroform. The mixture was subsequently vortexed for 15 seconds and rested at room temperature for 3 minutes, followed by centrifugation at 4°C at maximum speed of Microfuge 16 bench top centrifuge for 15 minutes. The aqueous phase was moved carefully by using a 200 µL pipette tip to transfer the solution to a new 1.5 mL microcentrifuge tube. The aqueous phase solution was then combined with 0.5 mL of 100% isopropanol, mixed thoroughly and rested at room temperature for 10 minutes, followed by centrifugation at 4°C at maximum speed of Microfuge 16 bench top centrifuge for 10 minutes. The supernatant was removed gently without interruption of the RNA pellet. The RNA precipitate was then washed gently with 1 mL of 75% ethanol (prepared with sterilized milliQ water), followed by centrifugation at 4°C at 7500 x g for 10 minutes. Following removal of the supernatant, the 1.5 mL microcentrifuge tube was air-dried for 10-15 minutes and RNA was eluted in 30 µL of nuclease-free water (Thermo Fisher Scientific (Ambion)) and incubated at 65°C for 10 minutes until the pellet was completely dissolved. RNA samples were then stored at -80°C until further usage. Genomic DNA contamination was removed using the TURBO DNA-free kit (Thermo Fisher

Scientific (Ambion)) prior to synthesis of cDNA templates (described below). The whole isolation procedure was performed at 4°C according to manufacturer's instructions unless stated otherwise.

In Chapter 5, RNA was extracted from isolated PCM1 (-/+) nuclei with TRIzol followed by Direct-zol RNA mini-prep kit (Zymo Research, Irvine, CA, USA), according to the manufacturer's recommended protocol, with DNase I treatment in the column to remove genomic DNA contamination. Briefly, isolated PCM1 (-/+) nuclei were lysed in 1 mL TRIzol, followed by 1 mL of 100% ethanol and mixed thoroughly. The mixture was then placed in a tube rotator and rotated for 5 minutes. The mixture was subsequently transferred carefully to a Zymo-Spin IIC Column and centrifuged at maximum speed for 30 seconds using Microfuge 18 bench top centrifuge (Beckman Coulter). The column was then washed with 400 µL RNA Wash Buffer and centrifuged for 30 seconds at maximum speed of Microfuge 18 bench top centrifuge. A premixed DNase treatment solution (5 µL of 6 U/µL DNase I and 75 µL DNA Digestion Buffer) was then added to the column matrix to remove genomic DNA contamination. The column was incubated in the DNase treatment solution for 15 minutes at room temperature, followed by addition of 400 µL Direct-zol RNA PreWash Buffer and centrifuged for 30 seconds at maximum speed of Microfuge 18 bench top centrifuge. The column was washed again with 700 µL RNA Wash Buffer and centrifuged for 2 minutes at maximum speed of Microfuge 18 bench top centrifuge to remove any residual liquid. 20 µL of preheated nuclease-free water was added directly to the column matrix, incubated for 5 minutes and centrifuged for 1 minute at maximum speed of Microfuge 18 bench top centrifuge. The whole isolation was performed under room temperature conditions according to manufacturer's instructions.

cDNA templates were synthesized using the SuperScript® III First-Strand Synthesis System (Thermo Fisher Scientific (Invitrogen)) using random hexamers. Briefly, 1 µg RNA was mixed with 150 ng random hexamers and 1 µL of 10 mM dNTPs to make a total 13 µL mixture. The mixture was then incubated at 65°C for 5 minutes followed by 4°C for at least 1 minute. The mixture was subsequently mixed with a premixed reverse transcription (RT) solution (4 µL 5x First Strand Buffer, 1 µL 0.1mM DTT, 1 µL RNAse Out and 1 µL Superscript III, when no-RT control was generated, 1 µL Superscript III was replaced with 1 µL nuclease-free water). The mixture was then incubated under the following cycling conditions: 25°C for 5 minutes, 50°C for 60 minutes, and 70°C for 15 minutes. The cDNA templates were then stored in -20°C until further usage. cDNA templates were diluted 5x with nuclease-free water before processing for qPCR.

qPCR was performed on the StepOnePlus™ Real-Time PCR System (Thermo Fisher Scientific (Applied Biosystems)) using SYBR® Green PCR Master Mix (Thermo Fisher Scientific (Invitrogen)), as previously described (Porrello et al., 2009). Standard PCR primers for qPCR are listed in **Table 2.1, 2.2**. 18S ribosomal RNA was used as a housekeeping control for all PCR reactions (**Table 2.3**). In Chapter 5, where RNA was extracted from the nucleus, primers were designed to span within single exon to ensure non-processed RNA was amplified with no-RT templates served as negative control, these primers are listed in **Table 2.4**. All used primers have efficiency at a range of ~80% -130%.

2.4. Histological analysis

Hearts were briefly rinsed in PBS (Thermo Fisher Scientific (Gibco)), fixed in 4% paraformaldehyde overnight, and then stored in PBS at 4˚C until paraffin embedding. Sections (5 μm thickness) were processed for H&E staining according to standard procedures, as previously described (Porrello et al., 2011a).

2.5. Immunofluorescence staining for Dnmts, cell proliferation and hypertrophy

Sections were de-paraffinized and washed with PBS prior to immunostaining as previously described (Porrello et al., 2011b). For Dnmt1, Dnmt3a and phosphorylated-histone H3 (pH3) immunostaining, sections underwent antigen retrieval by boiling in Tris-EDTA buffer (pH 9.0) at 110 ℃ for 20 minutes in the decloaking chamber (Biocare medical, Concord, CA, USA). Sections were then recovered in PBS for 20 minutes at room temperature, followed by permeabilisation in 0.3% Triton for 5 minutes, washing in PBS (3 x 3 minutes) and then blocking in 10% goat serum (in PBS) at room temperature for 20 minutes. Primary antibodies were diluted in 2% goat serum and incubated overnight at 4 ℃. The following primary antibodies were used for immunofluorescence staining: Dnmt1 (D63A6) (1:100, rabbit monoclonal #5032S, Cell Signaling, Danvers, MA, USA), Dnmt3a (D23G1) (1:100, rabbit monoclonal #5398S, Cell Signaling), cardiac Troponin-T (1: 100, mouse monoclonal MS-295-P1, Thermo Scientific, Waltham, MA, USA), pH3 (Ser10) (1:100, rabbit polyclonal 06-570, Merck Millipore, Darmstadt, Germany). Following primary antibody incubation, sections were washed in PBS (3 x 5 minutes) and then incubated with secondary antibodies conjugated with Alexa Fluor 488 or 555 (1: 400, Thermo Fisher Scientific (Molecular Probes)) and Hoechst 33342 (1:1000, H21492, Thermo Fisher Scientific (Invitrogen)) at room temperature for 1 hour in the dark. Sections were washed in PBS (3 x 3 minutes) before being

mounted with Fluoromount-G (Southern Biotech, Birmingham, AL, USA). For quantification of hypertrophy, heart sections were stained with wheat germ agglutinin (WGA, 50 μg/mL, W11261, Thermo Fisher Scientific (Molecular Probes)) as previously described (Porrello et al., 2011b). Quantitative analyses of cardiomyocyte mitosis and cross sectional area were performed using ImageJ as previously described (Porrello et al., 2011b).

2.6. Bisulphite sequencing

Bisulphite sequencing was performed on genomic DNA from cardiac ventricles obtained at P1, P7 and P28 (n=3 per time point). DNA samples underwent bisulphite conversion using the EZ DNA Methylation kit (Zymo Research). Bisulphite PCR primers are listed in **Table 2.5**. Bisulphite-converted DNA samples were then used as a template for PCR reactions using Hi Fidelity Platinum Taq DNA polymerase (Thermo Fisher Scientific (Invitrogen)) with the following cycling conditions: 95 ℃ for 3 minutes, 40 cycles of 95 ℃ for 30 seconds, 58 ℃ for 30 seconds, 72 ℃ for 45 seconds, followed by 72 ℃ for 5 minutes. The PCR product was purified using the QIAquick Gel Extraction Kit (Qiagen) and cloned into the TOPO plasmid (Thermo Fisher Scientific (Invitrogen)) for downstream sequencing. Following transformation and blue-white Xgal selection in competent E.coli (New England Biolabs, Ipswich, MA, USA), 6 positive clones per heart sample were picked and processed for Sanger sequencing (Australian Genome Research Facility, Brisbane, QLD, Australia). Bisulphite sequencing primers are listed in **Table 2.5**. Bisulphite sequencing results were then analysed using BISMA software, as previously described (Rohde et al., 2010).

2.7. Statistical analysis

All non-bioinformatics statistical analyses were performed using GraphPad Prism 6.0. For comparisons between two groups, a two-tailed unpaired Student's t-test was used. For multiple group comparisons, a one-way ANOVA followed by Bonferroni post-test was used. For comparison between multiple groups with multiple variables, a two-way ANOVA followed by Bonferroni post-test was used. All data are presented as mean ± s.e.m., except for the scatter plot of quantified cardiomyocyte cross-sectional surface area (**Figure 3.3I**), which is shown as a median. Detailed statistical analysis methods and sample sizes are indicated in the figure legends. For all statistical analyses: *P<0.05 and ** P <0.001. For bioinformatics analysis, including RNA-seq, MBD-seq and Gene Set Enrichment Analyses (GSEA), an false discovery rate (FDR) p- ≤ 0.05 using the correction procedure of Benjamini and Hochberg was used (Benjamini and Hochberg,

1995). Gene GO analysis (pathway/ process/network) of MetaCore from Thomson Reuters was performed using only statistically significant gene sets.

Table 2.1. List of primer sequences for SYBR Green qPCR analysis.

Targeted gene		Primer sequence (Human)	Primer sequence (Mouse)
18s	F'	GCTGAGAAGACGGTCGAACT	CCCTCCAATGGATCCTCGTT
18s	R'	CGCAGGTTCACCTACGGAAA	TCGAGGCCCTGTAATTGGAA
DNMT1	R'	-	GCCATCTCTTTCCAAGTCTTT
DNMT1	L'	-	TGTTCTGTCGTCTGCAACCT
DNMT2	F'	-	AGAGGATGGAACCTCTGCGT
DNMT2	R'	-	CCACATGTGCAGGGATATGA
DNMT3A	R'	-	GCTTTCTTCTCAGCCTCCCT
DNMT3A	L'	-	CCATGCCAAGACTCACCTTC
DNMT3B	F'	-	ATCCATAGTGCCTTGGGACC
DNMT3B	R'	-	CTGGCACCCTCTTCTTCATT
DNMT3L	R'	-	GCTTGCTCCTGCTTCTGACT
DNMT3L	L'	-	GGTGTGGAGCAACATTCCAG
TET1	F'	-	GGGAGCTCATGGAGACTAGG
TET1	R'	-	AGAGCTCTTCCCTTCCTTCC
TET2	F'	-	CTTCTCTGCTCATTCCCACA
TET2	R'	-	AGCTCCGACTTCTCGATTGT
TET3	R'	-	CAGCGATTGTCTTCCTTGGT
TET3	L'	-	GCCTGCATGGACTTCTGTG
GADD45A	F'	-	AAGACCGAAAGGATGGACAC
GADD45A	R'	-	ACCACGTTATCGGGGTCTAC
GADD45B	R'	-	TCTGCAGAGCGATATCATCC
GADD45B	L'	-	CGGCCAAACTGATGAATGT
GADD45G	R'	-	AAGTTCGTGCAGTGCTTTCC
GADD45G	L'	-	CGCACAATGACTCTGGAAGA

NEAT1	F'	-	TAGGTTCCGTGCTTCCTCTT
NEAT1	R'	-	ACATCCTCCACAGGCTTACC
IGF2BP3	R'	-	GGGCGGGATATTTCGTATCT
IGF2BP3	L'	-	GCGCTTTCAGGTAAAATGGA
CDK14	R'	-	CCAGGTGCTTGATCACTGAA
CDK14	L'	-	TCGCTCTGAAGAAAGAGGACA
CHTF18	R'	ACGCAGGAAGTTGTCAAACA	ACGGTGCTTAAGCTGGAGTC
CHTF18	L'	CTCACAGCGATTCTACCGTG	GTGACAAGGGCTCTCTGACC
CIT	R'	-	TTGGAGGTGTCATCGTCAGA
CIT	L'	-	CACCCTTTCTTTGCCAGAAC
CTDP1	R'	-	CTGTCATCACTGCCCTCTCC
CTDP1	L'	-	ACAACCCAGTATGTCCGAGG
GPSM2	R'	-	TTCAGCAGCACTTCAGCAAC
GPSM2	L'	-	TCCTAGTCTACGGCCAGAGG
IGF2	R'	-	TGAGAAGCACCAACATCGAC
IGF2	L'	-	CTTCTCCTCCGATCCTCCTG
IGF2BP2	R'	-	CCGAATCTGGATTCTTCTGC
IGF2BP2	L'	-	GACCCTCTCGGGTAAAGTGG
PAK4	R'	-	TACAGGCACCTGGTCTGAAG
PAK4	L'	-	GTACGCGGGCACAGAGTT
PRIM2	R'	-	GGTTGAGCAGAGGCTGAAGT
PRIM2	L'	-	GAACGAGTTTAGAGCCACGC
SH3PXD2B	R'	-	AAAGAACTTGCTGTAGCGCC
SH3PXD2B	L'	-	CGTGCCCAACAAGCATTA
UBE2C	R'	TTGTAAGGGTAGCCACTGGG	CACCCACTTGAACAGGTTGT
UBE2C	L'	TCAAATGGGTAGGGACCATC	CGGCTACAGCAGGAACTGAT
KLF9	R'	-	CGCGAGAACTTTTTAAGGCA

KLF9	L'	-	CAGTGGCTGTGGGAAAGTCT

Table 2.2. List of primer sequences for SYBR Green qPCR analysis (did not work).

Targeted gene		Primer sequence (Human)	Primer sequence (Mouse)
INSC	R'	-	CGAGTGGCTCTCATCAGTCA
INSC	L'	-	GCACACTGGCCTCTATCTGC
INSC	R'-2	-	GTCAAGATGTCAGCCAAGCA
INSC	L'-2	-	TAGCCCTCTTCAAGGTCTGC
KDM2B	R'	-	TCCTGCTGTTGTTCGGTTG
KDM2B	L'	-	GACGACTATGAATCGGAGCC
KDM2B	R'-2	-	AACTTGCCCTTAGGCCGAC
KDM2B	L'-2	-	GCTGCTCCAGCCATGTCA
POLD2	R'	-	GCTGCAGCTCACACAACTTC
POLD2	L'	-	ATATTTATGCCACCCGCCTC
POLD2	R'-2	-	GGACATGGCCTTGAACAGAG
POLD2	L'-2	-	AGATGAGACCGTTCCTGGTG
SMYD2	R'	-	CGTCCACATTTTGACAATCC
SMYD2	L'	-	ACCTCCTCTTCTCCTGCCC
SMYD2	R'-2	-	AGTAGAACGCCTGCTTGCAC
SMYD2	L'-2	-	CGACCTCCTCTTCTCCTGC
PTPRR	R'	-	GCTACTCCTTGGCGGAAGAT
PTPRR	L'	-	AATTCCAGCAGCAAATGTGA
PTPRR	R'-2	-	GAAGATCCGAAGCAGGGTTA
PTPRR	L'-2	-	CCTGCATATGACCCGTCTCT
CIT	R'	TCAGACTTGAGGGTGGGAAC	-
CIT	L'	GTTTGAAGGTCTTTGCTGCC	-
CIT	R'-2	GAGAGGATGAAACCCACGAA	-
CIT	L'-2	TTTGCTGCCATCCTTTCTTC	-

IGF2BP3	R'	CTGCAGTTTCCGAGTCAGTG	-
IGF2BP3	L'	ATCCCGCCTCATTTACAGTG	-
IGF2BP3	R'-2	ACAGCTCTCCACCACTCCAT	-
IGF2BP3	L'-2	GTCCCAAAAAGGCAAAGGAT	-

Table 2.3. Ct value of housekeeping gene 18s in different studies.

Studies	Conditions	Mean Ct value of 18s	± S.E.M
Mouse developmental profiling study	P1	6.97	0.03
	P7	7.10	0.05
	P14	7.22	0.05
	P28	7.08	0.06
	P56	7.11	0.02
Mouse 5aza-dC study	Saline	7.23	0.12
	5aza-dC	7.24	0.12
Human Heart-Dyno 5aza-dC study	Control	13.81	0.09
	10μM 5aza-dC	13.83	0.08
Mouse PCM1 study	P1-PCM1(-)	11.55	1.06
	P1-PCM1(+)	11.10	1.16
	P14-PCM1(-)	11.09	0.47
	P14-PCM1(+)	11.94	0.60
	P56-PCM1(-)	10.60	0.87
	P56-PCM1(+)	13.05	0.96
Human PCM1 study	Foetal (13-19 wks)-PCM1(-)	15.03	2.25
	Foetal (13-19 wks)-PCM1(+)	15.43	1.31
	0-10 yrs-PCM1(-)	13.95	0.36

	0-10 yrs-PCM1(+)	13.41	0.62
	10-30 yrs-PCM1(-)	16.23	0.89
	10-30 yrs-PCM1(+)	14.06	0.85
	30+ yrs-PCM1(-)	14.31	0.37
	30+ yrs-PCM1(+)	14.54	1.25

Table 2.4. List of primer sequences for SYBR Green real-time qPCR analysis targeting nuclei RNA.

Cell type markers	Targeted gene		Primer sequence (Human)	Primer sequence (Mouse)
House keeping gene	*18s*	F'	GCTGAGAAGACGGTCGAACT	CCCTCCAATGGATCCTCGTT
	18s	R'	CGCAGGTTCACCTACGGAAA	TCGAGGCCCTGTAATTGGAA
Cardio myocytes	*MYH6*	F'	TACCTCCGCAAGTCAGAGAA	AACTCAGCTGACCTGCTCAA
	MYH6	R'	CTCGGTTTCAGCAATGACC	GCCCCGATGGAATAGTACAC
	MYH7	F'	CCACTTCTCCCTGATCCACT	GTGAAGGAGGACCAGGTGAT
	MYH7	R'	TACAAGCCCACGACAGTCTC	TAGCGCTCCTTGAGGTTGTA
	TNNC1	F'	CCTTCGACATCTTCGTGCT	CTGCATCAGCACCAAGGA
	TNNC1	R'	TCCACCTCATCGATCATCTC	TCAATCATCTCCTGCAGCTC
	TNNI3	F'	CTTTGACCTTCGAGGCAAGT	AGCAGGAGATGGAACGAGAG
	TNNI3	R'	AGGTCCAGGGACTCCTTAGC	GCCCATCCAACTCCAAAG
Fibro blasts	*COL1A1*	F'	GTACTGGATTGACCCCAACC	CAATGGTGAGACGTGGAAAC
	COL1A1	R'	TACACGCAGGTCTCACCAGT	GGTTGGGACAGTCCAGTTCT
	COL3A1	F'	GGCAAAGATGGAACCAGTG	GCCACCTTGGTCAGTCCTAT
	COL3A1	R'	CTCAGATCCTCTTTCACCTCTG	GCAGTCTAGTGGCTCCTCATC
	FBN1	F'	GAAAGTGGCTGTCTCAATGG	GCTCCTCGAGTCCTACACG
	FBN1	R'	TCACACTGGGGTCCAGTAAA	CTCTTCTCTTGGCCCGATT
	DDR2	F'	GCCAGATTTGTCCGGTTC	TCCTGAGATTCCAGTGCAAC
	DDR2	R'	CAGACACAGCCGTAAAGCTC	GGGTCCCCACAAGAGTGATA
Immune cells	*ITGAM*	F'	GGGTTCAACTTGGACACTGA	GTGTCATGGCTTCAATCTGG
	ITGAM	R'	TCCCTGAAGCTGGACCAC	CAAGCTGGACCACACTCTGT
Endothelial cells	*VWF*	F'	GCCTCCAAAGGGCTGTATC	CTCTTTGGGGACGACTTCAT
	VWF	R'	CCGCAGGTCTTGTTGAAGTA	AAGGAACGTTTCTGGCAGTC

Table 2.5. List of primer sequences for bisulphite sequencing.

Targeted gene	Primer Sequence
Igf2bp3 **F'**	TAGGTAAAATGGAATTATATGGGAAAT
Igf2bp3 **R'**	ACAACAATAACCCAAAAACAAAAAC
Neat1 **F'**	GGTTGTGAATGTTTTAGATGAATGTT
Neat1 **R'**	CAAACTACAAAAACAAAAAAAATAAAC
Topo M13 Reverse	CAGGAAACAGCTATGAC

Chapter 3

Dynamic changes in the cardiac methylome during postnatal development

It is not the strongest of the species that survive,
nor the most intelligent,
but the one most responsive to change.
Charles Darwin.

Chapter 3. Dynamic changes in the cardiac methylome during postnatal development

Relatively little is known about the mechanisms of how epigenetics guides postnatal organ maturation. The goal of this chapter was to determine whether DNA methylation plays an important role in guiding transcriptional changes during the first two weeks of mouse heart development, which is an important period for cardiomyocyte maturation, loss of proliferative capacity and loss of regenerative potential. RNA-seq and MBD-seq identified dynamic changes in the cardiac methylome during postnatal development (2545 DMRs from P1 to P14 in the mouse). The vast majority (~80%) of DMRs were hypermethylated between P1 and P14 and these hypermethylated regions were associated with transcriptional shut down of important developmental signalling pathways, including Hedgehog, BMP, TGFβ, FGF and Wnt/β-catenin signalling. Postnatal inhibition of DNA methylation with 5aza-dC induced a marked increase (~3-fold) in cardiomyocyte proliferation and ~50% reduction in the percentage of binucleated cardiomyocytes compared to saline-treated controls. This chapter provides novel evidence for widespread alterations in DNA methylation during postnatal heart maturation and suggests that cardiomyocyte cell cycle arrest during the neonatal period is subject to regulation by DNA methylation.

3.1. Introduction

The mammalian heart undergoes several important physiological transitions during neonatal life, which allow the heart to adapt to the postnatal environment. In rodents, the first two weeks of postnatal heart development coincide with rapid cardiac growth, cardiomyocyte cell cycle withdrawal, a marked increase in the proportion of binucleated cardiomyocytes and cardiomyocyte hypertrophy. Additionally, there is a metabolic transition from glycolysis to fatty acid oxidation, increased extracellular matrix production and changes in the expression and organization of sarcomeric proteins (Porrello and Olson, 2014b). Importantly, it is also during this period, that the robust regenerative potential of the neonatal rodent heart diminishes (Porrello et al., 2011b; Porrello et al., 2013). These neonatal developmental transitions are associated with alterations in the expression of thousands of genes embedded within tightly controlled transcriptional networks. However, the transcriptional regulatory mechanisms that guide neonatal heart development remain poorly understood.

Epigenetic modifications have emerged as critical regulators of gene expression changes during heart development and disease. The control of gene expression is subject to diverse regulatory actions that involve DNA bound TFs including: ATP-dependent chromatin remodelling, covalent histone modifications such as acetylation and methylation, and DNA methylation. Genetic deletion of chromatin modifying proteins (including HMTs, acetylases, deacetylases and ATP-dependent remodelling factors) are implicated in cardiac developmental processes including defects in cardiomyocyte proliferation (Chang and Bruneau, 2012). Recent studies have further interrogated the relationship between chromatin modifications (histone acetylation and methylation) and gene transcription on a genome-wide scale, which has identified important relationships between chromatin transitions and transcription during cardiac lineage commitment (Wamstad et al., 2012). It has also become apparent that the cardiac cell cycle is under epigenetic control, as comparison of embryonic and adult rodent cardiomyocytes revealed an enrichment of H3K9me3 (associated with transcriptional repression) at the promoters of cell cycle genes during cardiac maturation (Sdek et al., 2011). A recent study has also identified numerous epigenetic modifications at Notch responsive promoters that appear to be important determinants of myocyte proliferative responses to Notch ligands (Felician et al., 2014a). Curiously, despite intensive interrogation of the roles of chromatin modifiers during cardiac development and disease, there have been few systematic studies on the impact of DNA methylation.

DNA methylation occurs by covalent modification at carbon 5 of cytosine, predominantly in the context of a cytosine-guanine dinucleotide (CpG) (Suzuki and Bird, 2008). The mechanisms for establishing and maintaining DNA methylation are well established and involve three methyltransferases (Dnmts) in mammals - Dnmt1, 3a and 3b (Wu and Zhang, 2014). Germline deletion studies in mice have established essential roles for Dnmts during embryonic heart development (Li et al., 1992). More recent genome-wide DNA methylation profiling studies have identified widespread alterations in DNA methylation patterns during early embryonic heart development and have revealed potentially important associations with transcriptional changes in cardiogenic genes (Chamberlain et al., 2014). Moreover, dynamic changes in DNA methylation patterns correlate with gene expression changes in heart failure (Movassagh et al., 2011) and dilated cardiomyopathy (Haas et al., 2013) in humans and inhibition of DNA methylation may be cardioprotective in settings of norepinephrine-induced cardiac hypertrophy (Xiao et al., 2013) and ischemic heart disease (Watson et al., 2013). These findings suggest that DNA methylation is important for cardiac gene expression during embryonic heart development and in various adult disease settings. However, the impact of DNA methylation during cardiac maturation in the neonatal period has not been investigated.

In this chapter, it was hypothesised that DNA methylation plays a key role in the repression of transcriptional networks governing cardiomyocyte proliferation during the neonatal period. The current chapter presents the first systematic analysis of DNA methylation during postnatal heart development. Two waves of DNA methylation have been identified during the neonatal period and demonstrate that inhibition of DNA methylation during neonatal heart development prolongs the proliferative capacity of cardiomyocytes and is associated with a profound reduction in cardiomyocyte binucleation. Moreover, a genome-wide approach have been taken to analyse neonatal changes in DNA methylation and transcription, which shows differential methylation events across thousands of loci, some of which are associated with transcriptional changes in important developmental signalling pathways for muscle growth and differentiation. These results provide new insight and information on the regulation of cardiac gene expression subject to changes by DNA methylation in the neonatal period.

3.2. Methodology

3.2.1. *In vivo* administration of 5aza-dC to neonatal mice

The hypomethylating agent 5aza-dC (Sigma-Aldrich, St. Louis, MO, USA) was made fresh daily by dissolved in saline and administered to neonatal ICR/CD-1 mice through daily subcutaneous injections (1 mg/kg) from P2 to P12. Control mice received a daily subcutaneous injection of an equivalent volume of saline. All animals were euthanized at P7 or P12 by asphyxiation with CO_2 followed by cervical dislocation. Hearts were harvested for DNA/RNA extraction, histology and cell isolations as described in Chapter 2.

3.2.2. Cardiomyocyte isolation and quantification of binucleation

Hearts were harvested and fixed in 4% PFA for 1 hour at room temperature. Cardiomyocytes were isolated by enzymatic digestion of fixed cardiac tissues using a combination of collagenase D (2.4 mg/mL, Roche, Basel, Switzerland) and collagenase B (1.8 mg/mL, Roche) with overnight shaking at 37℃ until the tissue was fully digested. Cell suspensions were then pelleted at 300 x g for 3 minutes at room temperature and then re-suspended in PBS. For nuclei staining, cell suspensions were stained with Hoechst 33342 (1:500, Thermo Fisher Scientific (Invitrogen)) for 10 minutes at room temperature. Cells were then pelleted at 300 x g for 3 minutes and washed in PBS before being re-suspended in Fluoromount-G (Southern Biotech) and mounted on slides. Bright field and fluorescence images were acquired for 100 cells per sample and overlayed for post-analysis in ImageJ (version 1.47v, National Institutes of Health, Bethesda, MD, USA). Quantification of cardiomyocyte nucleation, cell width and cell length were performed under blinded conditions.

3.2.3. Transcriptional profiling with RNA-seq

Cardiac ventricles were harvested at P1 and P14 (n=9 per group) from C57BL6/J mice as described above and were homogenised in PBS. Three individual hearts were pooled per replicate. This homogenate was divided between transcriptome and methylome assays. RNA was isolated by TRIzol extraction (Thermo Fisher Scientific (Ambion)) followed by QiaQuick MinElute (Qiagen) cleanup including on-column DNase digestion. RNA quality was verified with MultiNA bioanalyzer (Shimadzu, Kyoto, Kansai, Japan). Purified mRNA was prepared using Dynabeads® Oligo (dT) 25 (Thermo Fisher Scientific (Ambion)) enrichment. Libraries were generated using the NEBNext® mRNA Library Prep Reagent Set for Illumina (New England Biolabs). Libraries were

validated on MultiNA bioanalyzer and sequenced at a concentration of 10 pM (Illumina, San Diego, CA, USA). Base-calling was performed off-line with OLB v1.8.

3.2.4. MBD-seq

Genomic DNA for CpG methylation profiling was isolated using the DNeasy Blood & Tissue Kit (Qiagen). DNA was fragmented by BioRuptor sonication (Diagenode, Denville, NJ, USA). Fragmented DNA was analyzed with bioanalyzer, and 1 μg of sonicated DNA underwent methyl-CpG enrichment using the MethylMiner™ Methylated DNA Enrichment Kit (Thermo Fisher Scientific (Applied Biosystems)). Sequencing libraries were generated using the NEBNext® DNA Library Prep Reagent Set (New England Biolabs) for Illumina. Libraries were validated on MultiNA bioanalyzer and sequenced as above. MBD-seq measures average methyl-cytosine levels in the sequenced fragments (150-250 bp in length) (Stevens et al., 2013).

3.2.5. Bioinformatics analyses

Sequence reads underwent 3' base quality trimming using the Fastx toolkit with a minimum Phred quality score (Q) of 30 and a minimum read length of 20 nt. RNA-seq reads were aligned to the mouse genome sequence (GRCm38.70/mm10) using Olego with default settings (Wu et al., 2013). Reads aligning to Ensembl-annotated exons with a strict mapping quality (Q≥20) were counted with BedTools (Quinlan and Hall, 2010) and used to construct a data matrix comprising genes with an average of 10 reads or more per sample across the experiment. Differential gene expression analysis was performed using edgeR (v3.2.4) (Robinson et al., 2010). Heatmaps were generated from normalized and scaled gene expression values in R (Reich et al., 2006).

MBD-seq reads were aligned to the mouse genome (GRCm38.70/mm10) using Burrows Wheeler Aligner (BWA) with default settings (Li and Durbin, 2009). Reads from each developmental stage were pooled and a single large alignment file (bam format) prepared for P1 and P14. MACS (Zhang et al., 2008) was then used to directly compare P1 to P14 and identify regions of interest. MACS peak-calling was performed with a shift size of 75 bp and otherwise default parameters. DMRs were defined as coordinates initially identified using MACS peak calling determined to have a statistically significant signal difference (P1 vs. P14, FDR ≤ 0.05) and all DMRs exhibited greater than 30% fold change. Intersection between our DMRs and Ensembl genomic features was performed with BedTools. Likewise, intersection between DMRs and TF binding sites or DNaseI hypersensitivity sites defined by the Encyclopedia of DNA Elements (ENCODE) project (http://genome.ucsc.edu/ENCODE/downloadsMouse.html) was determined. Peak files from Mouse

ENCODE project (mm9) were converted to mm10 coordinates using liftOver tool (http://hgdownload.soe.ucsc.edu/admin/exe/) with the mm9 to mm10 chain file (http://hgdownload-test.cse.ucsc.edu/goldenPath/mm9/liftOver/mm9ToMm10.over.chain.gz) using the default settings. Enrichment of TF binding motifs between in P14 and P1 peaks was computed using Homer (http://homer.salk.edu/homer/ngs/index.html). Gene expression, methylation and gene set enrichments with an FDR p-value ≤ 0.05 were considered significant. Gene GO analysis (pathway/process/network) was performed using MetaCore from Thomson Reuters (https://portal.genego.com/cgi/data_manager.cgi) on significant gene sets. All network relationship analyses were performed using the direct interaction analysis function. GSEA was performed on these data as previously described (Subramanian et al., 2005) using publicly available gene sets (www.broadinstitute.org/gsea/msigdb).

3.2.6. Data access

RNA-seq and MBD-seq data from this project is available from GEO (http://www.ncbi.nlm.nih.gov/geo/) under accession number GSE59971.

3.3. Results

3.3.1. Dynamic regulation of DNA methylation machinery during postnatal cardiac maturation

Total DNA methylation was measured in mouse hearts at P1, P7, P14, P28 and P84. Genomic DNA methylation levels remained steady from P1 to P14 but markedly decreased thereafter (**Figure 3.1A**). Subsequently, the expression levels of Dnmts was measured by real-time qPCR in mouse hearts from P1 to P84 (**Figure 3.1B**). Consistent with an overall decrease in genomic DNA methylation levels after P14, qPCR profiling of *Dnmt1*, *Dnmt3a* and *Dnmt3b* confirmed decreased mRNA expression levels in postnatal maturation of cardiac tissue. This result was verified at the protein level by immunohistochemistry staining (**Figure 3.1C**). Dnmt1 and Dnmt3a were predominantly localized to the nucleus of cardiomyocytes with high expression levels at P1 and P7 (**Figure 3.1C**). While Dnmt1 exhibited a dramatic decrease in expression levels after P7, such that it became hardly detectable in cardiomyocytes by P14 and P28, Dnmt3a maintained its expression level until P14 but was undetectable in P28 hearts (**Figure 3.1C**). Dnmt1 and Dnmt3a were also expressed in non-myocytes at early developmental time-points but were undetectable in all cell types by P28 (**Figure 3.1C**). The expression levels of the non-canonical Dnmts, *Dnmt2* and *Dnmt3l* were also checked by qPCR analysis. While *Dnmt2* expression levels did not dramatically change throughout life, *Dnmt3l* was significantly up-regulated after P14 (**Figure 3.2A**).

Given the decrease in global DNA methylation levels after P14, the expression levels of TETs and Growth Arrest and DNA Damage 45 (*Gadd45s*) was profiled because they are implicated in active DNA demethylation (Wu and Zhang, 2014). Real-time qPCR analysis showed that *Gadd45a* and *Gadd45g* were up-regulated at P14 and *Gadd45a* expression continued to increase until P28 (**Figure 3.2B, C**). However, the mRNA expression levels of *Tet1-3* and *Gadd45b* all decreased during postnatal heart maturation (**Figure 3.2B, C**).

3.3.2. DNA methylation is required for cardiomyocyte cell cycle arrest and binucleation *in vivo*

To better understand the role of DNA methylation in regulating postnatal cardiac development, hypomethylating agent 5aza-dC was used to pharmacologically inhibit DNA methylation of neonatal mice from P2 (**Figure 3.3A**). 5aza-dC is a clinical medication for myelodysplastic syndromes and acute myeloid leukaemia. It effectively prevents DNA methylation by incorporating

into DNA as the analogue of cytidine, which cannot be methylated or through inhibition of Dnmts (Christman, 2002; Karahoca and Momparler, 2013). 5aza-dC treated mice grew normally for the first 5 days of exposure but stopped gaining weight thereafter and the experiment was terminated at P12 (**Figure 3.3A**). Systemic administration of 5aza-dC induced ~50% reduction of genomic DNA methylation levels in P12 hearts (**Figure 3.3B**). Inhibition of DNA methylation was associated with a significant increase in heart size, as indicated by a pronounced increase in the heart weight to body weight ratio (HW/BW) at P7 and P12 (**Figure 3.3C, D**).

To understand whether the increased heart weight following inhibition of neonatal DNA methylation was caused by cell proliferation, heart sections were stained with antibodies recognising pH3 and cTnnT to quantify the incidence of cardiomyocyte mitosis. At P7, an increase in the number of $pH3^{+}$ cells by ~50% in cardiomyocytes and ~25% in non-myocytes was observed in 5aza-dC treated hearts (**Figure 3.3E, F**) and was associated with a ~50% reduction in the percentage of binucleated cardiomyocytes (**Figure 3.3G**). A reduced percentage of binucleated cardiomyocytes in the 5aza-dC treated group was also noted at P12 (**Figure 3.3G**). While no effect of 5aza-dC on cell size was detected at P7, a modest increase in cell size was observed at P12 (**Figure 3.3H, I**). Interestingly, cardiomyocyte hypertrophy at P12 was associated with an increase in cell length in both mono- and bi-nucleated cardiomyocyte populations (**Figure 3.3J, K, L**). Together, these findings suggest that inhibition of DNA methylation during neonatal life prevents cardiomyocyte cell cycle arrest and binucleation, increasing heart size postnatally.

3.3.3. Neonatal cardiac maturation is associated with profound alterations in gene transcription

To understand the transcriptional changes during neonatal heart maturation, RNA-seq was performed in P1 and P14 hearts. A total of 6476 genes were differentially expressed (FDR ≤ 0.05) between P1 and P14 cardiac ventricles (**Figure 3.4A; Table 3.1**). Among these differentially expressed genes, 3233 genes were expressed at significantly higher levels at P14, whereas 3243 genes were expressed at higher levels at P1 (**Figure 3.4A, B; Table 3.1**). Gene GO pathway analysis revealed an increase in the expression of genes at P14 that were predominantly involved in metabolism (oxidative phosphorylation) and cytoskeletal remodelling which is consistent with the well known changes in metabolic substrate utilization and cytoskeletal rearrangement (Porrello and Olson, 2014b) that occur after birth in mammals (**Figure 3.4C**). On the other hand, the majority of genes that decreased in expression levels at P14 were associated with cell cycle checkpoints, DNA replication, the DNA damage response and cytoskeletal remodelling, consistent with the well-

established phenomenon of cardiomyocyte cell cycle arrest and ultrastructural maturation following birth (Porrello and Olson, 2014b) (**Figure 3.4C**).

3.3.4. Differential methylated regions characterize neonatal cardiac maturation

Given the importance of DNA methylation for postnatal cardiomyocyte cell cycle arrest and binucleation, whether there are alterations in DNA methylation across the genome have been assessed during neonatal cardiac maturation. DNA samples from P1 and P14 cardiac ventricles were processed for whole-genome DNA methylation sequencing (MBD-seq), known as MethylMiner, which have been previously validated (Pirola et al., 2011). Analysis of the total number of reads processed indicated that the numbers of aligned reads used in peak calling were similar for P1 and P14 sample groups (**Table 3.2**). The MBD-seq analysis identified 2545 DMRs between P1 and P14 (**Figure 3.5A; Table 3.1**). Among these DMRs, 2005 regions (~80%) were hypermethylated and 540 regions (~20%) were hypomethylated at P14 relative to P1 (**Figure 3.5A, B; Table 3.1**). Notably, P14 DMRs had a higher CpG dinucleotide content (28.95±0.006 / kilobase pair (kbp) at P14 vs. 13.02±0.012 / kbp at P1) and higher G/C nucleotide content (553.0±0.021 / kbp at P14 vs. 396.8±0.116 / kbp at P1) than the P1 DMRs. Interestingly, DNA hypermethylation was noted across all mouse chromosomes at P14 (**Figure 3.5C**). Intersection of differentially methylated peaks with the mouse genome revealed that approximately 4.8% of the genome was differentially methylated between P1 and P14 (**Figure 3.5D**). The majority of DNA methylation peaks at P14 occurred across protein coding DNA sequences (CDS) and exons, with almost one-third of coding regions displaying an increase in methylation levels from P1 to P14 (**Figure 3.5D**).

3.3.5. Gene expression changes implicated in cardiac maturation are subject to DNA methylation

Because neonatal cardiac development is subject to broad changes in DNA methylation we examined associations with gene expression by intersecting RNA-seq and MBD-seq data sets. In total, 564 DMRs overlapping promoters (+/- 3 kbp TSS) and gene bodies were associated with significant changes in mRNA expression levels between P1 and P14 (**Figure 3.6A, Top; Table 3.3; Appendix 7.1**). The majority of DMRs associated with gene expression changes at P14 overlapped protein coding sequences and exons (**Table 3.3**). In total, 143 hypermethylated regions were associated with transcriptional repression at P14, while a much larger number of hypermethylated regions (n=385) were associated with transcriptional activation during neonatal cardiac maturation (**Figure 3.6A, Bottom; Table 3.3; Appendix 7.1**). A smaller number of hypomethylated regions were similarly associated with either transcriptional repression or activation at P14 (**Figure 3.6A,**

Bottom; Table 3.3; Appendix 7.1). To explore relationships between DNA methylation and transcription in greater detail, statistical correlation analyses were performed between P14 methylation peaks across different genomic features and mRNA expression changes. At P14, DNA methylation across exons was highly positively correlated with gene expression (**Figure 3.7A**). Similarly, DNA methylation across promoter regions at P14 was also typically associated with increased transcription at P14 (**Figure 3.7B**). In contrast, DNA methylation across exons and promoter regions at P1 negatively correlated with gene expression levels (**Figure 3.7**). These observations are consistent with genome-wide methylation profiling studies in other cell types, which suggest the impact of DNA methylation on gene transcription is highly context-dependent (Jjingo et al., 2012).

To validate these novel associations between methylation and transcription during neonatal heart development, two of the most highly differentially methylated genes between P1 and P14 were analysed by qPCR and bisulphite sequencing. Igf 2 binding protein 3 (*Igf2bp3*) represented the top candidate for genes displaying increased methylation associated with decreased mRNA expression at P14, while the long non-coding RNA, nuclear paraspeckle assembly transcript 1 (*Neat1*), represented the top candidate for genes displaying decreased methylation and increased expression at P14 (**Figure 3.6A, Bottom**). Real-time qPCR analysis confirmed that *Igf2bp3* expression levels decreased from P1 to P84, while the expression level of *Neat1* significantly increased after birth (**Figure 3.6B**), consistent with the RNA-seq data. Bisulphite sequencing was also performed on these two gene loci (**Figure 3.6D**). Bisulphite sequencing results strongly validated our MBD-seq data and confirmed increased methylation across the *Igf2bp3* locus and decreased methylation across the *Neat1* locus from P1 to P28 (**Figure 3.6D, Figure 3.8**). To further confirm that the expression level of *Igf2bp3* and *Neat1* was regulated by DNA methylation, their mRNA expression level was also examined in heart samples from mice that were treated with 5aza-dC. Both *Igf2bp3* and *Neat1* exhibited higher expression levels in 5aza-dC treated groups (**Figure 3.6C**), which was consistent with their methylation/expression patterns during neonatal cardiac development.

3.3.6. DNA methylation regulates transcription of critical developmental signalling networks during neonatal life

Next, Gene GO analysis was performed to explore the potential mechanisms underlying relationships between DNA methylation and gene transcription during neonatal heart development. Gene GO was used for process network analysis of various gene sets representing different relationships between DNA methylation and gene transcription (**Figure 3.9A, 3.10A, 3.11A,**

Appendix 7.1). Process network analysis for genes with increased DNA methylation and reduced expression at P14 identified a highly significant enrichment for genes associated with several important developmental signalling pathways including Hedgehog, TGFβ, FGF, vascular endothelial growth factor (VEGF), Notch and the Wnt/β-catenin pathway (**Figure 3.9A**). In addition, genes with increased methylation and decreased expression during neonatal cardiac maturation were also highly enriched for genes associated with cell adhesion and extracellular matrix interactions (**Figure 3.9A**). Further analysis of this gene set revealed an interaction network centred on Smad3, a critical downstream TF for the TGFβ signalling pathway (**Figure 3.9B**). For genes displaying increased methylation and increased transcription at P14, Gene GO analysis also revealed a significant enrichment for genes associated with developmental signalling pathways such as Notch, but, in addition, this gene set was also highly enriched for genes associated with muscle contraction, inflammation and the immune response (**Figure 3.10A**). Analysis of this gene set identified multiple interaction nodes converging on Notch1, NF-κB and the CBP (**Figure 3.10B**). While no significant interaction networks was identified for the small subset of genes displaying decreased methylation and decreased expression at P14, analysis of the gene set associated with decreased methylation and increased expression identified a significant interaction network involving multiple components of the epidermal growth factor receptor (EGFR) and phosphoinositide 3-kinase (PI3K)/Akt signalling pathway (**Figure 3.11**). These findings suggest that DNA methylation regulates the expression of multiple components of key developmental signalling pathways for cardiac development during neonatal life.

3.3.7. Analysis of DNase hypersensitivity regions and TF binding sites associated with DNA methylation during neonatal cardiac maturation

DNA methylation peaks at P14 were intersected with DNase hypersensitivity sites, which are indicative of open chromatin and active transcription, using GSEA with reference to the mouse ENCODE project. Intersection of DNA methylation peaks at P14 with ENCODE data identified DNase hypersensitivity regions associated with undifferentiated mouse ESCs (**Figure 3.12A**). GSEA was also used to intersect P14 methylation peaks with ChIP-seq data from the mouse ENCODE project for identification of TF binding sites. Intersection of DNA methylation peaks at P14 with ENCODE revealed a significant overlap with ChIP-seq data sets for multiple TFs associated with muscle differentiation in C2C12 cells (**Figure 3.12B**). Notably, P14 methylation peaks displayed significant intersection with myogenic TF binding sites (e.g. myogenin (Myog) and Myod), as well as transcriptional repressors (neuron-restrictive silencer factor (Nrsf) and CCTC

binding factor (Ctcf)) and transcriptional effectors of Wnt signalling (transcription factor 3 (Tcf3)) (**Figure 3.12B**).

Additionally, a *de novo* search for enriched TF binding sites was performed to identify binding sites that overlapped with DNA methylation peaks at P1 and P14. Intersection of DNA methylation peaks at P14 with known TF binding motifs using Homer revealed a highly significant enrichment for several TF binding sites associated with myogenic differentiation including MADS-box, Tbx5, Smad2/3/4, and Foxh1 (**Figure 3.12C**). These findings point to a potential interaction between myogenic and Smad TFs with the DNA methylation machinery during neonatal heart maturation.

Table 3.1. Summary of the total number of differentially expressed genes and DMRs between P1 and P14 from RNA-seq and MBD-seq.

	Number of regions Higher at P1	Number of regions Higher at P14	Total
RNA-seq (FDR ≤ 0.05)	3243	3233	6476
MBD-seq (FDR ≤ 0.05)	540	2005	2545

Table 3.2. MBD-seq quality control summary.

	Total reads	QC passed reads	Aligned reads
P1-1	33903541	33675705	32911534
P1-2	34214266	33751319	33036386
P1-3	33554267	33361709	32690433
P14-1	30736962	30597908	30167706
P14-2	34335375	34131579	33532376
P14-3	32694036	32526986	31806532
P1 Total	101672074	100788733	98638353
P14 Total	97766373	97256473	95506614

Table 3.3. Summary of the total number of genes and distribution of DNA methylation marks with differential methylation levels and mRNA expression changes between P1 and P14 (CpG shore: CGS).

Correlation of mRNA expression levels and DNA methylation levels	Number of genes	%							
		TSS 1 kbp	TSS 3 kbp	Exon	CDS	CGI	CGS	Intergenic	Intron
↑CpG ↓mRNA	143	25.9	37.1	69.9	65.0	16.1	25.2	4.9	90.9
↓CpG ↑mRNA	36	19.4	41.7	22.2	16.7	0.0	16.7	2.8	88.9
↑CpG ↑mRNA	355	36.1	55.5	90.1	87.0	34.9	45.6	8.2	94.1
↓CpG ↓mRNA	30	16.7	30.0	43.3	30.0	0.0	13.3	10.0	86.7
Total number of genes	564								

*Please note that many DMRs overlapped multiple regions of a gene (e.g. a DMR can span exons and introns of the same gene). Therefore, the percentage of the distribution of DNA methylation marks does not sum up to 100%.

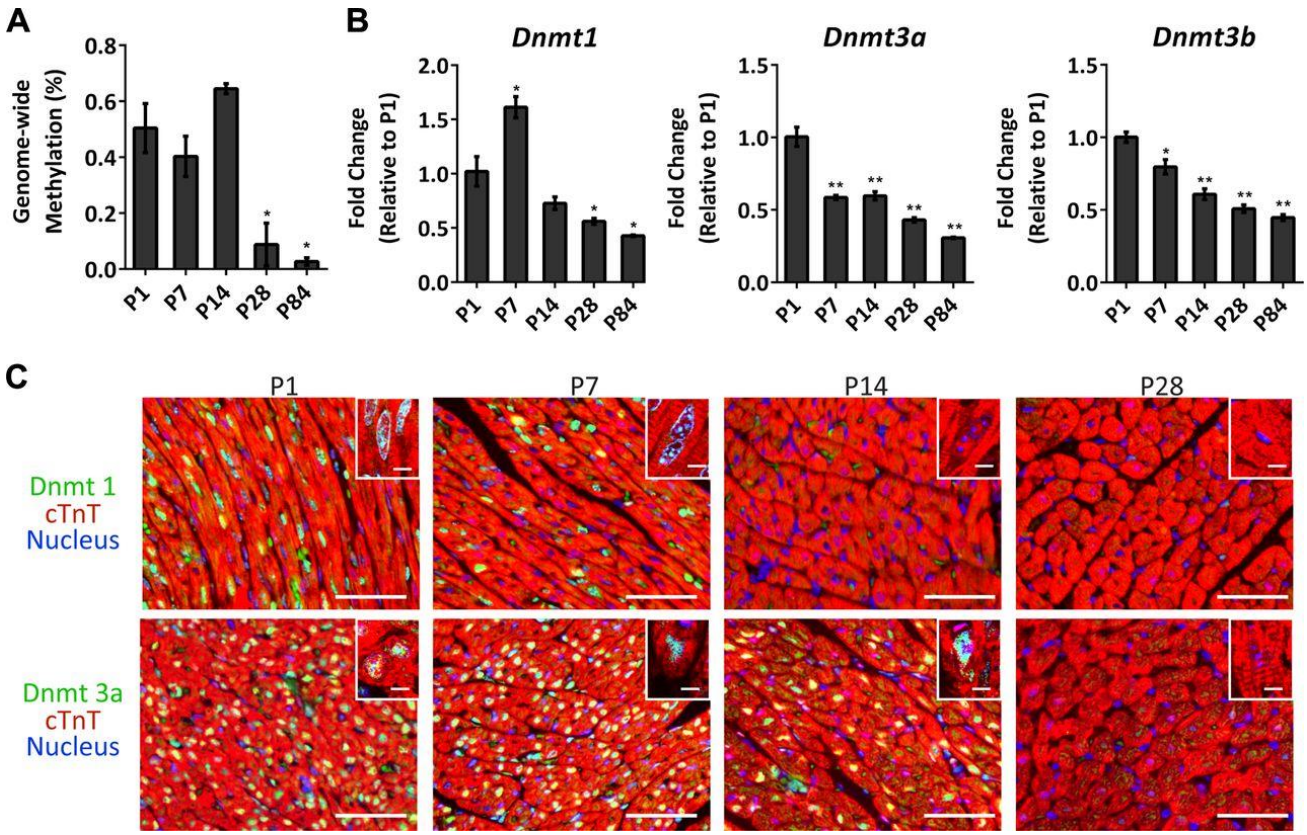

Figure 3.1. DNA methylation profiling during postnatal cardiac development.

A. Genomic DNA methylation levels in mouse cardiac ventricles from P1 to P84 (n=3 per time point; *P<0.05).

B. qPCR gene expression profiling of *Dnmt1*, *3a* and *3b* in mouse cardiac ventricles from P1 to P84. Expression levels of each Dnmt are normalized to 18S and represented as a fold change relative to P1 ventricles (n=3 per time point; *P<0.05, **P<0.001).

C. Immunohistochemistry staining for Dnmt1 and Dnmt3a in mouse hearts from P1 to P28. Red = cTnnT, green = Dnmt1 or Dnmt3a, blue = nuclei. Dnmt1/3a positive cardiomyocytes are also shown in the high magnification inset in the top right hand corner of each panel. Scale bar = 50 μm in main figure and 5 μm in high magnification inset.

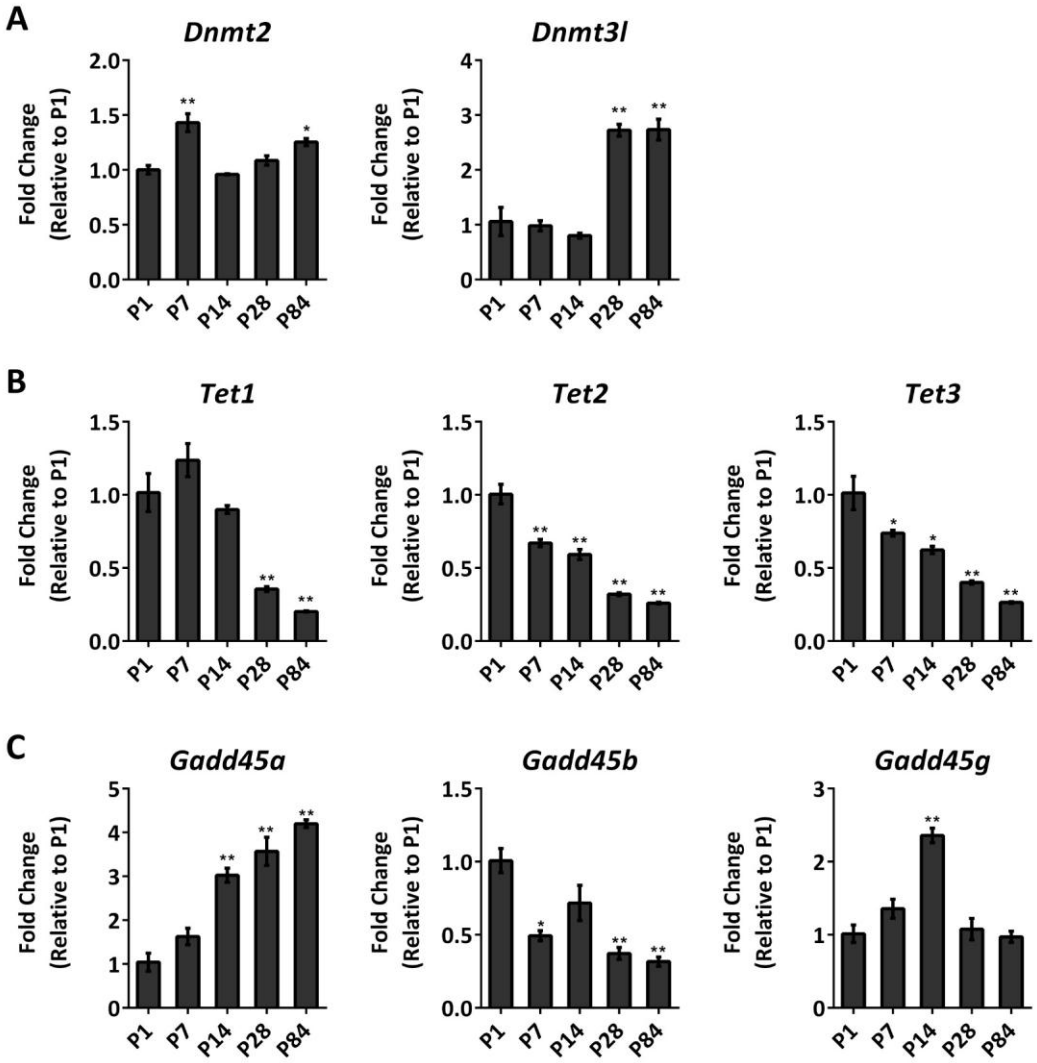

Figure 3.2. Expression profiling of non-canonical Dnmts and enzymes involved in active DNA demethylation during postnatal cardiac development.

A. qPCR gene expression profiling of *Dnmt2* and *Dnmt3l* in cardiac ventricles from P1 to 12 weeks-of-age. (n=3 per group).

B. qPCR gene expression profiling of Tet family enzymes from P1 to 12 weeks-of-age (n=3 per group).

C. qPCR gene expression profiling of Gadd45 family enzymes from P1 to 12 weeks-of-age (n=3 per group). All gene expression values are normalized to 18S and presented as a fold change relative to P1. All data are presented as mean ±s.e.m. *P<0.05, ** P <0.001).

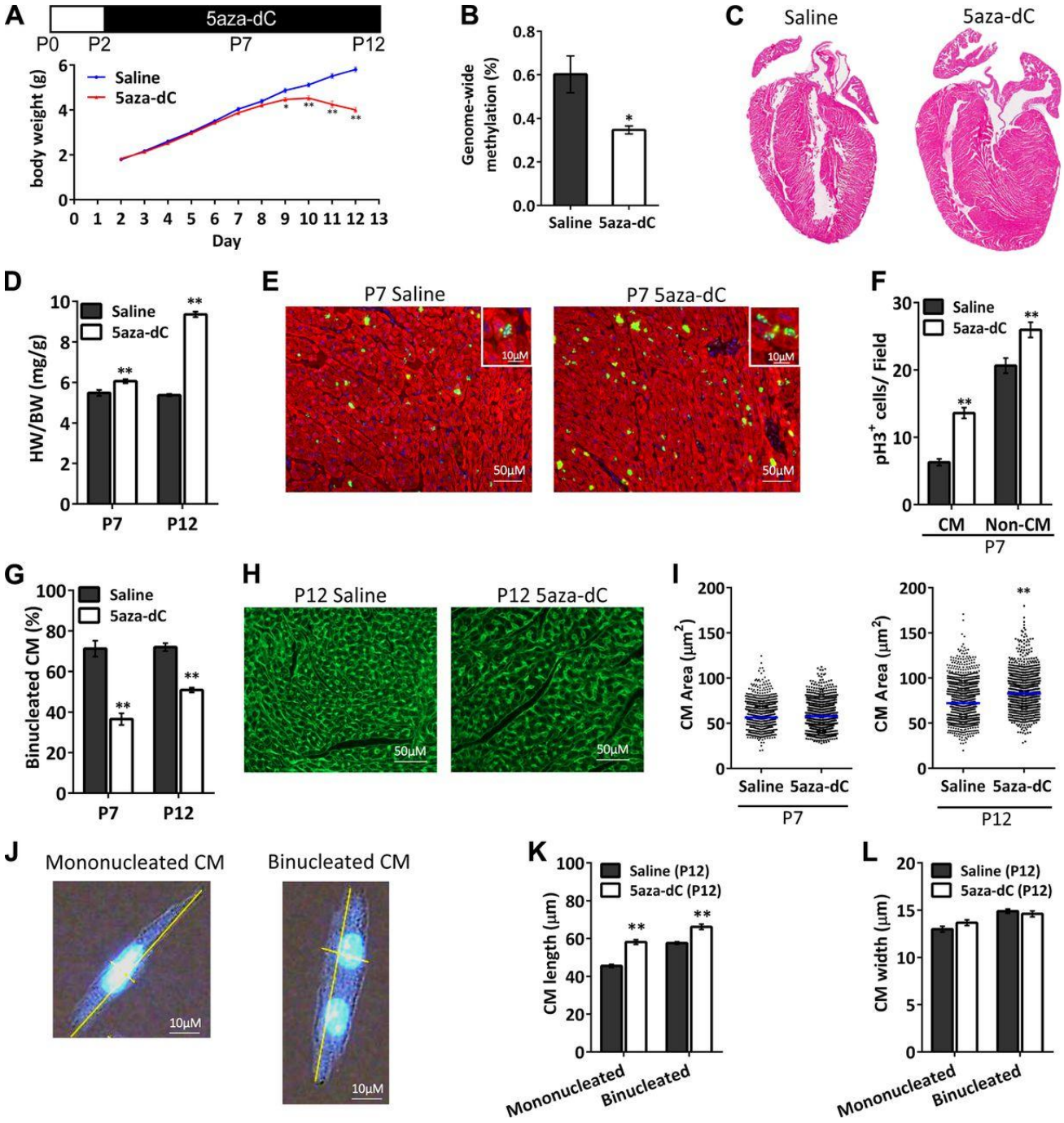

Figure 3.3. Pharmacological inhibition of DNA methylation during neonatal life promotes cardiac cell proliferation and blocks cardiomyocyte binucleation.

A. Growth curve for CD-1/ICR mice treated with 5aza-dC from P2 to P12 (*n*=14-15 per group). **P*<0.05, ***P*<0.001.

B. H&E staining of saline and 5aza-dC-treated hearts at P12.

C. Genomic DNA methylation levels of saline and 5aza-dC treated mice at P12 (*n*=4 per group; **P*<0.05).

D. Heart weight to body weight ratios for saline and 5aza-dC-treated mice at P7 (*n*=11-17 per group) and P12 (*n*=7-14 per group). ***P*<0.001.

E. Immunohistochemistry staining of saline and 5aza-dC-treated hearts at P7. Green = pH3, red = cardiac troponin T, blue = nuclei. $pH3^+$ cardiomyocytes are also shown in the high magnification inset in the top right hand corner of each panel. Scale bar = 50 μm in the main figure and 10 μm in the high magnification inset.

F. Quantification of $pH3^+$cardiomyocytes (CM) and non-cardiomyocytes (non-CM) in saline and 5aza-dC-treated hearts at P7. Data are presented as cells/field for n=4-6 independent samples per group (10 fields of cells assessed per heart). ***P*<0.001.

G. Quantification of the percentage of binucleated cardiomyocytes at P7 (*n*= 4-6 per group; *N*=100 cells per sample) and P12 (*n*= 3-5 per group; *N*=100 cells per sample). ***P*<0.001.

H. WGA staining of saline and 5aza-dC-treated hearts at P12. Scale bar = 50 μm.

I. Scatter plot of quantified cardiomyocyte cross-sectional surface area in saline and 5aza-dC-treated hearts at P7 (*n*=4-5 per group) and P12 (*n*= 3-5 per group) (10 fields of cells assessed per heart). Blue line represents median. ***P*<0.001.

J. Hoechst staining of mononucleated and binucleated cardiomyocytes. Scale bar = 10 μm.

K, L. Quantification of cardiomyocyte length (K) and width (L) in saline and 5aza-dC-treated hearts at P12 (*n*= 3-5 per group; *N*=100 cells per heart). Data are presented as average cell length or width per group. All values are presented as mean ± s.e.m. **P*<0.05, ***P*<0.001.

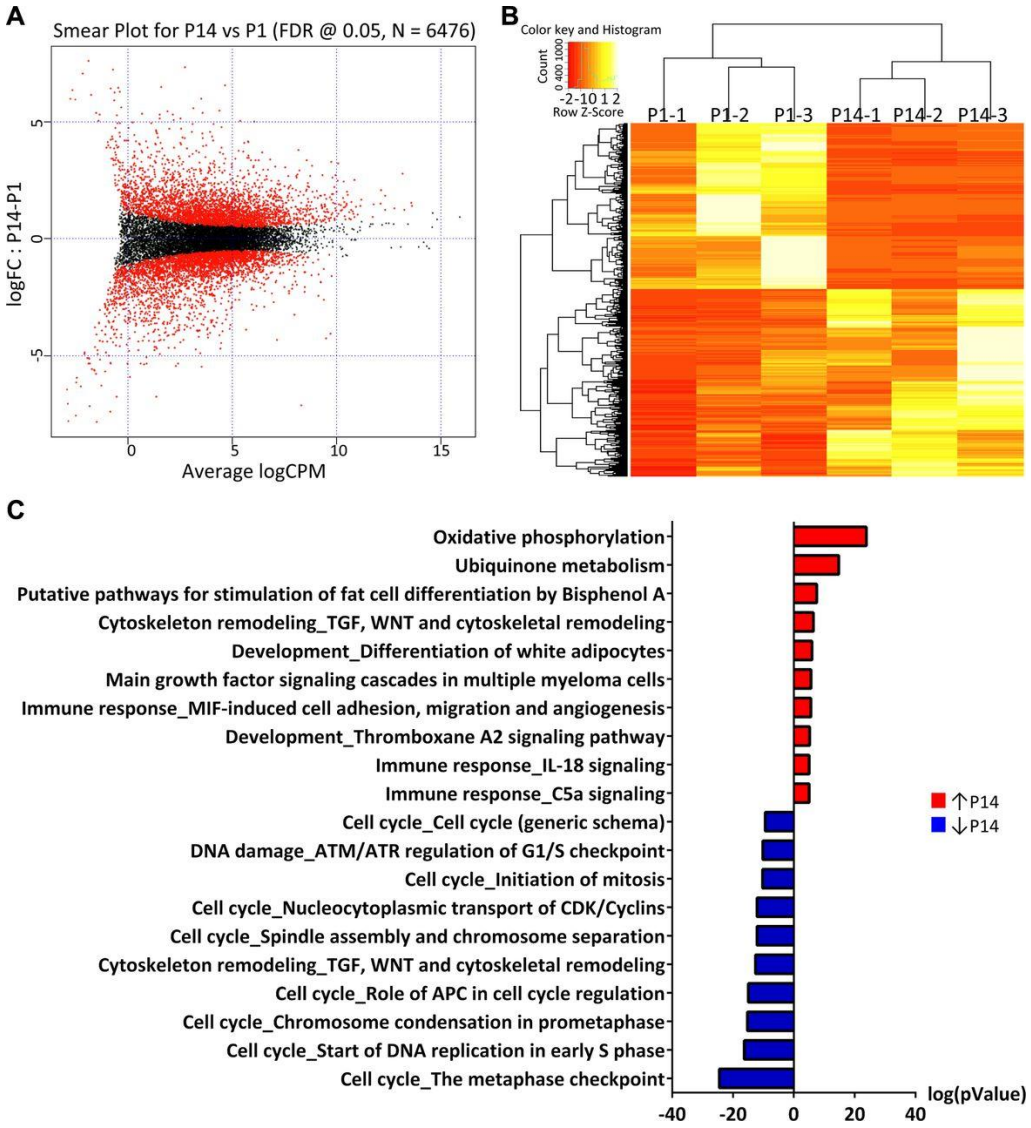

Figure 3.4. RNA-seq analysis of gene expression changes during neonatal heart development.

A. Smear plot of RNA-seq data showing average signal intensity (x-axis) versus log2 fold change in gene expression (P14/P1). Differentially expressed genes (FDR ≤ 0.05, *n*=6476) are shown in red and non-significant changes are shown in black.

B. Heatmap of differentially expressed genes from P1 to P14. Genes with higher expression levels are shown in yellow whereas genes with lower expression levels are shown in red.

C. Gene GO pathway analysis (MetaCore) for differentially regulated genes in P1 versus P14 hearts. Genes that have higher expression levels at P1 (Blue) or higher expression levels at P14 (Red).

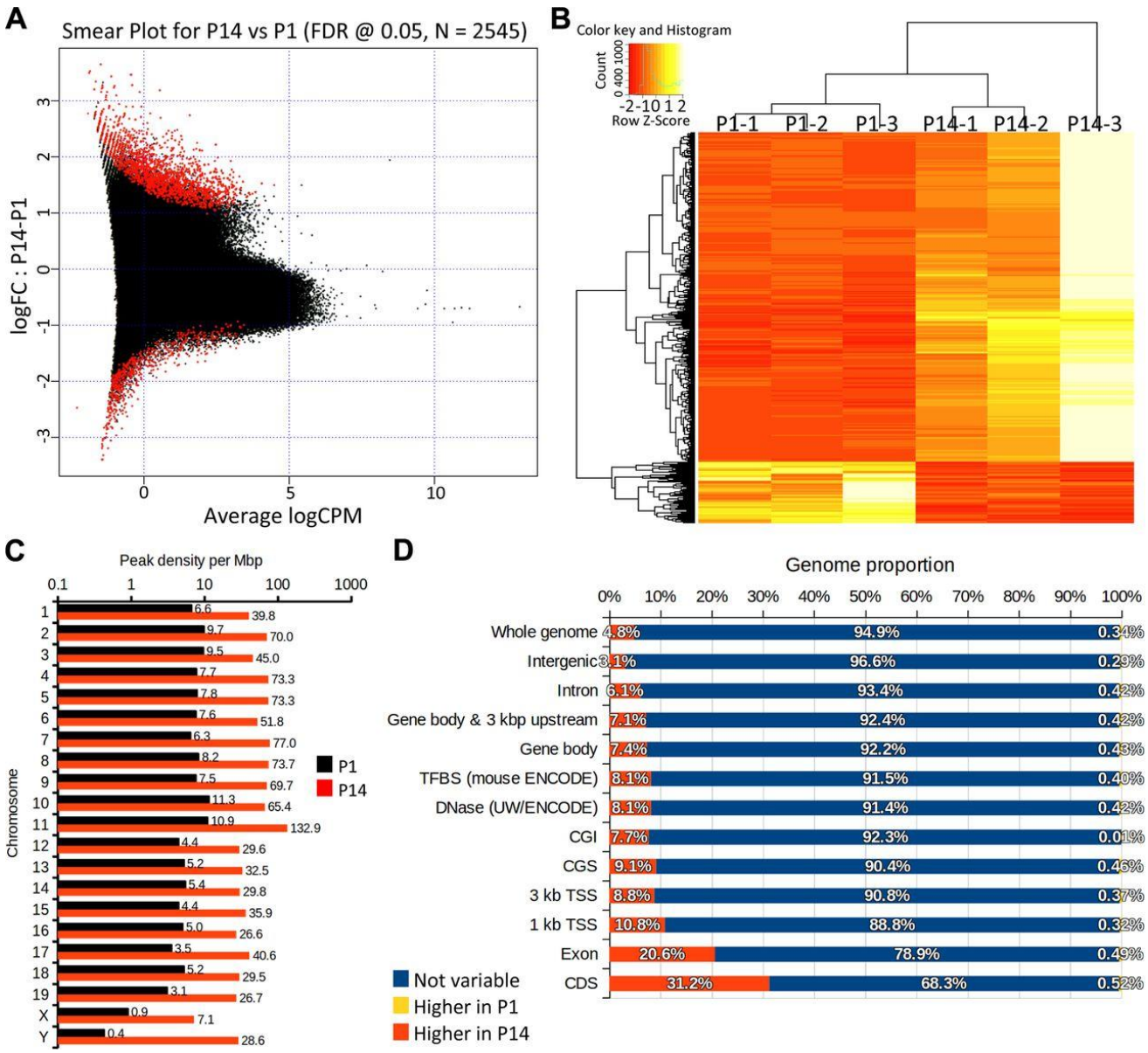

Figure 3.5. MBD-seq analysis of DNA methylation changes occurring during neonatal heart development.

A. Smear plot of MBD-seq data showing average signal intensity (x-axis) versus log2 fold change in MBD enrichment (P14/P1). DMRs (FDR ≤ 0.05, *n*=2545) are shown in red and non-significant changes are shown in black.

B. Heatmap of DMRs identified from MBD-seq. Regions with higher methylation levels are shown in yellow whereas regions with lower methylation levels are shown in red.

C. Distribution of DMRs across each chromosome at P1 (black) and P14 (red) for mouse (mm10) genome normalised by chromosome length.

D. Distribution of DMRs shown by genomic features. Hypermethylated regions at P1 are shown in yellow, hypermethylated regions at P14 are shown in red and regions without significant differential methylation are shown in blue.

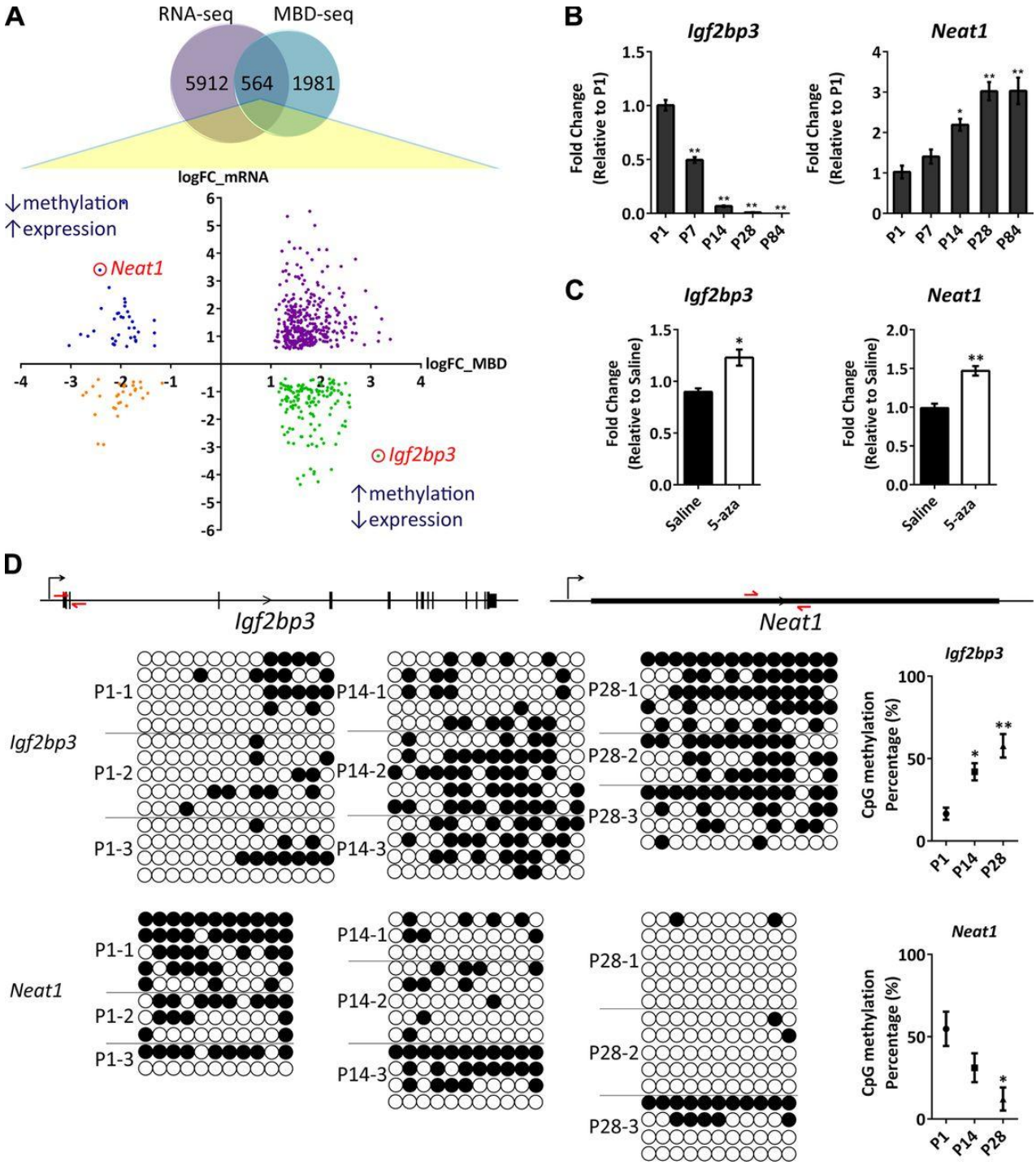

Figure 3.6. Integration of RNA-seq and MBD-seq identifies complex relationships between DNA methylation and transcription during neonatal heart development.

A. (Top) Venn diagram of differentially regulated genes from RNA-seq and MBD-seq data sets. 564 genes with differential methylation between P1 and P14 were also differentially expressed during this period. (Bottom) The scatter plot shows log2 fold changes in mRNA expression levels (y-axis) against log2 fold changes in MBD enrichment (x-axis).

B. qPCR gene expression profiling of *Igf2bp3* and *Neat1* in mouse cardiac ventricles from P1 to P84. Expression levels of *Igf2bp3* and *Neat1* are normalized to 18S and represented as a fold change relative to P1 ventricles (*n*=3 per group). Data are presented as mean ± s.e.m. **P*<0.05, ***P*<0.001.

C. qPCR gene expression profiling of *Igf2bp3* and *Neat1* in saline and 5aza-dC treated hearts at P7. Expression levels of *Igf2bp3* and *Neat1* are normalized to 18S and represented as a fold change relative to P1 ventricles (*n*=4-6 per group). Data are presented as mean ± s.e.m. **P*<0.05, ***P*<0.001.

D. Bisulphite sequencing of *Igf2bp3* and *Neat1* in cardiac ventricles at P1, P14 and P28 (*n*=3 per group). A schematic of the genomic region selected for bisulphite sequencing is shown above with the sequenced region denoted by red arrows. Black dot: methylated CpG site, white dot: unmethylated CpG site. Quantification of the percentage of CpG methylation of target genes at P1, P14 and P28 is also shown. Data are presented as mean ± s.e.m. **P*<0.05, ***P*<0.001.

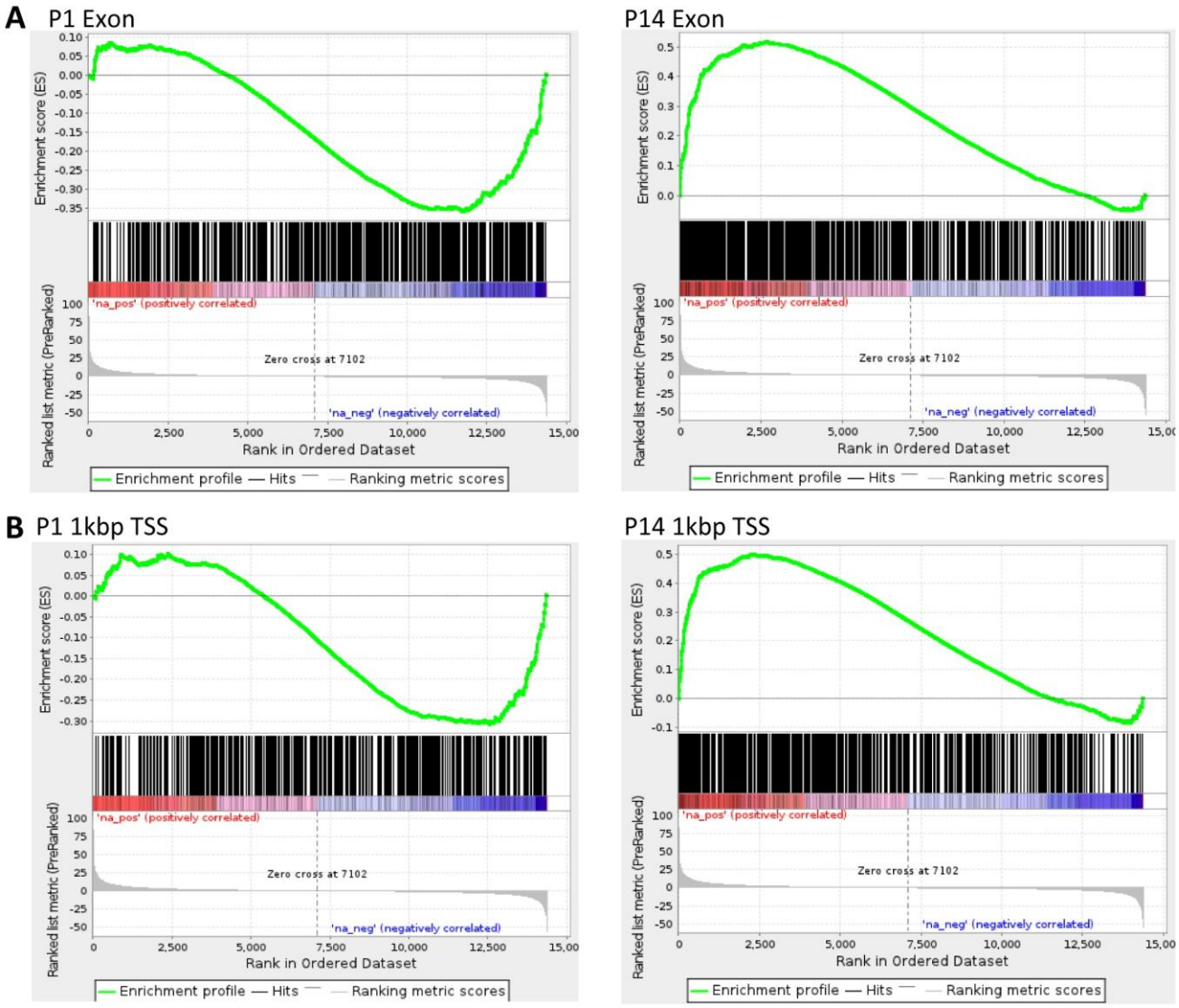

Figure 3.7. Statistical correlation analysis of DMRs with gene expression changes at P1 and P14.

A. GSEA identifies a positive correlation between exon methylation and gene transcription at P14. In contrast, methylation across exon at P1 was negatively correlated with gene expression levels at P1.

B. GSEA identifies a positive correlation between TSS methylation and gene transcription at P14. In contrast, methylation across TSS at P1 was negatively correlated with gene expression at P1.

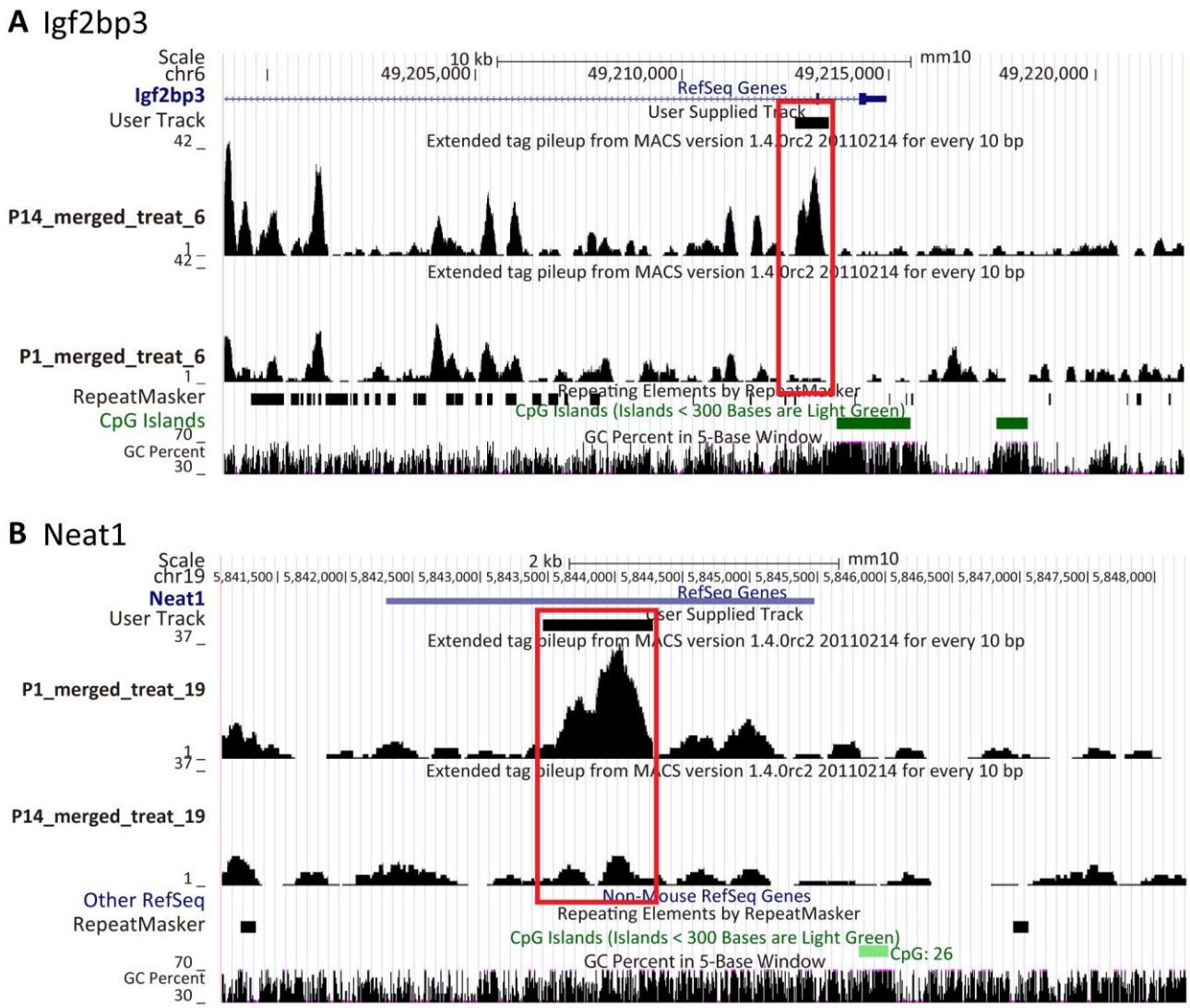

Figure 3.8. Map of MBD-seq reads across the *Igf2bp3* and *Neat1* loci in P1 and P14 hearts.

A. Map of MBD-seq reads across the *Igf2bp3* locus between P1 and P14. DMR highlighted in red.

B. Map of MBD-seq reads across the *Neat1* locus between P1 and P14. DMR highlighted in red.

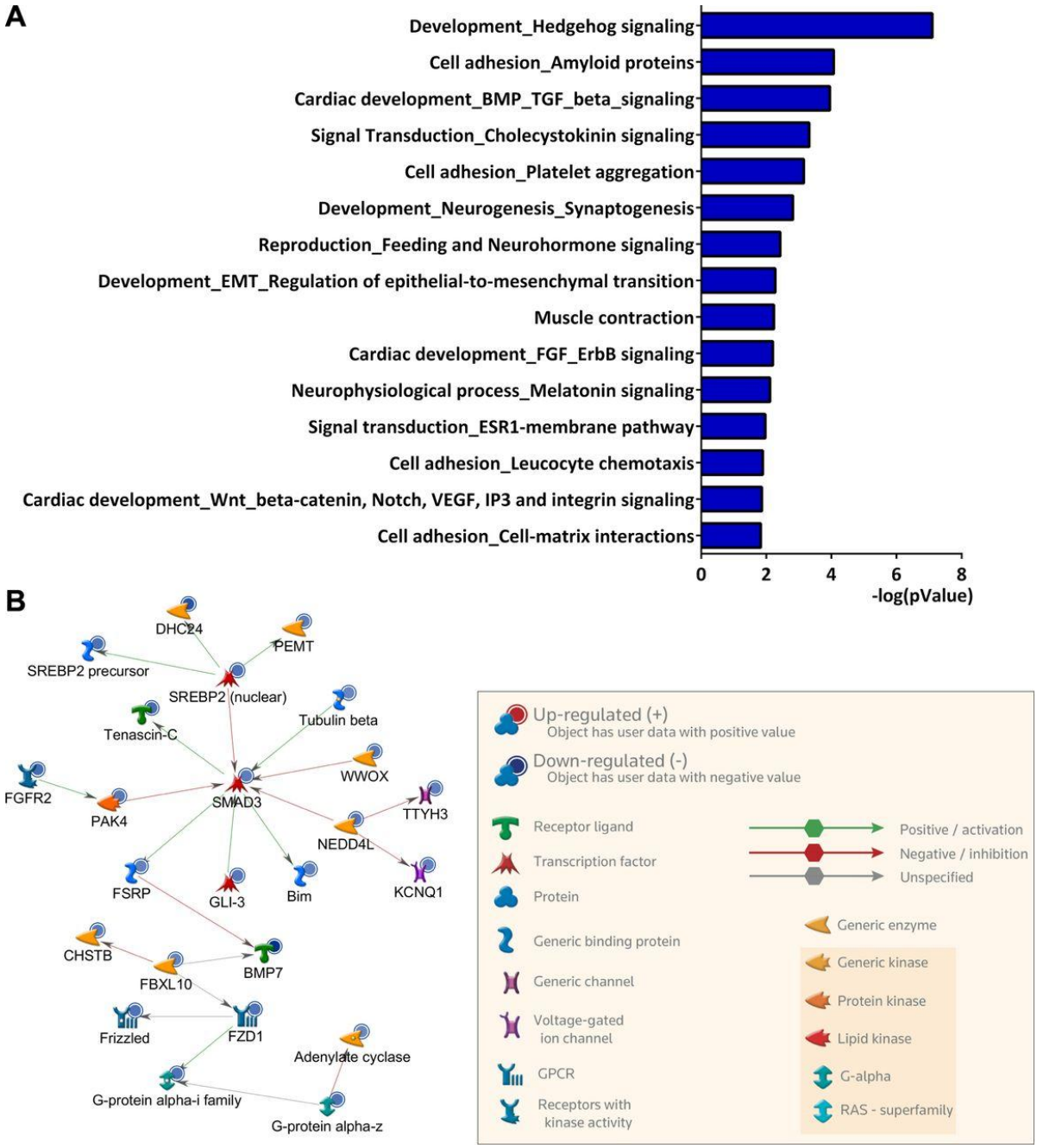

Figure 3.9. Gene ontology and biological network analysis for hypermethylated genes associated with transcriptional repression during neonatal cardiac maturation.

A. Gene GO process network analysis for the 143 genes with increased methylation and decreased mRNA expression from P1 to P14.

B. Interaction network created by Gene GO using genes with increased DNA methylation and decreased mRNA expression levels from P1 to P14.

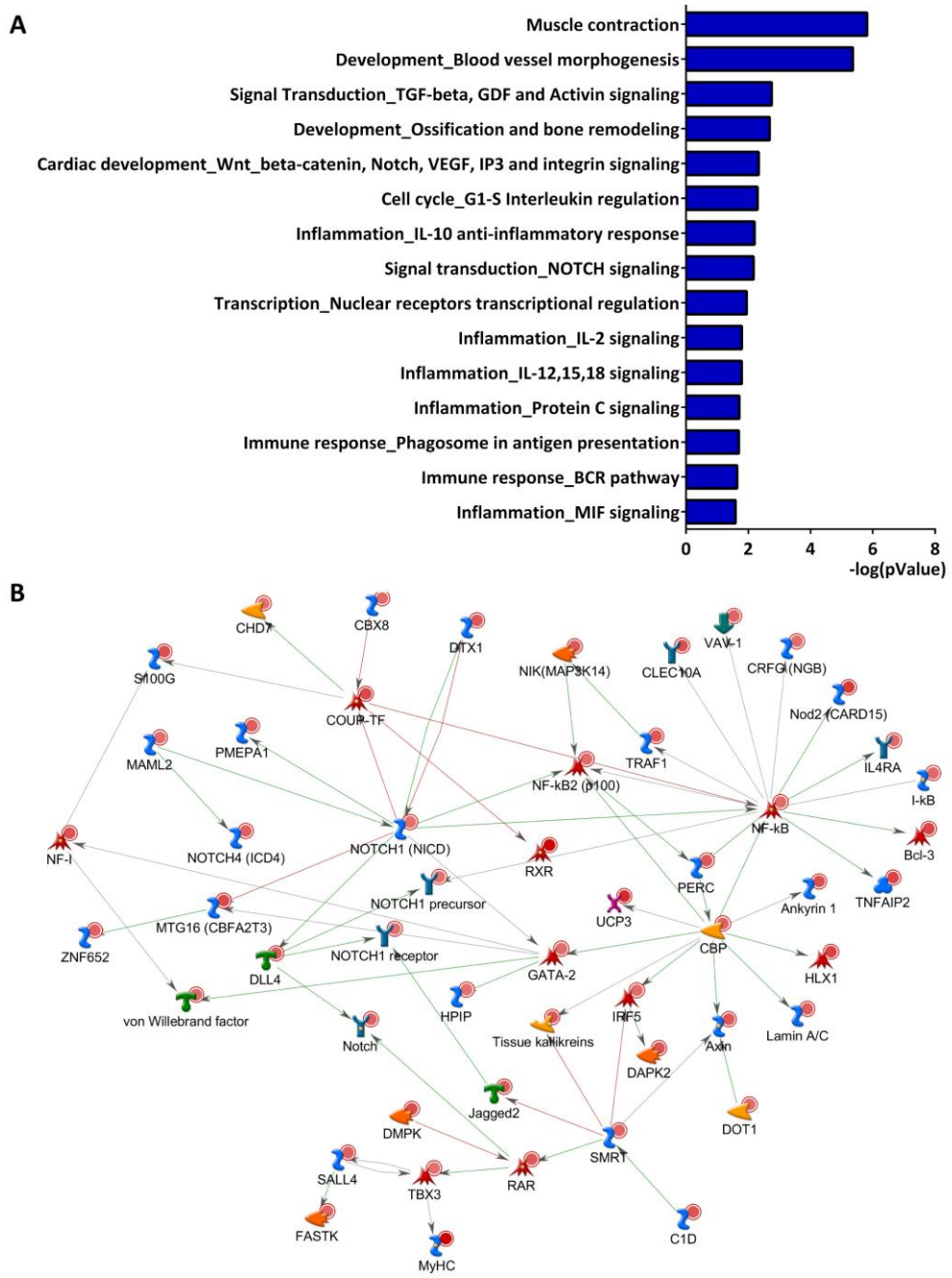

Figure 3.10. Gene ontology and biological network analysis for hypermethylated genes associated with transcriptional activation during neonatal cardiac maturation.

A. Gene GO process network analysis for the 355 genes with increased methylation and increased mRNA expression from P1 to P14.

B. Interaction network created by Gene GO using genes with increased DNA methylation and increased mRNA expression levels from P1 to P14.

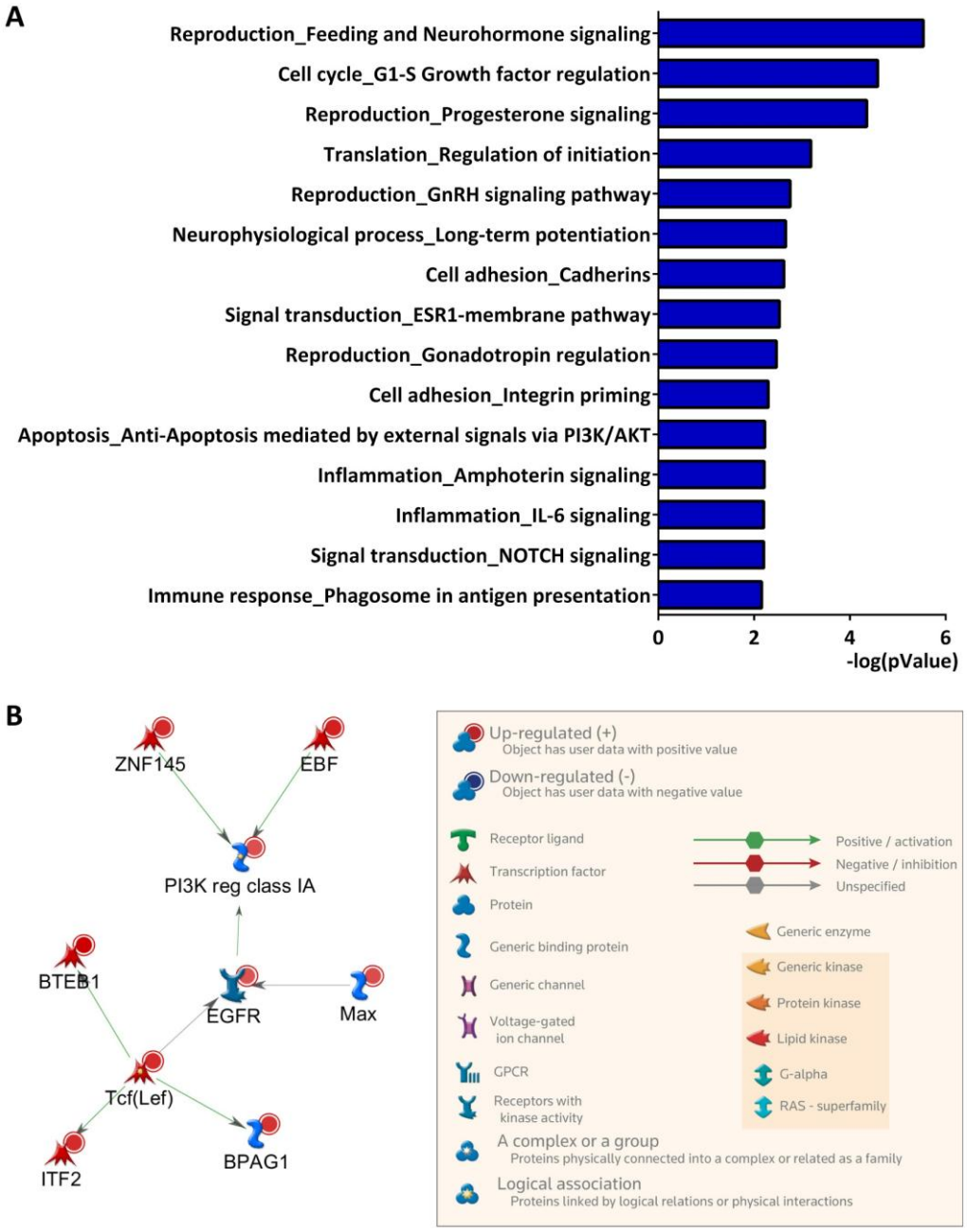

Figure 3.11. Gene ontology and biological network analysis for hypomethylated genes associated with transcriptional activation during neonatal cardiac maturation.

A. Gene GO process network analysis for the 36 genes with decreased methylation and increased mRNA expression from P1 to P14.

B. Interaction network created by Gene GO using genes with decreased DNA methylation and increased mRNA expression levels from P1 to P14.

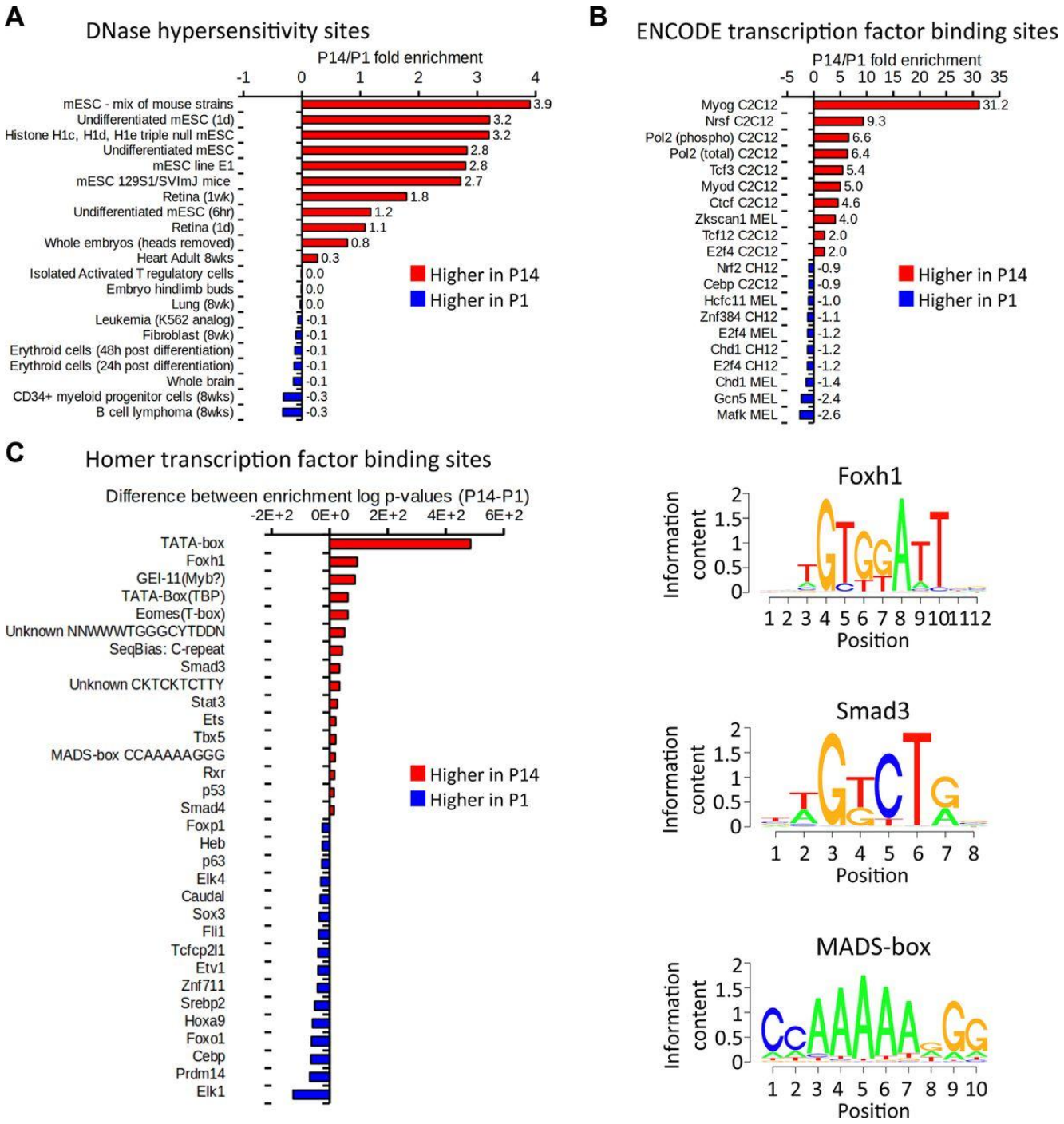

Figure 3.12. Analysis of DMRs for enriched DNase hypersensitivity sites and enriched TF binding sites at P14.

A. Relative fold enrichment of Mouse ENCODE DNase hypersensitivity between P14:P1 peak sets. Peak intersections with a positive value show enrichment in P14 peak regions (hypermethylation), while negative values depict enrichment in the P1 peak regions (hypomethylation).

B. Relative fold enrichment of Mouse ENCODE TF binding sites between P14:P1 peak sets. Peak intersections with a positive value show enrichment in P14 peak regions (hypermethylation), while negative values depict enrichment in the P1 peak regions (hypomethylation).

C. *De novo* analysis of enriched TF binding sites between P14 and P1 using Homer. TF binding motifs for Foxh1, Smad3 and MADS-box are displayed on the right.

3.4. Discussion and conclusion

This chapter demonstrates, for the first time, that DNA methylation events are associated with changes in cardiac gene expression during neonatal heart development. The findings indicate that DNA methylation levels are not static during postnatal heart development but rather undergo dynamic alterations during neonatal life. Specifically, two postnatal waves of DNA methylation were identified in the rodent heart involving increased site-specific methylation from P1 to P14, followed by a global decrease in genomic methylation levels after P14. Importantly, global inhibition of DNA methylation during the neonatal period promotes cardiac cell proliferation and inhibits cardiomyocyte binucleation, suggesting that DNA methylation is required for neonatal cardiac maturation. Bioinformatics analyses suggest that this process might be regulated through methylation of several canonical developmental and differentiation-associated signalling pathways including Hedgehog, TGFβ, FGF, Notch and Wnt. Notably, DMRs were highly enriched for MyoG, Tbox and Smad 2/3/4 TF binding sites, suggesting that interplay between myogenic TFs and the epigenetic machinery might contribute to the regulation of gene expression networks during neonatal cardiac differentiation. The current chapter identifies a novel role for DNA methylation during neonatal heart development and is consistent with an epigenetic mechanism for cell cycle arrest in the postnatal heart.

One of the most surprising observations of the current study was the identification of two postnatal waves of DNA methylation; one coinciding predominantly with increases in site-specific methylation from P1 to P14 and another involving global hypomethylation after P14. This phenomenon is highly reminiscent of previously reported patterns of DNA methylation associated with aging and cancer (Issa, 2014). Specifically, methylation drift occurs during aging and cancer development, with numerous studies identifying an increase in site-specific DNA methylation (e.g. at promoter regions), occurring coincident with global hypomethylation across intergenic regions and repeat sequences (Issa, 2014). This DNA methylation pattern is conserved between species and across multiple organs during aging. Notably, a prominent methylation shift is observed in more proliferative tissues, including colon, stomach and liver (Issa, 2014). Interestingly, multiple studies suggest that age-related changes in DNA methylation predominantly occur at genes associated with developmental signalling pathways and organogenesis (Issa, 2014), which is similar to the findings of the current study in neonatal hearts. While the functional significance and specific genomic regions affected by the global hypomethylation after P14 are currently unclear, this process may reflect an age-dependent loss of DNA integrity during postnatal cardiac maturation. A recent report provided evidence for a progressive increase in oxidative DNA damage during postnatal cardiac

maturation (Puente et al., 2014) and several studies have suggested that the presence of unrepaired lesions in DNA substantially alters the methylation capacity of Dnmts, leading to DNA hypomethylation (Cerda and Weitzman, 1997; James et al., 2003). Interestingly, Gadd45a, which is induced by DNA damage and has been implicated in active DNA demethylation (Niehrs and Schafer, 2012), increased at P14. However, transcription of other enzymes implicated in DNA demethylation such as Tet1-3 decreased during postnatal heart development. It is currently unclear whether these DNA demethylating enzymes play a major role in the hypomethylation of the cardiac genome after P14 and further studies will be required to determine whether this is a cardiac-specific phenomenon or whether it has broader implications for postnatal maturation of other tissues..

These findings suggest that DNA methylation events during the first two weeks of life in rodents are required for cardiomyocyte cell cycle arrest and binucleation *in vivo*. While the study design does not permit exclusion of a possible contribution of systemic effects of 5azato the observed cardiac phenotype, the *in vivo* findings are consistent with two recent *in vitro* studies in cultured neonatal rat cardiomyocytes , which suggested that 5azainduces cardiomyocyte proliferation and inhibits endothelin-induced cardiomyocyte binucleation (Felician et al., 2014b; Kou et al., 2010; Paradis et al., 2014). These striking effects of 5azaon cardiomyocyte binucleation are particularly interesting given that hypomethylating agents such as 5azaare commonly used as anti-cancer drugs and have anti-proliferative effects in other cell types. However, it is also known that DNA methylation can have either positive or negative effects on cell proliferation depending on the epigenetic modification of different sub-sets of genes (e.g. oncogenes or tumour suppressor genes). In the present chapter, complex relationships have been identified between DNA methylation during neonatal life and multiple components of key developmental signalling pathways. Neonatal cardiac maturation is associated with hypermethylation of multiple genes associated with critical cardiac developmental signalling pathways such as Hedgehog, FGF, TGFβ, Notch and Wnt signalling. Interestingly, many of these signalling pathways play key roles in the maintenance of cardiomyocyte proliferation during zebrafish heart regeneration (Choi et al., 2013) and activation of these pathways drives precocious proliferation of neonatal rodent cardiomyocytes (Porrello and Olson, 2014b). However, re-activation of developmental signalling in adult cardiomyocytes does not robustly re-induce cell cycle activity in adult binucleated cardiomyocytes (Felician et al., 2014a; Porrello and Olson, 2014b). These findings suggest that epigenetic regulation of key developmental signalling pathways during neonatal life contributes to cardiomyocyte terminal differentiation.

It is noteworthy that DMRs at P14 were highly enriched for TF binding motifs for myogenic TFs (e.g. MADS-box, Tbx5) and Smad-related TFs (e.g. Smad2/3/4 and Foxh1). The over-

representation of these TF binding sites is particularly interesting given the critical role of TGFβ and myogenic TFs during muscle differentiation. For example, Smad TFs interact with Mef2 to target critical components of the myogenic transcription machinery during C2C12 differentiation (Liu et al., 2004). While the precise mechanism by which the DNA methylation machinery is recruited to specific DNA sequences during neonatal heart development is currently unclear, this process may involve interactions between de novo methyltransferases (Dnmt3a/b) and myogenic TFs (Hervouet et al., 2009). Moreover, the role of TGFβ signalling warrants further investigation, as a recent study suggests that TGFβ-induced anti-proliferative responses involve the recruitment of DNA methylation/de-methylation enzymes to Smad2/3 target genes (Thillainadesan et al., 2012). A recent study also suggests that interactions between Foxh1/Smad2/3 transcriptional complexes and switch-enhancer elements for pluripotency genes underlie context-specific responses to TGFβ mesoendoderm specification (Beyer et al., 2013). Interestingly, we observed significant enrichment for pluripotency-related genes at DNase hypersensitivity regions, as well as enrichment for Smad2/3/4 and Foxh1 binding sites, suggesting that a similar mechanism may be engaged during cardiomyocyte terminal differentiation. Future studies will be required to dissect the potential involvement of TGFβ signalling, as well as interactions between the DNA methylation machinery and myogenic TFs, during cardiomyocyte terminal differentiation.

Overall, the present chapter provides novel insights into the regulatory role of DNA methylation during neonatal cardiac maturation. Although further work is required to elucidate the mechanisms that induce specific methylation changes in the postnatal heart, the current chapter provides support for an epigenetic mechanism for cardiomyocyte terminal differentiation. Additional interrogation of the role of DNA methylation during neonatal heart development may provide an enhanced understanding of the mechanisms that drive cardiac cell cycle arrest and binucleation.

3.5. Summary and future direction

This chapter provides novel evidence for DNA methylation during postnatal heart maturation and suggests that cardiomyocyte cell cycle arrest during the neonatal period is subject to regulation by DNA methylation. However, the mechanism by which DNA methylation shuts down the cardiac cell cycle after birth remains unclear. In the following chapter, the role of DNA methylation in regulating cell proliferation genes as well as human cardiomyocyte proliferation are examined to further understand the mechanism of postnatal cardiomyocyte maturation in rodents and humans.

Chapter 4

DNA methylation is essential for cell cycle regulation in mouse and human cardiomyocytes

Persistence in scientific research leads to what I call instinct for truth.

Louis Pasteur.

Chapter 4. DNA methylation is essential for cell cycle regulation in mouse and human cardiomyocytes

4.1. Introduction

In Chapter 3, DNA methylation was found to be an essential upstream regulator of cardiomyocyte proliferation during early postnatal heart development in the mouse. However, a direct relationship between DNA methylation and the expression of proliferative gene networks during neonatal myocyte development was not evident in previous studies (Chapter 3). As DNA methylation is known for its ability to induce long-lasting transcriptional repression, it was hypothesised that DNA methylation regulates early postnatal cardiomyocyte proliferation through direct repression of cell cycle promoters.

DNA methylation status has been repeatedly linked with cancer cell proliferation through repression of tumour suppressor genes or activation of oncogenes, both of which play a critical role in regulating cell cycle activity (Baylin, 2005; Ehrlich, 2002; Luczak and Jagodzinski, 2006). With respect to heart development, Li et al reported that loss of DNA methylation leads to foetal lethality by E10.5 with cardiac developmental defects, suggesting an indispensible role of DNA methylation during embryonic heart development (Li et al., 1992). A more recent study by Felician and colleagues has demonstrated that hypermethylation in the promoter region of Notch signalling components and target genes occurs concomitant with the developmental shutdown of this critical signalling pathway during cardiomyocyte terminal differentiation (Felician et al., 2014a). Treatment of 5aza-dC caused hypomethylation at promoter loci of Notch signalling components (Notch1, Hes1, cell cycle promoters) and increased expression levels of associated genes. Moreover, 5aza-dC caused activation of cell proliferation in neonatal cardiomyocytes, suggesting DNA methylation modulates cardiomyocyte proliferation through transcriptional repression (Felician et al., 2014a). Furthermore, another recent study has reported that inhibition of neonatal rat cardiomyocyte proliferation following treatment with dexamethasone is due to promoter hypermethylation and transcriptional repression of cell cycle genes, including Ccnd2 (Gay et al., 2016). Gay et al. also demonstrated that 5aza-dC reactivated cell proliferation in dexamethasone-treated cardiomyocytes through restoration of *Ccnd2* expression, providing further support for a direct role for DNA methylation in regulating transcription of cell cycle genes (Gay et al., 2016). Therefore,

identification of the direct targets of DNA methylation at specific cell cycle genes is critical to understand the mechanism of postnatal cardiomyocyte cell cycle arrest.

In the present chapter, the relationship between DNA methylation and transcription of specific genes involved in cell proliferation were investigated in both mouse and human cardiomyocytes. Cross-referencing the RNA-seq and MBD-seq datasets from Chapter 3 identified a subset of cell proliferation genes that were differentially methylated during mouse heart development. Moreover, *in vitro* cell culture of human ESC differentiated cardiomyocytes demonstrated that DNA methylation was crucial for human cardiomyocyte proliferation. However, only 1 out of 4 of the validated DNA methylation target genes was conserved between mouse and human cardiomyocytes, implicating potential species differences in the cardiomyocyte cell cycle regulatory network. These results provide further evidence for a role of DNA methylation in regulating genes involved in cell proliferation during cardiomyocyte maturation and also suggest potential species differences between rodents and humans.

4.2. Methodology

4.2.1. Identification of differentially regulated and methylated cell cycle related genes

Utilizing the genes that were previously identified from RNA-seq and MBD-seq in Chapter 3 (**Appendix 7.1**), 143 genes with hypermethylation associated with transcriptional repression, as well as 36 genes with hypomethylation associated with transcriptional activation were isolated from the list. Genes that were previously known to be involved in cell cycle and proliferation activities were then selected using the NCBI (http://www.ncbi.nlm.nih.gov/) and GeneCards (www.genecards.org) databases for further experimental validation.

4.2.2. *In vitro* administration of 5aza-dC to 3D hESC differentiated cardiomyocytes

Briefly, the embryonic stem cell line H9 (WiCell, Madison, WI, USA) was maintained in mTeSR (Stemcell Technologies, Vancouver, Canada) on Matrigel (Corning, Tewksbury, MA, USA) coated flasks and was passaged using TypLE (Thermo Fisher Scientific (Gibco)). ESCs were differentiated into cardiac cells using 2D cardiomyocyte differentiation protocol yielding ~75% cardiomyocytes and ~25% stromal cells. Differentiated cardiomyocytes were then seeded into a 96-well cardiac tissue engineering platform (Heart-Dyno) recently developed in the Cardiac Regeneration Lab which facilitates mechanical loading during culture to form hCOs (**Figure 4.5A, B**). Tissues formed over 2 days and were cultured for another 5 days (**Figure 4.5A)**. For 5aza-dC treatment experiments, 5aza-dC was added 7 days after differentiated cardiomyocytes were seeded in the Heart-Dyno. 5aza-dC was prepared fresh daily in culture media and a final concentration of 10μM 5aza-dC was used to treat hCOs with no treatment (media alone) used as control.

4.2.3. DNA and RNA extraction of 3D hESC derived cardiomyocytes

For DNA or RNA extraction of hCOs, 3 hCOs were pooled together prior processing using standard methods (described in Chapter 2 – 2.2, 2.3).

4.2.4. Immunostaining of hCOs for proliferation

48 hours after hCOs were treated with 10μM 5aza-dC, tissues were washed wish PBS followed by fixation with 1% PFA at room temperature for 20 minutes. Tissues were then washed with PBS and

then blocked in blocking buffer (PBS, 5% FBS, 0.025% Triton X-100) for 5 minutes at room temperature. Primary antibodies were diluted in blocking buffer and incubated overnight at 4 ℃. The following primary antibodies were used for immunofluorescence staining: ACTN2 (EA-53, 1:1000, mouse monoclonal A7811, Sigma-Aldrich) and pH3 (Ser10) (1:100, rabbit polyclonal 06-570, Merck Millipore). Following primary antibody incubation, sections were washed in blocking buffer for 1 hour at 4 ℃ and then incubated with secondary antibodies conjugated with Alexa Fluor 488 or 555 (1: 400, Thermo Fisher Scientific (Molecular Probes)) and Hoechst (1:1000, H21492, Thermo Fisher Scientific (Molecular Probes)) overnight at 4 ℃. Tissues were washed in blocking buffer for 1 hour at 4 ℃ followed by another wash in PBS before being mounted with Fluoromount-G (Southern Biotech). Photos were taken under Olympus FV1000 Inverted Confocal Microscope (Olympus, Shinjuku, Tokyo, Japan). Quantitative analyses of cardiomyocyte mitosis were performed using ImageJ as previously described (Porrello et al., 2011b)

4.2.5. Visualization of ENCODE ChIP-seq peaks (H3K4me1, H3K4me3 and H3K27ac) in UCSC genome browser

The *Igf2bp3* and *Ube2c* genomic loci were visualized using the UCSC genome browser (http://genome.ucsc.edu) with tracks for CGI and ENCODE ChIP-seq results for H3K4me1, H3K4me3 and H3K27ac turned on.

4.3. Results

4.3.1. Identification of cell cycle and proliferation genes regulated by DNA methylation during mouse heart development

To further understand the role of DNA methylation in regulating postnatal cardiomyocyte cell cycle arrest, a set of genes with previously reported functions in regulating cell cycle activity and cell proliferation were selected for further analysis (**Figure 4.1; Table 4.1**). As DNA methylation is known for its canonical role in transcriptional repression, this analysis focused on identifying cell proliferation genes that exhibited an inverse relationship between transcription and DNA methylation (**Figure 4.1**). Specifically, cell proliferation genes were selected from 2 correlations of DNA methylation and transcription, which were increased DNA methylation associated with decreased expression of cell cycle activators or decreased DNA methylation associated with increased expression of cell cycle inhibitors (**Figure 4.1; Table 4.1**). From P1 to P14, a total of 16 cell cycle genes were identified that were hypermethylated and transcriptionally repressed. In contrast, only 2 cell cycle genes were hypomethylated and transcriptionally activated from P1 to P14 (**Figure 4.1; Table 4.1**).

qPCR analysis was performed to examine the mRNA levels of selected proliferation genes between P1 to P84. *Insc, Kdm2b, Pold2* and *Smyd2* were not analysed because they could not be efficiently detected after testing 2 different qPCR primer sets (**Table 2.2**). For proliferation genes displaying hypermethylation associated with transcriptional repression, *Igf2, Igf2bp2, Igf2bp3,* and *Pak4* were significantly down-regulated between P1 and P14, consistent with the RNA-seq datasets presented in Chapter 3 (**Figure 4.2**). The rest of the candidates exhibited no statistically significant changes in gene expression between P1 and P14 (**Figure 4.2**). The same analysis was also performed on the proliferation genes displaying hypomethylation associated with transcriptional activation between P1 and P14 (except for *Ptprr*, which failed to be efficiently detected after testing 2 different qPCR primer sets). None of these candidates were significantly regulated by qPCR (**Figure 4.3A**).

To further validate the relationship between DNA methylation and transcription of the selected cell proliferation genes, qPCR analysis was performed to examine their expression levels in heart samples from mice that were treated with 5aza-dC. Consistent with the expression profiling during development (**Figure 4.2**), *Igf2bp3* exhibited higher expression levels in 5aza-dC treated mice, confirming the relationship between its expression levels and DNA methylation (**Figure 4.4**). Interestingly, while *Chtf18*, *Cit* and *Ube2c* were not significantly regulated between P1 and P14,

their expression levels were significantly up-regulated in 5aza-dC treated mice, suggesting that DNA methylation is essential for their transcriptional regulation during early postnatal heart development in the mouse (**Figure 4.4**). On the other hand, the expression levels of cell proliferation genes that were hypomethylated and associated with transcriptional activation were also examined but these were not significantly regulated by 5aza-dC (**Figure 4.3B**). Together, these findings suggest a subset of genes involved in cell proliferation is subject to regulation by DNA methylation during postnatal heart development in the mouse.

4.3.2. DNA methylation is linked to human cardiomyocyte proliferation

As previously discussed in this thesis, mouse and human hearts have some significant differences in their physiological characteristics (**Table 1.1**). Therefore, it is important to understand whether DNA methylation plays a conserved role in regulating transcription of cell proliferation genes in human cardiomyocytes. Employing a 96-well miniaturized human cardiac organoid platform that was previously established in the lab (**Figure 4.5A, B**), 10 μM 5aza-dC was administered to cultured hCOs to inhibit global DNA methylation levels. The concentration of 10 μM was selected based on previous studies where it was shown to efficiently inhibit DNA methylation without causing pathological effects (Palii et al., 2008; Zhou et al., 2015).

Administration of 5aza-dC induced >50% inhibition of genomic DNA methylation levels in the Heart-Dyno tissues, although this did not reach statistical significance (P=0.77) (**Figure 4.5C**). To test whether inhibition of DNA methylation induced cardiomyocyte proliferation, hCOs were stained with pH3 and the cardiac marker ACTN2 to quantify the incidence of cardiomyocyte mitosis. A 2-fold (from ~1% to ~2%) increase in the number of $pH3^+$ cells by in cardiomyocytes was observed in 5aza-dC treated human cardiac organoids (**Figure 4.5 D, E**), suggesting that DNA methylation is linked to human cardiomyocyte proliferation.

4.3.3. DNA methylation of cell proliferation target genes is not conserved between mice and humans

In order to determine whether the regulation of cell cycle genes by DNA methylation is conserved between mice and humans, the expression levels of the 4 validated cell cycle and proliferation genes (*CHTF18, CIT, IGF2BP3,* and *UBE2C*) in section 4.3.1 (**Figure 4.4**) were examined in the 5aza-dC treated hCOs. *CIT* and *IGF2BP3* could not be detected in hCOs after testing with 2 different qPCR primer sets (**Table 2.2**). qPCR analysis showed that only the expression levels of *CHTF18* were increased following inhibition of DNA methylation in hCOs (**Figure 4.6**),

suggesting that DNA methylation is required for transcription of this gene in both mouse and human cardiomyocytes.

Table 4.1. Summary of cell cycle and proliferation related genes with differential methylation levels and mRNA expression changes between P1 and P14 (NA: not available, UC: unchanged).

Cell cycle related genes in ↑CpG associated with ↓mRNA gene set (16/ 143)						
Genes	**Comments**	**Cell cycle promoter or repressor**	**Expression changes in developmental mouse heart (P1 to P84)**	**Expression changes in 5aza treated mouse heart**	**Expression changes in 5aza treated human Heart-Dynos**	**References**
CDK14	Cyclin-dependent kinase 14. Regulates cell cycle and proliferation through interaction with CCND3. siRNA inhibition led to cell cycle arrest at G1 phase. Regulates Wnt signalling through LRP6 during G2/M phase.	Promoter	↓	UC	NA	(Davidson et al., 2009; Shu et al., 2007)
CHTF18	Chromosome transmission fidelity factor 18. Associate with other component to form replication factor C (RFC) to load	Promoter	↓	↑	↑	(Shiomi et al., 2007)

	proliferating cell nuclei antigen (PCNA) onto DNA during S phase.					
CIT	Citron rho-interacting serine/threonine kinase. Components of central spindle associate with KIF14 to regulate cytokinesis.	Promoter	↓	↑	NA	(Gruneberg et al., 2006; Liu et al., 2003)
CTDP1	Carboxy-terminal domain phosphatase subunit 1. Regulate transcription through phosphorylation of C-terminal domain of RNA polymerase II. Inhibition of CTDP1 led to cell growth repression.	Promoter	↓	UC	NA	(Nguyen et al., 2003; Zhong et al., 2016)
GPSM2	G-protein signalling modulator 2. Forms complex that guide mitotic spindle organization with LGL2 during mitosis.	Promoter	↓	UC	NA	(Yasumi et al., 2005)
IGF2	Insulin-like growth factor 2. Member of insulin family of polypeptide growth factors. Governing development and	Promoter	↓	UC	NA	(Chao and D'Amore, 2008)

	growth process.					
IGF2BP2	Insulin-like growth factor 2 binding protein 2. Member of IGF2 mRNA-binding protein. Binds to IGF2 and regulates IGF2 translation. Regulate myoblast proliferation together with HMGA2.	Promoter	↓	UC	NA	(Li et al., 2012)
IGF2BP3	Insulin-like growth factor 2 binding protein 2. Member of IGF2 mRNA-binding protein. Binds to IGF2 and regulates IGF2 translation. Strong relationship with cancer development and malignancy.	Promoter	↓	↑	UC	(Ennajdaoui et al., 2016; Lederer et al., 2014)
INSC	Inscuteable homolog. Regulates mitotic spindle orientation.	Promoter	NA	NA	NA	(Hughes et al., 2004)
KDM2B	Lysine demethylase 2B. Regulates cell proliferation and senescence through p15.	Promoter	NA	NA	NA	(He et al., 2008)

PAK4	p21 (RAC1) activated kinase 4. Regulates cell cycle through normal degradation of CDKN1A. Overexpression led to uncontrolled proliferation.	Promoter	↓	UC	NA	(Nekrasova and Minden, 2011, 2012; Tian et al., 2011)
POLD2	DNA polymerase delta 2, accessory subunit. Catalytic subunit of DNA polymerase delta. DNA polymerase delta interacts with PCNA to control DNA synthesis during DNA replication and repair.	Promoter	NA	NA	NA	(Lu et al., 2002; Perez et al., 2000)
PRIM2	Primase (DNA) subunit 2. Subunit of DNA primase (key enzyme for DNA replication).	Promoter	↓	UC	NA	(Zerbe and Kuchta, 2002; Zhang et al., 2014)
SH3PXD2B	SH3 and PX domains 2B. Scaffold protein. siRNA inhibition led to	Promoter	↓	UC	NA	(Hishida et al., 2008)

	mitotic clonal expansion repression of adipocyte.					
SMYD2	SET and MYND domain containing 2. Lysine methyltransferase. Regulate cell proliferation through methylation of p53 and RB.	Promoter	NA	NA	NA	(Cho et al., 2012; Huang et al., 2006)
UBE2C	Ubiquitin conjugating enzyme E2 C. Member of E2 ubiquitin conjugating enzyme family. Regulates cell proliferation through cyclin B.	Promoter	↓	↑	UC	(van Ree et al., 2010)

Cell cycle related genes in ↓CpG associated with ↑mRNA gene set (2/ 36)						
Genes	**Comments**	**Cell cycle activator or repressor**	**Expression changes in developmental mouse heart (P1 to P14)**	**Expression changes in 5aza treated mouse heart**	**Expression changes in 5aza treated human Heart-Dynos**	**References**
KLF9	Kruppel-like factor 9. Member of Kruppel-like transcriptional regulator family. Inhibition of KLF9 promoted glioma cell proliferation.	Repressor	UC	UC	NA	(Huang et al., 2015)
PTPRR	Protein tyrosine phosphatase receptor type R. Member of protein tyrosine phosphatase (PTP) family. PTP family is one of the key mechanisms of cell division and proliferation governing.	Repressor	NA	NA	NA	(Chernoff, 1999)

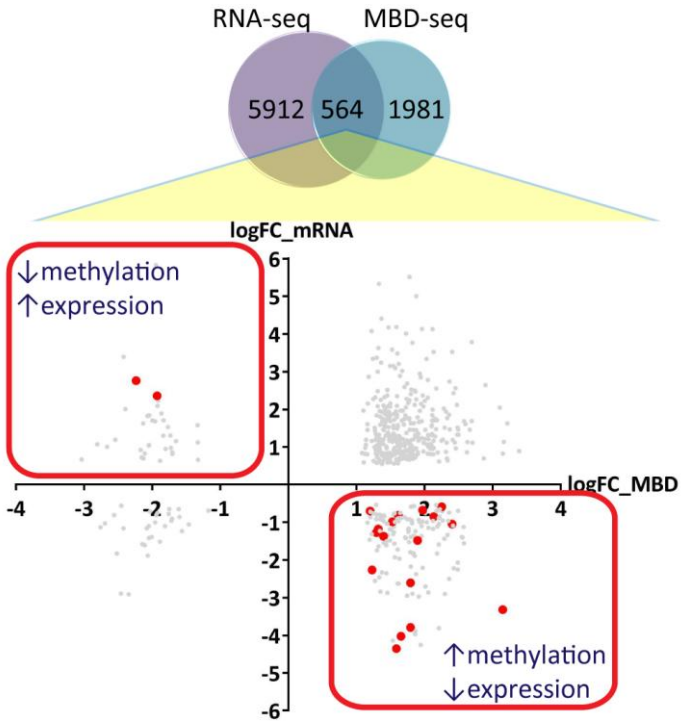

Figure 4.1. Identification of genes involved in cell proliferation from differentially methylated and transcribed genes during neonatal heart development.

The scatter plot demonstrates differentially regulated and methylated genes from Chapter 3. The scatter plot shows log2 fold changes in mRNA expression levels (y-axis) against log2 fold changes in MBD enrichment (x-axis). Genes with increased (or decreased) methylation levels associated with decreased (or increased) transcription levels were selected for further cell cycle and proliferation analysis (framed by red rectangles). Genes that with previously reported functions in cell proliferation or cell cycle regulation were selected for further analysis (in red dots).

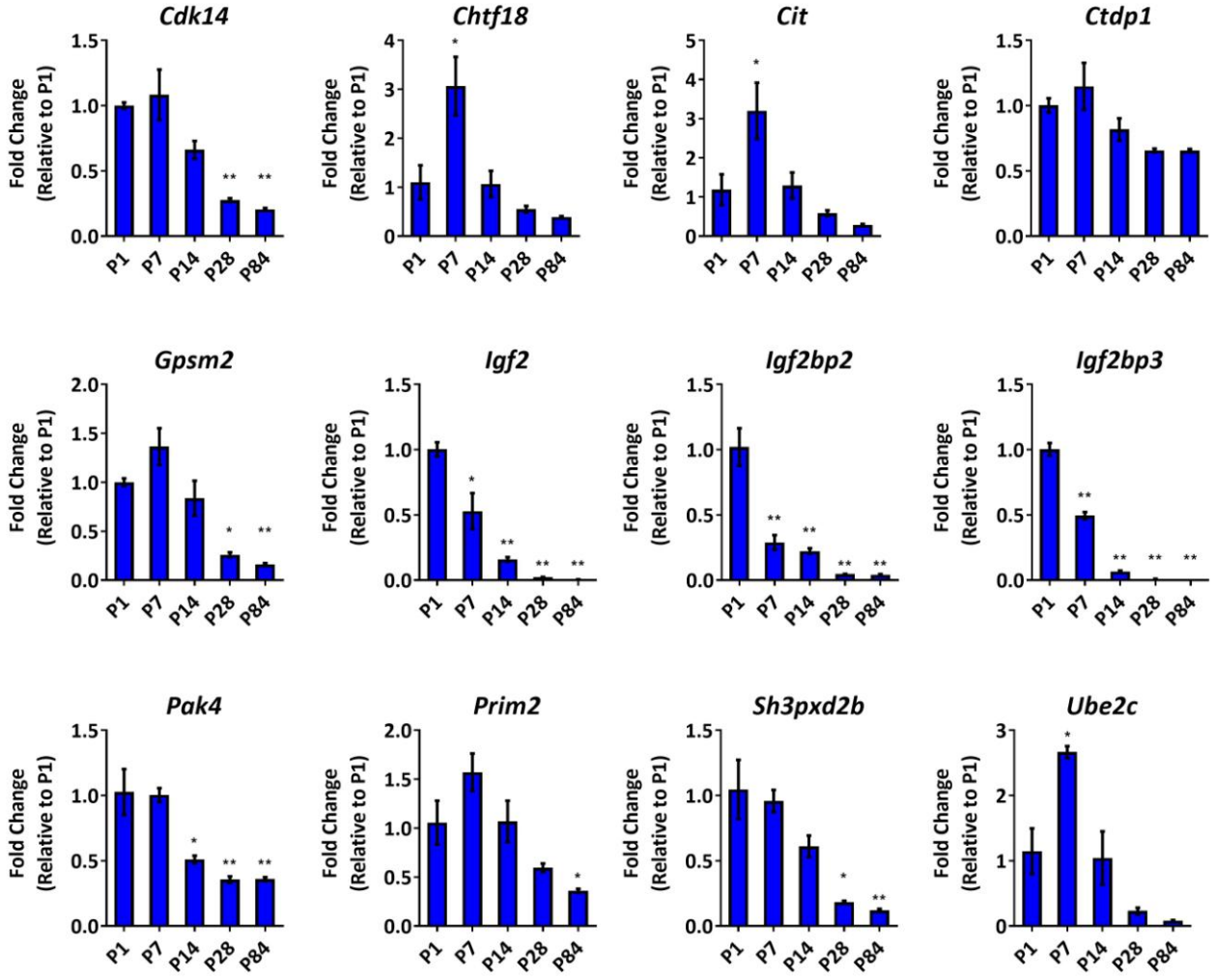

Figure 4.2. Profiling of cell cycle genes (hypermethylation associated with transcriptional repression) during heart development.

qPCR gene expression profiling of cell cycle and proliferation candidate genes (hypermethylated and transcriptionally repressed) in mouse cardiac ventricles from P1 to P84. Expression levels are normalized to 18S and represented as a fold change relative to P1 ventricles (n=3 per group). Data are presented as mean ± s.e.m. *P<0.05, **P<0.001.

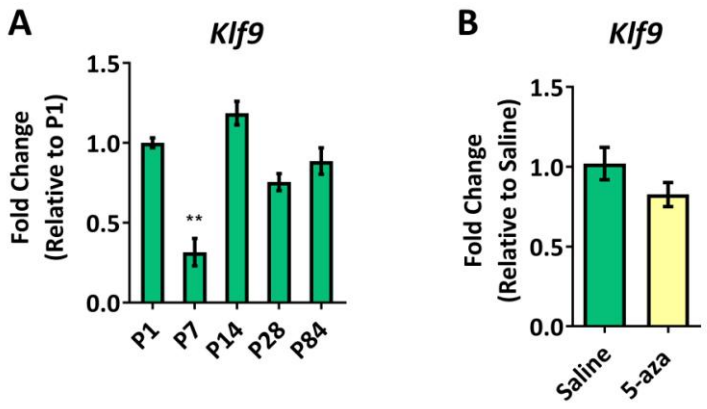

Figure 4.3. Profiling of the cell cycle gene, *Klf9*, (hypomethylation associated with transcriptional activation) during heart development and following 5aza-dC treatment in mice.

A. qPCR gene expression profiling of *Klf9* (hypomethylation associated with transcription activation group) in mouse cardiac ventricles from P1 to P84. Expression levels are normalized to 18S and represented as a fold change relative to P1 ventricles (n=3 per group). Data are presented as mean ± s.e.m. **P<0.001.

B. qPCR gene expression profiling of *Klf9* in saline and 5aza-dC treated hearts at P7. Expression levels are normalized to 18S and represented as a fold change relative to P1 ventricles (n=4-6 per group). Data are presented as mean ± s.e.m.

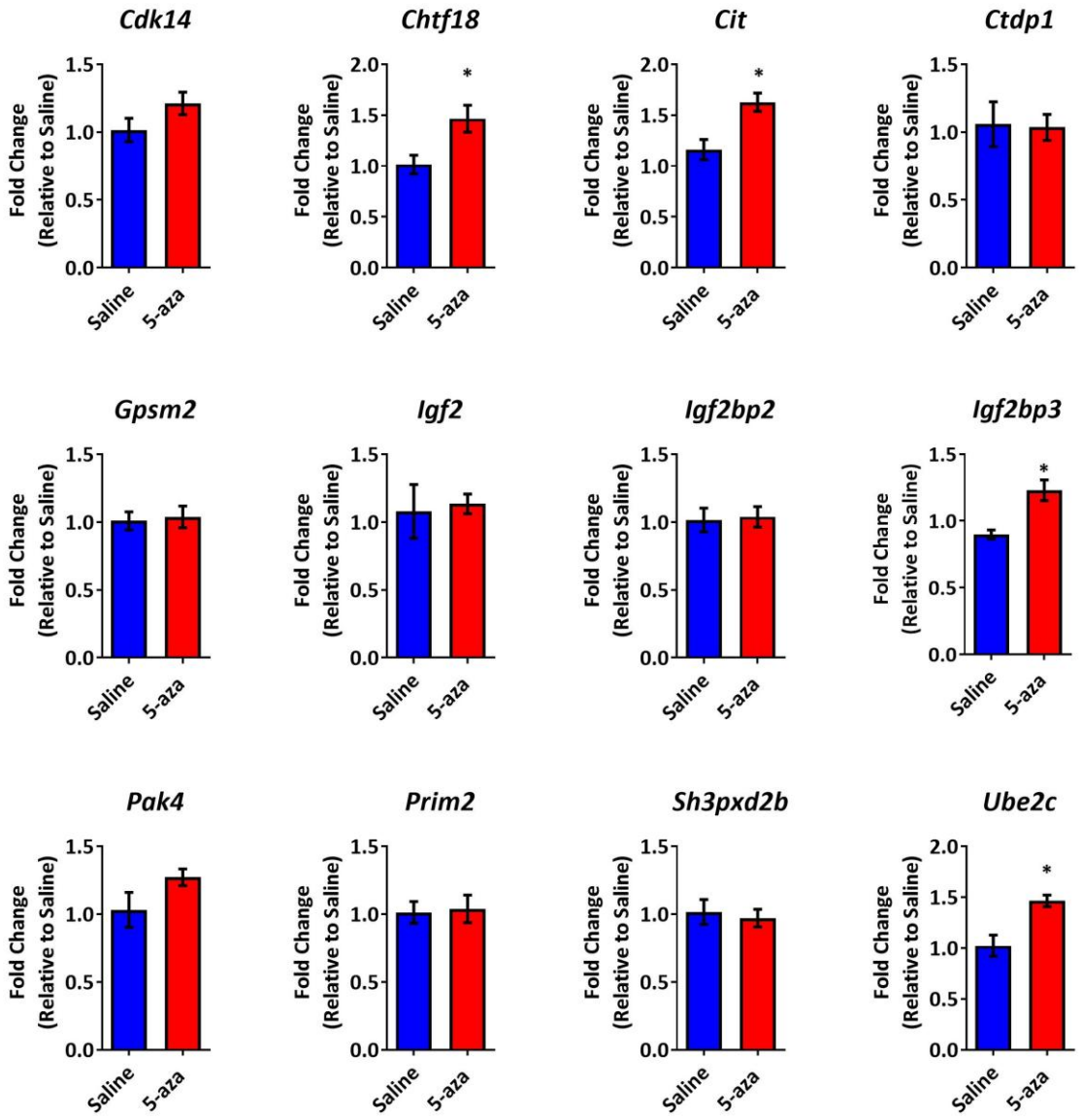

Figure 4.4. Transcription of cell cycle genes (hypermethylation associated with transcriptional repression) are subjected to DNA methylation in 5aza-dC treated mouse hearts.

qPCR gene expression profiling of cell cycle gene candidates (from hypermethylation associated with transcriptional repression group) in saline and 5aza-dC treated hearts at P7. Expression levels are normalized to 18S and represented as a fold change relative to P1 ventricles (n=4-6 per group). Data are presented as mean ±s.e.m. *P<0.05.

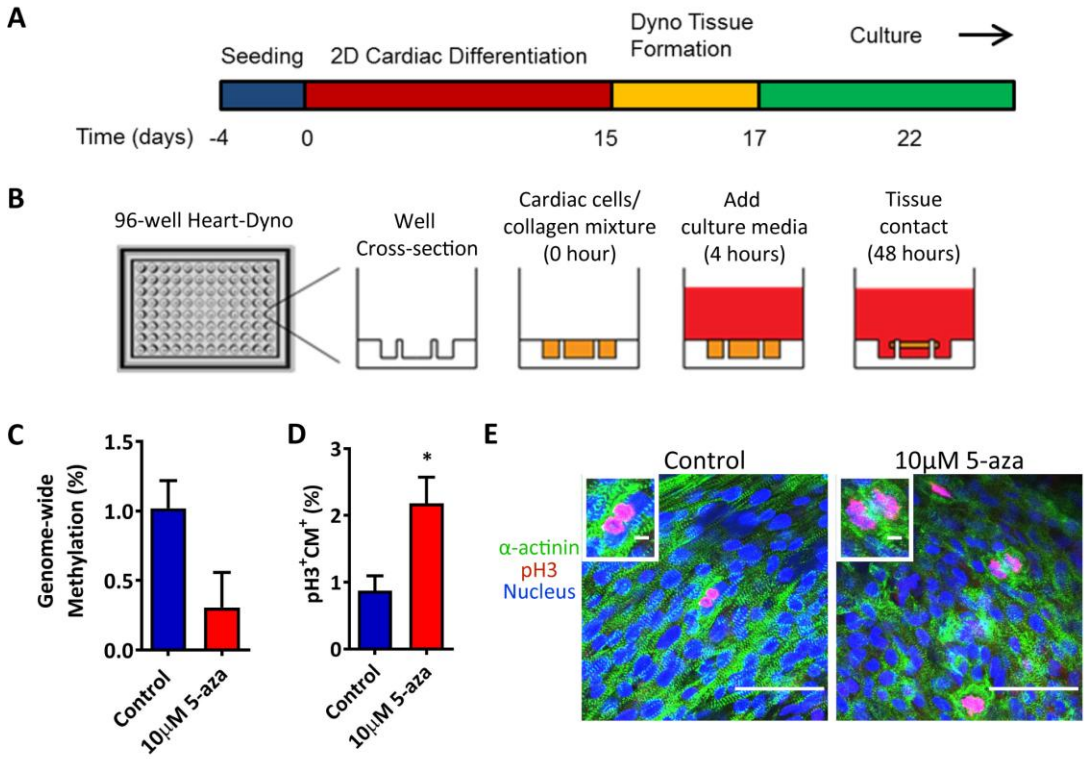

Figure 4.5. DNA methylation is linked to cardiomyocyte proliferation in 3D cultured hCOs.

A. Timeline of human ESC culture, differentiation and 3D hCOs culture.

B. Schematic of 96-well Heart Dyno platform. (*Figure A and B are kindly provided by Dr Richard Mills.)

C. Genomic DNA methylation levels in hCOs treated with saline or 5aza-dC (*n*=3 pooled samples, each pooled sample contained 3 hCOs).

D. Quantification of $pH3^{+}$cardiomyocytes in control and 5aza-dC-treated hCOs. Data are presented as % of cardiomyocytes/hCOs for n=13-15 independent hCOs tissue per group (3 fields of cells assessed per hCO). **P*<0.05.

E. Immunohistochemistry staining of saline and 5aza-dC-treated hCOs. Green = ACTN2, red = pH3, blue = nuclei. pH3 positive cardiomyocytes with disassembled sarcomeres are also shown in the high magnification inset in the top left hand corner of each panel. Scale bar = 50 μm in main figure and 5 μm in high magnification inset.

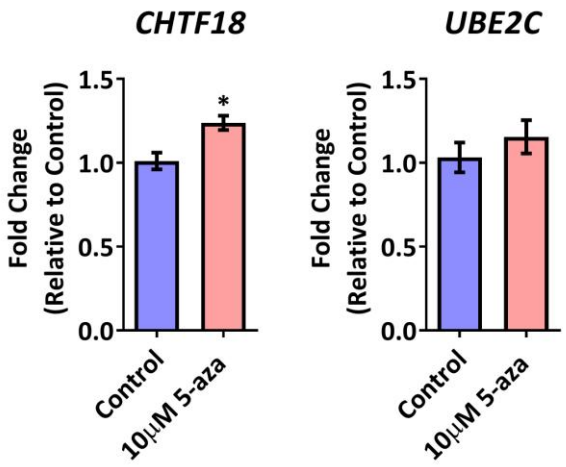

Figure 4.6. Profiling of validated cell cycle genes in 5aza-dC treated hCOs.

qPCR gene expression profiling of validated cell cycle candidates (from hypermethylation associated with transcriptional repression group) in control and 5aza-dC treated hCOs. Expression levels are normalized to 18S and represented as a fold change relative to control (n=9 pooled samples, each pooled sample contained 3 hCOs). Data are presented as mean ± s.e.m. *P<0.05.

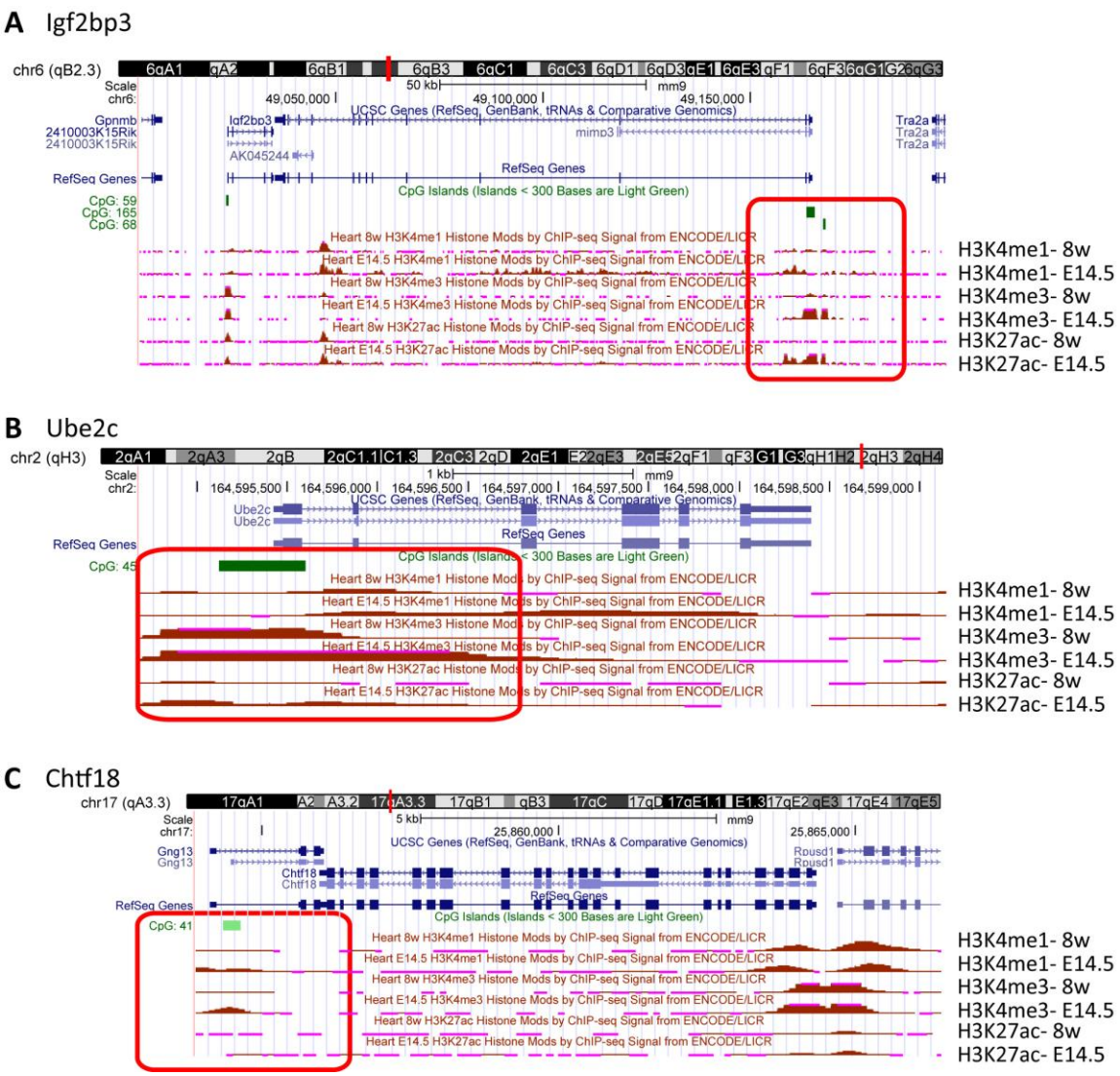

Figure 4.7. Maps of ENCODE H3K4me1, H3K4me3 and H3K27ac ChIP-seq peaks across the *Igf2bp3, Ube2c* and *Chtf18* loci at E14.5 and 8 weeks old hearts.

A. Maps of ENCODE H3K4me1, H3K4me3 and H3K27ac ChIP-seq peaks across the *Igf2bp3* locus in E14.5 and 8 week-old mouse hearts. Selected region highlighted by red box.

B. Maps of ENCODE H3K4me1, H3K4me3 and H3K27ac ChIP-seq peaks across the *Ube2c* locus in E14.5 and 8 weeks-old mouse hearts. Selected region highlighted by red box.

C. Maps of ENCODE H3K4me1, H3K4me3 and H3K27ac ChIP-seq peaks across the *Chtf18* locus in E14.5 and 8 weeks-old mouse hearts. Selected region highlighted by red box.

4.4. Discussion and conclusion

This chapter uncovers an essential role for DNA methylation in the regulation of cardiomyocyte proliferation in both rodent and human cardiac cells for the first time. These experimental findings indicate that DNA methylation is involved in regulating several cell cycle promoters during early postnatal cardiac development. Specifically, 4 cell proliferation genes (*Chtf18*, *Cit*, *Igf2bp3*, and *Ube2c*) were validated as being subject to regulation by DNA methylation during mouse heart development. Importantly, global inhibition of DNA methylation in human cardiac organoids also promoted cardiomyocyte proliferation, suggesting that the effect of global DNA methylation in restraining cardiomyocyte proliferation is conserved between rodents (Chapter 3) and humans. Notably, out of 4 validated DNA methylation targets involved in cell proliferation in the mouse, only *CHTF18* was also validated as a putative DNA methylation target in human cardiac cells. This result indicates that the mechanism by which DNA methylation regulates cardiomyocyte proliferation may differ in mice and humans.

One of the most interesting observations in this chapter is that inhibition of DNA methylation induces cardiomyocyte proliferation in human ESC-derived cardiomyocytes, which is similar to the result previously observed in the developing mouse heart (Chapter 3). This result suggests that DNA methylation plays an essential role in restraining cardiomyocyte proliferation in both rodents and humans. This is a potentially important finding as inhibition of DNA methylation using hypomethylating agents such as 5-aza is currently used as a clinical therapeutic approach for myelodysplastic syndromes and acute myeloid leukaemia (Christman, 2002). However, it is important to note that the effects of DNA methylation inhibitors on cardiomyocyte proliferation were observed in immature cardiomyocytes and DNA methylation likely plays diverse roles in regulating cell proliferation at different stages of development. Human ESC-derived cardiomyocytes have been previously characterized to be similar to foetal or embryonic cardiomyocytes (Veerman et al., 2015). While the current results provide supporting evidence for a role of DNA methylation in guiding cardiomyocyte cell cycle shutdown during development, it is unclear whether inhibiting DNA methylation at later stages of development (i.e. in adulthood) is sufficient for cardiomyocyte cell cycle re-entry. Interestingly, recent studies have demonstrated that 5aza improves cardiac function and fibrosis following MI in the adult mouse heart via modulation of macrophages (Jeong et al., 2015; Kim et al., 2014). However, none of the studies have reported the effects of 5aza on cardiomyocyte proliferation in the adult heart following injury. Future characterization of the effects of modulating DNA methylation on cardiomyocyte proliferation in

the setting of adult heart disease could provide new therapeutic avenues towards cardiac regeneration.

Although DNA methylation clearly constrains cardiomyocyte proliferation, very few cell cycle genes appear to be directly by DNA methylation at their gene promoters during cardiomyocyte maturation. The analyses undertaken in this chapter reveal that only 4 out of 179 differentially methylated cell cycle genes showed a direct relationship between DNA methylation levels and gene transcription. This result implies that while DNA methylation is essential for cardiomyocyte proliferation, the direct regulation of cell cycle genes is uncommon. Similarly, a recent whole genome methylation analysis of mouse heart development also found limited evidence for direct methylation of cell cycle genes during cardiomyocyte maturation (Gilsbach et al., 2014). It is possible that DNA methylation regulates cardiomyocyte proliferation through modulation of other signalling components including TFs instead of direct regulation of cell cycle genes. In fact, research in the cancer biology and cellular reprogramming fields has revealed that a few TFs can single-handedly alter cellular behaviour or even cell identity. For instance, a recent study has shown that transcription of FOXF2 is highly sensitive to regulation by DNA methylation in breast cancer cells, and is sufficient to drive the cascade of events triggering (or repressing) breast cancer (Tian et al., 2015). Moreover, another study found that cancer cells could be directly reprogrammed to less proliferative states by targeting Dnmt3a to differentially methylated SOX2 binding sites (Rivenbark et al., 2012). Notably, one of the DNA methylation target genes, Ube2c, regulates protein degradation by catalysing ubiquitin modifications of proteins (Hao et al., 2012). DNA methylation may regulate subsets of genes by mediating Ube2c without directly influencing their transcription. Overexpression of Ube2c leads to degradation of cyclin B, which has been shown to increase susceptibility to carcinogens (van Ree et al., 2010). Together, these results illustrate that DNA methylation can affect cell proliferation simply through regulation of a few TFs without direct regulation of a subset of cell cycle genes. Future studies are required to identify the TF networks that are targeted by DNA methylation during cardiomyocyte maturation, which might provide further understanding of how DNA methylation regulates cardiomyocyte proliferation.

Although DNA methylation does not directly regulate the majority of cell proliferation genes at cell cycle promoters, 4 methylated cell cycle genes were identified in this chapter. Chtf18, Cit, and Ube2c have been previously reported as cell cycle regulators (Shiomi et al., 2007, Gruneberg et al., 2006; Liu et al., 2003, van Ree et al., 2010). Specifically, Cit can regulate cell cycle through forming a complex with Klf14 at central spindle and midbody during G2/M stage transition (Gruneberg et al., 2006; Liu et al., 2003). In addition, Chtf18 has been previously shown to drive

cell cycle by forming a complex with the replication factor C to load proliferating cell nuclear antigen (PCNA) to DNA. DNA polymerase η will then be activated following the loading of PCNA to DNA to initiate DNA synthesis (Shiomi et al., 2007). Notably, Chtf18 is the only conserved DNA methylation target gene that was identified in this Chapter, supporting a previous study that has demonstrated its conservation for DNA replication between yeast, flies and mammals (Berkowitz et al., 2008). Furthermore, Igf2bp3 is an important member of a critical upstream signalling pathway that drives cell proliferation (Ennajdaoui et al., 2016; Lederer et al., 2014, Chernoff, 1999). In particular, Igf2bp3 (Palanichamy et al., 2016; Schaeffer et al., 2010) and Ube2c (Bajaj et al., 2016; Chou et al., 2014; Shen et al., 2013; Shuliang et al., 2013) have been widely studied in various cancers, confirming their ability to promote cell proliferation. Interestingly, their expression levels are substantially down-regulated during postnatal cardiac development. However, it is also apparent that reactivation of their expression levels following treatment of 5-aza in both mouse and human systems are very modest. This could be due to other epigenetic regulatory mechanisms, such as H3K4me1, H3K4me3 and H3K27ac. For example, utilizing the ENCODE ChIP-seq results through UCSC genome browser, it was found that these genes progressively lose these active histone marks during heart development from E14.5 to 8 weeks of age (**Figure 4.7**). It is important to note that transcription is collectively influences by various epigenetic marks rather than DNA methylation alone. Therefore, the developmental shutdown of these proliferation genes might due to the combined effects of DNA methylation, histone methylation as well as histone acetylation. Modification of one epigenetic mark might not provide enough stimulation for the reactivation of these genes. It will therefore be important in the future to look at the epigenome in its entirety to better understand underlying relationships between epigenetic modifications and transcription during cardiomyocyte maturation.

While animals are widely used in research studies and have greatly contributed our understanding of various developmental and disease processes, many biological differences between rodents and humans have prevented translation of many experimental results into the clinic (Mak et al., 2014; Shanks et al., 2009). In fact, it was previously reported that the successful rate of experimental translation from mouse to human clinical trials in cancer research is less than 8% (Mak et al., 2014). Moreover, recent studies have revealed the distinct differences between mice and humans from proximal and distal regulatory elements to TF landscape (Cheng et al., 2014; Monaco et al., 2015; Pishesha et al., 2014; Shay et al., 2013). In particular, only ~30% of the top 500 human expressed genes have equivalent orthologous in the top 500 expressed genes in stage-matched mouse erythroid cells (Pishesha et al., 2014). Moreover, these studies have demonstrated that while promoter regions generally demonstrate high interspecies fidelity, promoter sequences with less

than 65% conservation show little correlation to gene expression levels across species (Cheng et al., 2014; Pishesha et al., 2014), suggesting diverse TF regulation and promoter usage in different species. These variations in the control of gene transcription might contribute to important physiological differences between mice and humans. However, it is also important to be aware that the previous study of DNA methylation in the mouse was observed under the dynamic *in vivo* process of heart development. On the other hand, the engineered human heart tissue is a static *in vitro* culture system that might not completely recapitulate the cardiomyocyte maturation and development processes. Furthermore, it is noteworthy that previous RNA-seq and MBD-seq (Chapter 3) datasets were derived from whole ventricular tissue lysates, which comprise mixed cell populations. As such, differentially transcribed and methylated genes could be caused by artefacts related to changes in cellular composition during postnatal heart maturation. Future interrogation of the regulatory role of DNA methylation in purified mouse and human cardiomyocyte populations is essential in order to shed further light on the underlying epigenetic basis for postnatal cardiomyocyte maturation.

4.5. Summary and future direction

This chapter provides supporting evidence for direct regulation of a small subset of cell proliferation genes by DNA methylation during postnatal cardiomyocyte maturation. The current findings suggest that DNA methylation restrains both mouse and human cardiomyocyte proliferation. However, given the technical limitations imposed by analysis of DNA methylation events in whole tissue preparations in Chapters 3 and 4, the epigenetic mechanisms underlying postnatal cardiac cell cycle arrest, especially in human cardiomyocytes, remains elusive. In the following chapter, a series of refined and cell type specific analyses are conducted to further delineate relationships between the chromatin landscape and transcription during postnatal cardiomyocyte maturation in rodents and humans.

Chapter 5

Chromatin accessibility dynamics during human and mouse cardiac development

We cannot solve our problems
with the same thinking we used when we created them.
Albert Einstein.

Chapter 5. Chromatin accessibility dynamics during human and mouse cardiac development

5.1. Introduction

In Chapter 4, it was shown that DNA methylation is essential for cardiomyocyte proliferation. However, DNA methylation did not increase at the majority of cell cycle gene promoters, suggesting that DNA methylation regulates cardiomyocyte proliferation via an alternative mechanism. However, the previous chapters also identified several technical limitations, such as lack of cellular resolution and a reliance on single epigenetic marks, which may have precluded identification of cardiomyocyte specific epigenetic mechanisms that guide postnatal maturation and cell cycle arrest. In this chapter, two state-of-the-art experimental approaches are adapted to directly interrogate dynamic changes in the chromatin landscape during postnatal rodent and human cardiomyocyte maturation.

Classic approaches for isolation of different cell populations from the adult heart require perfusion of enzymatic solutions followed by fluorescence-activate cell sorting (FACS), which requires the integrity of the whole heart structure and the use of fresh tissue. This approach is not suitable for archival specimens (Bell et al., 2011), which is a major limitation for research using human material. Recent publications have reported an alternative method for isolation of cardiomyocytes from frozen heart tissue, which combines cellular fractionation and immunostaining with the cardiomyocyte-specific marker PCM1 to isolate myocyte specific nuclei (Alkass et al., 2015; Bergmann and Jovinge, 2012; Bergmann et al., 2015; Preissl et al., 2015a). This method has been used to isolate cardiomyocyte nuclei from human and mouse heart tissue and various studies have demonstrated the utility of this approach for downstream transcriptomic and epigenomic assessments, including RNA-seq and ChIP-seq (Alkass et al., 2015; Bergmann et al., 2015; Gilsbach et al., 2014; Preissl et al., 2015a). Therefore, this approach provides a relatively simple method for the isolation of cardiomyocyte specific nuclei for epigenetic studies in both rodents and humans.

It is evident that various epigenetic modifications collectively regulate chromatin accessibility, which dictates the transcription of underlying genes (Gillette and Hill, 2015; Han et al., 2011; Quaife-Ryan et al., 2016). The chromatin landscape alternates between euchromatin (a relatively

open structure that is accessible for transcriptional activation) and heterochromatin (more compacted chromatin state that is associated with transcriptional repression). These alternative chromatin states are influenced by chemical modifications of histone proteins and DNA (see Chapter 1). Recent genome-wide approaches have begun to assess the epigenetic landscape using next-generation sequencing methods coupled with biochemical pull-down approaches for individual epigenetic marks. Some of the most common approaches include MBD-seq or methylated DNA immunoprecipitation (MeDIP-seq) (for DNA methylation) (Harris et al., 2010) and ChIP-seq (for individual histone modifications) (Furey, 2012). Despite their undisputed utility, these approaches only interrogate individual epigenetic modifications without investigating the integrated influence of multiple epigenetic marks on chromatin structure. In contrast, other approaches such as DNase I hypersensitive site sequencing (DNase-seq) (Boyle et al., 2008) and high-throughput sequencing for formaldehyde-assisted isolation of regulatory elements (FAIRE-seq) (Gaulton et al., 2010) have been developed to bypass individual epigenetic marks and investigate their integrated product – the chromatin accessibility landscape. While DNase-seq and FAIRE-seq have illuminated our understanding of chromatin structure and the influence of regulatory elements on transcriptional regulation (Gerstein et al., 2012), they often require large amounts of starting materials (>1 million cells), which is a challenge for research involving human tissue biopsy specimens. More recently, ATAC-seq was developed, which utilizes the properties of transposase to sequence accessible regions of open chromatin (Buenrostro et al., 2013)., ATAC-seq provides a new strategy to investigate the global chromatin landscape and TF occupancy at the same time. A major advantage of this approach is that it requires minimal starting material (500 to 50,000 cells), with more recent studies further refining this approach for single cells (Buenrostro et al., 2015b; Cusanovich et al., 2015). This significant reduction in the input material requirements for sequencing of accessible chromatin increases the feasibility of this approach for numerous biological studies including those involving human tissue.

In this chapter, PCM1 isolation of cardiomyocytes, ATAC-seq and RNA-seq are combined to define the relationship between the global chromatin landscape, TFs and transcriptional regulation during cardiomyocyte maturation in rodents (P1, P14 and P56) and humans (foetal (14-19 wks), 0-10 yrs, 10-30 yrs and 30+ yrs). Integrating RNA-seq and ATAC-seq datasets revealed a positive correlation between chromatin accessibility and active transcription states in cardiomyocytes. Furthermore, motifs for several TFs that are essential for cell proliferation were associated with chromatin compaction and transcriptional repression of cell cycle genes during cardiomyocyte maturation. Together, these results provide novel insight into the relationship between chromatin

accessibility and transcription during cardiomyocyte maturation and suggest a potential epigenetic mechanism for postnatal cardiomyocyte cell cycle arrest.

5.2. Methodology

5.2.1. Experimental human tissue collection

All protocols were approved by The University of Queensland Institutional Human Research Ethics Committee (SBS/2014000329).

In collaboration with Professor Cristobal G. dos Remedios and Dr Sean Lal from the University of Sydney, human heart tissues spanning a large developmental period, from foetal (13-19 wks) (provided by commercial supplier – Advanced Bioscience Resource, Alameda, CA, USA), 0-10 yrs, 10-30 yrs, and 30+ yrs were obtained from The Sydney Human Heart Tissue Bank. All human heart specimens were donated from healthy, non-diseased donors and the tissues have been archived in liquid nitrogen since collection (**Table 5.1**). Left ventricular cardiac tissues from donors were selected for this study.

5.2.2. PCM1 isolation of cardiomyocyte nuclei

Cardiomyocyte specific nuclei were isolated according to a previous publication (Bergmann and Jovinge, 2012). Mouse hearts were pooled to obtain enough material for sequencing (P1: 12 hearts/ sample, P14 and P56: 6-7 hearts/ sample). For human samples, ~1g of ventricular tissue was used per sample, left ventricular tissue samples were then dissected and minced into approximately $1mm^3$ cube and electrically homogenised in 15mL lysis buffer (0.32M sucrose, 10mM Tris-HCl (pH = 8), 5mM $CaCl_2$, 5mM magnesium acetate, 2.0mM EDTA, 0.5mM EGTA, 1mM DTT and 1X Complete protease inhibitor (all chemical reagents were acquired from Sigma-Aldrich). Heart lysate was combined with another 15mL lysis buffer and subsequently homogenised for 10-15 strokes using dounce tissue grinder (Wheaton, Millville, NJ, USA). Cell lysate was then filtered through a 70μM filter followed by a 40μM cell strainer (Becton Dickinson, Franklin Lakes, NJ, USA) and centrifuged to pellet nuclei at 1000 x g (Allegra X-15R, Beckman Coulter) for 5 mins. Nuclei pellets were then resuspend in 2-4mL sucrose buffer (1M sucrose, 10mM Tris-HCl (pH = 8), 5mM magnesium acetate, 1mM DTT and 1X Complete protease inhibitor) and the suspension was cushioned on top of 2 times volume of the sucrose buffer, followed by centrifugation to pellet nuclei at 1000xg (Allegra X-15R, Beckman Coulter) for 5 mins. Nuclei pellets were then washed 1 time in 1mL nuclei storage buffer (NSB, 0.44M sucrose, 10mM Tris-HCl (pH = 7.2), 70mM KCl, 10mM $MgCl_2$, 1.5mM spermine and 1x Complete protease inhibitor). Washed nuclei pellets were then resuspended in NSB and stained for cardiomyocyte nuclear specific marker, PCM1 antibody (1:200, HPA023374, Sigma-Aldrich) at 4℃ for 45 minutes. Omitting the primary antibody served

as a control for positive staining. Nuclei were washed twice in NSB and stained for secondary antibody conjugated with Alexa Fluor 633 (1:500, Thermo Fisher Scientific (Molecular Probes)) or Brilliant Violet 421 (1:400, #406410, Biolegend, San Diego, CA, USA) at 4℃ for 30 minutes. Nuclei were washed twice in NSB and resuspended in PBS before being processed for FACS. PCM1 (-/+) nuclei were separated by FACS. Collected PCM1 (-/+) nuclei were pelleted at 1500 x g (Allegra X-15R, Beckman Coulter) for 15 minutes (**Figure 5.1**). (Note: Various protocols for PCM1 isolation of nuclei were compared and are summarized in **Appendix 7.2.**)

5.2.3. PCM1^{+} nuclei purity confirmation

For confirmation of cardiomyocyte purity, sorted PCM (-/+) nuclei were resuspended in 1mL TRIzol (Thermo Fisher Scientific (Ambion)) and stored in -80°C prior to processing. RNA was extracted according to RNA extraction protocol listed in Chapter 2 and profiled for several cardiomyocyte, fibroblast, endothelial and immune cell markers through real-time qPCR (**Table 2.4**).

5.2.4. Transcriptional expression profiling with RNA-seq

RNA extraction was performed according to the protocol described in Chapter 2. RNA quality was examined with the MultiNA bioanalyzer (Shimadzu) before library preparation. Ribosomal RNA was depleted from total RNA using NEBNext rRNA Depletion Kit (Human/Mouse/Rat) (E6310, New England Biolabs) followed by library generation using NEBNext Ultra Directional RNA Library Prep Kit for Illumina (E7420, New England Biolabs) according to the manufacturer's protocol. Size selection was performed according to NEBNext® Ultra II DNA Library Prep Kit for Illumina (E7645, New England Biolabs) size selection to select library fragment sizes of 200-400bp. Libraries were validated on MultiNA bioanalyzer and diluted to a concentration of 10 pM for 100 cycle, 40 million reads, single end sequencing on HiSeq2500 with version 4 reagents (Illumina). Base-calling was performed with RTA (version 1.8.66.3) and converted to fastq file using bcl2fastq (version 2.17.1.14). (Note: all human samples were extracted and sorted for cardiomyocyte nuclei in order to do RNA-seq and ATAC-seq. However, only selected samples were used for RNA-seq due to limited sample material (see **Table 5.1, 5.2, 5.3**).)

5.2.5. Chromatin accessibility profiling with ATAC-seq

Following PCM1 nuclei isolation, ATAC-seq libraries were generated according to the methods described in a previous publication (Buenrostro et al., 2015a). Briefly, nuclei pellets underwent

transposition reaction using Nextera DNA library preparation kit (FC-121-1030, Illumina) followed by purification using MinElute PCR purification kit (#28004, Qiagen), PCR amplification and qPCR strictly according to the published protocol. An extra PCR cycle step for library amplification was determined by qPCR for individual samples (**Table 5.3, 5.4**). Size selection by agarose gel was performed after PCR to select for library fragment sizes of 200-400bp. Libraries were validated on MultiNA bioanalyzer and diluted to a concentration of 10 pM for 100 cycle, 60 million reads, single end sequencing (for mouse) or 80 million reads, paired end sequencing (for human) on HiSeq2500 with version 4 reagents (Illumina). Base-calling was performed with RTA (version 1.8.66.3) and converted to fastq file using bcl2fastq (version 2.17.1.14).

5.2.6. Bioinformatics analyses (summarized pipeline at Table 5.5)

RNA-seq Sequence reads underwent 3' base quality trimming using the Fastx toolkit with a minimum Phred quality score (Q) of 30 and a minimum read length of 20 nt. RNA-seq reads were aligned to the reference genome sequence (mouse: GRCm38.p4/mm10, human: GRCh38.p7/hg38) using STAR with default settings (Dobin et al., 2013). Reads aligning to Ensembl-annotated whole genes on the correct strand with a strict mapping quality (Q≥20) were counted with featureCounts (Liao et al., 2014) and used to construct a data matrix comprising genes with an average of 10 reads or more per sample across the experiment. Differential gene expression analysis was performed using edgeR (v3.2.4) (Robinson et al., 2010). Heatmaps were generated from normalized and scaled gene expression values with R in RStudio (Reich et al., 2006; RStudio, 2012).

ATAC-seq Paired sequence reads underwent quality trimming using the Skewer (0.1.122r) with default setting (Jiang et al., 2014) and aligned to the mouse genome (GRCm38.p4/mm10) using Burrows Wheeler Aligner (BWA, version 0.7.10-r806-dirty) with default settings (Li and Durbin, 2009). Duplicate reads were removed before further analysis. Reads aligning to Ensembl-annotated 1kp up- and down-stream of a TSS with a strict mapping quality (Q≥20) were counted with featureCounts (Liao et al., 2014) and used to construct a data matrix comprising genes with an average of 10 reads or more per sample across the experiment. Differential gene expression analysis was performed using edgeR (v3.2.4) (Robinson et al., 2010). Heatmaps were generated from normalized and scaled gene expression values with R in RStudio (Reich et al., 2006; RStudio, 2012). Reads from each developmental stage were pooled and a single large alignment file (bam format) prepared for P1, P14 and P56. MACS (Zhang et al., 2008) was then used to directly compare P1 to P56 , P1 to P14 and P14 to P56 and identify regions of interest. MACS peak-calling was performed with a shift size of 75 bp and otherwise default parameters. Differentially accessible regions were defined as coordinates initially identified using MACS peak calling determined to

have a statistically significant signal difference (P1 vs. P56, FDR ≤ 0.05). Intersection between differential accessible chromatin regions and Ensembl genomic features was performed with BedTools (Quinlan and Hall, 2010).

GSEA of RNA-seq and ATAC-seq Gene GO process analysis was performed using MetaCore from Thomson Reuters (https://portal.genego.com/cgi/data_manager.cgi) on significant gene sets that formed different clusters. GSEA was performed on these data as previously described (Subramanian et al., 2005) using publicly available gene sets (www.broadinstitute.org/gsea/msigdb) to determine the enrichment of Reactome or TF binding sites.

Intersection of RNA-seq and ATAC-seq A two-way enrichment analysis was used to identify gene sets simultaneously altered in gene expression and chromatin accessibility. First, genes in RNA and ATAC profiles were ranked by the sign of the fold change divided by the nominal p-value. These data were merged, followed by MANOVA test to determine the two-dimensional enrichment of gene sets. All statistical analyses were performed in R (Unpublished software by Antony Kaspi).

Statistical analysis Gene expression, chromatin structure and gene set enrichments with a FDR p-value ≤ 0.05 were considered significant.

5.3. Results

5.3.1. Isolated PCM1 nuclei are enriched for cardiomyocyte specific markers

To interrogate myocyte specific transcriptome and chromatin accessibility dynamics during cardiac maturation, cardiomyocyte specific nuclei were isolated from frozen ventricular mouse hearts from P1, P14 and P56 (**Figure 5.1**). Following the isolation of PCM1 (-/+) nuclei, nuclear RNA was processed for real-time qPCR for analysis of cell type specific markers (**Figure 5.2, 5.3, 5.4**). PCR profiling data of myocyte markers (*Myh6, Myh7*), slow skeletal and cardiac type troponin C1 (*Tnnc1*) and *Tnni3*, showed significant enrichment of cardiomyocyte specific markers in $PCM1^+$ nuclei populations in P1, P14 and P56 samples (**Figure 5.2**). Next, the non-myocyte markers for fibroblasts (collagen type 1 or 3 alpha 1 chain (*Col1a1*, *Col3a1*), fibrillin 1 (*Fbn1*) and discoidin domain receptor tyrosine kinase 2 (*Ddr2*)) (**Figure 5.3**), endothelial cells (von Willebrand factor (*Vwf*)) and immune cells (integrin subunit alpha M (*Itgam*)) (**Figure 5.4**) were examined in the PCM1 (-/+) populations. $PCM1^-$ populations were significantly enriched for non-myocyte specific markers at all 3 developmental stages. These findings confirm the purity of the isolated $PCM1^+$ populations that were subsequently used for sequencing.

5.3.2. RNA-seq of $PCM1^+$ nuclei identifies dynamic changes in the cardiomyocyte transcriptome during postnatal development

RNA-seq was performed on the isolated myocyte specific $PCM1^+$ fraction from P1, P14 and P56 to examine transcriptional changes during postnatal cardiomyocyte development. More than 92% of generated reads were uniquely mapped to the mouse genome with >83% of reads assigned to a specific gene, confirming the high quality of data generated in this RNA-seq experiment (**Table 5.6**). Furthermore, multidimensional scaling (MDS) analyses were performed on all RNA-seq datasets to assess the degree of similarity of individual samples within the datasets. MDS plot showed clear separation of clusters for the P1, P14 and P56 samples and tight clustering of replicates within the sample groups (P1, P14 and P56) (**Figure 5.5A**), confirming the specificity and reproducibility of the sequencing datasets.

Gene sets that were differentially transcribed (FDR p-value <0.05) between P1 vs. P14, P1 vs. P56 or P14 vs. P56 were then selected to generate differential heatmap profiles (**Figure 5.5B**). The heatmap shows the formation of 5 distinct transcriptional clusters. Gene sets from different clusters were examined for their roles in different biological processes through ontology analysis. Gene sets

that were highly expressed in P1 cardiomyocytes and gradually shut down during development (cluster 5) were enriched for genes that were involved in cell cycle activities and cellular structure arrangement. Gene sets that were primarily repressed between P1 and P14 (cluster 3) were enriched for genes that participated in cell cycle S phase and DNA damage regulation. Conversely, gene sets that were significantly enriched in P14 and/or P56 cardiomyocytes (relative to P1) were associated with muscle contraction, skeletal muscle development, cell adhesion, inflammation and the immune response (cluster1).

5.3.3. Analysis of transcriptional changes during defined windows of postnatal cardiomyocyte maturation

To further understand specific transcriptional changes during different windows of postnatal development, the RNA-seq data were analysed according to the following comparisons: P1 vs. P14, P14 vs. P56 and P1 vs. P56. Between P1 vs. P14, there were 8193 differentially expressed genes with 4350 up-regulated and 3843 down-regulated at P14 (**Figure 5.6A; Table 5.7**). GSEA analysis revealed that genes that were highly expressed at P1 were largely involved in cell cycle activities, supporting the previous results from the heatmap cluster analysis (**Figure 5.5B**). Furthermore, these gene sets were enriched for E2f4 and Foxm1 regulated targets, which are cell cycle-related TFs (**Figure 5.6B, C; 5.8B, C**).

A total of 7113 genes were differentially expressed between P14 and P56 with 3790 up-regulated and 3323 down-regulated at P56 (**Figure 5.7A; Table 5.7**). To understand the biological processes that were regulated at P14, genes enriched at P14 from the two comparisons (P1 vs. P14 and P14 vs. P56) were analysed. Together, genes that were highly enriched at P14 were associated with vascular reactivity, cell adhesion, extracellular matrix processes, muscle contraction and relaxation, immune response as well as metabolic activities, consistent with the maturation processes observed during postnatal heart maturation (**Figure 5.6B, 5.7B**). TFs that were known for regulating the aforementioned biological processes, such as Brg1 (Han et al., 2016; Zhang et al., 2011), Stat1 (Gatto et al., 2014; Sisler et al., 2015); (Kim et al., 2015), Suz12 (Pasini et al., 2007) as well as MTA3 (Fujita et al., 2004; Fujita et al., 2003) were also enriched in these gene sets (**Figure 5.6C, 5.7C)**. Collectively, this suggested the establishment of terminal cardiomyocyte differentiation and immune responses by P14.

Overall there were 10369 genes that were differentially expressed between P1 and P56, with 5281 up-regulated at P1 and 5088 up-regulated at P56 (**Figure 5.8A; Table 5.7**). There was a marked

enrichment of genes that participated in cell cycle activities and that were regulated by the cell cycle TFs E2f4 and Foxm1 in P1 cardiomyocytes (**Figure 5.8B, C)**. Interestingly, genes that were highly expressed at P56 (relative to P1) were largely associated with metabolic activities, especially tricarboxylic acid (TCA) cycle (**Figure 5.7B, 5.8B**). In addition, P56 up-regulated genes were regulated by TFs Stat1 and Pgc1a, a key inducer of mitochondria metabolism, consistent with the observation in the ontology analysis (**Figure 5.7C, 5.8C**).

Together, the analysis between P1 vs. P14, P14 vs. P56 and P1 vs. P56 indicated distinct biological processes were taking place in cardiomyocytes during two defined postnatal developmental windows.

5.3.4. Dynamic changes in the chromatin accessibility landscape during cardiomyocyte development

In order to understand the changes in chromatin landscape during cardiomyocyte maturation, ATAC-seq was performed on the sorted $PCM1^+$ nuclei samples. As previous papers have reported that TSSs are enriched in accessible chromatin regions, I focused on analysing the sequencing data within 1 kbp±TSS and genes assigned to these regions. Quality control results from BWA (Q10: confident in correcting mapped sequences >99%, Q20: confident in correcting mapped sequences >99.99%) indicated that at least 54% of the sequenced reads were correctly mapped and ~3-4.5% were mapped to TSS (**Table 5.8**). Next, MDS analysis was performed to understand the similarity between different samples and showed that unique clusters were formed by the 3 replicates in P1 and P56 group but not P14 group (**Figure 5.9A**). Gene sets with differential chromatin structure (FDR p-value ≤0.05) between P1 vs. P14, P1 vs. P56 or P14 vs. P56 were used to generate differential heatmap profiles (**Figure 5.9B**). The heatmap demonstrated the formation of 3 clusters. Interestingly, gene sets that had highly accessible TSSs at P1 with reduced accessibility by P56 (cluster 3) were enriched for genes associated with cell adhesion, olfactory transduction and inflammation (**Figure 5.9B**). On the other hand, gene sets that had more compacted TSS at P1 and gradually gained accessibility by P56 were enriched for genes associated with cell adhesion, muscle development, cytoskeleton rearrangement and muscle contraction (cluster 1 and 2). Together, these results suggest that the chromatin landscape of cardiomyocytes underwent significant transitions from P1 to P56.

Due to the variability of the P14 ATAC-seq datasets, which might be due to sample quality or reflect vibrant biological changes during this critical developmental transition, further analysis was

focused on P1 vs. P56. First, P1 vs. P56 ATAC-seq data was used to generate peak sets that mapped across the mouse chromosome regions to understand the distribution of open chromatin regions during development (**Figure 5.9C**). The data suggested that chromosomes 1,3,6,7 and 12 were relatively open at P1 while chromosomes 9, 11, 17 and 19 were relatively open at P56. Moreover, while the distribution of open chromatin signatures at GC regions was fairly similar (**Figure 5.9D**), P56 CpG sites were more accessible at P1 (**Figure 5.9E**). In addition, various genome features were mapped using P1 vs. P56 sequencing reads and indicated the enrichment of open chromatin at P56 on CGIs, TSSs, introns, exons, enhancers, and TFBS, except intergenic regions (**Figure 5.9F**), suggesting the P56 cardiomyocyte genome encoded for more accessible chromatin regions.

Differential analysis on P1 vs. P56 ATAC-seq datasets revealed that 882 genes had significant changes in chromatin structure within 1 kbp±TSS (**Figure 5.10A; Table 5.9**). GSEA analysis suggested that most of these regions were associated with genes involved in metabolism, especially fatty acid oxidation pathway and TCA cycle (**Figure 5.10B**). Moreover, analysis of enriched TFBS suggested an enrichment of Erra (essential for mitochondria biogenesis (Schreiber et al., 2004)) and BCL3 (critical component for adaptive immune response (Herrington and Nibbs, 2016)) (**Figure 5.10C**).

In summary, these data suggested a progressively open chromatin landscape at gene promoters was established during cardiomyocyte maturation between P1 and P56, which primarily occurred at the promoters of genes involved in cardiomyocyte metabolism and the immune response.

5.3.5. Chromatin accessibility is reduced at E2f4 and Foxm1 sites during postnatal cardiomyocyte maturation

RNA-seq and ATAC-seq (1 kbp±TSS) datasets were next intersected to understand the relationship between chromatin accessibility and transcriptional regulation. Importantly, the integration of both sequencing data sets demonstrated a strong positive correlation of active transcription with open chromatin at TSSs (**Figure 5.11A**). Analysis of the TFBS suggested that genes that were highly expressed and associated with open chromatin at P1 were significantly enriched for several critical TFs for cell proliferation, such as E2f4, E2f1 and Foxm1 binding sites (**Figure 5.11B**). Conversely, Pol2, Bcl3 and Erra binding sites were enriched in gene sets that were up-regulated with open chromatin at P56 (**Figure 5.11C**). In sum, these data revealed a positive relationship between transcription and open chromatin structure and identified several critical TFs that might participate in the cardiomyocyte maturation process.

5.3.6. Isolation of human cardiomyocyte nuclei for RNA-seq and ATAC-seq

To fully understand the key developmental processes that govern mammalian cardiomyocyte maturation, a similar strategy was applied to archival human ventricular samples at various stages of development. RNA-seq and ATAC-seq of human cardiomyocyte nuclei would provide an understanding of cardiomyocyte specific transcriptional programs and chromatin landscape dynamics during human cardiac maturation for the first time (**Table 5.1**). Briefly, 4 sample groups were included for human RNA-seq and ATAC-seq, including foetal (13-19 wks), 0-10 yrs, 10-30 yrs and 30+ yrs.

Similar to mouse studies, $PCM1^+$ nuclei were isolated from frozen human ventricular heart tissue samples from different age groups. Cardiomyocyte specificity of the $PCM1^+$ nuclei was tested by real-time qPCR for cell type specific markers (cardiomyocytes: MYH6, MYH7, TNNC1, TNNI3; fibroblast: COL1A1, COL3A1, FBN1, DDR2; endothelial cells: VWF and immune cells: ITGAM) (**Figure 5.12**). The results confirmed that human $PCM1^+$ nuclei were highly enriched for cardiomyocyte specific markers. Next, isolated $PCM1^+$ samples were processed for RNA-seq and ATAC-seq. Initial preliminary analysis of RNA-seq data showed that at least 89% of sequencing reads were uniquely mapped to the human genome and at least 75% were assigned to a gene, suggesting high quality sequencing data were generated (**Table 5.2**). In addition, MDS analysis of the sequenced samples revealed distinct clusters were formed by foetal, 0-10 yrs and 30+ yrs groups (**Figure 5.13**). Bioinformatics analysis of human RNA-seq and ATAC-seq data sets are underway. Unfortunately, due to time constraints, these data will not be included in this PhD Thesis. Nevertheless, this Thesis outlines the methodological pipelines for RNA-seq and ATAC-seq of mammalian cardiomyocyte nuclei, which will be used in the future to characterise the chromatin accessibility landscape of human cardiomyocytes for the first time.

Table 5.1. Selected human heart specimens for RNA-seq and ATAC-seq.

Bin	Age	Code	Sex	Heart Tissue	ATAC-seq	RNA-seq
Foetal	13 wks	9773	F	LV	x	x
	14 wks	9770	F	LV	√	√
	16 wks	9768	F	LV	√	√
	19 wks	9763	F	LV	√	√
0-10 yrs	3 wks	6012	M	LV	√	√
	10 wks	4087	F	LV/ IVS	√	√
	2 yrs	705	M	LV	√	√
	4 yrs	4152	M	LV	√	√
10-30 yrs	14 yrs	4043	M	LV	√	√
	16 yrs	7072	M	LV	√	√
	17 yrs	3134	M	LV	√	x
	17 yrs	7060	M	LV	√	x
	19 yrs	7012	M	LV	√	x
	23 yrs	4013	M	LV	√	x
	25 yrs	6038	M	LV	√	x
	29 yrs	5086	M	LV	√	x
30+ yrs	37 yrs	7040	M	LV	√	x
	40 yrs	6008	M	LV	√	√

	44 yrs	3122	M	LV	√	√
	48 yrs	6052	M	LV	√	x
	55 yrs	4062	M	LV	√	x
	62 yrs	7028	M	LV	√	√

* Note:

1. Foetal 13 wks sample only used for real-time qPCR due to no enough quantity for RNA-seq or ATAC-seq.

Table 5.2. Quality control of human PCM1^{+} nuclei RNA-seq reads by STAR and featureCounts (f: foetal, w: weeks, y: years).

	Total reads	% Uniquely mapped reads	% Multi-mapped	% Un-mapped	Assigned reads	% Assigned reads
f14w	72,644,087	95.27%	3.19%	1.22%	59,636,409	82.09%
f16w	52,242,769	95.77%	2.88%	1.11%	42,734,181	81.80%
f19w	70,098,883	95.14%	3.16%	1.37%	56,937,531	81.22%
3w	51,134,960	90.56%	6.92%	1.95%	38,386,008	75.07%
10w	55,190,224	95.14%	3.05%	1.32%	44,175,023	80.04%
2y	58,143,412	95.12%	3.29%	1.28%	45,813,276	78.79%
4y	47,382,739	93.34%	4.52%	1.81%	36,925,972	77.93%
14y	59,159,454	89.55%	8.66%	1.44%	44,714,807	75.58%
16y	56,402,691	94.23%	4.21%	1.28%	44,517,834	78.93%
40y	66,859,238	95.77%	2.73%	1.19%	52,788,846	78.96%

44y	47,682,840	93.59%	4.25%	1.58%	36,944,090	77.48%
62y	56,246,363	95.10%	3.30%	1.28%	42,489,260	75.54%

Table 5.3. Additional PCR amplification cycle during human PCM1^{+} nuclei ATAC-seq libraries construction (f: foetal, w: weeks, y: years).

Sample	Rn (top)	Rn (low)	Rn (Sum)= Rn (top)- Rn (low)	Extra PCR cycle
f14w	0.8	0.06	0.74	11
f16w	0.75	0.085	0.665	11
f19w	0.8	0.09	0.71	11
3w	0.73	0.065	0.665	11
10w	0.85	0.09	0.76	10
2y	0.625	0.09	0.535	14
4y	0.8	0.06	0.74	10
14y	0.775	0.12	0.655	11
16y	0.71	0.05	0.66	12
17y-3134	0.76	0.07	0.69	12
17y-7060	0.775	0.075	0.7	11
19y	0.74	0.14	0.6	11
23y	0.675	0.08	0.595	13
25y	0.59	0.06	0.53	14
29y	0.755	0.095	0.66	12
37y	0.765	0.075	0.69	11
40y	0.795	0.12	0.675	12

44y	0.725	0.045	0.68	10
48y	0.75	0.08	0.67	12
55y	0.64	0.065	0.575	14
62y	0.785	0.09	0.695	11

Table 5.4. Additional PCR amplification cycle during mouse PCM1^{+} nuclei ATAC-seq libraries construction.

Sample	Rn (top)	Rn (low)	Rn (Sum)= Rn (top)- Rn (low)	Extra PCR cycle
P1-1	2.2	0.3	1.90	5
P1-2	2.4	0.4	2.00	7
P1-3	2.3	0.25	2.05	7
P14-1	2.3	0.3	2.00	8
P14-2	2.25	0.3	1.95	9
P14-3	2.25	0.25	2.00	9
P56-1	2.25	0.25	2.00	8
P56-2	2.25	0.5	1.75	7
P56-3	2.3	0.65	1.65	8

Table 5.5. Bioinformatics analysis pipeline.

	Function	Software	Input file type	Reference file type	Output file type
1	Qualicty control, trimming of poor quality sequencing reads	Fastx toolkit (RNA)	.fastq.gz	-	.fastq.gz
		Skewer (DNA)			
↓					
2	Mapping	STAR (RNA)	.fastq.gz	.fa (generated by STAR indexing)	.bam
		BWA (DNA)		.fa (generated by BWA indexing)	
				.gtf	
↓					
3	Peak calling (DNA only)	MACS	.bam	-	.saf / .bed
↓					
4	Count reads and generate matrix	feature Counts	to quantify at genes or specific genome feature: .bam (from BWA or	.gtf / custom genome feature .saf	.mx

			STAR)		
			to quantifiy global peak distribution: .bam (from BWA)	.saf (generated from MACS by merging all peaksets)	.mx
↓					
5	Sample similarity test	Rstudio	.mx	-	MDS plot (.pdf / .jpg)
↓					
6	Differential gene expression	Rstudio-edgeR	.mx	-	DGE spreadsheet (.xls)
↓					
7	Ontology	GSEA	.rnk (generated from logFC and adjusted p-value of edgeR)	.gmt	.xls / .pdf
↓					
8	TF motifs analysis (DNA peaks only)	Homer	.bed (generated from .mx)	unchange peak sets (.bed) and .fa	.html

Table 5.6. Quality control of mouse PCM1^{+} nuclei RNA-seq reads by STAR and featureCounts.

Sample	Total reads	%Uniquely mapped	%Multimapped	%Unmapped	%Assigned reads	Assigned reads
P1-1	68,512,799	94.32%	2.00%	3.68%	85.48%	58,567,486
P1-2	57,754,801	94.05%	1.99%	3.96%	85.21%	49,214,558
P1-3	58,487,025	93.53%	2.13%	4.34%	84.78%	49,587,028
P14-1	43,495,718	92.52%	2.40%	5.08%	84.24%	36,641,831
P14-2	44,842,478	92.06%	2.28%	5.66%	83.71%	37,539,561
P14-3	46,359,284	92.11%	2.22%	5.67%	83.90%	38,894,187
P56-1	54,482,507	93.68%	2.46%	3.86%	84.22%	45,886,211
P56-2	57,325,021	93.79%	2.20%	4.01%	84.53%	48,455,170
P56-3	58,734,172	93.80%	2.15%	4.05%	84.37%	49,554,405

Table 5.7. Differential expression of mouse PCM1^{+} nuclei RNA-seq between P1 vs. P14, P14 vs. P56 and P1 vs. P56.

	DGE	Up	Dn
P1 vs. P14	8193	4350	3843
P1 vs. P56	10369	5088	5281
P14 vs. P56	7113	3323	3790

Table 5.8. Quality control of mouse PCM1^{+} nuclei ATAC-seq reads by BWA and featureCounts.

Sample	Total reads	Mapped Q10	Mapped Q20	%MapQ	Total Q20 reads	TSS assigned	TSS assigned %	Gene Assigned
P1-1	72,517,156	53,640,927	53,640,927	73.97%	176,640,656	2674544	3.69%	3519093
P1-2	77,059,406	48,347,793	48,347,793	62.74%		2576882	3.34%	3592856
P1-3	111,552,674	74,651,936	74,651,936	66.92%		4106252	3.68%	5829840
P14-1	109,087,985	70,455,399	70,455,399	64.59%	181,838,251	3896994	3.57%	5437797
P14-2	95,137,466	64,086,045	64,086,045	67.36%		3723605	3.91%	5296468
P14-3	86,128,542	47,296,807	47,296,807	54.91%		2595565	3.01%	3621401
P56-1	75,413,580	55,506,944	55,506,944	73.60%	138,382,130	3365470	4.46%	4780900
P56-2	71,660,454	49,474,315	49,474,315	69.04%		3091933	4.31%	4651638
P56-3	46,835,518	33,400,871	33,400,871	71.32%		2079152	4.44%	3019502

Table 5.9. Differential chromatin landscape of mouse PCM1$^+$ nuclei ATAC-seq between P1 vs. P14, P14 vs. P56 and P1 vs. P56.

	DGE	Up	Dn
P1 vs. P14	55	40	15
P1 vs. P56	882	476	406
P14 vs. P56	62	53	9

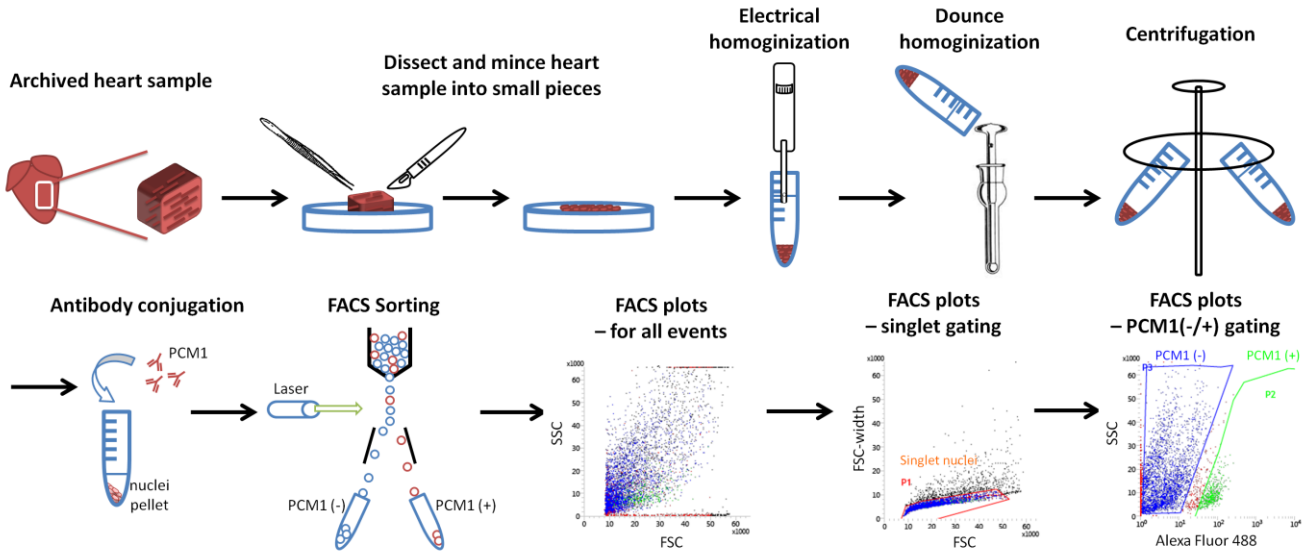

Figure 5.1. Schematic of the isolation of cardiomyocyte specific nuclei.

Left ventricular heart tissue was isolated from individual hearts and archived in liquid nitrogen. Archived heart samples were dissected and minced into approximately 1mm^3 cubes, followed by two stages of homogenization and centrifugation. Nuclei pellets were then stained with PCM1 antibody and PCM1 (-/+) nuclei were separated through FACS. All nuclei that went through FACS process were plotted according to forward scatter (FSC) versus side scatter (SSC). Singlet nuclei were further selected through FSC versus FSC width setting. Singlet nuclei were then plotted according to SSC and secondary antibody signal (Alexa Fluor 633 or Brilliant Violet 421).

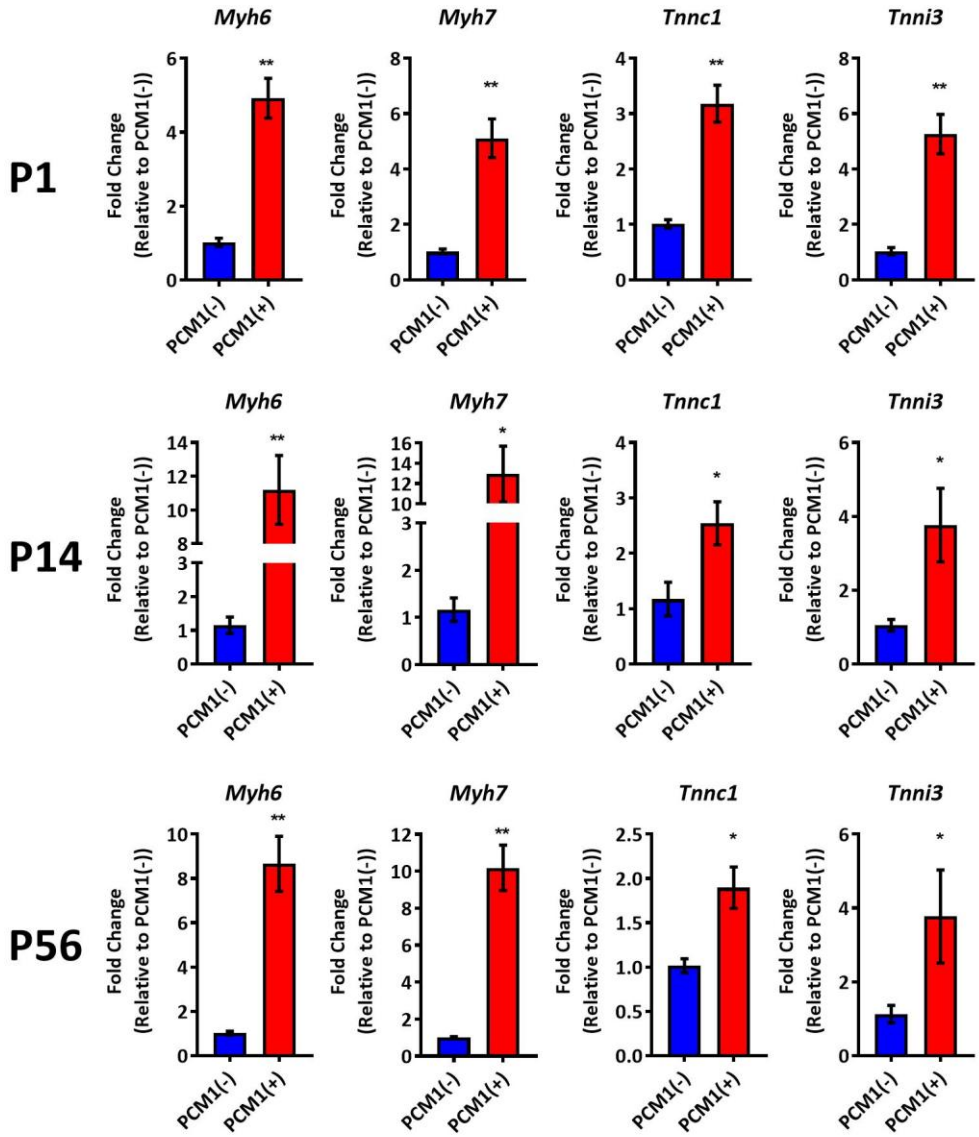

Figure 5.2. PCM1^{+} nuclei enriches for cardiomyocyte specific markers during heart development.

qPCR gene expression profiling of *Myh6, Myh7, Tnnc1* and *Tnni3* in PCM1 (-/+) cardiomyocyte populations from P1 to P14 and P56. (n=3 per group). All gene expression values are normalized to 18S and presented as a fold change relative to PCM1^{-}. All data are presented as mean ±s.e.m. *P<0.05, ** P <0.001).

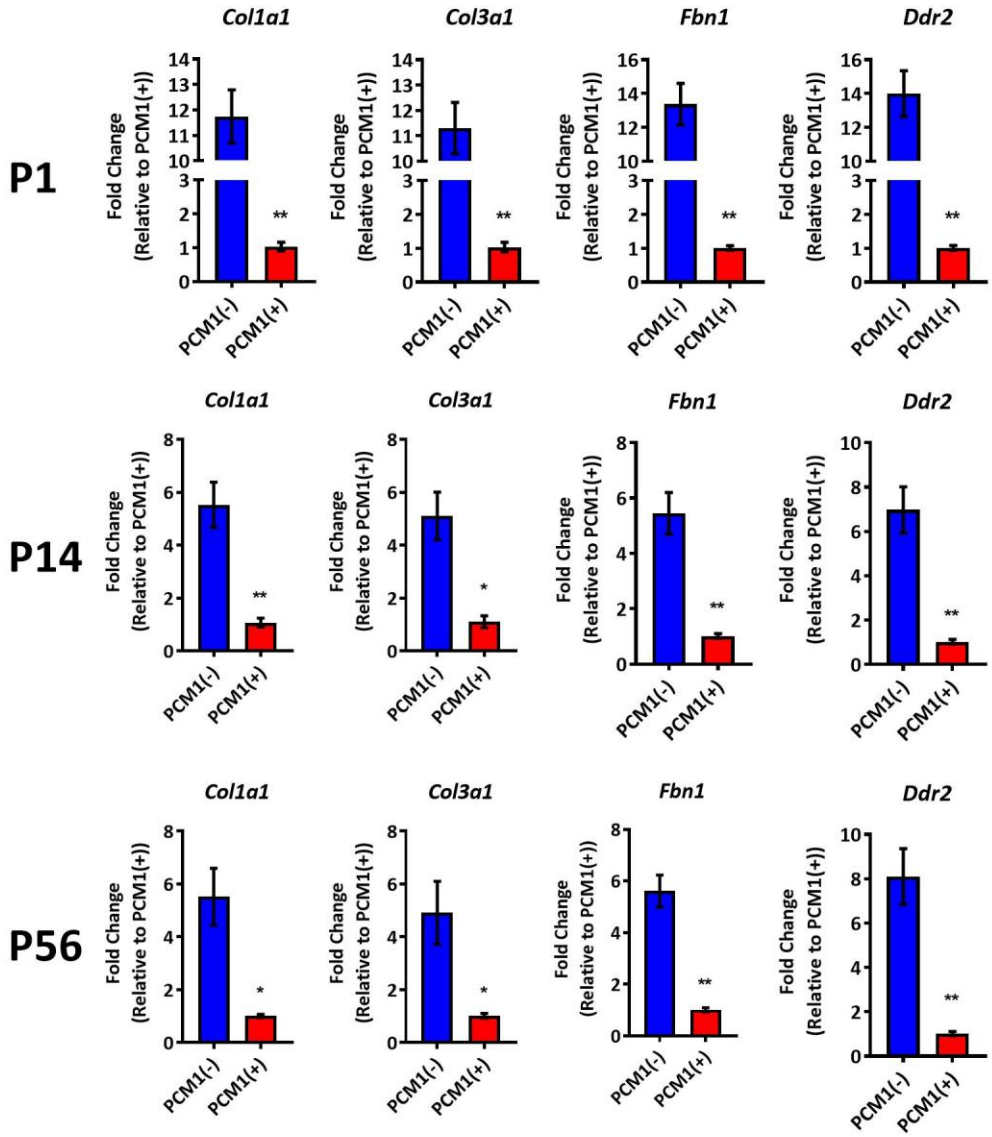

Figure 5.3. PCM1$^-$ nuclei enriches for fibroblast specific markers during heart development.

qPCR gene expression profiling of *Col1a1, Col3a1, Fbn1* and *Ddr2* in PCM1 (-/+) cardiomyocyte populations from P1 to P14 and P56. (n=3 per group). All gene expression values are normalized to 18S and presented as a fold change relative to PCM1$^+$. All data are presented as mean ±s.e.m. *P<0.05, ** P <0.001).

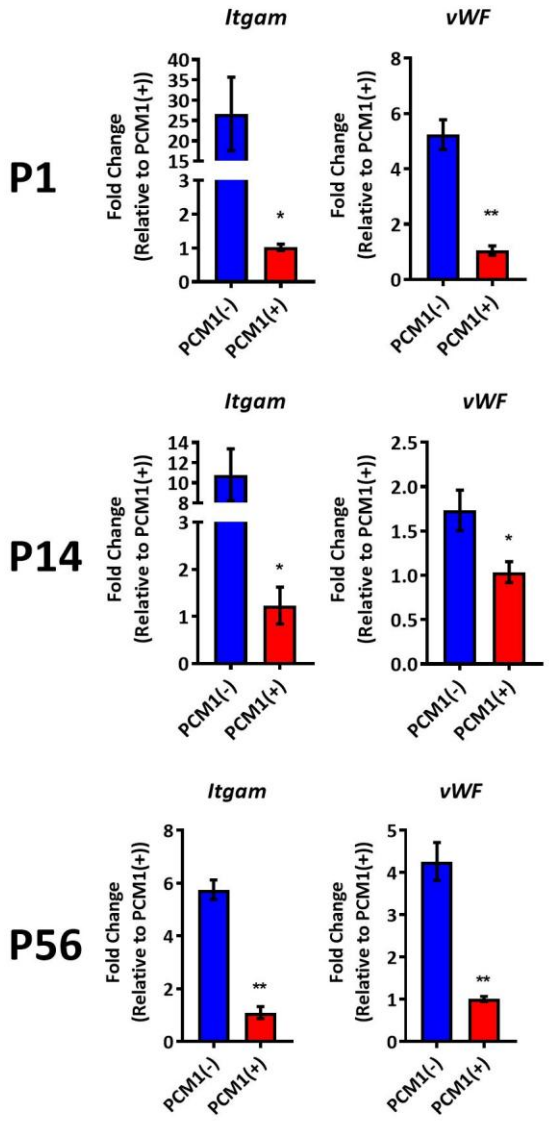

Figure 5.4. PCM1$^-$ nuclei enriches for endothelial and immune cell specific markers during heart development.

qPCR gene expression profiling of *Itgam* and *Vwf* in PCM1 (-/+) cardiomyocyte populations from P1 to P14 and P56. (n=3 per group). All gene expression values are normalized to 18S and presented as a fold change relative to PCM1$^-$. All data are presented as mean ±s.e.m. *P<0.05, ** P <0.001).

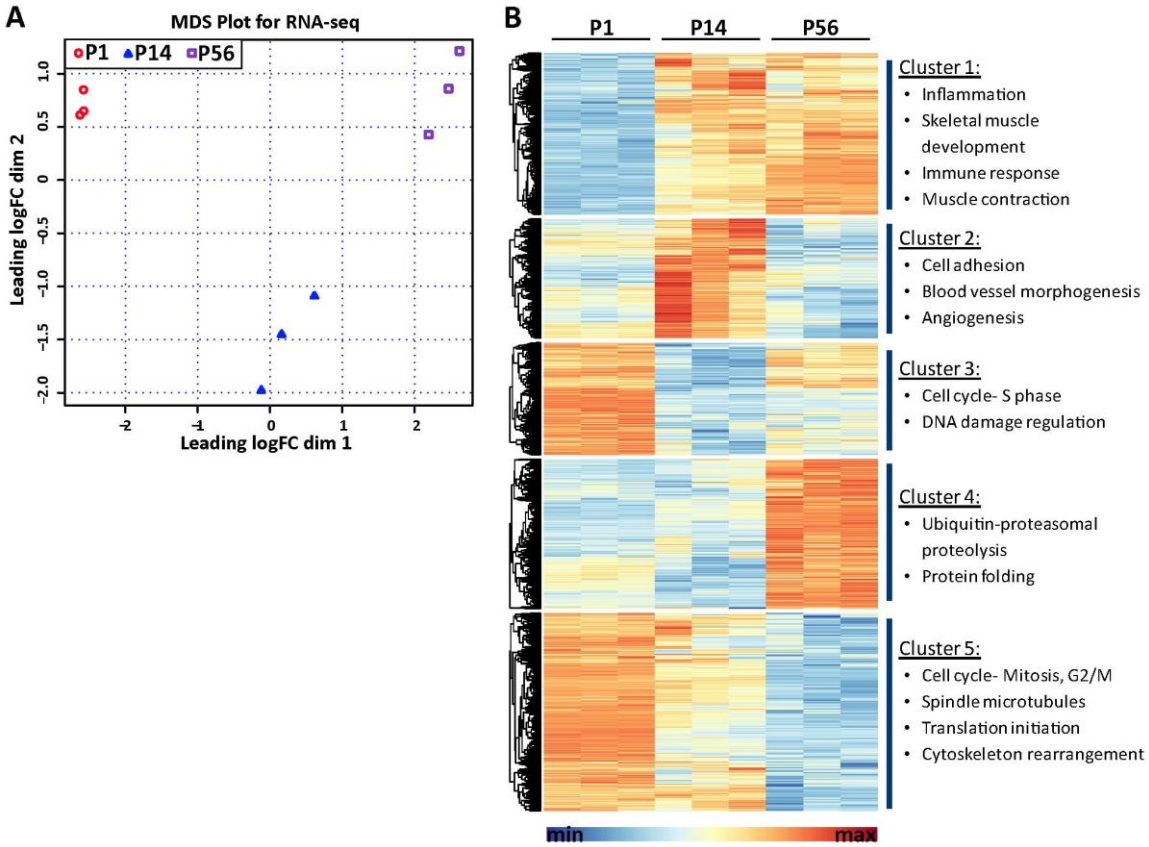

Figure 5.5. RNA-seq analysis of cardiomyocyte specific gene expression during heart development.

A. MDS plot of RNA-seq data showing distinct clusters formed by 3 replicates of individual time point from P1 to P56.

B. Heatmap of differentially expressed genes from P1 to P14 and P56. Genes with higher expression levels are shown in red whereas genes with lower expression levels are shown in blue. 5 clusters were formed by the datasets. Gene GO process analysis (MetaCore) revealed the involved functional processes.

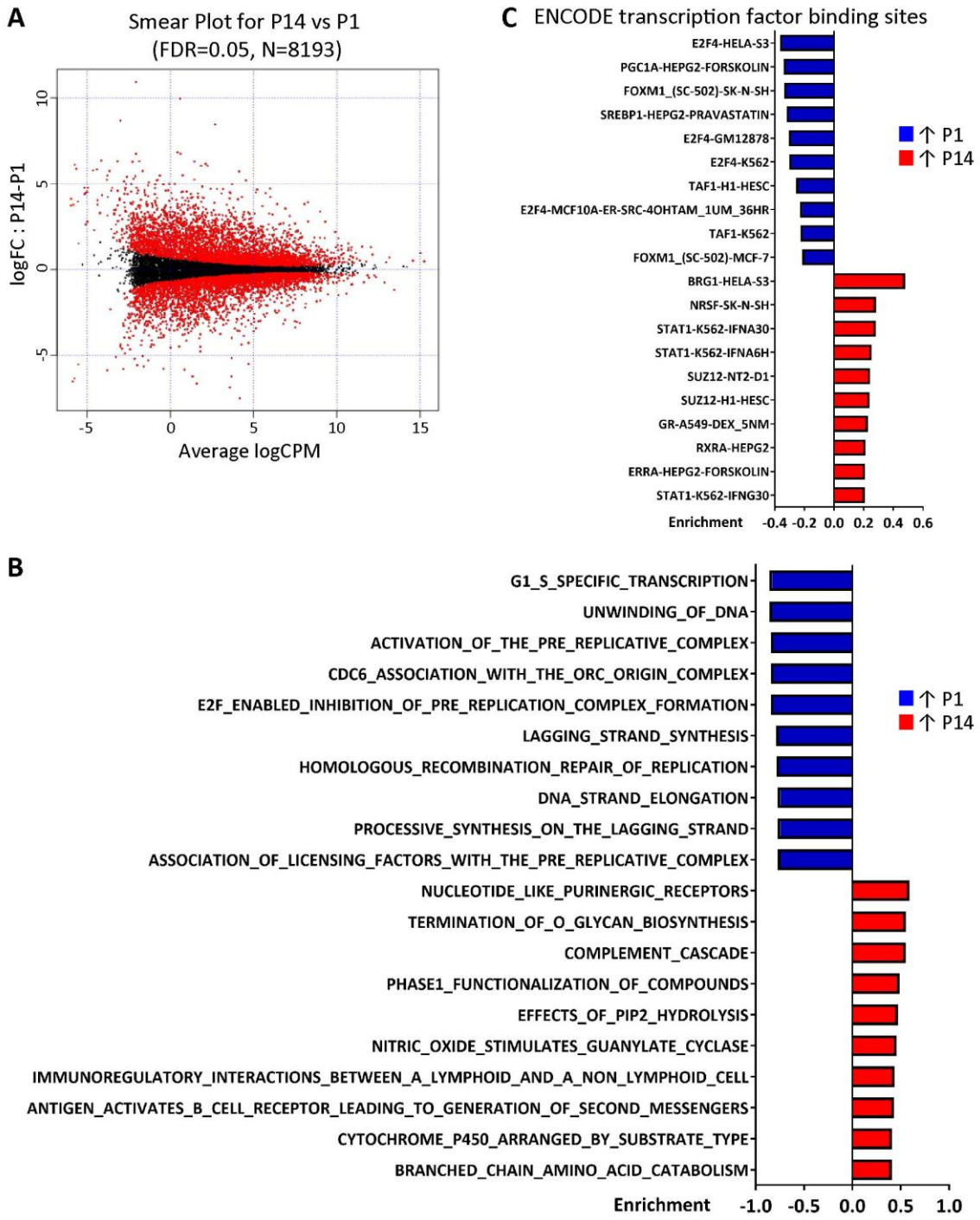

Figure 5.6. RNA-seq analysis of cardiomyocyte specific gene expression revealed cell cycle shut down activity during P1 and P14.

A. Smear plot of RNA-seq data showing average signal intensity (x-axis) versus log2 fold change in gene expression (P14/P1). Differentially expressed genes (FDR ≤ 0.05, *n*=8193) are shown in red and non-significant changes are shown in black.

B. GSEA reactome analysis of differentially expressed genes from P1 to P14. Reactome that are enriched at P1 (Blue) or enriched at P14 (Red).

C. GSEA TFBS analysis of differentially expressed genes from P1 to P14. TFBS that are enriched at P1 (Blue) or enriched at P14 (Red).

.

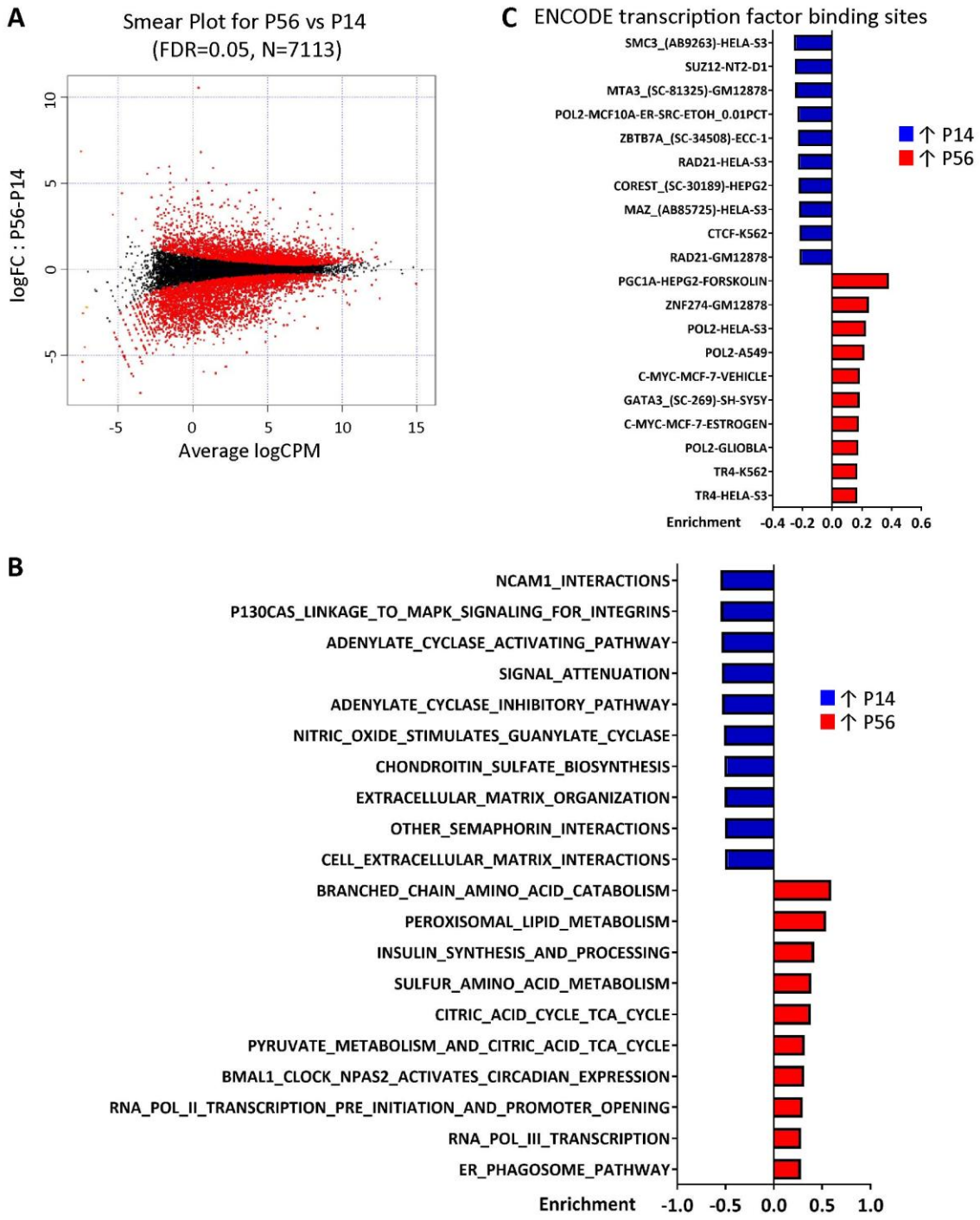

Figure 5.7. RNA-seq analysis of cardiomyocyte specific gene expression revealed the activation of TCA cycle during P14 and P56.

A. Smear plot of RNA-seq data showing average signal intensity (x-axis) versus log2 fold change in gene expression (P56/P14). Differentially expressed genes (FDR ≤ 0.05, *n*=7113) are shown in red and non-significant changes are shown in black.

B. GSEA reactome analysis of differentially expressed genes from P14 to P56. Reactome that are enriched at P14 (Blue) or enriched at P56 (Red).

C. GSEA TFBS analysis of differentially expressed genes from P14 to P56. TFBS that are enriched at P14 (Blue) or enriched at P56 (Red).

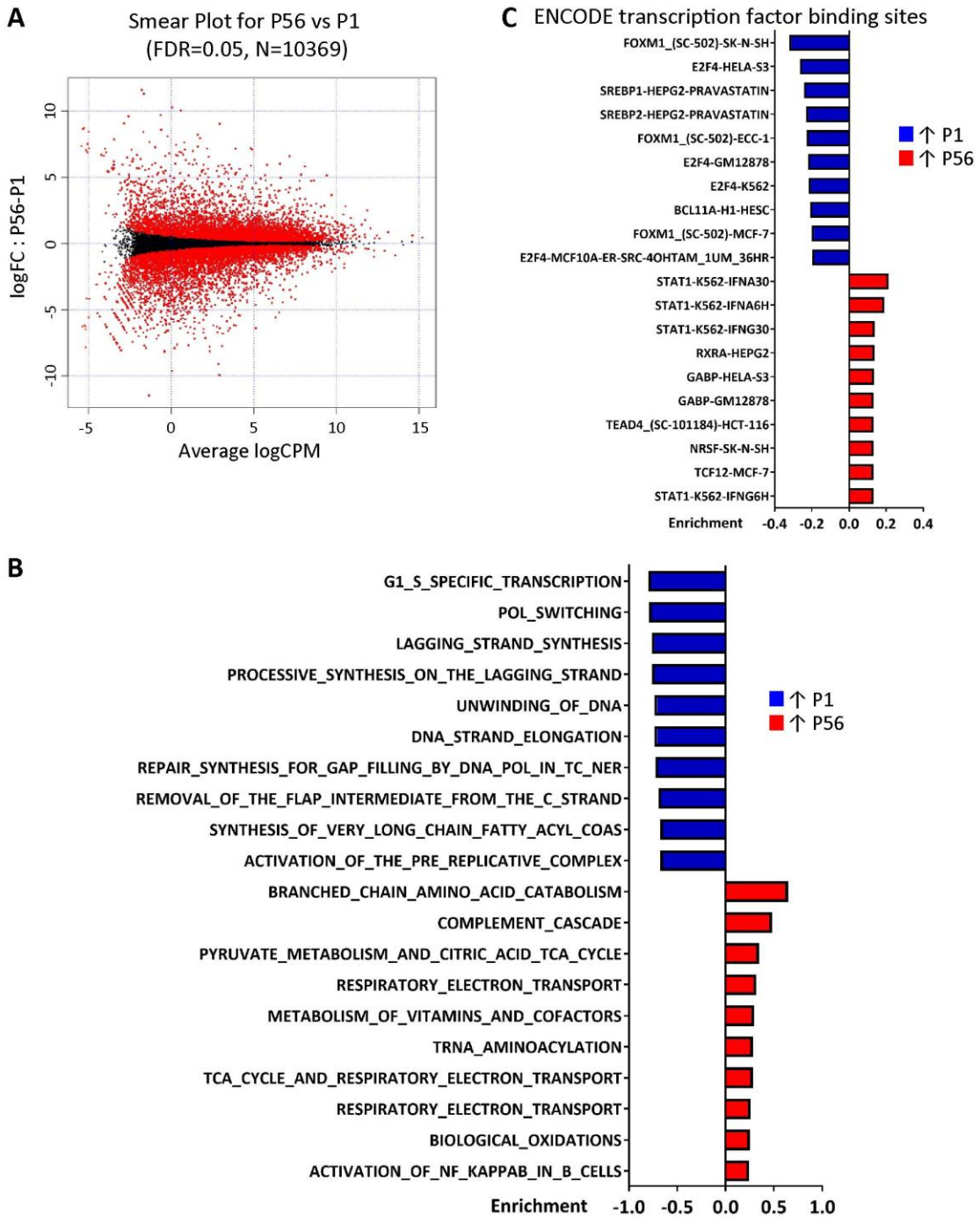

Figure 5.8. RNA-seq analysis of cardiomyocyte specific gene expression revealed cell cycle shut down and activation of TCA cycle during P1 and P56.

A. Smear plot of RNA-seq data showing average signal intensity (x-axis) versus log2 fold change in gene expression (P56/P1). Differentially expressed genes (FDR ≤ 0.05, *n*=10369) are shown in red and non-significant changes are shown in black.

B. GSEA reactome analysis of differentially expressed genes from P56 to P1. Reactome that are enriched at P1 (Blue) or enriched at P56 (Red).

C. GSEA TFBS analysis of differentially expressed genes from P56 to P1. TFBS that are enriched at P1 (Blue) or enriched at P56 (Red).

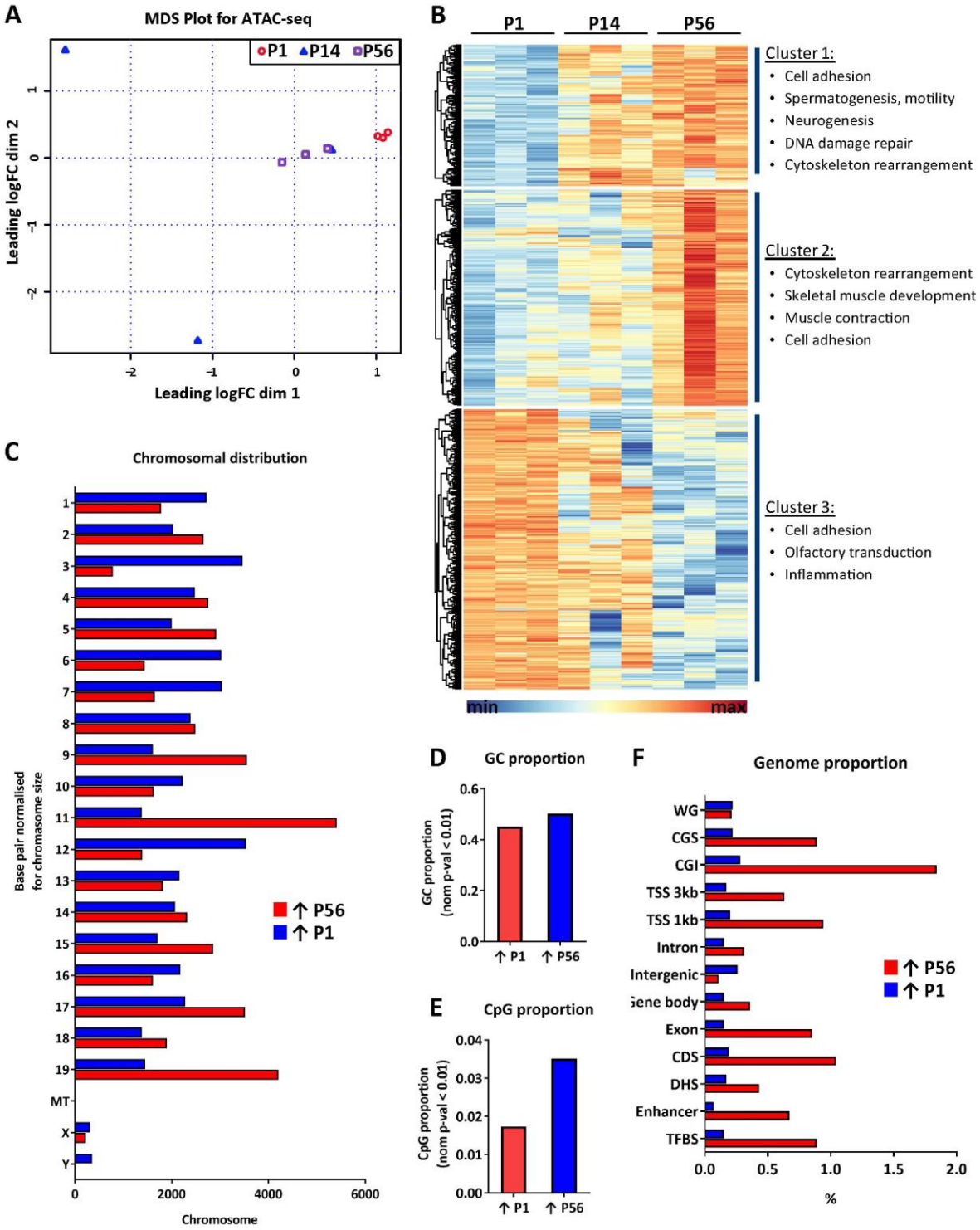

Figure 5.9. ATAC-seq analysis of cardiomyocyte specific chromatin structure during heart development.

A. MDS plot of ATAC-seq data showing distinct clusters formed by 3 replicates of P1 and P56.

B. Heatmap of differentially expressed genes from P1 to P14 and P56. Genes with higher expression levels are shown in red whereas genes with lower expression levels are shown in blue. 3 clusters were formed by the datasets. Gene GO process analysis (MetaCore) revealed the involved functional processes.

C. Distribution of differentially accessible regions across each chromosome at P1 (blue) and P56 (red) for mouse (mm10) genome normalised by chromosome length.

D. Distribution of differentially accessible regions across GC component at P1 (red) and P56 (blue) in mouse (mm10) genome.

E. Distribution of differentially accessible regions across CpG sites at P1 (red) and P56 (blue) in mouse (mm10) genome.

F. Distribution of differentially accessible regions shown by genomic features. Open chromatin regions at P1 are shown in blue, accessible chromatin regions at P56 are shown in red.

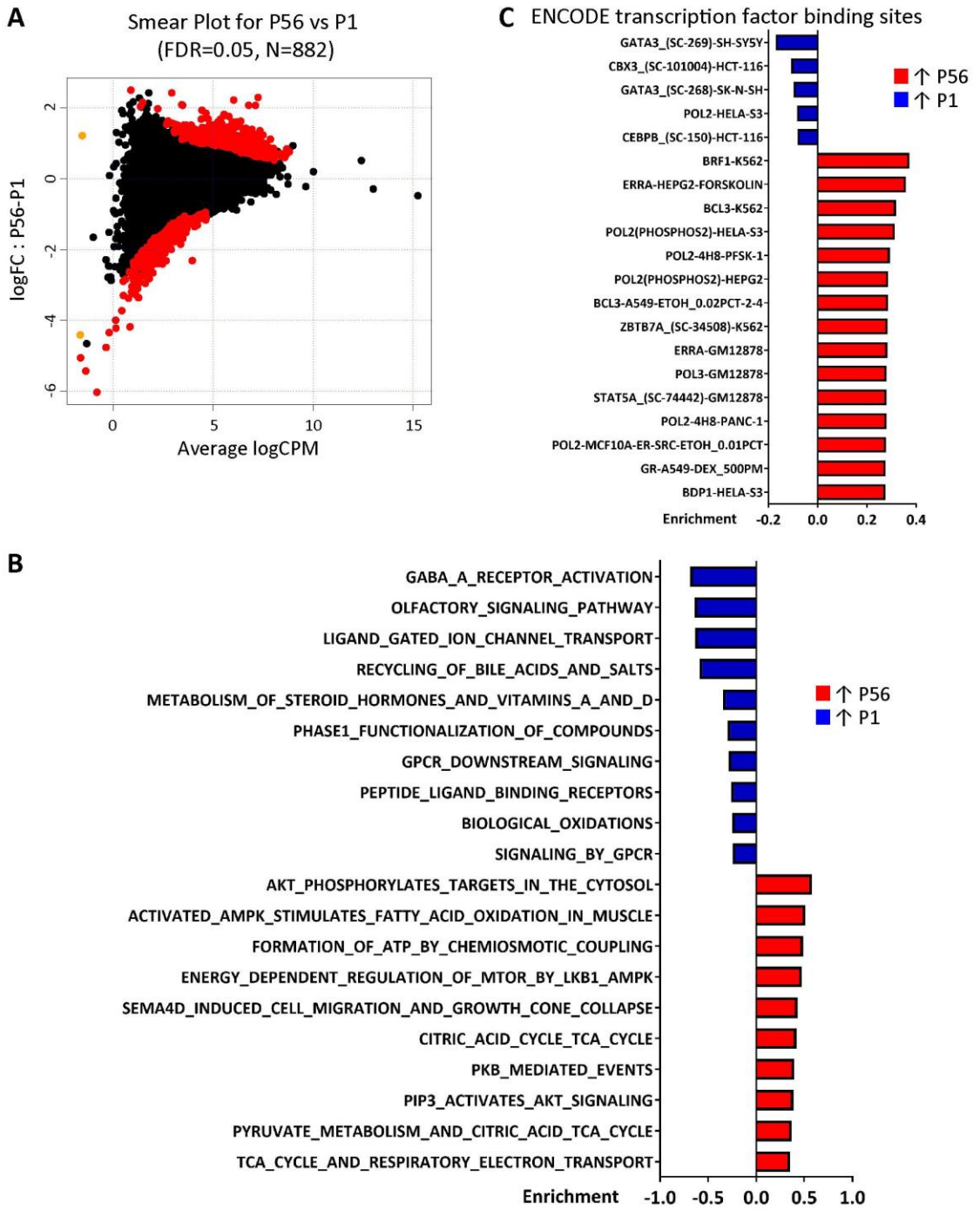

Figure 5.10. ATAC-seq analysis of cardiomyocyte specific chromatin structure showed enrichment of pathway for matured metabolism pathway between P1 and P56.

A. Smear plot of ATAC-seq data showing average signal intensity (x-axis) versus log2 fold change in chromatin accessibility (P56/P1). Differentially accessible genes (FDR ≤ 0.05, *n*=882) are shown in red and non-significant changes are shown in black.

B. GSEA reactome analysis of differentially accessible genes from P56 to P1. Reactome that are enriched at P1 (Blue) or enriched at P56 (Red).

C. GSEA TFBS analysis of differentially accessible genes from P56 to P1. TFBS that are enriched at P1 (Blue) or enriched at P56 (Red).

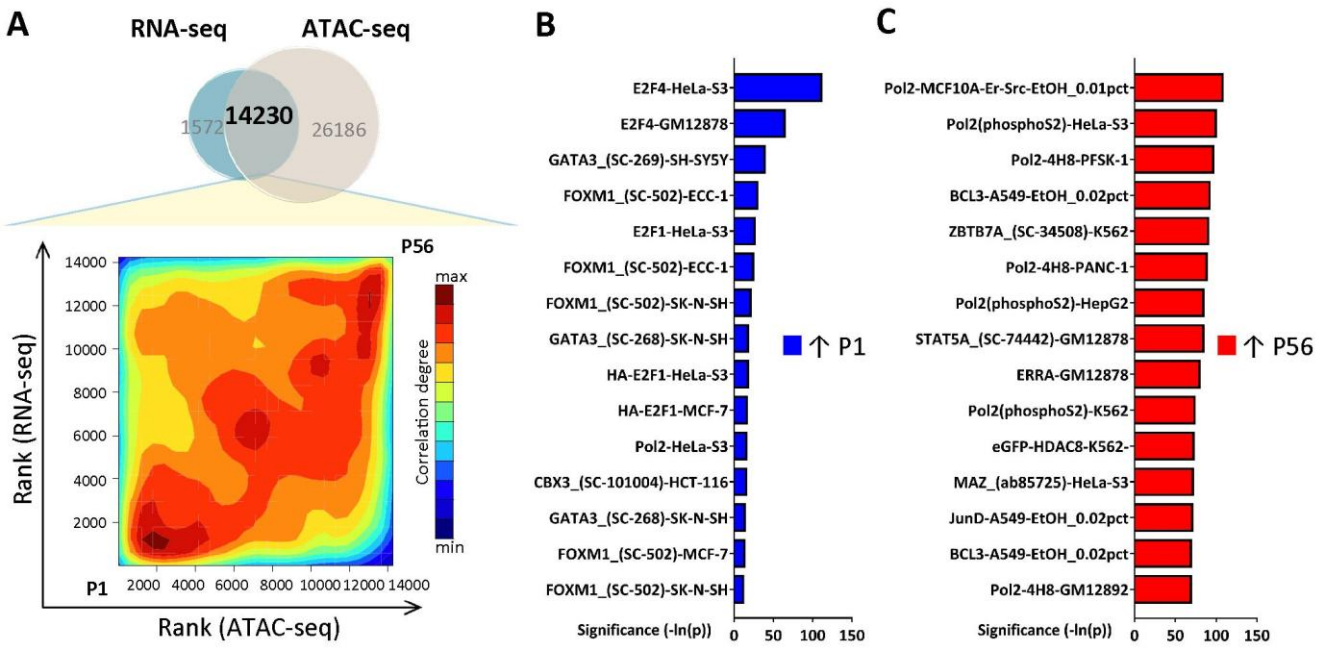

Figure 5.11. Integration of RNA-seq and ATAC-seq demonstrated a positive correlation of gene expression with chromatin structure between P1 and P56, with the enrichment of TF, E2F4 at P1.

A. (Top) Venn diagram of all differentially regulated genes (no p-value threshold) from RNA-seq and ATAC-seq 1 kbp±TSS data sets. A total of 14230 genes were detected in both data sets. (Bottom) Heatmap contour of integration of RNA-seq and ATAC-seq data showed positive correlation between active transcription and open chromatin structure. The degree of positive correlation is shown from red (highest) to blue (lowest).

B. GSEA TFBS analysis of differentially regulated genes from RNA-seq and ATAC-seq between P1 to P56. TFBS that are enriched at P1 open chromatin and actively transcripted genes are shown in blue.

C. GSEA TFBS analysis of differentially regulated genes from RNA-seq and ATAC-seq between P1 to P56. TFBS that are enriched at P56 open chromatin and actively transcripted genes are shown in red.

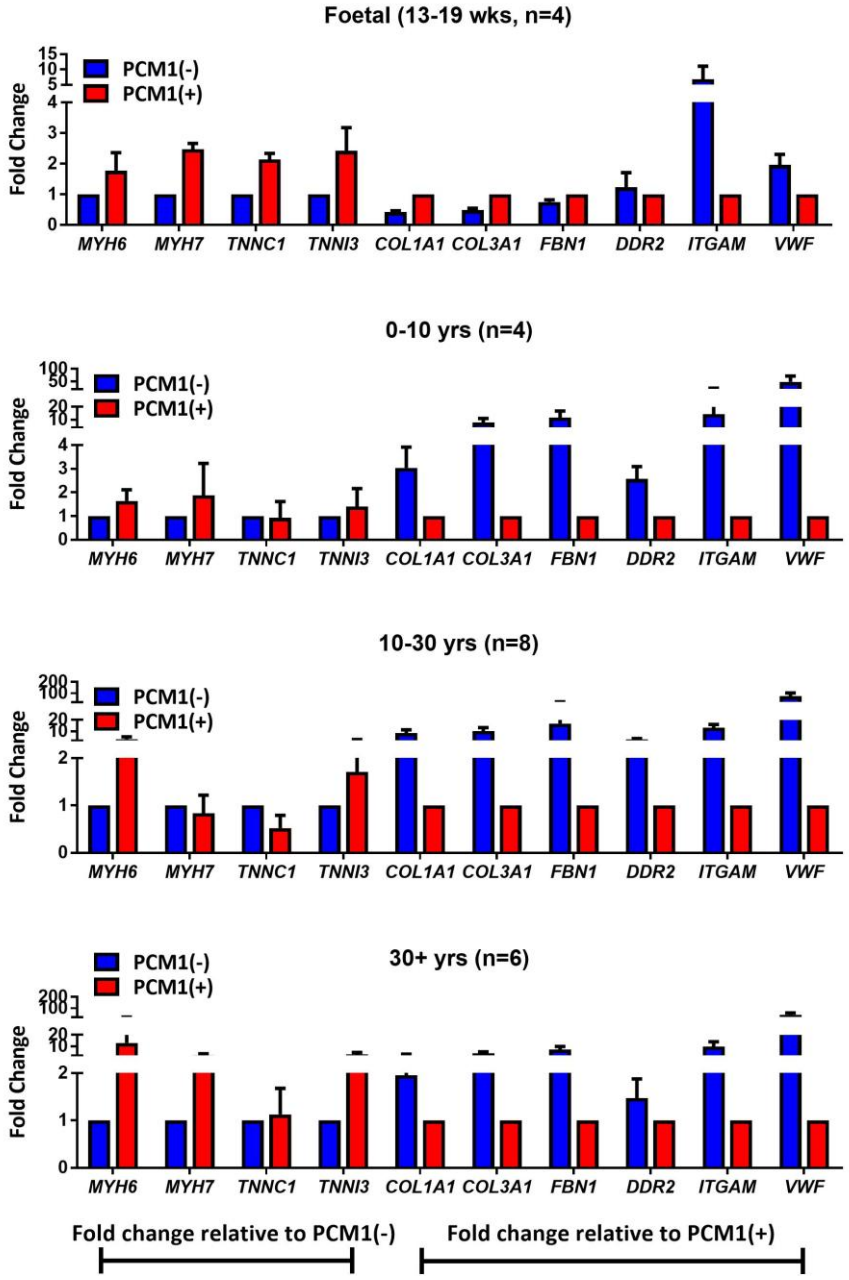

Figure 5.12. PCM1^{+} nuclei enriches for cell type specific markers during human heart development.

qPCR gene expression profiling of *MYH6, MYH7, TNNC1, TNNI3; COL1A1, COL3A1, FBN1, DDR2; ITGAM* and *VWF* in human PCM1 (-/+)cardiomyocyte populations from foetal, 0-10 yrs, 10-30 yrs and 30+ yrs group (n=4-8 per group). All gene expression values are normalized to 18S and presented as a fold change relative to PCM1 (-/+). All data are presented as mean ±s.e.m.

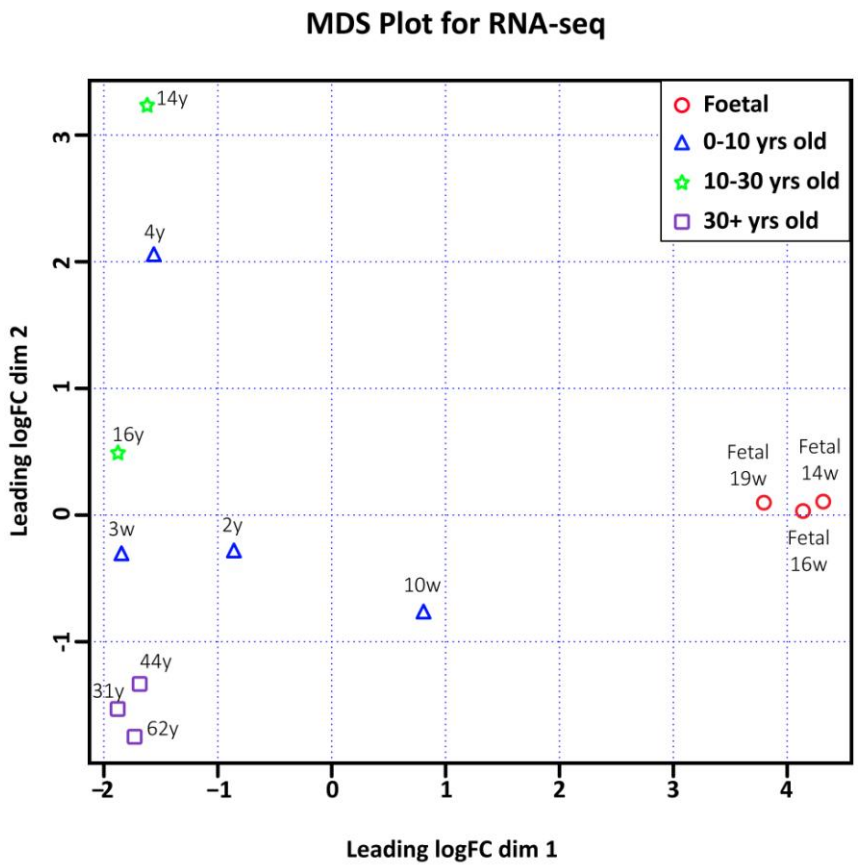

Figure 5.13. RNA-seq analysis of cardiomyocyte specific gene expression during human heart development.

MDS plot of RNA-seq data showing distinct clusters formed by replicates of individual time point from foetal, 0-10 yrs, 10-30 yrs and 30+ yrs.

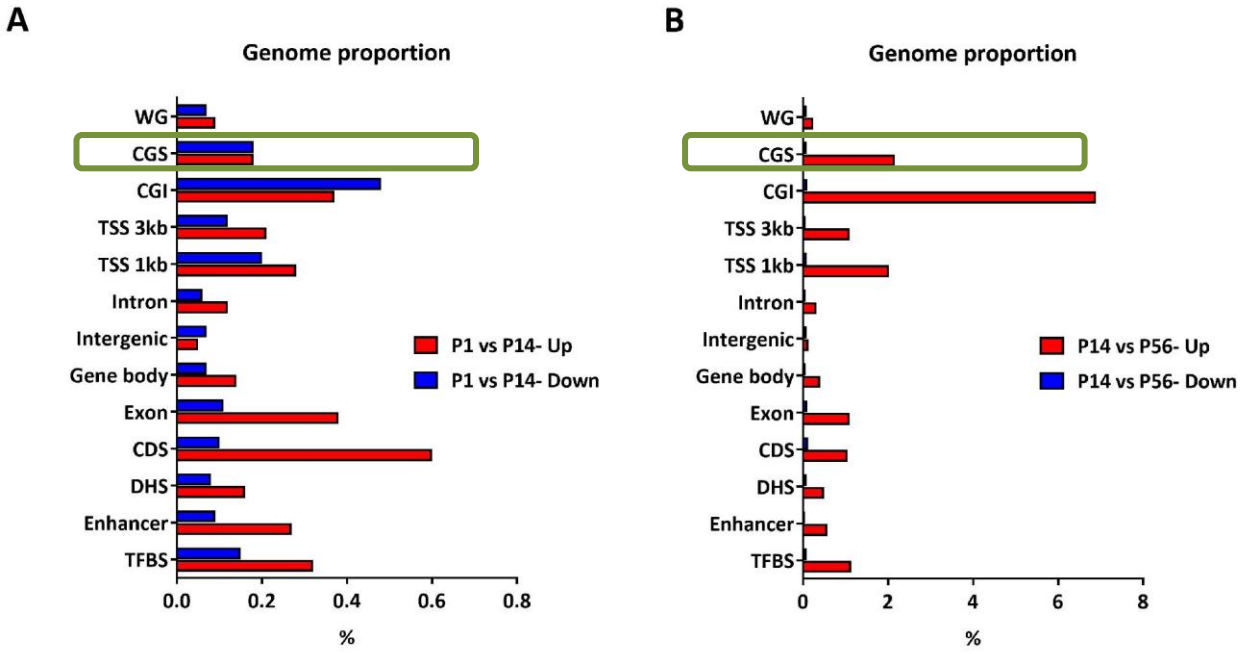

Figure 5.14. Genomic feature analysis of ATAC-seq peak sets between P1 vs. P14 and P14 vs. P56.

A. Distribution of differentially accessible regions shown by genomic features. Open chromatin regions at P1 are shown in blue, accessible chromatin regions at P14 are shown in red. CGI is marked in green box.

B. Distribution of differentially accessible regions shown by genomic features. Open chromatin regions at P14 are shown in blue, accessible chromatin regions at P56 are shown in red. CGI is marked in green box.

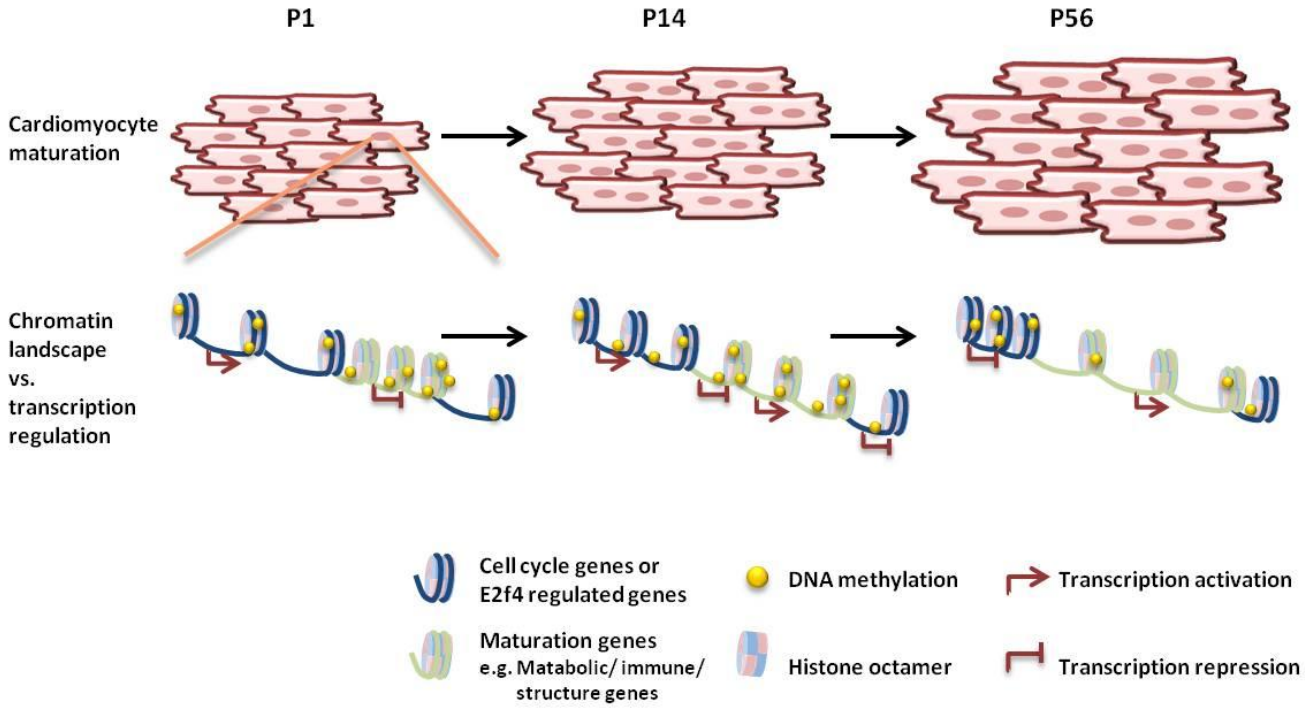

Figure 5.15. Schematic of proposed model for chromatin landscape, DNA methylation and transcription regulation during postnatal cardiomyocyte maturation.

In the proposed model, cell cycle related genes undergo chromatin compaction between P1 to P14 and completely closed by P56, with potential increase methylation at CpG island of E2f4 regulated genes. Meanwhile, maturation required genes undergo hypomethylation and become more accessible between P14 to P56.

5.4. Discussion and conclusion

The current chapter has shown for the first time that the chromatin landscape of cardiomyocytes is positively correlated with transcriptome changes during postnatal maturation. Current findings suggest that the cardiomyocyte transcriptome exhibits distinct biological changes during postnatal development from P1 to P14 and P14 to P56. Specifically, 2 distinct waves of transcriptional regulation have been identified involving the repression of cell cycle activities from P1 to P14 and the transition towards an adult metabolic system from P14 to P56. Importantly, bioinformatics analyses identified critical TF binding motifs that are enriched at these 3 distinct developmental time points, corresponding to the biological processes that are regulated during these critical stages of postnatal cardiac development. Furthermore, the chromatin landscape demonstrated a progressively open chromatin structure between P1 and P56, which was associated with the acquisition of an open chromatin state at the promoter regions of metabolic genes in adult cardiomyocytes. Moreover, a strong positive correlation between open chromatin structure in promoter regions and transcriptional activity was identified. Notably, the binding motifs of several core cell cycle TFs, such as E2f4, E2f1 and Foxm1, underwent chromatin compaction during cardiomyocyte maturation from P1 to P56, suggesting the postnatal repression of cardiomyocyte cell cycle genes could be related to chromatin remodelling at cell cycle promoters in cardiomyocytes. The current chapter identifies novel relationships between the chromatin accessibility landscape and transcription during postnatal cardiomyocyte maturation and is consistent with an epigenetic mechanism for postnatal cardiomyocyte cell cycle arrest.

An important finding of the current chapter is the identification of a positive correlation between chromatin accessibility at gene promoters and active transcription of downstream genes in cardiomyocytes using ATAC-seq couples with RNA-seq. Moreover, this analysis enabled the identification of TFs governing cardiomyocyte transcriptional programs between P1 vs. P56. While the concept of chromatin accessibility enabling transcriptional activation is well accepted (Song et al., 2011; Thurman et al., 2012), this is the first time that cardiomyocyte transcriptome dynamics has been linked to the accessible chromatin landscape on a genome-wide scale during cardiomyocyte maturation. Importantly, the developmental acquisition of a condensed chromatin state at cell cycle related genes was associated with transcriptional repression of the cardiomyocyte proliferation program. Furthermore, transcriptional activity of cell cycle genes in P1 cardiomyocytes was associated with accessible chromatin containing motifs for several cell proliferation TFs, such as E2f4, E2f1 and Foxm1. These findings support the hypothesis that postnatal cardiomyocyte cell cycle arrest is epigenetically regulated. Several lines of evidence

indicate that E2f1, E2f4 and Foxm1 comprise core TFs required for cardiomyocyte proliferation. A previous study has reported that E2f4 is localized in nuclei during cardiomyocyte mitosis and is essential for neonatal rat cardiomyocyte proliferation *in vitro*.(van Amerongen et al., 2010). Inhibition of E2f4 leads to premature repression of cardiomyocyte mitotic events (van Amerongen et al., 2010). However, overexpression of E2f4 led to restricted expression of E2f4 in the cytoplasm instead of the nucleus and failed to induce proliferation in neonatal rat cardiomyocyte *in vitro*. Similarly, E2f1 was reported to regulate cardiomyocyte proliferation (Ebelt et al., 2006). In addition, in vivo knock-out of Foxm1 caused embryonic lethality in mice due to ventricular wall thinning (Bolte et al., 2011; Bolte et al., 2012). Collectively, these TFs are highly associated with cardiomyocyte proliferation and it would be important to investigate their capacity to induce adult cardiomyocyte proliferation *in vivo* to fully understand their role in regulation of postnatal myocyte cell cycle shut down. Furthermore, as previously discussed in Chapter 1, many studies have shown that factors which can lead to potent activation of neonatal cardiomyocyte proliferation have failed to serve the same purpose in adult cardiomyocytes. The more compacted chromatin landscape around cell cycle genes in adult cardiomyocytes could provide an explanation for this phenomenon. Without pioneer TFs to open the chromatin structure at cell proliferation genes, mitogenic stimuli may not be able to reach their full potential in promoting cell cycle activation in the adult heart (Denny et al., 2016). Therefore, it will be important in the future to determine whether these TFs can initiate the open chromatin structure and compete with nucleosomes as pioneer TFs in adult cardiomyocytes. These studies will be important in determining therapeutic strategies for inducing cardiomyocyte proliferation in the injured adult heart.

Another interesting result from this chapter is the regulation of distinct biological processes during defined windows of postnatal cardiac development. Cell cycle activity is repressed in mouse cardiomyocytes from P1 to P14, initiation of cell-cell contacts, immune system development and activation of adult metabolic pathways occurs from P1 to P14 and the full activation of the mature cardiomyocyte metabolic system is established between P14 and P56. These results not only support the previously well-known early postnatal cell cycle shut down of cardiomyocytes between P1 and P14 (Alkass et al., 2015; Soonpaa et al., 1996), but also provide novel understanding regarding the timing of different cellular transitions towards the acquisition of the final terminally differentiated, mature cardiomyocyte phenotype. In addition, the identification of TFs that drive these postnatal maturation processes at individual time points further supports the proposal of core TFs driving the cardiomyocyte maturation process (Consortium, 2012; Gerstein et al., 2012; Song et al., 2011). Future validation of these TFs *in vivo* and in human cardiomyocytes will provide a more complete understanding of their role during postnatal cardiac development.

Globally, the chromatin accessibility landscape appears to open between P1 and P56 across almost every genomic feature except intergenic regions. However, reflecting the transcriptional changes observed between P1, P14 and P56, chromatin accessibility also dynamically changes from P1 to P14 and P56, especially at the CGI regions (**Figure 5.14**). Interestingly, it was found that chromatin regions around CGI are compacted between P1 and P14 and then open between P14 and P56. This is particularly interesting, as previously in Chapter 3 (**Figure 3.1A, B**) it was shown that the cardiac methylome is hypermethylated between P1 and P14 and globally hypomethylated after P14. As CGI is enriched for CpG and DNA methylation prefers CpG sites, the current result provides supporting evidence for our previously proposed model whereby two waves of DNA methylation shape the cardiomyocyte epigenome during postnatal heart development. A working model is proposed whereby the transcription of cardiomyocyte cell cycle genes is gradually shut down due to chromatin compaction between P1 to P14. In contrast, a progressively open chromatin landscape is acquired between P14 and P56, which is associated with hypomethylation of cardiomyocyte structural (Gilsbach et al., 2014), immune-related and metabolic genes, without affecting the previously compacted cell proliferation genes. Together, these epigenetic modifications collaborate to re-structure the chromatin landscape and direct postnatal cardiomyocyte maturation (**Figure 5.15**).

5.5. Summary and future direction

The experimental platform developed in this study has demonstrated developmental stage- and cell type-specific changes in the chromatin landscape and transcriptome during heart development. The positive correlation of chromatin landscape and transcription indicates a potential regulatory mechanism between the two. However, whether chromatin landscape is the cause of transcription regulation and postnatal cell cycle shutdown or simply a consequence of transcription status remains unclear. Future studies are required to interrogate this relationship during postnatal cardiomyocyte maturation.

Chapter 6

General Discussion

An experiment is a question which science poses to Nature
And a measurement is the recording of Nature's answer.
Max Planck.

Chapter 6. General Discussion

6.1. Overview

The mammalian heart has traditionally been recognised as an organ of limited regenerative capacity. This notion has recently been challenged by the observation that neonatal mice retain a transient capacity for heart regeneration for a short period after birth (Porrello et al., 2011b). Cardiac regeneration in neonatal mice, as well as adult zebrafish, is driven by cardiomyocyte proliferation (Haubner et al., 2012; Jopling et al., 2010; Kikuchi et al., 2010; Porrello et al., 2011b; Porrello et al., 2013). Concordantly, many studies have demonstrated that mitogenic stimuli that promote cardiomyocyte proliferation in neonates fail to deliver the same outcome in adulthood (refer to Section 1.1.3). Therefore, there is intensive interest in defining the mechanisms that shut down cardiomyocyte proliferative capacity and drive cardiac maturation in the postnatal period. The role of epigenetics in postnatal cardiac maturation has gained considerable attention as one possible mechanism for cardiomyocyte terminal differentiation (refer to Section 1.5.1, 1.5.2), but this hypothesis has not been formally tested. Moreover, the roles of DNA methylation and chromatin dynamics in postnatal cardiomyocyte maturation remain largely unstudied and poorly understood.

In this Thesis, 3 major questions have been asked and addressed (Figure 1.7):

1. What is the role of DNA methylation in transcriptional regulation during cardiac maturation?
2. Does DNA methylation regulate cardiomyocyte proliferation during mammalian heart development?
3. What is the relationship between the chromatin accessibility landscape and transcription during mammalian cardiomyocyte maturation?

The major findings of this Thesis are (Figure 6.1):

1. The murine heart experiences two postnatal waves of DNA methylation and transcriptional remodelling during cardiac maturation (**Chapter 3 and 5**).
    - Between P1 and P14, the cardiac transcriptome transitions from a pro-proliferative state towards the acquisition of a mature structural, immune and metabolic state (**Figure 3.4, 5.5**). Site-specific hypermethylation occurs across thousands of genomic loci during this developmental window (**Figure 3.1, 3.5**).

- Between P14 to P56, the cardiomyocyte transcriptome shifts towards an oxidative metabolic system (**Figure 5.5**), which is associated with global hypomethylation of the cardiomyocyte genome (**Figure 3.1**).

2. DNA methylation is essential for rodent and human cardiomyocyte proliferation (**Chapter 3: Figure 3.3, Chapter 4: Figure 4.5**).
3. Identification of novel relationships between DNA methylation, chromatin accessibility and TFs (**Chapter3 and 5**):
    - Several canonical developmental and differentiation-associated signalling pathways including Hedgehog, TGFβ, FGF, Notch and Wnt are hypermethylated and transcriptionally repressed between P1 and P14. These hypermethylated regions are highly enriched for Smad TF motifs (**Figure 3.9**).
    - E2f4, E2f1 and Foxm1 dependent gene promoters become compacted during cardiomyocyte maturation, which is associated with transcriptional repression of cell cycle genes. In contrast, Erra dependent gene promoters become more accessible and transcriptionally activated postnatally (**Figure 5.6B, 5.7B, 5.8B, 5.11B, C**).
4. The cardiomyocyte chromatin landscape is dynamically altered during development and is positively associated with transcription (**Chapter 5: Figure 5.10A, 5.11**).

This PhD Thesis provides new insight into the role of DNA methylation and chromatin dynamics during cardiac development. This Thesis identifies novel relationships between DNA methylation, chromatin accessibility and transcription during cardiac development, suggesting a significant role for epigenetic modifications in the loss of cardiomyocyte proliferative potential during postnatal maturation. In addition, this Thesis uncovers previously unappreciated relationships between chromatin accessibility and core cell cycle TFs, which might contribute towards postnatal terminal differentiation of cardiomyocytes. Collectively, this Thesis supports the hypothesis that cardiomyocyte terminal differentiation and maturation are under epigenetic control. The following sections will discuss the importance of these findings and their broad implications for our understanding of cardiac developmental and regenerative biology.

6.2. Postnatal remodelling of the cardiomyocyte epigenome – physiological adaptation with pathophysiological consequences?

The research outcomes from this PhD Thesis demonstrate that the cardiac DNA methylome undergoes dynamic alterations during postnatal development. Specifically, two waves of postnatal

DNA methylation were identified, where focal hypermethylation occurs from P1 to P14 and global hypomethylation predominates from P14 to P56. Thousands of DMRs were identified during the critical P1 to P14 developmental window when cardiac regenerative capacity is lost in mice. Hypermethylation was associated with transcriptional repression of several components of signalling pathways associated with early cardiac development and proliferation and these hypermethylated regions were enriched for TF binding motifs related to TGFβ/Smad signalling, including Smad3, Foxh1 and Tbx5 (Sim et al., 2015). These results are supported by another study that has investigated the cardiac DNA methylome between ESCs, neonatal and adult cardiomyocytes (Gilsbach et al., 2014) (refer to section 1.5.1, 1.5.4). Combining the two datasets, it is becoming clearer that developmental signalling pathways are hypermethylated and repressed, while some maturation related signalling pathways (related to structural remodelling, metabolism and contraction) are progressively hypomethylated and expressed during cardiac maturation.

Importantly, the phenomenon of focal hypermethylation at CGIs followed by global hypomethylation has been widely observed in both senescent and cancer cells when compared to "young" cells or non-cancerous cells, respectively (Berman et al., 2011; Cruickshanks et al., 2013; Hansen et al., 2011). In cancerous cells, this shift in DNA methylation is thought to act acts as a defence system enabling cell cycle shutdown in senescent cells. However, it also leads to DNA epigenome instability, which makes the cell vulnerable to carcinogenic stimuli and which cancerous cells eventually employ to overcome the cell cycle shutdown barrier (Cruickshanks et al., 2013; Gomez et al., 2016). Unlike cardiomyocytes, most cells that develop cancer retain proliferation capacity throughout life, which means that more proliferation events increase the exposure rate to carcinogens and therefore increase the likelihood for mutational events that can overcome intrinsic cell cycle regulatory mechanisms. Could this same DNA methylome drift happen during postnatal cardiac development and contribute to cardiomyocyte cell cycle arrest? Or could this phenomenon represent a physiological adaptation that induces cell cycle shutdown by acquiring a "senescent-like" cardiac methylome to maintain lifelong function of terminally differentiated cardiomyocytes? While cancer cells metastasise through the blood system, which passes through the heart, myocardial tumours are extraordinarily rare (~0.3-0.7% vs. high incident type cancer such as breast cancer at 12%) (DeSantis et al., 2014; Leja et al., 2011). From an evolutionary perspective, such a mechanism could promote organismal survival over the maintenance of specific organ regenerative capacity.

While the current Thesis points towards an essential role for DNA methylation during postnatal cardiac maturation, there is still considerable debate regarding the requirement of Dnmts for normal

heart development. Several studies and results from this PhD Thesis have shown that Dnmt1, Dnmt3a and Dnmt3b are indispensible for heart development and maturation (Fang et al., 2016; Gilsbach et al., 2014; Li et al., 1992; Okano et al., 1999; Sim et al., 2015). Also, Gilsbash et al have shown that Dnmt3a/3b is essential for cardiac gene expression in the adult heart (Gilsbach et al., 2014). However, a subsequent study from the same lab has suggested that Dnmt3a/3b are dispensable for the maintenance of postnatal cardiomyocyte function (Nuhrenberg et al., 2015) (refer to section1.5.4). Notably, while Dnmt1 has traditionally been known as a DNA methylation maintenance enzyme, recent studies have exhibited its *de novo* methylation ability (see (Jeltsch and Jurkowska, 2014) for detailed discussion), providing a potential compensatory effect for Dnmt3a/3b knockout in the study by Nuhrenberg et al. Furthermore, the results from this PhD Thesis indicate that DNA methylation is controlled during specific developmental windows, which may have been missed in the aforementioned studies. Due to the stage-specific activation and inhibition of the DNA methylation machinery, future studies should employ genetic tools that enable temporal deletion of DNA methyltransferases in cardiomyocytes at defined stages of postnatal development that coincide with the major methylome transitions reported here.

It is also important to note that while the results from this PhD Thesis have reported hypermethylation at gene bodies at P14, Gilsbach et al reported a demethylation at gene bodies from foetal to adult stages (Gilsbach et al., 2014; Sim et al., 2015). This might potentially be due to the limitation of the selected sequencing approach, as MBD-seq is an enrichment-based genome-wide sequencing approach that lacks the base-pair resolution of whole genome bisulphite sequencing, which was used by Gilsbach et al (Gilsbach et al., 2014; Sim et al., 2015). Also, a large cohort of hypermethylated genes was paradoxically up-regulated during development in Chapter 3. Importantly, the study from Chapter 3 was performed on whole heart tissue and this observation could be due to the presence of mixed cell populations in whole tissues. Nonetheless, this phenomenon has previously been observed in other genome-wide methylation studies (Ball et al., 2009; Lister et al., 2009) and could reflect more complex relationships between region-specific DNA methylation patterns and gene transcription, or could be a general artefact of genome-wide studies using heterogeneous cell populations from whole tissues.

Together, it is clear that DNA methylation has a role in postnatal regulation of cardiac development and maturation. Future studies are required to carefully investigate the developmental stage- and ventricular cardiomyocyte-specific functions of DNA methylation, which will provide a clearer picture of the requirement of DNA methylation for cardiomyocyte maturation. In addition, it is well-accepted that DNA methylation and other histone marks act in concordance to modify the

epigenome and transcription (Romanoski et al., 2015). It will therefore be important to take a broader view of the epigenome beyond single epigenetic marks in order to gain a more complete mechanistic understanding of the transcriptional control of cardiac development.

6.3. Harnessing the DNA methylome for cardiac regeneration

An interesting outcome of this PhD thesis was the observation that pharmacological inhibition of DNA methylation via the hypomethylating agent 5aza-dC induces proliferation of immature rodent and human cardiomyocytes (Chapter 3 and 4). Interestingly, 5aza-dC also reduced cardiomyocyte binucleation *in vivo*, which is consistent with another *in vitro* study showing reduced rates of binucleation in 5aza treated cardiomyocytes following agonist stimulation with endothelin (Paradis et al., 2014). Notably, the most successful clinical targets of 5aza or 5aza-dC - advanced myelodysplastic syndrome, chronic myeloid leukaemia and acute myeloid leukaemia - are all associated with mutations in TET2 and isocitrate dehydrogenase 1 or 2 (both associated with DNA hypomethylation) (Figueroa et al., 2010). This might explain why 5aza-dC is effective in this clinical setting. In fact, as 5aza and 5aza-dC are already FDA-approved for clinical use, their effects in promoting immature cardiomyocyte proliferation could indicate a potential usage for heart disease patients to stimulate cardiac regeneration. Interestingly, recent studies have administered 5aza post-MI in adult rodent hearts and demonstrated improved functional outcomes, which were associated with changes in macrophage activity including increased anti-inflammatory macrophage (M2) number and decreased pro-inflammatory macrophage (M1) number (Jeong et al., 2015; Kim et al., 2014). However, cardiomyocyte proliferation rates were not examined in these studies. It is possible that 5aza is targeting upstream TFs that control the cardiac cell cycle (via hypomethylation) and immune system (via hypermethylation) to de-differentiate adult cardiomyocytes to a neonatal state post-MI. Future studies are required to understand the role of 5aza in promoting cardiomyocyte proliferation in the adult heart, which would help inform downstream clinical therapeutic possibilities.

Beside the well-described de-methylating effects of 5-aza, the pharmacological mechanisms of 5aza and 5aza-dC remain unknown. Recent studies have linked both of these compounds to the regulation of cellular metabolism, including effects on mitochondrial copy number and oxidative phosphorylation in various cell lines, suggesting a possible link to metabolic regulation (San Martin et al., 2011; Sok AJ, 2014; Wen et al., 2013). Notably, a recent study has proposed that the postnatal transition to a high oxygen environment provides a key trigger for oxidative metabolism, DNA damage and cardiomyocyte cell cycle arrest (Puente et al., 2014). It is possible that the effects

of 5aza-dC on cardiomyocyte proliferation (and transcription) could be due to unexplored actions on cardiomyocyte metabolism. Further studies are required to assess the mechanistic basis for these effects and whether 5aza is sufficient to promote (or facilitate) cell cycle re-entry in adult cardiomyocytes.

Maturation of human PSC-derived cardiomyocytes is another major barrier in the field (Veerman et al., 2015). The finding that DNA methylation facilitates cardiomyocyte cell cycle arrest and maturation also has important ramifications for the cell therapy field and for disease modelling applications. While transplanted immature cardiomyocytes can proliferate, mature and engraft within the injured heart over time in small animals (Funakoshi et al., 2016; Riegler et al., 2015), previous studies have shown that the injection of these immature cardiomyocytes into the infarcted primate heart leads to transient cardiac arrhythmias (Chong et al., 2014). Targeting the DNA methylome could provide one strategy for controlling cardiomyocyte proliferative potential and maturation prior to implantation. Future studies should focus on understanding the maturation effects of DNA methylation or 5aza-dC in hPSC-derived cardiomyocyte or organoid models. In summary, DNA methylation (or 5aza-dC) could be harnessed for multiple applications in regenerative medicine: (1) transient treatment for cardiomyocyte cell cycle re-entry in the adult heart or (2) promotion of cardiomyocyte proliferation or maturation in hPSC-derived cardiomyocytes.

6.4. Chromatin accessibility and TF activity – towards a mechanistic understanding of cardiomyocyte maturation

Over the decade, the ENCODE, FANTOM and EPIGENOME ROADMAP projects have revealed complex relationships between the epigenome and transcription. It has been shown that enhancers are one of the most critical components of a genomic module. Enhancers often exhibit exquisite cell type or tissue-specific expression patterns, which translate into cell type-specific functions and influence genotype-phenotype associations (Ashburner et al., 2000; Koche et al., 2011; Rada-Iglesias et al., 2011; Roadmap Epigenomics et al., 2015). Accordingly, each cell type encompasses from 20,000 to 40,000 enhancers to drive its transcriptional profile. However, similar groups of enhancers are enriched for common motifs of various TFs (Roadmap Epigenomics et al., 2015), suggesting enhancers are common regulatory elements targeted by specific TFs to drive specific cellular functions and thereby modulate organismal development. This is further supported by previous studies in the reprogramming field where differential expression of TFs and dynamic regulation of target genes synchronizes and drives PSC differentiation into different germ layers

(Thomson et al., 2011; Tsankov et al., 2015). Previous studies have also illustrated that the same TF can regulate different target genes at different developmental stages by binding to unique enhancers or promoters to orchestrate differentiation events (Thomson et al., 2011; Tsankov et al., 2015). Others have provided supporting linkages for the gaps between TFs and enhancer or promoter regulation of target genes through chromatin remodelling via epigenetic modifications, suggesting that epigenomic modifications can precede transcriptional regulation (Koche et al., 2011; Roadmap Epigenomics et al., 2015; Romanoski et al., 2015). This Thesis identifies novel relationships between several cardiomyocyte developmental stage-specific TFs and transcription. It is possible that these specific TFs govern the chromatin landscape and transcription of target genes during the maturation process of cardiomyocytes. Future studies should elucidate whether these TFs directly modulate chromatin accessibility at cell cycle genes or whether chromatin modifications preclude binding of TFs to critical cell cycle regulatory regions.

It is important to note that the cell cycle-associated TF, E2f4, which was identified in this PhD Thesis as significantly associated with open chromatin regions in neonatal cardiomyocytes, has been previously reported to associate with various epigenetic modifiers. E2F4 has been shown to form multimolecular complexes with pRb2, p130, HDAC1, SUV39H1 and p300 (or DNMT1) to regulate the transcription of estrogen receptor α through DNA methylation, histone deacetylation or histone methylation in breast cancer (Macaluso et al., 2003). A subsequent study has also validated that E2F4 recruited SIN3-HDAC complexes for transcriptional repression, while the HCF1-E2F1 complex recruited MLL and SET1 H3K4 histone methyltransferase complexes for transcriptional activation during the cell cycle (Tyagi et al., 2007). Additionally, E2F4 can coordinate with KDM5A (histone demethylase) for strong repression of cell cycle genes during differentiation of ESCs. Notably, not only can E2f4 recruit epigenetic modifiers, it can also associate with chromatin remodellers to modify chromatin structure. A recent study has shown that E2f4 restricted liver regeneration by remodelling the chromatin landscape of cell cycle associated genes by forming E2f4-SWI/SNF-Arid1a complexes (Sun et al., 2016). Collectively, these results have indicated the potential of E2f4 to act as an upstream TF or even a pioneer TF to regulate chromatin structure and therefore the transcription of its target genes. Future studies are needed to validate whether E2f4 could act as one of the most upstream TF for modulation of the chromatin landscape and transcription of cell cycle genes during postnatal cardiomyocyte maturation.

So what environmental signals could dictate the activity of cell cycle TFs and chromatin accessibility changes during postnatal cardiac maturation? As previously mentioned, a recent study has linked the postnatal switch to an oxygen-rich environment and the subsequent transition

towards oxygen-dependant fatty acid metabolism as a central trigger for postnatal cardiomyocyte cell cycle shutdown (Puente et al., 2014). This switch from glycolysis to fatty acid metabolism could potentially have a direct impact on the downstream one-carbon metabolism pathway, which is a branching pathway of glucose metabolism and has been shown to be critical for tumour development (Gao and Locasale, 2016; Locasale, 2013; Maddocks et al., 2016). One-carbon metabolism is essential for cell proliferation as it utilises the glucose input and distributes the carbon units through downstream folate cycle, methionine cycle and trans-sulphuration pathway to govern various cellular process including biosynthesis, redox regulation and production of methyl groups for DNA methylation (Locasale, 2013). One-carbon metabolism is also indispensable for pluripotency of stem cells and the up-regulation of this pathway has been previously linked with hypermethylation and tumourigenesis (Locasale, 2013; Shyh-Chang et al., 2013; Wang et al., 2009). Notably, the methyl groups derived from the methionine cycle are required for DNA and histone methylation, which could potentially explain the loss of global DNA methylation that was observed between P1 and P14 in the mouse heart (Chapter 3). Furthermore, it is important to note that the oxygen-rich environment, oxidative metabolism and other environmental insults such as heat, UV radiation, H_2O_2 and cytokines can also lead to the generation of reactive oxygen species (ROS) (Finkel and Holbrook, 2000; Ziech et al., 2011). An imbalance between antioxidant components and ROS production in the cell can lead to an excess of ROS and oxidative stress. Importantly, previous studies have reported that ROS can activate several canonical signalling pathways, such as NF-κB, p53, PI3K/AKT, MAPK/ERK, Hippo and Wnt/β-catenin signalling pathways during aging, cancers, differentiation and disease, which in turn could activate downstream TFs controlling the cell cycle (Finkel and Holbrook, 2000; Holmstrom and Finkel, 2014; Korswagen, 2006; Mao et al., 2015). Furthermore, ROS has also been shown to mediate the transcription of several TFs, such as AP1, NF-κB, and PGC1α (co-activator of TF PPARγ) in Alzheimer's disease (Shi and Gibson, 2007). Notably, ROS has direct influences on epigenetic modifications. Several studies have shown that free radicals can induce DNA lesions, which if unrepaired can cause genomic instability, which in turn causes DNA hypomethylation as the modified DNA bases fail to act as substrates for Dnmts (Franco et al., 2008; Ziech et al., 2011). In addition, previous studies have also shown that increased ROS regulates the activity of Sirt1 (deacetylase), which can also drive downstream epigenetic modifications (Shi and Gibson, 2007; Ziech et al., 2011). Recent studies have proposed that free radicals could also serve as nucleophiles or electrophiles to interfere with the methyl and acetyl transfer process of DNA methylation as well as histone methylation and acetylation (Afanas'ev, 2014, 2015). Together, oxidative stress could potentially act as an initiator of signalling pathways for transcriptional regulation or by triggering the expression of upstream TFs. Alternatively, ROS

could also regulate the epigenetic landscape and thereby alter chromatin accessibility for transcription regulation.

Collectively, several models are proposed for the postnatal modification of the cardiomyocyte epigenetic and chromatin landscape (**Figure 6.2**). Future studies are needed to experimentally test these proposed models for an enhanced understanding of postnatal cardiomyocyte maturation.

6.5. Summary and future directions

The heart acquires specialized functions during postnatal development that allow it to cope with the increased demands of life outside the womb. The specialized transcriptional program that gives adult cardiomyocytes their unique identity is epigenetically imprinted during neonatal life. Lessons from developmental studies suggest that the very same epigenetic signatures that give adult cardiomyocytes their identity might also present a roadblock to regeneration. It is likely that re-introduction of regenerative capacity in the adult heart will require a combinatorial strategy targeting both the critical regenerative signalling pathways and the epigenetic brakes to regeneration. Locus-specific targeting of the epigenome will be critical in order to re-activate specific transcriptional networks but very few tools currently exist for site-directed engineering of the epigenome. Re-awakening developmental mechanisms for endogenous regeneration of the adult heart requires a deeper understanding of cell-type specific epigenetic signatures during cardiac development and the continued development of technologies for cellular reprogramming and epigenomic engineering. However, even under cell type and locus-specific targeting strategy, whether a fully developed and functioning adult heart can allow localized dedifferentiation, reprogramming and re-differentiation events which often link to structural remodelling, loss of contractile function and arrhythmia remains a question. Maybe the mammalian heart is not evolutionarily equipped for regeneration in adulthood and cell cycle shutdown represents an important physiological adaptation to oxygen-rich terrestrial life (Celine J Vivien, 2016). Regardless, a more comprehensive understanding of the relationships between the epigenome and transcription during cardiac development and postnatal maturation is necessary and could shape the future of regenerative medicine.

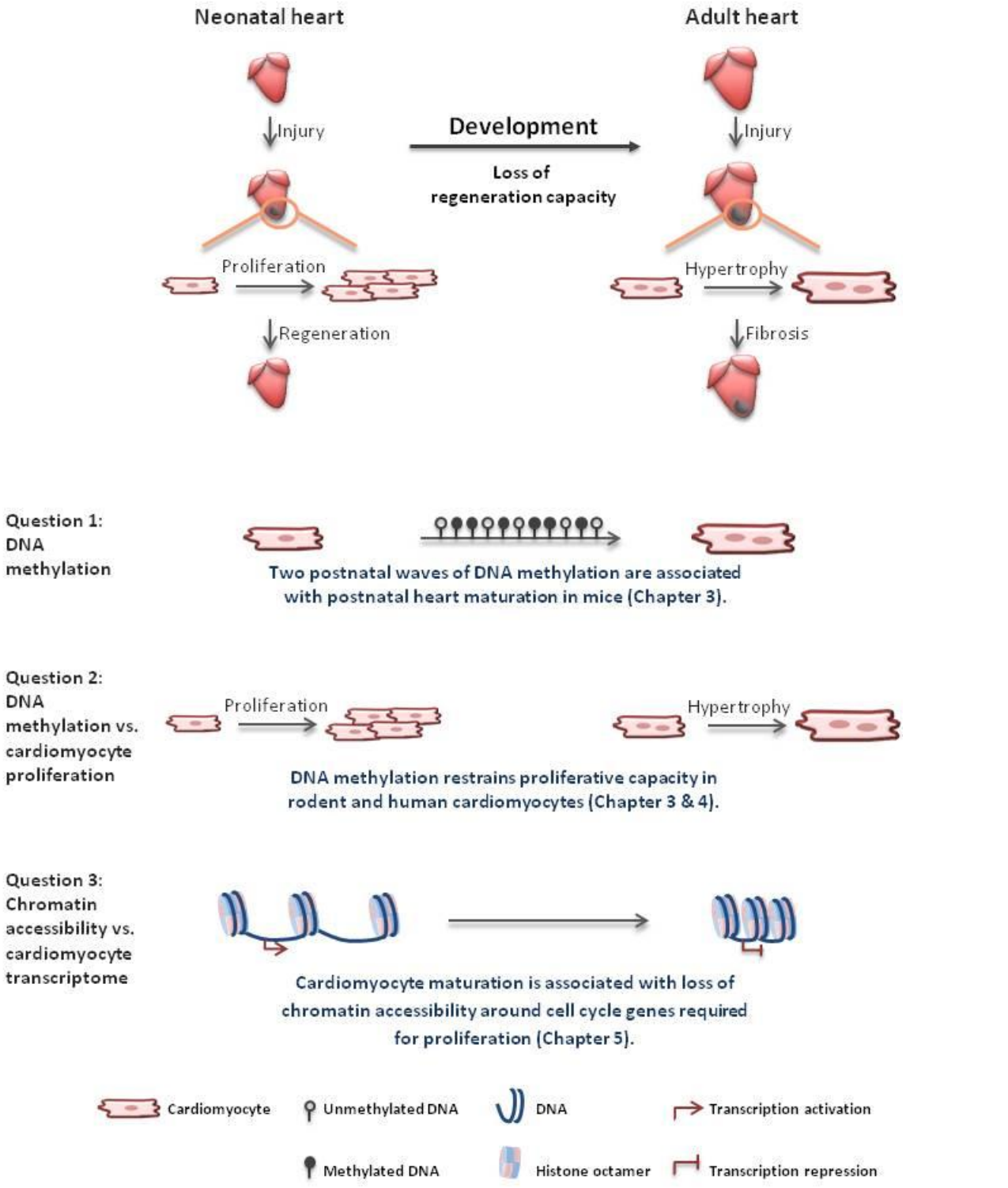

Figure 6.1. Summary of the 3 major findings of this PhD Thesis in current research models.

The 3 major findings of this PhD Thesis are: 1. Two postnatal waves of DNA methylation are associated with postnatal heart maturation in mice (Chapter 3). 2. DNA methylation restrains proliferative capacity in rodent and human cardiomyocytes (Chapter 3 & 4). 3. Cardiomyocyte maturation is associated with loss of chromatin accessibility around cell cycle genes required for proliferation (Chapter 5).

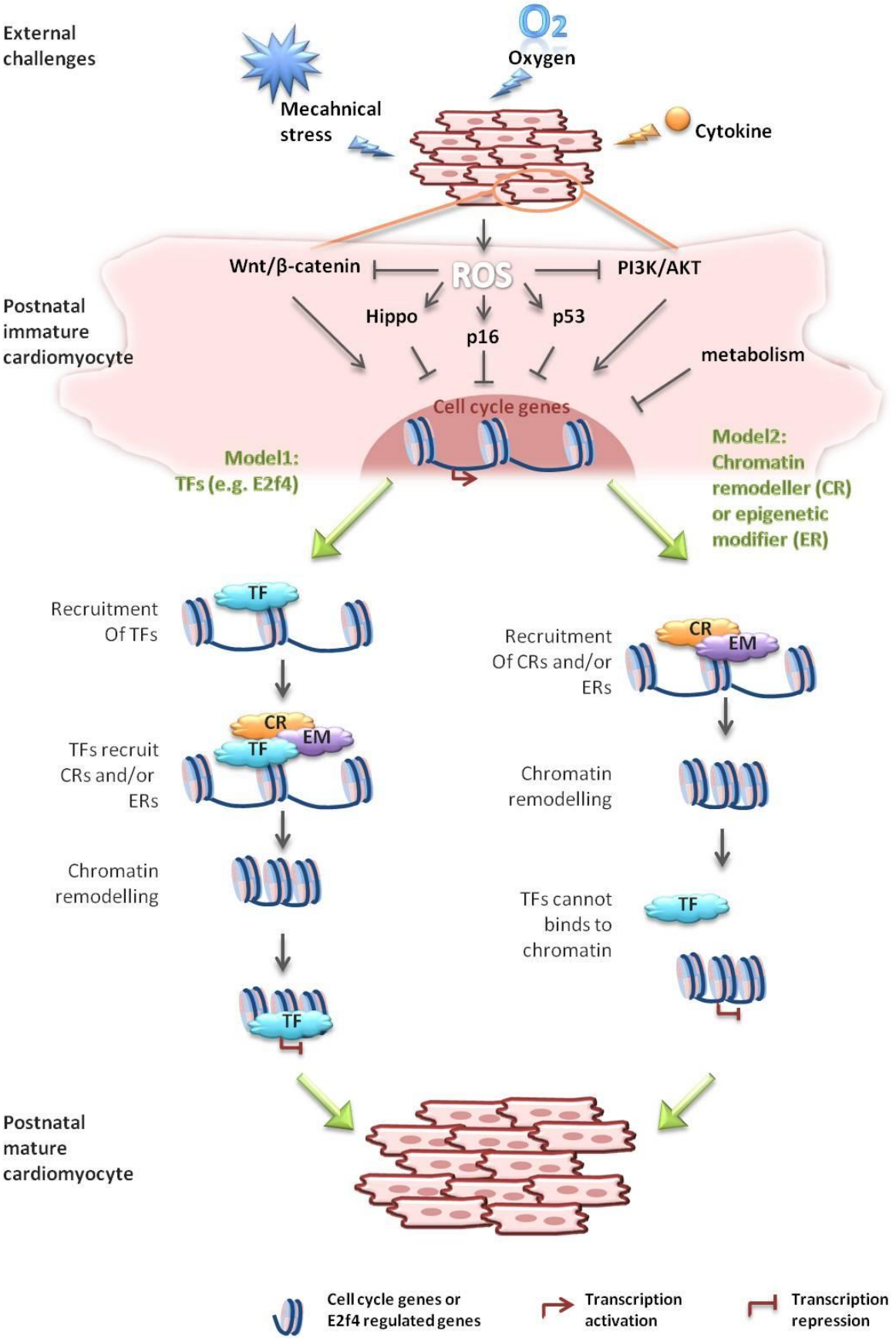
External challenges
O2
Oxygen
Mecahnical stress
Cytokine
Wnt/β-catenin
ROS
PI3K/AKT
Postnatal immature cardiomyocyte
Hippo
p16
p53
metabolism
Cell cycle genes
Model1: TFs (e.g. E2f4)
Model2: Chromatin remodeller (CR) or epigenetic modifier (ER)
Recruitment Of TFs
TF
TFs recruit CRs and/or ERs
CR
EM
Chromatin remodelling
Recruitment Of CRs and/or ERs
TFs cannot binds to chromatin
Postnatal mature cardiomyocyte
Cell cycle genes or E2f4 regulated genes
Transcription activation
Transcription repression

Figure 6.2. Schematic of site specific chromatin remodelling during postnatal cardiomyocyte cell cycle shutdown.

Cardiomyocytes encounter various external challenges (such as oxygen-rich environment, mechanical stress and cytokines stimulation) following birth, generating ROS and oxidative stress, which leads to activation of several signalling pathways. Activated signalling pathway could lead to the expression of TFs, chromatin remodellers (CRs) or epigenetic modifiers (ERs, such as HATs, HDACs, HMTs and Dnmts). In model 1, the expressed TFs can actively recruit CRs to perform chromatin remodelling and lead to the changes in transcription of downstream target genes. In model 2, the activated signalling pathways activates CRs or ERs and therefore changes the chromatin accessibility, allowing TFs to bind (or cannot bind) to open chromatin (or compacted chromatin) for transcription activation (or fail to activate) of downstream target genes.

Chapter 7

Appendices

A dream written down with a date becomes a goal.

A goal broken down into steps becomes a plan.

A plan backed by action makes your dreams come true.

Greg Reid.

Chapter 7. Appendices

7.1. Summary of genes with differential methylation levels and mRNA expression changes between P1 and P14 (from Chapter 3).

Gene Name	MBD-Seq						RNA-Seq		
	Pattern	logFC	p-value	DMRs co-ordinates			Pattern	logFC	p-value
4831426I19Rik	↑	1.55	2.20E-02	104962279	-	104963658	↓	-1.26	1.39E-02
4930427A07Rik	↑	1.88	2.01E-02	113160898	-	113162262	↓	-2.38	2.52E-08
4933413G19Rik	↑	1.62	3.35E-02	128379233	-	128380307	↓	-2.63	4.02E-04
9830001H06Rik	↑	1.93	4.82E-02	157059909	-	157060752	↓	-0.99	2.31E-03
Acan	↑	1.49	3.34E-02	79093143	-	79094561	↓	-1.48	2.06E-03
Adcy5	↑	2.26	2.26E-02	35156499	-	35157497	↓	-0.70	1.48E-02
AI661453	↑	1.34	4.56E-02	47467093	-	47469664	↓	-2.46	4.17E-09
Ankrd6	↑	1.46	4.32E-02	32863841	-	32865107	↓	-1.34	3.71E-03
App	↑	2.19	4.64E-02	85104550	-	85105050	↓	-1.11	2.88E-05
Arhgap39	↑	1.55	1.92E-02	76807751	-	76809479	↓	-1.12	4.66E-03
Arsg	↑	2.21	4.65E-02	109502987	-	109503533	↓	-0.88	4.77E-02

Atl1	↑	1.19	4.81E-02	69907646	-	69909652	↓	-1.46	6.25E-05
Bai2	↑	2.43	6.04E-03	129991875	-	129993335	↓	-2.22	5.84E-06
BC022687	↑	1.85	2.50E-02	112807400	-	112808107	↓	-1.37	6.52E-04
Bcl2l11	↑	1.82	2.03E-02	128124261	-	128125467	↓	-1.02	1.02E-03
Bmp7	↑	1.53	3.60E-02	172923549	-	172924414	↓	-4.14	3.27E-28
C530008M17Rik	↑	1.92	2.34E-02	76857912	-	76859345	↓	-2.97	1.11E-15
Cacna2d2	↑	1.27	4.78E-02	107414024	-	107415347	↓	-2.56	5.52E-10
Ccdc85c	↑	1.73	2.81E-02	108205536	-	108206709	↓	-1.42	2.89E-02
Cd276	↑	1.33	4.79E-02	58536269	-	58537710	↓	-1.64	6.78E-08
Cdh4	↑	2.21	4.96E-02	179770421	-	179771118	↓	-3.81	6.77E-07
Cdk14	↑	2.13	4.79E-02	5381612	-	5382585	↓	-0.85	6.03E-03
Cdkn1c	↑	2.18	2.33E-03	143458486	-	143461261	↓	-0.70	9.47E-03
Celsr1	↑	1.34	3.73E-02	86029863	-	86032946	↓	-0.80	2.26E-02
Chst11	↑	2.12	2.99E-02	83050381	-	83051161	↓	-1.17	1.55E-04
Chtf18	↑	1.32	3.45E-02	25721671	-	25724363	↓	-1.18	2.57E-02
Cit	↑	1.53	3.60E-02	115906891	-	115909185	↓	-0.99	7.48E-03
Cnn2	↑	2.21	2.27E-02	79994102	-	79994873	↓	-1.04	6.60E-04

Col12a1	↑	1.60	3.67E-02	79599511	-	79600348	↓	-2.63	8.73E-16
Col18a1	↑	1.40	4.13E-02	77054486	-	77056107	↓	-1.54	5.08E-05
Cpne5	↑	1.72	2.66E-02	29160931	-	29161811	↓	-1.40	2.76E-04
Ctdp1	↑	2.40	6.28E-03	80433814	-	80434769	↓	-1.05	9.15E-04
Cttn	↑	2.21	4.70E-02	144438518	-	144439229	↓	-0.89	1.70E-04
D430042O09Rik	↑	2.22	3.61E-02	125803070	-	125803816	↓	-0.85	2.55E-03
D630045J12Rik	↑	1.36	3.10E-02	38176726	-	38177991	↓	-0.92	3.63E-02
Dbn1	↑	1.29	4.61E-02	55475909	-	55478323	↓	-0.92	3.01E-03
Dcaf15	↑	1.41	4.15E-02	84094363	-	84098192	↓	-0.84	2.37E-02
Dhcr24	↑	2.05	2.81E-02	106581748	-	106582543	↓	-2.87	2.83E-19
Dstn	↑	1.83	2.50E-02	143933955	-	143934771	↓	-1.82	8.11E-10
Etv6	↑	1.87	3.49E-02	134211046	-	134211870	↓	-1.24	1.78E-06
Fam171a2	↑	2.34	2.32E-03	102437116	-	102439296	↓	-1.34	8.42E-03
Fam53c	↑	1.54	4.32E-02	34768017	-	34769176	↓	-0.78	4.57E-03
Fam73a	↑	2.57	8.17E-03	152312817	-	152313541	↓	-1.13	9.55E-04
Fbxl7	↑	2.21	4.92E-02	26622960	-	26623831	↓	-1.59	4.89E-02
Fgfr2	↑	2.18	2.61E-02	132711566	-	132712610	↓	-1.83	3.88E-05

Fstl3	↑	1.35	4.78E-02	79780908	-	79782124	↓	-0.91	1.58E-02
Ftcd	↑	1.86	3.68E-02	76576136	-	76576982	↓	-3.97	8.44E-18
Fzd1	↑	2.58	1.28E-02	4755620	-	4756485	↓	-1.56	1.07E-07
Gli3	↑	1.32	4.95E-02	15724296	-	15725929	↓	-1.34	3.07E-04
Gm12892	↑	1.44	3.16E-02	122007888	-	122009735	↓	-1.03	8.49E-03
Gm14024	↑	2.36	3.73E-02	129259248	-	129259930	↓	-2.50	2.90E-09
Gm16323	↑	1.83	4.75E-02	30409794	-	30410776	↓	-1.36	2.03E-02
Gm16599	↑	2.30	1.05E-02	136274367	-	136275609	↓	-2.90	9.71E-04
Gm20431	↑	1.91	6.15E-03	167653945	-	167655010	↓	-0.93	3.27E-02
Gna13	↑	2.49	3.99E-02	109392522	-	109393132	↓	-0.70	7.46E-03
Gnaz	↑	1.77	4.78E-02	74977448	-	74978176	↓	-1.52	1.33E-02
Gpr124	↑	1.49	4.38E-02	27120205	-	27122377	↓	-1.19	1.23E-05
Gpsm2	↑	1.40	4.38E-02	108686535	-	108687390	↓	-1.37	6.00E-06
Grik5	↑	2.12	1.28E-02	25013237	-	25014148	↓	-0.96	1.43E-02
Igf2	↑	1.79	3.08E-02	142667454	-	142668464	↓	-2.60	8.24E-14
Igf2as	↑	1.79	3.08E-02	142667454	-	142668464	↓	-3.79	3.45E-19
Igf2bp2	↑	1.23	4.00E-02	22063185	-	22064361	↓	-2.27	7.50E-16

Igf2bp3	↑	3.15	6.28E-03	49212755	-	49213556	↓	-3.32	1.59E-27
Igf2r	↑	1.63	3.62E-02	12701614	-	12702649	↓	-1.96	4.33E-11
Insc	↑	1.59	4.24E-02	114790713	-	114791592	↓	-4.35	1.39E-16
Iqgap3	↑	1.87	3.08E-02	88115564	-	88116242	↓	-3.89	1.56E-19
Itgad	↑	1.86	4.40E-02	128205463	-	128206325	↓	-1.89	6.55E-04
Jub	↑	1.95	1.28E-02	54569928	-	54570907	↓	-1.37	5.37E-07
Kalrn	↑	2.55	4.32E-02	34081506	-	34082057	↓	-1.39	4.78E-07
Kcnq1	↑	1.40	2.50E-02	143375067	-	143377464	↓	-0.97	2.20E-04
Kdm2b	↑	1.61	3.92E-02	122888157	-	122889107	↓	-0.81	3.65E-02
Klf14	↑	2.49	3.43E-02	30957472	-	30958197	↓	-2.26	7.83E-04
Lrrc4b	↑	1.56	3.82E-02	44460601	-	44462954	↓	-1.93	9.96E-03
Lrrfip1	↑	1.80	3.74E-02	91008215	-	91009342	↓	-0.59	2.84E-02
Mex3b	↑	1.97	1.51E-02	82869062	-	82870549	↓	-2.21	5.76E-04
Micalcl	↑	1.97	4.67E-02	112406957	-	112407917	↓	-0.98	3.26E-02
Micall1	↑	1.85	2.72E-02	79120460	-	79121265	↓	-0.57	2.44E-02
Mtap1a	↑	1.20	4.24E-02	121299258	-	121302682	↓	-0.87	1.56E-03
Mtrr	↑	2.36	3.55E-02	68568579	-	68569068	↓	-0.74	1.68E-02

Myh7	↑	1.94	3.58E-02	54978527	-	54979854	↓	-4.26	3.05E-21
Nat8l	↑	1.62	3.99E-02	33997861	-	33998850	↓	-0.97	4.65E-02
Nedd4l	↑	1.80	2.33E-03	65083377	-	65085824	↓	-1.39	1.28E-08
Nptxr	↑	2.35	2.81E-02	79787807	-	79788443	↓	-0.96	5.13E-03
Osbpl5	↑	1.56	4.67E-02	143721250	-	143721869	↓	-0.99	9.61E-04
Pak4	↑	1.29	4.81E-02	28559296	-	28561303	↓	-1.27	2.51E-04
Parva	↑	2.06	3.67E-02	112444663	-	112445335	↓	-1.15	4.37E-06
Pcdhga3	↑	1.34	2.61E-02	37765911	-	37768755	↓	-1.23	4.53E-07
Peg12	↑	2.49	1.67E-02	62463262	-	62464576	↓	-2.07	3.98E-05
Pemt	↑	2.42	2.00E-02	59977251	-	59977757	↓	-1.09	1.52E-02
Phactr2	↑	1.56	3.90E-02	13314214	-	13315120	↓	-0.76	5.01E-03
Phc1	↑	1.76	4.82E-02	122322869	-	122323627	↓	-1.26	7.79E-07
Pip5k1b	↑	2.26	2.81E-02	24527350	-	24527984	↓	-0.96	1.75E-04
Plekha7	↑	1.82	3.35E-02	116170303	-	116171098	↓	-2.90	1.58E-12
Pold2	↑	1.20	3.81E-02	5871934	-	5875424	↓	-0.70	3.82E-02
Prim2	↑	1.90	2.29E-02	33635843	-	33637012	↓	-1.48	3.00E-05
Prkag2	↑	1.80	2.27E-02	24947124	-	24947798	↓	-2.17	9.54E-16

Prss57	↑	1.35	4.78E-02	79780908	-	79782124	↓	-0.92	1.41E-02
Ptgfrn	↑	1.78	4.65E-02	101064201	-	101064813	↓	-0.92	2.87E-04
Ptprf	↑	1.40	3.62E-02	118244152	-	118246567	↓	-0.82	3.20E-03
Rap1gds1	↑	1.81	4.82E-02	139017427	-	139018011	↓	-0.95	2.55E-04
Rasl11b	↑	2.01	4.75E-02	74197812	-	74198891	↓	-0.76	3.10E-03
Rbm19	↑	1.25	4.80E-02	120179111	-	120180670	↓	-0.76	3.56E-02
Rgl1	↑	1.62	4.78E-02	152636946	-	152637663	↓	-0.89	2.04E-04
Rnf157	↑	1.16	4.13E-02	116341764	-	116345014	↓	-1.01	2.36E-03
Ror2	↑	1.74	2.34E-02	53118499	-	53119674	↓	-2.95	6.40E-12
Rph3al	↑	1.55	4.51E-02	75859379	-	75860200	↓	-1.57	2.33E-05
Scd2	↑	1.45	4.78E-02	44303931	-	44304694	↓	-2.87	1.96E-24
Sdc1	↑	1.30	4.75E-02	8790077	-	8793016	↓	-0.79	1.47E-02
Sdk1	↑	2.01	3.10E-02	142172229	-	142172963	↓	-2.71	2.04E-10
Sergef	↑	1.74	3.67E-02	46568573	-	46569888	↓	-0.92	9.63E-03
Sh3pxd2b	↑	2.25	2.80E-02	32361566	-	32362296	↓	-0.59	2.60E-02
Sipa1l2	↑	2.17	2.42E-02	125447181	-	125448083	↓	-0.54	4.98E-02
Slc16a3	↑	1.35	4.81E-02	120954965	-	120957405	↓	-2.84	1.05E-10

Slc8a2	↑	2.29	1.94E-02	16144571	-	16145709	↓	-1.44	2.53E-03
Slco2a1	↑	1.60	3.67E-02	103067275	-	103068253	↓	-1.72	4.80E-09
Smad3	↑	1.96	2.60E-02	63754693	-	63755837	↓	-1.11	1.42E-05
Smoc1	↑	1.76	2.71E-02	81138784	-	81139783	↓	-1.19	1.84E-04
Smyd2	↑	1.97	2.61E-02	189883230	-	189884052	↓	-0.68	2.60E-02
Spon2	↑	1.83	4.72E-02	33215219	-	33216043	↓	-1.84	1.64E-08
Spry2	↑	2.17	5.96E-03	105892647	-	105893752	↓	-0.70	1.23E-02
Spsb4	↑	1.70	3.35E-02	96995232	-	96996490	↓	-0.86	3.51E-03
Srebf2	↑	1.44	3.96E-02	82169726	-	82171851	↓	-1.61	1.17E-08
Stx11	↑	1.51	3.97E-02	12940482	-	12942121	↓	-1.20	2.74E-02
Stxbp1	↑	1.60	4.18E-02	32808779	-	32809565	↓	-0.91	4.09E-04
Sv2a	↑	1.77	9.45E-03	96184806	-	96185680	↓	-1.16	7.18E-05
Synpo2l	↑	2.56	2.42E-02	20662081	-	20662762	↓	-1.40	1.92E-07
Tdrd7	↑	2.23	3.52E-02	46032327	-	46033068	↓	-0.66	1.42E-02
Tenm4	↑	1.37	4.95E-02	96729116	-	96730078	↓	-2.33	9.77E-10
Tmem138	↑	1.66	4.60E-02	10571020	-	10571650	↓	-0.88	2.01E-02
Tnc	↑	1.79	3.73E-02	64016596	-	64018467	↓	-1.79	1.48E-10

Tnrc18	↑	1.44	3.24E-02	142774890	-	142776953	↓	-1.50	9.55E-04
Tox2	↑	1.22	4.35E-02	163317579	-	163320971	↓	-1.31	4.99E-03
Ttyh3	↑	1.45	3.35E-02	140634936	-	140636362	↓	-1.04	1.64E-03
Tubb6	↑	1.64	2.79E-02	67401040	-	67402500	↓	-0.75	4.40E-03
Ube2c	↑	1.65	4.41E-02	164767375	-	164768370	↓	-4.02	1.11E-27
Vps8	↑	1.29	4.70E-02	21626553	-	21628510	↓	-0.54	4.26E-02
Wdr19	↑	1.54	3.44E-02	65245769	-	65246856	↓	-1.31	1.10E-03
Wwox	↑	1.76	2.65E-02	114455852	-	114456850	↓	-1.22	1.42E-04
Ypel2	↑	2.03	4.79E-02	86945995	-	86946736	↓	-1.00	1.27E-03
Zbed3	↑	1.30	4.78E-02	95335582	-	95336997	↓	-1.74	2.63E-10
Zfp395	↑	1.20	4.32E-02	65384528	-	65386692	↓	-0.72	1.04E-02
Zfp608	↑	1.35	4.78E-02	54891516	-	54892275	↓	-0.83	3.80E-02
Zfp618	↑	1.44	1.63E-02	63132022	-	63134627	↓	-2.35	5.41E-07
1110002E22Rik	↑	1.38	2.14E-02	138064713	-	138070690	↑	0.55	3.47E-02
2200002D01Rik	↑	1.35	4.71E-02	29246392	-	29247578	↑	1.12	7.67E-03
2310050B05Rik	↑	1.54	3.81E-02	81199006	-	81201489	↑	0.91	2.32E-03
2310067B10Rik	↑	2.08	4.39E-02	115785838	-	115786703	↑	1.07	2.87E-03

2510049J12Rik	↑	1.93	3.77E-02	115586257	-	115587125	↑	1.96	6.51E-04
2610027K06Rik	↑	1.89	2.61E-02	85801164	-	85802106	↑	1.27	9.30E-03
2900092E17Rik	↑	1.49	3.15E-02	127001072	-	127002125	↑	0.82	1.66E-02
4632433K11Rik	↑	1.56	3.55E-02	5028736	-	5032390	↑	0.83	2.87E-02
4931428F04Rik	↑	1.92	4.73E-02	105290242	-	105291059	↑	1.20	1.77E-05
6030419C18Rik	↑	1.88	4.56E-02	58489808	-	58490602	↑	0.96	1.63E-02
A530058N18Rik	↑	1.90	4.69E-02	114051529	-	114052331	↑	0.86	3.49E-03
Aatk	↑	1.62	1.74E-02	120008927	-	120013270	↑	1.29	1.26E-02
Abca7	↑	1.87	6.04E-03	80013034	-	80016328	↑	0.73	3.56E-02
Abcc10	↑	1.33	3.82E-02	46305150	-	46307867	↑	1.06	9.55E-03
Abcc8	↑	1.71	3.48E-02	46124532	-	46125834	↑	0.72	2.25E-02
Abhd2	↑	1.51	3.43E-02	79359632	-	79360858	↑	0.75	6.64E-03
Abi3	↑	2.11	3.37E-03	95830140	-	95831709	↑	1.70	1.35E-09
Ablim2	↑	2.18	2.97E-02	35879955	-	35880829	↑	1.71	1.40E-07
Ablim3	↑	1.35	4.12E-02	61800435	-	61801820	↑	1.11	1.31E-05
Acacb	↑	1.59	4.83E-02	114248291	-	114249266	↑	1.79	1.01E-09
Ace	↑	2.01	5.96E-03	105987558	-	105989356	↑	1.45	1.96E-06

Acvr2b	↑	1.25	4.07E-02	119425891	-	119428951	↑	2.27	2.39E-04
Acvrl1	↑	1.33	4.78E-02	101136864	-	101137912	↑	1.10	1.11E-04
Adamts7	↑	2.19	2.61E-02	90182460	-	90183351	↑	0.85	1.14E-02
Adamtsl5	↑	2.37	1.86E-03	80340925	-	80342953	↑	1.47	7.71E-09
Ahdc1	↑	1.34	3.66E-02	133060480	-	133066597	↑	1.22	1.79E-02
Aldh4a1	↑	1.61	1.05E-02	139639535	-	139640837	↑	0.56	3.98E-02
Ank1	↑	1.31	4.79E-02	23032909	-	23034768	↑	2.08	1.67E-15
Ankrd33b	↑	1.42	2.71E-02	31296810	-	31299372	↑	0.80	7.45E-03
Ankrd54	↑	1.40	4.81E-02	79054920	-	79055806	↑	0.74	4.17E-02
Ankrd9	↑	2.13	1.63E-02	110976219	-	110977849	↑	3.52	4.54E-29
Anks1	↑	1.16	4.69E-02	28051315	-	28054218	↑	1.61	3.36E-08
Ano8	↑	1.78	2.30E-02	71483938	-	71485388	↑	0.66	4.65E-02
Appl2	↑	2.46	2.14E-02	83615675	-	83616433	↑	0.96	4.06E-04
Arhgap27	↑	1.88	1.63E-02	103332543	-	103334658	↑	1.45	2.78E-06
Arhgef1	↑	1.33	3.97E-02	24921135	-	24924291	↑	0.99	1.79E-03
Arhgef10l	↑	1.80	4.31E-02	140514668	-	140515586	↑	0.96	1.35E-02
Arhgef17	↑	1.48	2.20E-02	100880932	-	100883944	↑	0.80	2.07E-03

Arhgef37	↑	2.66	1.67E-02	61506953	-	61507616	↑	1.46	3.95E-02
Armc2	↑	1.55	4.92E-02	41924239	-	41924954	↑	1.28	2.99E-04
Asb10	↑	1.74	4.67E-02	24533104	-	24534196	↑	2.69	5.25E-23
Asb2	↑	2.16	4.06E-02	103324714	-	103325734	↑	1.28	6.26E-04
Atp2a3	↑	1.76	3.07E-02	72975083	-	72975875	↑	2.16	1.62E-12
Atp2b1	↑	2.05	3.96E-02	98967161	-	98967864	↑	1.32	1.41E-04
Atp9a	↑	1.37	4.79E-02	168690151	-	168691337	↑	0.78	5.74E-03
Atxn1	↑	1.49	3.36E-02	45566330	-	45568721	↑	0.67	4.09E-02
Axin2	↑	1.78	1.05E-02	108941460	-	108943506	↑	1.76	2.84E-04
BC020535	↑	2.58	4.04E-02	153070695	-	153071137	↑	1.68	2.31E-09
Bcas3	↑	1.78	1.95E-02	85780813	-	85781640	↑	1.08	7.31E-05
Bcl3	↑	1.45	4.81E-02	19808545	-	19810090	↑	2.51	3.96E-09
Bcl6b	↑	1.62	4.98E-02	70225757	-	70227092	↑	0.85	4.86E-04
Cabp1	↑	1.86	1.25E-02	115175032	-	115175781	↑	2.12	1.50E-06
Cacnb2	↑	1.54	4.47E-02	14738896	-	14740088	↑	0.81	2.63E-03
Cadm4	↑	1.60	4.88E-02	24502318	-	24503078	↑	1.03	1.49E-03
Cbfa2t3	↑	1.28	3.80E-02	122636751	-	122639445	↑	2.32	3.72E-13

Cbx6	↑	1.34	3.40E-02	79826778	-	79829612	↑	0.97	5.27E-05
Cbx8	↑	2.11	2.53E-02	119037479	-	119038285	↑	0.95	1.03E-02
Ccdc94	↑	1.79	4.83E-02	55966198	-	55967029	↑	0.96	1.68E-02
Cd79b	↑	1.91	2.01E-02	106313981	-	106314805	↑	1.35	2.41E-03
Cdh13	↑	2.44	2.20E-02	119109393	-	119110003	↑	1.12	1.72E-05
Cdh23	↑	2.03	9.96E-03	60564192	-	60565446	↑	3.34	5.09E-11
Cdk20	↑	1.84	4.71E-02	64438465	-	64439150	↑	1.20	1.88E-03
Chd7	↑	1.25	4.79E-02	8865394	-	8866951	↑	0.63	4.05E-02
Chpf	↑	1.40	4.78E-02	75474632	-	75476856	↑	1.74	1.71E-05
Chrna10	↑	1.96	2.01E-02	102112729	-	102113969	↑	4.13	5.62E-08
Chst12	↑	1.42	3.74E-02	140523278	-	140525345	↑	1.54	1.76E-03
Cilp2	↑	2.40	3.12E-02	69880872	-	69882280	↑	3.52	2.25E-08
Clec3b	↑	2.45	2.14E-02	123156454	-	123157414	↑	2.56	3.38E-14
Clpb	↑	2.05	2.86E-02	101763240	-	101763996	↑	1.00	8.15E-05
Cmss1	↑	2.21	2.34E-02	57390893	-	57392014	↑	0.62	2.72E-02
Col11a2	↑	1.89	3.35E-02	34045687	-	34046595	↑	1.79	6.40E-04
Cox6a2	↑	1.86	4.40E-02	128205463	-	128206325	↑	2.50	2.81E-08

Crat	↑	1.83	4.75E-02	30409794	-	30410776	↑	0.69	4.46E-02
Crebbp	↑	1.43	3.64E-02	4083974	-	4086395	↑	1.31	1.19E-03
Crlf2	↑	1.35	4.38E-02	109554287	-	109556834	↑	1.59	6.71E-03
Cryab	↑	2.08	2.61E-02	50751198	-	50752439	↑	0.81	4.98E-02
Cryba4	↑	1.82	2.66E-02	112246226	-	112247125	↑	3.77	1.02E-13
Cuedc1	↑	2.11	3.87E-02	88192165	-	88192832	↑	1.31	7.32E-07
Cul9	↑	1.65	2.61E-02	46539966	-	46540932	↑	1.06	6.07E-03
Cux2	↑	2.27	8.48E-03	121868851	-	121869943	↑	1.19	2.12E-04
Cxxc5	↑	1.28	4.03E-02	35857859	-	35859800	↑	0.83	8.03E-03
Cyth1	↑	1.43	4.86E-02	118165163	-	118166291	↑	0.72	3.75E-03
D630044L22RIK	↑	1.60	2.72E-02	25958845	-	25961076	↑	1.29	1.65E-02
Dapk2	↑	1.65	4.43E-02	66220181	-	66221262	↑	1.96	4.19E-06
Dbh	↑	1.62	3.77E-02	27162124	-	27163060	↑	3.21	2.12E-24
Dgkz	↑	1.78	4.38E-02	91944567	-	91946043	↑	0.89	6.04E-03
Dlg4	↑	1.27	4.69E-02	70040961	-	70044102	↑	1.44	8.35E-04
Dlgap4	↑	1.08	3.33E-02	156761594	-	156764750	↑	0.84	3.34E-03
Dll4	↑	2.49	2.34E-02	119323656	-	119324479	↑	1.46	9.18E-08

Dmpk	↑	2.00	1.28E-02	19091437	-	19093106	↑	2.23	1.52E-15
Dnaaf1	↑	1.17	4.85E-02	119595994	-	119599745	↑	2.15	4.53E-08
Dnaaf3	↑	1.49	2.82E-02	4526667	-	4527949	↑	3.15	7.38E-19
Dnase2a	↑	2.71	1.13E-03	84911854	-	84912943	↑	1.11	8.24E-04
Dnm1	↑	1.60	4.35E-02	32308588	-	32309377	↑	1.13	5.19E-03
Dock6	↑	1.37	4.59E-02	21838437	-	21840223	↑	1.09	6.36E-05
Dock8	↑	1.26	4.93E-02	25172102	-	25173129	↑	1.00	1.01E-03
Dok5	↑	1.80	3.62E-02	170870228	-	170871157	↑	1.63	1.28E-02
Dos	↑	1.60	4.12E-02	80129310	-	80133513	↑	1.85	8.63E-10
Dot1l	↑	1.72	2.92E-02	80790415	-	80793069	↑	0.92	1.50E-03
Dpysl4	↑	1.36	4.62E-02	139097630	-	139098985	↑	3.24	1.27E-16
Dtx1	↑	2.15	3.15E-02	120682047	-	120682905	↑	1.75	1.39E-02
Dysf	↑	2.33	3.61E-02	84105780	-	84106539	↑	1.77	8.09E-13
Efcab4a	↑	1.78	3.88E-02	141464116	-	141465390	↑	1.46	2.63E-06
Enthd2	↑	1.40	2.81E-02	120092636	-	120095123	↑	1.21	4.59E-05
Fam109a	↑	1.57	2.82E-02	121851379	-	121853604	↑	1.17	9.38E-05
Fam193b	↑	1.41	4.12E-02	55552576	-	55553427	↑	2.05	4.15E-11

Fam19a5	↑	1.71	3.18E-02	87757245	-	87758346	↑	2.59	4.70E-06
Fastk	↑	1.63	4.15E-02	24445489	-	24446363	↑	1.16	4.96E-04
Fbrsl1	↑	1.14	4.67E-02	110430308	-	110433488	↑	1.06	8.12E-04
Fbxl6	↑	1.22	4.02E-02	76539453	-	76541380	↑	1.16	7.45E-03
Fbxo31	↑	1.45	3.36E-02	121555894	-	121557173	↑	2.37	1.25E-13
Fbxo46	↑	1.42	4.45E-02	19135155	-	19137519	↑	1.59	6.93E-04
Fgd2	↑	1.67	3.84E-02	29362452	-	29363770	↑	3.02	8.99E-12
Fhl2	↑	2.05	4.52E-02	43131386	-	43132086	↑	0.82	3.00E-02
Flcn	↑	1.83	3.74E-02	59812366	-	59813073	↑	0.72	5.94E-03
Fmnl1	↑	1.78	9.45E-03	103191725	-	103193440	↑	2.24	6.95E-15
Foxo6	↑	2.48	5.96E-03	120266920	-	120268099	↑	1.51	5.89E-03
Gabbr1	↑	2.17	3.88E-02	37050784	-	37051486	↑	1.47	9.19E-05
Galntl2	↑	1.64	4.61E-02	32054837	-	32055650	↑	2.89	1.32E-20
Gata2	↑	3.15	5.51E-04	88190013	-	88191408	↑	0.82	2.80E-02
Gm11264	↑	2.36	2.50E-02	82065919	-	82066666	↑	1.86	4.88E-04
Gm11474	↑	1.63	3.05E-02	167538394	-	167539498	↑	0.70	4.80E-03
Gm11598	↑	2.11	3.96E-02	100243028	-	100243806	↑	1.58	2.41E-02

Gm11651	↑	2.01	5.96E-03	105987558	-	105989356	↑	1.21	1.52E-02
Gm12992	↑	1.55	3.56E-02	131922232	-	131923460	↑	0.56	4.65E-02
Gm14232	↑	1.48	3.99E-02	131170987	-	131173103	↑	1.90	8.58E-07
Gm14290	↑	1.31	4.55E-02	167103828	-	167106903	↑	3.00	1.62E-17
Gm14492	↑	1.93	3.93E-02	142507428	-	142508190	↑	2.94	1.12E-22
Gm15821	↑	1.74	3.77E-02	34214944	-	34215755	↑	1.17	1.77E-02
Gm5303	↑	1.47	4.69E-02	28361642	-	28362905	↑	1.30	1.33E-02
Gngt2	↑	2.34	1.63E-02	95833356	-	95834506	↑	0.65	1.63E-02
Gp1bb	↑	1.80	4.07E-02	18624301	-	18625756	↑	0.72	3.62E-02
Gtdc2	↑	1.35	4.70E-02	121981790	-	121983969	↑	1.80	4.20E-06
Gtpbp3	↑	1.78	2.30E-02	71483938	-	71485388	↑	0.80	2.40E-02
Hagh	↑	1.62	3.68E-02	24856347	-	24857128	↑	0.64	3.62E-02
Hcn2	↑	1.52	3.41E-02	79734717	-	79742099	↑	3.58	1.34E-29
Hipk2	↑	1.61	4.82E-02	38715821	-	38716402	↑	1.08	1.41E-02
Hk3	↑	1.42	2.53E-02	55002079	-	55007503	↑	1.87	9.61E-04
Hlx	↑	2.89	6.04E-03	184727158	-	184728438	↑	2.65	1.56E-15
Hmha1	↑	1.87	6.04E-03	80013034	-	80016328	↑	2.47	1.46E-08

Hr	↑	1.73	4.39E-02	70556254	-	70557093	↑	4.01	3.60E-32
Hspa12b	↑	1.86	9.45E-03	131144410	-	131145548	↑	1.31	1.73E-07
Hspb2	↑	2.08	2.61E-02	50751198	-	50752439	↑	0.96	1.52E-03
Ift172	↑	1.11	4.82E-02	31251204	-	31254190	↑	0.59	1.93E-02
Igfbp6	↑	1.36	4.88E-02	102144457	-	102146515	↑	4.41	1.12E-28
Igsf8	↑	1.45	2.61E-02	172317128	-	172319710	↑	0.84	2.90E-03
Il3ra	↑	1.37	2.61E-02	14348533	-	14351571	↑	1.15	4.56E-02
Il4ra	↑	2.13	4.75E-02	125576094	-	125576787	↑	0.97	7.90E-04
Inha	↑	1.86	2.30E-02	75509225	-	75510231	↑	0.78	3.16E-02
Inpp4a	↑	1.83	3.13E-02	37357599	-	37358365	↑	0.92	4.39E-03
Insl3	↑	1.81	6.04E-03	71683606	-	71686499	↑	2.53	3.40E-06
Ints1	↑	1.54	1.36E-02	139756700	-	139760883	↑	1.57	2.61E-04
Ipo13	↑	1.42	2.61E-02	117900366	-	117901879	↑	1.53	3.01E-07
Irf5	↑	1.57	3.60E-02	29535360	-	29536310	↑	0.83	2.68E-03
Islr	↑	1.50	4.74E-02	58156645	-	58158564	↑	2.16	1.36E-14
Jag2	↑	1.43	1.69E-02	112919364	-	112921979	↑	1.55	1.46E-03
Jak3	↑	1.81	6.04E-03	71683606	-	71686499	↑	1.04	1.43E-02

Kcnb1	↑	1.31	4.55E-02	167103828	-	167106903	↑	2.48	4.21E-13
Kcnip3	↑	2.32	2.20E-02	127510479	-	127511233	↑	1.11	2.87E-02
Kcnk6	↑	2.03	1.36E-02	29224919	-	29226072	↑	1.07	3.65E-03
Kcnq4	↑	1.68	4.79E-02	120711111	-	120712013	↑	1.96	9.23E-07
Kif6	↑	2.62	2.61E-02	49830654	-	49831250	↑	0.86	3.01E-02
Klc3	↑	1.61	3.45E-02	19392593	-	19396052	↑	1.58	5.76E-03
Klhl18	↑	1.12	3.67E-02	110426577	-	110429397	↑	0.82	4.54E-03
Klhl26	↑	1.65	4.67E-02	70450800	-	70453197	↑	0.81	2.19E-02
Leng9	↑	1.96	3.67E-02	4151167	-	4152089	↑	1.68	2.06E-05
Lgi4	↑	1.58	2.74E-02	31066612	-	31068126	↑	4.18	4.87E-19
Lgr6	↑	2.43	1.02E-02	134986885	-	134988243	↑	2.43	8.81E-17
Lhx6	↑	2.50	1.36E-03	36090262	-	36091972	↑	1.33	2.92E-04
Lingo3	↑	1.74	3.74E-02	80833655	-	80836518	↑	2.28	3.77E-09
Lmna	↑	1.27	4.95E-02	88483038	-	88485480	↑	1.51	5.81E-05
Lrg1	↑	1.88	3.35E-02	56123056	-	56125215	↑	5.00	3.68E-55
Lrp1	↑	1.68	3.16E-02	127594590	-	127595717	↑	1.96	3.21E-08
Lrp3	↑	1.48	4.33E-02	35202132	-	35205838	↑	1.86	2.63E-07

Lrrc14	↑	1.13	4.67E-02	76712854	-	76714915	↑	0.98	5.36E-04
Lrrn4cl	↑	1.70	2.23E-02	8851645	-	8852674	↑	1.74	2.39E-04
Ltbp4	↑	2.28	2.61E-02	27329343	-	27330499	↑	2.02	1.34E-05
Lysmd1	↑	1.54	2.44E-02	95138879	-	95141161	↑	1.51	1.28E-02
Macrod1	↑	1.49	2.20E-02	7094765	-	7097602	↑	1.79	6.04E-11
Maml2	↑	1.90	2.99E-02	13641092	-	13641763	↑	0.81	2.01E-02
Map3k14	↑	1.42	3.32E-02	103229857	-	103232232	↑	1.66	5.96E-05
Map3k6	↑	2.05	9.97E-03	133250744	-	133252158	↑	2.31	2.84E-16
Mapkapk3	↑	1.58	3.34E-02	107263251	-	107264228	↑	0.88	2.86E-03
Mast3	↑	1.48	3.55E-02	70779080	-	70781823	↑	0.84	1.36E-02
Mcf2l	↑	1.18	4.04E-02	13000444	-	13004454	↑	2.87	6.76E-25
Megf8	↑	1.67	1.72E-02	25337346	-	25338865	↑	0.74	1.13E-02
Mfsd12	↑	1.74	3.67E-02	81362408	-	81364394	↑	0.68	3.99E-02
Mgll	↑	1.46	3.35E-02	88822787	-	88823769	↑	2.08	2.12E-12
Mir208b	↑	1.94	3.58E-02	54978527	-	54979854	↑	2.85	2.19E-08
Mn1	↑	1.73	1.69E-02	111418980	-	111421997	↑	1.37	3.56E-05
Mon1a	↑	1.51	3.29E-02	107900797	-	107903266	↑	1.31	4.60E-03

Mri1	↑	1.46	3.69E-02	84253835	-	84255149	↑	0.73	2.53E-02
Mrpl34	↑	1.68	1.05E-02	71460614	-	71462721	↑	0.86	1.05E-03
Mrps28	↑	1.58	4.82E-02	8881829	-	8882995	↑	0.67	6.64E-03
Mrps6	↑	1.53	2.47E-02	92060796	-	92062119	↑	0.78	3.35E-03
Mrvi1	↑	3.21	5.96E-03	110923076	-	110923802	↑	1.63	9.07E-09
Msx1	↑	1.80	4.07E-02	37820909	-	37822016	↑	2.41	3.14E-11
Mvp	↑	1.49	3.15E-02	127001072	-	127002125	↑	1.81	9.76E-06
Mxra8	↑	1.49	4.30E-02	155841408	-	155843078	↑	0.60	3.17E-02
Myh11	↑	1.41	4.81E-02	14200357	-	14201353	↑	2.32	2.61E-17
Myh14	↑	1.78	6.22E-03	44629695	-	44632638	↑	5.52	1.45E-61
Myh6	↑	1.72	3.33E-02	54959588	-	54961529	↑	1.84	3.09E-05
Myo10	↑	1.28	3.27E-02	25779454	-	25782156	↑	1.19	5.63E-04
Myo18b	↑	1.71	2.62E-02	112879074	-	112880299	↑	1.03	1.20E-04
Myo1d	↑	1.46	4.12E-02	80489627	-	80491772	↑	0.71	1.79E-02
Myo5c	↑	1.37	4.70E-02	75293796	-	75295062	↑	1.93	3.05E-06
Mypop	↑	1.69	4.79E-02	18987590	-	18988344	↑	1.59	2.08E-03
Nacc2	↑	1.53	3.99E-02	26059829	-	26060817	↑	1.19	6.74E-05

Naif1	↑	1.60	4.67E-02	32452481	-	32453336	↑	0.89	1.28E-02
Ncf4	↑	1.78	4.59E-02	78250081	-	78251187	↑	1.14	2.29E-02
Nckipsd	↑	1.34	2.81E-02	108813724	-	108815970	↑	0.94	1.13E-02
Ncor2	↑	1.63	4.50E-02	125028100	-	125029563	↑	1.28	2.06E-04
Ndufaf2	↑	1.77	4.78E-02	108062158	-	108062761	↑	0.92	6.47E-04
Nfix	↑	2.31	6.22E-03	84785098	-	84786543	↑	1.94	8.28E-09
Nfkb2	↑	1.29	3.23E-02	46309430	-	46313711	↑	0.89	1.01E-02
Nfkbie	↑	2.13	2.45E-02	45558957	-	45559719	↑	0.98	4.11E-02
Ng23	↑	1.24	4.79E-02	35030396	-	35032291	↑	3.34	2.31E-13
Nlgn2	↑	1.67	2.61E-02	69823847	-	69826349	↑	1.04	1.27E-03
Nod1	↑	1.72	1.41E-02	54942824	-	54945174	↑	2.05	8.89E-14
Nod2	↑	1.57	2.39E-02	88663461	-	88665842	↑	3.09	1.02E-07
Notch1	↑	1.67	1.98E-02	26464579	-	26465962	↑	0.69	3.66E-02
Notch4	↑	1.88	3.35E-02	34566957	-	34567807	↑	1.33	2.66E-07
Npr1	↑	2.31	4.78E-02	90464375	-	90465207	↑	0.87	1.81E-03
Npr2	↑	1.88	1.63E-02	43632112	-	43633215	↑	1.28	3.96E-08
Nr2f1	↑	1.97	2.46E-02	78194390	-	78196105	↑	2.37	4.00E-08

Osbp2	↑	1.70	3.41E-02	3862859	-	3863730	↑	1.10	2.35E-03
Osgin1	↑	1.60	4.51E-02	119444619	-	119445849	↑	3.48	9.52E-08
Otud7b	↑	1.30	3.97E-02	96154484	-	96155879	↑	0.58	4.02E-02
P2ry2	↑	1.47	3.52E-02	100997662	-	100999384	↑	1.79	1.59E-11
Palm	↑	1.28	4.78E-02	79818628	-	79821266	↑	0.93	3.40E-02
Papln	↑	1.46	1.67E-02	83773583	-	83779594	↑	1.73	4.48E-05
Pbxip1	↑	1.46	4.78E-02	89432141	-	89433846	↑	0.59	1.99E-02
Pcsk6	↑	2.10	4.86E-02	65871200	-	65871865	↑	1.55	8.21E-09
Pde2a	↑	1.44	4.40E-02	101504016	-	101505555	↑	1.01	1.20E-04
Pdss2	↑	2.13	3.83E-02	43303465	-	43304210	↑	0.80	4.28E-03
Pear1	↑	2.06	6.89E-03	87756120	-	87757146	↑	1.21	1.71E-04
Peli2	↑	1.30	3.81E-02	48255615	-	48257024	↑	0.77	1.72E-02
Per3	↑	1.41	3.60E-02	151011911	-	151014065	↑	1.57	2.67E-07
Phc3	↑	1.71	3.97E-02	30948304	-	30948991	↑	0.70	3.62E-02
Phldb1	↑	1.93	3.08E-02	44733265	-	44734109	↑	1.67	2.07E-09
Phospho1	↑	2.11	3.37E-03	95830140	-	95831709	↑	1.84	1.88E-11
Pitpnm2	↑	1.44	4.67E-02	124120169	-	124124457	↑	0.70	8.56E-03

Plec	↑	1.91	2.99E-02	76205330	-	76206319	↑	1.16	1.23E-03
Plekha6	↑	1.55	4.48E-02	133293353	-	133294301	↑	1.87	3.30E-13
Plekhg5	↑	2.41	1.36E-03	152107318	-	152108849	↑	1.19	4.52E-04
Plxdc2	↑	2.48	4.75E-02	16586295	-	16586847	↑	2.12	4.55E-11
Pmepa1	↑	1.61	3.35E-02	173234133	-	173235416	↑	1.54	9.21E-11
Podn	↑	1.22	4.77E-02	108020699	-	108022954	↑	4.08	3.86E-22
Polrmt	↑	1.52	3.41E-02	79734717	-	79742099	↑	1.16	3.68E-04
Ppargc1b	↑	1.49	4.81E-02	61307050	-	61308172	↑	1.68	5.94E-06
Ppp1r10	↑	1.55	3.82E-02	35930029	-	35932186	↑	1.72	2.64E-07
Ppp1r3c	↑	1.95	4.32E-02	36731165	-	36731830	↑	2.15	8.03E-16
Psd	↑	1.29	3.23E-02	46309430	-	46313711	↑	1.84	9.99E-04
Psmb8	↑	1.98	2.20E-02	34196368	-	34197296	↑	2.08	1.13E-08
Ptch2	↑	1.35	4.25E-02	117107836	-	117111873	↑	1.08	4.30E-02
Ptgir	↑	1.59	4.98E-02	16906565	-	16907934	↑	2.09	7.00E-04
Rab6b	↑	1.38	3.59E-02	103118970	-	103120332	↑	1.68	6.72E-09
Ralbp1	↑	1.14	4.75E-02	65848552	-	65851402	↑	1.19	1.43E-06
Rap1gap	↑	1.48	4.39E-02	137719871	-	137720952	↑	1.89	2.68E-05

Rarg	↑	2.14	4.83E-02	102249686	-	102250299	↑	1.70	4.78E-07
Relb	↑	3.39	6.89E-03	19619260	-	19620102	↑	0.89	1.01E-02
Rfx1	↑	1.41	4.15E-02	84094363	-	84098192	↑	0.83	3.25E-02
Rgl3	↑	1.43	3.35E-02	21990931	-	21992404	↑	1.73	3.29E-04
Rps6ka4	↑	1.57	1.75E-02	6829671	-	6832708	↑	0.81	1.32E-02
Rusc2	↑	1.52	2.61E-02	43414409	-	43417141	↑	1.15	7.05E-04
Rxrg	↑	1.33	4.66E-02	167631802	-	167632993	↑	5.33	2.46E-66
Safb2	↑	1.54	3.93E-02	56565671	-	56567317	↑	1.36	1.06E-06
Sall4	↑	1.28	3.60E-02	168754073	-	168757130	↑	1.35	1.92E-03
Sbk1	↑	1.58	2.61E-02	126290775	-	126293217	↑	1.29	1.90E-05
Scara5	↑	1.87	3.52E-02	65730174	-	65731429	↑	1.30	1.63E-04
Scarf2	↑	2.48	2.17E-03	17802131	-	17804955	↑	1.32	1.16E-03
Scube2	↑	2.10	4.80E-02	109837913	-	109838588	↑	1.06	1.60E-04
Sdccag8	↑	1.55	4.69E-02	177017866	-	177018686	↑	0.97	1.97E-03
Sema6b	↑	1.88	3.35E-02	56123056	-	56125215	↑	2.27	1.82E-05
Sgca	↑	1.73	4.94E-02	94963049	-	94963630	↑	1.78	1.44E-08
Sgta	↑	1.33	4.82E-02	81043791	-	81045761	↑	0.67	4.58E-02

Sh3tc1	↑	1.70	4.67E-03	35705494	-	35708182	↑	0.81	2.20E-02
Shank3	↑	2.60	4.67E-03	89556952	-	89558524	↑	1.61	1.88E-08
Sipa1	↑	1.53	8.76E-03	5653761	-	5656625	↑	1.14	4.59E-04
Slc25a29	↑	1.30	4.95E-02	108825446	-	108828040	↑	3.37	1.72E-16
Slc39a3	↑	1.84	2.30E-02	81030517	-	81032070	↑	1.63	4.54E-07
Slc45a3	↑	1.99	2.30E-02	131981009	-	131981843	↑	1.11	1.35E-02
Slc7a10	↑	1.48	4.33E-02	35202132	-	35205838	↑	1.93	1.93E-04
Slco3a1	↑	3.10	6.04E-03	74421951	-	74422723	↑	2.05	1.87E-17
Smcr7	↑	1.40	3.96E-02	60730159	-	60732094	↑	2.10	2.99E-16
Solh	↑	1.60	2.72E-02	25958845	-	25961076	↑	1.49	1.03E-02
Sorl1	↑	1.96	3.18E-02	41979093	-	41979796	↑	1.24	1.23E-03
Spef1	↑	1.48	3.99E-02	131170987	-	131173103	↑	1.23	2.20E-05
Speg	↑	1.47	3.35E-02	75405935	-	75407470	↑	1.52	1.13E-08
Sstr3	↑	2.05	3.88E-02	78543835	-	78544755	↑	2.78	3.94E-08
St3gal3	↑	1.16	3.58E-02	118096582	-	118098689	↑	0.81	3.99E-03
Stab1	↑	1.35	3.88E-02	31139464	-	31142361	↑	0.87	8.86E-03
Stap2	↑	1.40	4.39E-02	55999044	-	56001363	↑	1.45	8.56E-08

Stard8	↑	2.13	2.61E-02	99072348	-	99073231	↑	1.17	1.81E-05
Stk11	↑	1.60	4.12E-02	80129310	-	80133513	↑	1.20	6.97E-05
Stoml1	↑	1.48	3.84E-02	58259800	-	58260562	↑	1.17	2.39E-04
Taf1c	↑	1.10	4.69E-02	119600176	-	119603791	↑	1.96	2.49E-07
Taf3	↑	1.46	4.02E-02	9930279	-	9931159	↑	1.39	1.42E-05
Tap1	↑	1.98	2.20E-02	34196368	-	34197296	↑	0.88	3.19E-02
Tap2	↑	1.74	3.77E-02	34214944	-	34215755	↑	0.90	1.61E-02
Tbc1d2	↑	1.29	4.60E-02	46606251	-	46607428	↑	1.26	1.47E-02
Tbx3	↑	2.33	4.19E-03	119680061	-	119681185	↑	0.70	3.10E-02
Tbxa2r	↑	1.92	2.72E-02	81332045	-	81333506	↑	1.66	1.06E-04
Tcap	↑	2.69	2.01E-02	98383882	-	98384795	↑	3.79	1.05E-18
Tcf15	↑	1.58	3.59E-02	152140278	-	152141332	↑	1.94	1.62E-06
Tecpr1	↑	1.42	3.55E-02	144205843	-	144207095	↑	1.99	1.02E-13
Tecr	↑	2.63	8.51E-03	83573567	-	83574196	↑	1.13	1.77E-04
Tesc	↑	1.47	3.67E-02	118060928	-	118061955	↑	4.17	1.64E-39
Tmem104	↑	1.84	3.66E-02	115242983	-	115244469	↑	0.97	1.57E-02
Tmem200b	↑	1.55	3.56E-02	131922232	-	131923460	↑	1.50	1.02E-02

Tmub1	↑	1.63	4.15E-02	24445489	-	24446363	↑	0.95	3.77E-02
Tnfaip2	↑	2.17	2.14E-02	111444844	-	111446519	↑	2.55	1.21E-17
Tnfaip8l2	↑	1.54	2.44E-02	95138879	-	95141161	↑	3.15	3.86E-08
Tnni3	↑	1.49	2.82E-02	4526667	-	4527949	↑	2.07	1.53E-06
Tnrc6b	↑	1.68	3.73E-02	80876028	-	80876967	↑	1.21	1.16E-03
Tnrc6c	↑	1.16	4.12E-02	117757887	-	117761940	↑	1.46	2.04E-07
Tnxb	↑	2.12	2.50E-02	34670273	-	34673576	↑	1.99	2.05E-08
Tppp3	↑	1.34	4.39E-02	105472175	-	105473374	↑	1.95	5.43E-07
Traf1	↑	1.67	1.38E-02	34943457	-	34944493	↑	1.70	2.43E-03
Trim11	↑	1.60	3.73E-02	58989998	-	58991076	↑	0.61	2.76E-02
Trim56	↑	1.30	3.38E-02	137112677	-	137114840	↑	0.72	2.59E-02
Trim72	↑	2.12	2.15E-02	128009711	-	128010714	↑	4.13	1.25E-46
Trpv4	↑	2.37	2.74E-02	114630265	-	114631025	↑	2.74	2.91E-10
Tshz3	↑	3.16	4.99E-03	36695045	-	36695782	↑	1.13	1.25E-02
Ttc28	↑	1.33	3.67E-02	111269978	-	111271874	↑	0.60	4.29E-02
Ttc7	↑	1.84	4.01E-02	87311949	-	87312805	↑	1.45	2.69E-04
Tyrobp	↑	2.30	4.19E-02	30414242	-	30414800	↑	1.52	9.99E-07

Ubxn10	↑	1.35	2.29E-02	138719194	-	138722070	↑	2.25	1.46E-08
Ucp3	↑	1.32	4.17E-02	100479196	-	100481533	↑	3.63	5.47E-18
Ulk4	↑	1.73	4.79E-02	121154949	-	121155696	↑	0.76	6.23E-03
Unc13a	↑	1.85	2.61E-02	71662276	-	71663908	↑	0.97	4.93E-04
Unc93b1	↑	1.33	4.19E-02	3942187	-	3944517	↑	1.32	2.97E-06
Ush1c	↑	1.77	4.93E-02	46208528	-	46209358	↑	1.09	3.55E-03
Ushbp1	↑	1.60	2.26E-02	71386905	-	71388152	↑	2.35	5.39E-13
Vav1	↑	2.25	1.52E-02	57278825	-	57279692	↑	1.16	2.85E-03
Vegfb	↑	1.69	3.52E-02	6985122	-	6985876	↑	0.88	2.91E-03
Vps18	↑	1.39	3.87E-02	119296487	-	119298278	↑	1.08	3.22E-02
Vwf	↑	1.30	2.67E-02	125641811	-	125643512	↑	1.04	2.08E-03
Wdr81	↑	1.63	9.83E-03	75443611	-	75446317	↑	0.91	1.68E-02
Wdtc1	↑	2.87	3.93E-02	133294094	-	133294565	↑	0.70	2.13E-02
Wfs1	↑	1.46	3.24E-02	36966382	-	36968901	↑	1.93	1.69E-16
Wipf3	↑	2.69	4.64E-02	54485559	-	54486263	↑	1.69	1.79E-10
Zbtb48	↑	1.32	3.52E-02	152019157	-	152022502	↑	1.19	4.62E-03
Zbtb7a	↑	1.56	4.32E-02	81143558	-	81145675	↑	1.27	2.21E-03

Zc3h18	↑	1.41	4.72E-02	122402949	-	122403746	↑	0.75	3.10E-02
Zdhhc1	↑	1.34	4.39E-02	105472175	-	105473374	↑	0.86	2.36E-02
Zfhx3	↑	1.40	1.05E-02	108954613	-	108957252	↑	1.46	3.41E-05
Zfp629	↑	1.66	3.74E-02	127610585	-	127612444	↑	1.20	1.69E-06
Zfp641	↑	1.81	4.07E-02	98288346	-	98289173	↑	0.84	1.41E-02
Zfp652	↑	2.11	3.37E-03	95830140	-	95831709	↑	1.35	9.56E-08
Zfp668	↑	1.44	3.27E-02	127865867	-	127868548	↑	0.96	2.40E-02
Zfp775	↑	1.77	2.32E-02	48619171	-	48621394	↑	1.74	4.40E-08
Zfp787	↑	1.79	1.79E-02	6131469	-	6133450	↑	1.17	1.65E-05
Zfyve21	↑	1.66	4.15E-02	111810494	-	111811422	↑	0.69	1.17E-02
Zmynd8	↑	1.39	4.62E-02	165889339	-	165890943	↑	0.63	1.78E-02
Bnip2	↓	-2.17	2.81E-02	69997546	-	69998309	↑	0.92	4.85E-04
C1qtnf7	↓	-2.81	1.40E-02	43555085	-	43555778	↑	1.07	1.86E-03
Cmya5	↓	-2.07	4.67E-02	93145841	-	93146925	↑	1.82	1.02E-09
D9Ertd402e	↓	-1.91	4.52E-02	122808301	-	122808996	↑	2.23	7.75E-16
Derl2	↓	-1.73	2.14E-02	71020535	-	71021954	↑	0.97	4.79E-04
Dnajc21	↓	-1.33	4.39E-02	10466438	-	10468104	↑	0.66	3.26E-02

Dnm3	↓	-2.39	3.59E-02	162018394	-	162019194	↑	2.01	9.05E-08
Dst	↓	-1.83	4.81E-02	34054081	-	34054715	↑	1.71	3.10E-05
Ebf1	↓	-1.92	3.97E-02	44627615	-	44628511	↑	2.09	2.51E-05
Egfr	↓	-1.80	4.39E-02	16886677	-	16887318	↑	0.95	1.29E-02
Frmd6	↓	-1.88	2.81E-02	70872447	-	70873246	↑	0.64	1.43E-02
Gpatch2	↓	-1.70	4.39E-02	187220824	-	187221949	↑	0.82	1.14E-02
Grm1	↓	-1.95	4.78E-02	10809589	-	10810388	↑	5.83	5.71E-20
Hadha	↓	-1.33	4.15E-02	30140414	-	30141494	↑	1.58	4.16E-06
Immp2l	↓	-1.96	4.55E-02	41580807	-	41581481	↑	1.68	4.27E-09
Klf7	↓	-2.66	2.55E-02	64117428	-	64118155	↑	1.00	4.54E-04
Klf9	↓	-2.24	1.28E-02	23150327	-	23151006	↑	2.76	2.64E-26
Max	↓	-1.33	3.73E-02	76955993	-	76957657	↑	1.12	1.00E-05
Mbnl2	↓	-2.16	4.01E-02	120302265	-	120302906	↑	0.72	1.65E-02
Mfn1	↓	-2.13	2.36E-02	32532277	-	32533052	↑	0.69	2.12E-02
Nceh1	↓	-1.84	4.03E-02	27187439	-	27188208	↑	1.30	8.30E-07
Neat1	↓	-2.42	1.90E-03	5843466	-	5844277	↑	3.39	2.11E-18
Pik3r1	↓	-2.05	2.78E-02	101713227	-	101713992	↑	1.05	2.09E-03

Ppap2a	↓	-2.05	3.90E-02	112802901	-	112803453	↑	1.04	5.02E-05
Ppap2b	↓	-2.54	3.32E-02	105159954	-	105160823	↑	1.19	8.10E-07
Prune2	↓	-2.13	3.23E-02	17078101	-	17078805	↑	1.63	1.25E-05
Ptprr	↓	-1.93	3.93E-02	116049566	-	116050157	↑	2.36	3.51E-05
Rcan2	↓	-3.04	2.20E-02	43968520	-	43969005	↑	0.67	1.47E-02
Ryr2	↓	-1.65	4.82E-02	11751798	-	11752652	↑	1.16	9.93E-03
Sgcd	↓	-1.73	4.80E-02	47203138	-	47203703	↑	1.30	6.17E-05
Srgn	↓	-1.77	3.73E-02	62506139	-	62506905	↑	1.53	2.87E-07
Tcf4	↓	-2.05	3.61E-02	69581499	-	69582257	↑	1.84	7.86E-12
Upf2	↓	-1.70	4.66E-02	6010546	-	6011377	↑	0.86	1.10E-02
Zbtb16	↓	-1.87	4.96E-02	48734322	-	48734883	↑	1.89	1.31E-06
Zfp703	↓	-2.00	4.49E-02	26974168	-	26974914	↑	1.70	8.84E-07
Zfp827	↓	-2.11	2.13E-02	79126106	-	79126995	↑	0.83	4.72E-03
1110018J18Rik	↓	-1.81	3.20E-02	64309872	-	64310578	↓	-1.10	1.72E-04
Bmpr1a	↓	-1.71	3.39E-02	34435613	-	34437154	↓	-0.91	2.69E-03
Cetn3	↓	-1.60	4.79E-02	81782190	-	81782787	↓	-0.86	4.78E-03
Chic2	↓	-1.94	4.69E-02	75019723	-	75020325	↓	-0.81	5.39E-03

Dcaf13	↓	-2.45	4.04E-02	39139987	-	39140604	↓	-0.56	4.79E-02
Diap3	↓	-2.46	3.48E-02	86963147	-	86963860	↓	-2.89	2.56E-12
Fam151b	↓	-2.76	1.74E-02	92486922	-	92487525	↓	-1.13	1.42E-02
Fam48a	↓	-2.05	3.88E-02	54707950	-	54708490	↓	-1.10	3.62E-03
Herc3	↓	-2.05	3.74E-02	58834199	-	58834857	↓	-1.42	5.68E-07
Herpud2	↓	-1.61	4.80E-02	25135646	-	25136712	↓	-0.65	2.10E-02
Kif26b	↓	-2.35	3.55E-02	178702892	-	178703541	↓	-2.91	7.69E-13
Lass6	↓	-2.11	4.39E-02	68866458	-	68867045	↓	-1.61	8.41E-07
Map4k3	↓	-1.76	4.77E-02	80630120	-	80630734	↓	-0.78	1.24E-02
Mapk1ip1l	↓	-1.56	4.12E-02	47302783	-	47303676	↓	-1.23	5.62E-05
Nudt21	↓	-2.56	6.32E-03	94028763	-	94029608	↓	-0.81	3.32E-02
Orc5	↓	-1.92	2.79E-02	22547464	-	22548312	↓	-0.75	1.33E-02
Pam	↓	-2.15	3.62E-02	97900281	-	97901054	↓	-1.58	1.46E-07
Parg	↓	-2.42	4.88E-02	32213077	-	32213570	↓	-1.16	2.84E-04
Pdcl	↓	-1.72	4.66E-02	37351660	-	37352545	↓	-0.96	1.68E-03
Pias2	↓	-2.69	2.16E-02	77144877	-	77145549	↓	-1.03	5.98E-05
Pitrm1	↓	-1.17	4.82E-02	6549449	-	6551096	↓	-0.69	4.88E-03

Ptpn9	↓	-1.89	4.07E-02	57048831	-	57049518	↓	-1.51	1.66E-08
Rad21	↓	-2.52	4.39E-02	51962496	-	51963121	↓	-1.83	4.68E-14
Scfd1	↓	-1.96	4.82E-02	51431523	-	51432144	↓	-1.00	1.20E-03
Sowahc	↓	-2.07	3.67E-02	59225878	-	59226582	↓	-1.89	1.44E-04
Sri	↓	-2.03	3.96E-02	8059823	-	8060539	↓	-0.72	7.17E-03
St6galnac3	↓	-2.08	3.62E-02	153310189	-	153310858	↓	-1.16	4.32E-02
Thsd4	↓	-1.46	4.85E-02	60466595	-	60467605	↓	-1.05	5.35E-03
Zdhhc6	↓	-1.75	4.67E-02	55313676	-	55315273	↓	-0.65	2.55E-02
Zfpm2	↓	-2.01	4.76E-02	41080783	-	41081495	↓	-1.39	5.44E-05

7.2. Comparison of PCM1 staining and sorting protocol (from Chapter 5).

Year			2009	2011	2012	2014	2015	2015	2015
Lab and reference			**Bergmann (Bergmann et al., 2009)**	**Bergmann (Bergmann et al., 2011)**	**Bergmann (Bergmann and Jovinge, 2012)**	**Hein (Gilsbach et al., 2014)**	**Hein (Preissl et al., 2015a)**	**Bergmann (Bergmann et al., 2015)**	**Bergmann (Alkass et al., 2015)**
Note			TnnT, TnnI	TnnT, TnnI, PCM1	PCM1 Method	Refer 2011 Bergmann	refer 2014 Hein	Human (more similar to 2011)	mouse, refer 2015 human
Buffer	1. Lysis Buffer	0.32 M sucrose	√	√	√	√	-	√	√
		10 mM Tris-HCl (pH √ 8)	√	√	√	√	√	√	√
		5 mM CaCl2	√	√	√	√	√	√	√
		5 mM magnesium	3mM	3mM	√	3mM	3mM	√	√

		acetate							
		2.0 mM EDTA	√	√	√	√	√	√	√
		0.5 mM EGTA	√	√	√	√	√	√	√
		1 mM DTT	√	√	√	√	√	√	√
		proteinase inhibitor	√	NA	NA	NA	√	NA	NA
	2. Sucrose buffer	2.1 M sucrose	(2.1 & 2.2 M only has different in sucrose)	√	√	√	1M	√	√
		10 mM Tris-HCl (pH √ 8)	√	√	√	√	√	√	√
		5 mM magnesium acetate	3mM	3mM	√	3mM	3mM	√	√
		1 mM DTT	√	√	√	√	-	-	-

	3. Nuclei storage buffer (NSB plus)	0.44 M sucrose	0.43M	0.43M	√	0.43M	use staining buffer (PBS+ 5%BSA+ 0.2% Igepal CA-630)	√	√
		10 mM Tris-HCl (pH √ 7.2)	√	√	√	√		√	√
		70 mM KCl	√	√	√	√		√	√
		10 mM MgCl2	2mM	2mM	√	2mM		√	√
		1.5 mM spermine	-	-	√	-		√	√
		5mM EGTA	√	√	-	√		-	-
Isolation protocol	1	tissur amount	10g	NA	1g	NA	NA	8-10g	NA
	2	50 ml Falcon tube filled with 15 ml of lysis buffer	200mL	200mL	√	2011 Bergmann protocol	3mL	no vol	NA
	3	blend with speed 9, 10 min	√	√	-		-	√	-
	4	Homogenize at	20000rpm,	20000rpm,	√		NA	√	√

		24,000 rpm for 10 sec.	8s	10s					
	5	Add 15 ml of lysis buffer to dilute the homogenate to 30 ml.	add triton x-100 to 0.2%, no add more lysis	-	√		3mL + 0.4% Triton-X	no add more lysis buffer	NA
	6	Perform 8 strokes use a glass douncer.	√	√	√		-	√	√
	7	Filter: 70 μm nylon mesh cell strainer.	100->70 um strainer	100->70 um strainer	100->70 um strainer		40um	100->60 um strainer	100->60 um strainer
	8	1000 x g, 10 min, 4 ℃	divide 6 tube, 8min	700g, 8min	700g		2mL (with 0.2% Triton-X) then spin, 5min	700g	600g
	9	resuspense	√	no vol	√		no vol, 1M	no vol	no vol

		30mL 2.1M sucrose buffer					sucrose		
	10	layer on 10mL 2.2M sucrose	√	same vol, 2.1M	√		no vol, 1M sucrose	same vol, 2.1M	same vol, 2.1M
	11	30000g, 1h, 4 ℃	√	√	13000g		1000g, 5min	13000g	13000g
	12	1 ml of nuclei storage buffer	1.5mL	1.5mL	√		0.5mL staining buffer	no vol	no vol
FACS	13	Primary Ab, 4 ℃, ON	at least 30mins	NA	√	30min	NA	√	√
		PCM1 (Sigma), 1:100	-	(1:1000)	(1:500)	(1:1000)	(1:1000)	Santa, 1:200	Santa, 1:200
		TnnT (Thermo), 1:100	-	direct conjugate A488	-	-	-	-	-
		TnnT (Abcam Ab10214), 1:100	-		-	-	-	-	-
		TnnT (Abcam	√		-	-	-	-	-

		Ab10224), 1:800						
		TnnI (Millipore MAB3152), 1:800	√		-	-	-	-	-
	14	add double vol of primary Ab	NA		no vol, (at least 1 time)	NA	NA	NA	NA
	15	1000 x g, 10 min, 4 ℃	NA		700g	NA	NA	700g	NA
	16	secondary Ab 1:500, 4 ℃, 1h	NA		A488, 1:1000	A488/ A647, 1:1000 (not sure direct conjugation)	1:1000 (not sure direct conjugation)	PE, Santa, 1:100	A488, no dilution
	17	add double vol of primary Ab	NA		no vol, (at least 1 time)	NA	NA	NA	NA
	18	1000 x g, 10	NA	NA	700g	NA	NA	700g	NA

		min, 4 ℃							
	19	nuclei fix in BD fix/Perm 20mins, 4 ℃ before sort	-	-	-	-	-	NA	√
	20	1500g, 15mins	NA	NA	√	NA	NA	1200g	NA
Nuclei marker	Nuclei marker	Hoechst	for ploidy	NA	DRAQ5, 1:500	7-AAD, 1:500	DRAQ7, 1:200	DRAQ5, 1:1000	Hoechst
		DAPI	-	NA	-	(1:1000)	(1:1000)	-	-
			DRAQ5						

Chapter 8

List of References

All we have to decide
is what to do with the time that is given us.
Gandalf in The Lord of the Ring.

Chapter 8. List of References

Afanas'ev, I. (2014). New nucleophilic mechanisms of ros-dependent epigenetic modifications: comparison of aging and cancer. Aging Dis *5*, 52-62.

Afanas'ev, I. (2015). Mechanisms of superoxide signaling in epigenetic processes: relation to aging and cancer. Aging Dis *6*, 216-227.

Ahuja, P., Sdek, P., and MacLellan, W.R. (2007). Cardiac myocyte cell cycle control in development, disease, and regeneration. Physiological reviews *87*, 521-544.

Alkass, K., Panula, J., Westman, M., Wu, T.D., Guerquin-Kern, J.L., and Bergmann, O. (2015). No Evidence for Cardiomyocyte Number Expansion in Preadolescent Mice. Cell *163*, 1026-1036.

Ang, S.Y., Uebersohn, A., Spencer, C.I., Huang, Y., Lee, J.E., Ge, K., and Bruneau, B.G. (2016). KMT2D regulates specific programs in heart development via histone H3 lysine 4 di-methylation. Development (Cambridge, England) *143*, 810-821.

Arceci, R.J., King, A.A., Simon, M.C., Orkin, S.H., and Wilson, D.B. (1993). Mouse GATA-4: a retinoic acid-inducible GATA-binding transcription factor expressed in endodermally derived tissues and heart. Molecular and cellular biology *13*, 2235-2246.

Arner, E., Daub, C.O., Vitting-Seerup, K., Andersson, R., Lilje, B., Drablos, F., Lennartsson, A., Ronnerblad, M., Hrydziuszko, O., Vitezic, M., *et al.* (2015). Gene regulation. Transcribed enhancers lead waves of coordinated transcription in transitioning mammalian cells. Science (New York, NY) *347*, 1010-1014.

Ashburner, M., Ball, C.A., Blake, J.A., Botstein, D., Butler, H., Cherry, J.M., Davis, A.P., Dolinski, K., Dwight, S.S., Eppig, J.T., *et al.* (2000). Gene ontology: tool for the unification of biology. The Gene Ontology Consortium. Nature genetics *25*, 25-29.

Assmus, B., Schachinger, V., Teupe, C., Britten, M., Lehmann, R., Dobert, N., Grunwald, F., Aicher, A., Urbich, C., Martin, H., *et al.* (2002). Transplantation of Progenitor Cells and Regeneration Enhancement in Acute Myocardial Infarction (TOPCARE-AMI). Circulation *106*, 3009-3017.

Baccarelli, A., Rienstra, M., and Benjamin, E.J. (2010). Cardiovascular epigenetics: basic concepts and results from animal and human studies. Circulation Cardiovascular genetics *3*, 567-573.

Backs, J., and Olson, E.N. (2006). Control of cardiac growth by histone acetylation/deacetylation. Circulation research *98*, 15-24.

Bajaj, S., Alam, S.K., Roy, K.S., Datta, A., Nath, S., and Roychoudhury, S. (2016). E2 Ubiquitin-conjugating Enzyme, UBE2C Gene, Is Reciprocally Regulated by Wild-type and Gain-of-Function Mutant p53. The Journal of biological chemistry *291*, 14231-14247.

Ball, M.P., Li, J.B., Gao, Y., Lee, J.H., LeProust, E.M., Park, I.H., Xie, B., Daley, G.Q., and Church, G.M. (2009). Targeted and genome-scale strategies reveal gene-body methylation signatures in human cells. Nature biotechnology *27*, 361-368.

Bannister, A.J., and Kouzarides, T. (2011). Regulation of chromatin by histone modifications. Cell Research *21*, 381-395.

Bartholomew, B. (2014). Regulating the chromatin landscape: structural and mechanistic perspectives. Annual review of biochemistry *83*, 671-696.

Bartolomei, M.S., Zemel, S., and Tilghman, S.M. (1991). Parental imprinting of the mouse H19 gene. Nature *351*, 153-155.

Baylin, S.B. (2005). DNA methylation and gene silencing in cancer. Nat Clin Pract Oncol *2 Suppl 1*, S4-11.

Bearzi, C., Rota, M., Hosoda, T., Tillmanns, J., Nascimbene, A., De Angelis, A., Yasuzawa-Amano, S., Trofimova, I., Siggins, R.W., Lecapitaine, N., *et al.* (2007). Human cardiac stem cells. Proceedings of the National Academy of Sciences of the United States of America *104*, 14068-14073.

Beato, M., and Eisfeld, K. (1997). Transcription factor access to chromatin. Nucleic acids research *25*, 3559-3563.

Bell, R.M., Mocanu, M.M., and Yellon, D.M. (2011). Retrograde heart perfusion: the Langendorff technique of isolated heart perfusion. Journal of molecular and cellular cardiology *50*, 940-950.

Beltrami, A.P., Barlucchi, L., Torella, D., Baker, M., Limana, F., Chimenti, S., Kasahara, H., Rota, M., Musso, E., Urbanek, K., *et al.* (2003). Adult cardiac stem cells are multipotent and support myocardial regeneration. Cell *114*, 763-776.

Benjamini, Y., and Hochberg, Y. (1995). Controlling the False Discovery Rate - a Practical and Powerful Approach to Multiple Testing. J Roy Stat Soc B Met *57*, 289-300.

Bergmann, O., Bhardwaj, R.D., Bernard, S., Zdunek, S., Barnabe-Heider, F., Walsh, S., Zupicich, J., Alkass, K., Buchholz, B.A., Druid, H., *et al.* (2009). Evidence for cardiomyocyte renewal in humans. Science *324*, 98-102.

Bergmann, O., and Jovinge, S. (2012). Isolation of cardiomyocyte nuclei from post-mortem tissue. Journal of visualized experiments : JoVE.

Bergmann, O., Zdunek, S., Alkass, K., Druid, H., Bernard, S., and Frisen, J. (2011). Identification of cardiomyocyte nuclei and assessment of ploidy for the analysis of cell turnover. Experimental cell research *317*, 188-194.

Bergmann, O., Zdunek, S., Felker, A., Salehpour, M., Alkass, K., Bernard, S., Sjostrom, S.L., Szewczykowska, M., Jackowska, T., Dos Remedios, C., *et al.* (2015). Dynamics of Cell Generation and Turnover in the Human Heart. Cell *161*, 1566-1575.

Berkowitz, K.M., Kaestner, K.H., and Jongens, T.A. (2008). Germline expression of mammalian CTF18, an evolutionarily conserved protein required for germ cell proliferation in the fly and sister chromatid cohesion in yeast. Mol Hum Reprod *14*, 143-150.

Berman, B.P., Weisenberger, D.J., Aman, J.F., Hinoue, T., Ramjan, Z., Liu, Y., Noushmehr, H., Lange, C.P., van Dijk, C.M., Tollenaar, R.A., *et al.* (2011). Regions of focal DNA hypermethylation and long-range hypomethylation in colorectal cancer coincide with nuclear lamina-associated domains. Nature genetics *44*, 40-46.

Bernstein, B.E., Mikkelsen, T.S., Xie, X., Kamal, M., Huebert, D.J., Cuff, J., Fry, B., Meissner, A., Wernig, M., Plath, K., *et al.* (2006). A bivalent chromatin structure marks key developmental genes in embryonic stem cells. Cell *125*, 315-326.

Bersell, K., Arab, S., Haring, B., and Kuhn, B. (2009). Neuregulin1/ErbB4 signaling induces cardiomyocyte proliferation and repair of heart injury. Cell *138*, 257-270.

Beyer, T.A., Weiss, A., Khomchuk, Y., Huang, K., Ogunjimi, A.A., Varelas, X., and Wrana, J.L. (2013). Switch enhancers interpret TGF-beta and Hippo signaling to control cell fate in human embryonic stem cells. Cell reports *5*, 1611-1624.

Bicknell, K.A., Coxon, C.H., and Brooks, G. (2004). Forced expression of the cyclin B1-CDC2 complex induces proliferation in adult rat cardiomyocytes. The Biochemical journal *382*, 411-416.

Bolli, R., Chugh, A.R., D'Amario, D., Loughran, J.H., Stoddard, M.F., Ikram, S., Beache, G.M., Wagner, S.G., Leri, A., Hosoda, T., *et al.* (2011). Cardiac stem cells in patients with ischaemic cardiomyopathy (SCIPIO): initial results of a randomised phase 1 trial. Lancet *378*, 1847-1857.

Bolte, C., Zhang, Y., Wang, I.C., Kalin, T.V., Molkentin, J.D., and Kalinichenko, V.V. (2011). Expression of Foxm1 transcription factor in cardiomyocytes is required for myocardial development. PloS one *6*, e22217.

Bolte, C., Zhang, Y., York, A., Kalin, T.V., Schultz Jel, J., Molkentin, J.D., and Kalinichenko, V.V. (2012). Postnatal ablation of Foxm1 from cardiomyocytes causes late onset cardiac hypertrophy and fibrosis without exacerbating pressure overload-induced cardiac remodeling. PloS one *7*, e48713.

Botting, K.J., Wang, K.C., Padhee, M., McMillen, I.C., Summers-Pearce, B., Rattanatray, L., Cutri, N., Posterino, G.S., Brooks, D.A., and Morrison, J.L. (2012). Early origins of heart disease: low birth weight and determinants of cardiomyocyte endowment. Clinical and experimental pharmacology & physiology *39*, 814-823.

Bouveret, R., Waardenberg, A.J., Schonrock, N., Ramialison, M., Doan, T., de Jong, D., Bondue, A., Kaur, G., Mohamed, S., Fonoudi, H., *et al.* (2015). NKX2-5 mutations causative for congenital heart disease retain functionality and are directed to hundreds of targets. eLife *4*.

Boyle, A.P., Davis, S., Shulha, H.P., Meltzer, P., Margulies, E.H., Weng, Z., Furey, T.S., and Crawford, G.E. (2008). High-resolution mapping and characterization of open chromatin across the genome. Cell *132*, 311-322.

Buenrostro, J.D., Giresi, P.G., Zaba, L.C., Chang, H.Y., and Greenleaf, W.J. (2013). Transposition of native chromatin for fast and sensitive epigenomic profiling of open chromatin, DNA-binding proteins and nucleosome position. Nature methods *10*, 1213-1218.

Buenrostro, J.D., Wu, B., Chang, H.Y., and Greenleaf, W.J. (2015a). ATAC-seq: A Method for Assaying Chromatin Accessibility Genome-Wide. Curr Protoc Mol Biol *109*, 21 29 21-29.

Buenrostro, J.D., Wu, B., Litzenburger, U.M., Ruff, D., Gonzales, M.L., Snyder, M.P., Chang, H.Y., and Greenleaf, W.J. (2015b). Single-cell chromatin accessibility reveals principles of regulatory variation. Nature *523*, 486-490.

Canseco, D.C., Kimura, W., Garg, S., Mukherjee, S., Bhattacharya, S., Abdisalaam, S., Das, S., Asaithamby, A., Mammen, P.P., and Sadek, H.A. (2015). Human ventricular unloading induces cardiomyocyte proliferation. Journal of the American College of Cardiology *65*, 892-900.

Cao, Y., Yao, Z., Sarkar, D., Lawrence, M., Sanchez, G.J., Parker, M.H., MacQuarrie, K.L., Davison, J., Morgan, M.T., Ruzzo, W.L., *et al.* (2010). Genome-wide MyoD binding in skeletal muscle cells: a potential for broad cellular reprogramming. Developmental cell *18*, 662-674.

Carninci, P., Kasukawa, T., Katayama, S., Gough, J., Frith, M.C., Maeda, N., Oyama, R., Ravasi, T., Lenhard, B., Wells, C., *et al.* (2005). The transcriptional landscape of the mammalian genome. Science (New York, NY) *309*, 1559-1563.

Carroll, J.S., Liu, X.S., Brodsky, A.S., Li, W., Meyer, C.A., Szary, A.J., Eeckhoute, J., Shao, W., Hestermann, E.V., Geistlinger, T.R., *et al.* (2005). Chromosome-wide mapping of estrogen receptor binding reveals long-range regulation requiring the forkhead protein FoxA1. Cell *122*, 33-43.

Carvalho, A.B., and de Carvalho, A.C. (2010). Heart regeneration: Past, present and future. World journal of cardiology *2*, 107-111.

Cassano, M., Berardi, E., Crippa, S., Toelen, J., Barthelemy, I., Micheletti, R., Chuah, M., Vandendriessche, T., Debyser, Z., Blot, S., *et al.* (2012). Alteration of cardiac progenitor cell potency in GRMD dogs. Cell transplantation *21*, 1945-1967.

Celine J Vivien, J.E.H.E.R.P. (2016). Evolution, comparative biology and ontogeny of vertebrate heart regeneration. Regenerative Medicine *1*.

Cerda, S., and Weitzman, S.A. (1997). Influence of oxygen radical injury on DNA methylation. Mutation research *386*, 141-152.

Chablais, F., Veit, J., Rainer, G., and Jazwinska, A. (2011). The zebrafish heart regenerates after cryoinjury-induced myocardial infarction. BMC developmental biology *11*, 21.

Chamberlain, A.A., Lin, M., Lister, R.L., Maslov, A.A., Wang, Y., Suzuki, M., Wu, B., Greally, J.M., Zheng, D., and Zhou, B. (2014). DNA methylation is developmentally regulated for genes essential for cardiogenesis. J Am Heart Assoc *3*, e000976.

Chang, C.P., and Bruneau, B.G. (2012). Epigenetics and cardiovascular development. Annual review of physiology *74*, 41-68.

Chang, S., McKinsey, T.A., Zhang, C.L., Richardson, J.A., Hill, J.A., and Olson, E.N. (2004). Histone deacetylases 5 and 9 govern responsiveness of the heart to a subset of stress signals and play redundant roles in heart development. Mol Cell Biol *24*, 8467-8476.

Chao, W., and D'Amore, P.A. (2008). IGF2: epigenetic regulation and role in development and disease. Cytokine Growth Factor Rev *19*, 111-120.

Chaudhry, H.W., Dashoush, N.H., Tang, H., Zhang, L., Wang, X., Wu, E.X., and Wolgemuth, D.J. (2004). Cyclin A2 mediates cardiomyocyte mitosis in the postmitotic myocardium. The Journal of biological chemistry *279*, 35858-35866.

Chen, J., Huang, Z.P., Seok, H.Y., Ding, J., Kataoka, M., Zhang, Z., Hu, X., Wang, G., Lin, Z., Wang, S., *et al.* (2013). mir-17-92 cluster is required for and sufficient to induce cardiomyocyte proliferation in postnatal and adult hearts. Circulation research *112*, 1557-1566.

Chen, L., Ma, Y., Kim, E.Y., Yu, W., Schwartz, R.J., Qian, L., and Wang, J. (2012). Conditional ablation of Ezh2 in murine hearts reveals its essential roles in endocardial cushion formation, cardiomyocyte proliferation and survival. PloS one *7*, e31005.

Chen, T., and Dent, S.Y. (2014). Chromatin modifiers and remodellers: regulators of cellular differentiation. Nature reviews Genetics *15*, 93-106.

Cheng, H.L., Mostoslavsky, R., Saito, S., Manis, J.P., Gu, Y., Patel, P., Bronson, R., Appella, E., Alt, F.W., and Chua, K.F. (2003). Developmental defects and p53 hyperacetylation in Sir2 homolog (SIRT1)-deficient mice. Proceedings of the National Academy of Sciences of the United States of America *100*, 10794-10799.

Cheng, Y., Ma, Z., Kim, B.H., Wu, W., Cayting, P., Boyle, A.P., Sundaram, V., Xing, X., Dogan, N., Li, J., *et al.* (2014). Principles of regulatory information conservation between mouse and human. Nature *515*, 371-375.

Chernoff, J. (1999). Protein tyrosine phosphatases as negative regulators of mitogenic signaling. Journal of cellular physiology *180*, 173-181.

Cho, H.S., Hayami, S., Toyokawa, G., Maejima, K., Yamane, Y., Suzuki, T., Dohmae, N., Kogure, M., Kang, D., Neal, D.E., *et al.* (2012). RB1 methylation by SMYD2 enhances cell cycle progression through an increase of RB1 phosphorylation. Neoplasia *14*, 476-486.

Choi, S.W., and Friso, S. (2010). Epigenetics: A New Bridge between Nutrition and Health. Adv Nutr *1*, 8-16.

Choi, W.Y., Gemberling, M., Wang, J., Holdway, J.E., Shen, M.C., Karlstrom, R.O., and Poss, K.D. (2013). In vivo monitoring of cardiomyocyte proliferation to identify chemical modifiers of heart regeneration. Development (Cambridge, England) *140*, 660-666.

Choi, W.Y., and Poss, K.D. (2012). Cardiac regeneration. Current topics in developmental biology *100*, 319-344.

Chong, J.J., Chandrakanthan, V., Xaymardan, M., Asli, N.S., Li, J., Ahmed, I., Heffernan, C., Menon, M.K., Scarlett, C.J., Rashidianfar, A., *et al.* (2011). Adult cardiac-resident MSC-like stem cells with a proepicardial origin. Cell stem cell *9*, 527-540.

Chong, J.J., Yang, X., Don, C.W., Minami, E., Liu, Y.W., Weyers, J.J., Mahoney, W.M., Van Biber, B., Cook, S.M., Palpant, N.J., *et al.* (2014). Human embryonic-stem-cell-derived cardiomyocytes regenerate non-human primate hearts. Nature *510*, 273-277.

Chou, C.P., Huang, N.C., Jhuang, S.J., Pan, H.B., Peng, N.J., Cheng, J.T., Chen, C.F., Chen, J.J., and Chang, T.H. (2014). Ubiquitin-conjugating enzyme UBE2C is highly expressed in breast microcalcification lesions. PloS one *9*, e93934.

Christman, J.K. (2002). 5-Azacytidine and 5-aza-2'-deoxycytidine as inhibitors of DNA methylation: mechanistic studies and their implications for cancer therapy. Oncogene *21*, 5483-5495.

Citro, L., Naidu, S., Hassan, F., Kuppusamy, M.L., Kuppusamy, P., Angelos, M.G., and Khan, M. (2014). Comparison of human induced pluripotent stem-cell derived cardiomyocytes with human mesenchymal stem cells following acute myocardial infarction. PloS one *9*, e116281.

Consortium, E.P. (2012). An integrated encyclopedia of DNA elements in the human genome. Nature *489*, 57-74.

Coulombe, K.L., Bajpai, V.K., Andreadis, S.T., and Murry, C.E. (2014). Heart regeneration with engineered myocardial tissue. Annu Rev Biomed Eng *16*, 1-28.

Cruickshanks, H.A., McBryan, T., Nelson, D.M., Vanderkraats, N.D., Shah, P.P., van Tuyn, J., Singh Rai, T., Brock, C., Donahue, G., Dunican, D.S., *et al.* (2013). Senescent cells harbour features of the cancer epigenome. Nature cell biology *15*, 1495-1506.

Cusanovich, D.A., Daza, R., Adey, A., Pliner, H.A., Christiansen, L., Gunderson, K.L., Steemers, F.J., Trapnell, C., and Shendure, J. (2015). Multiplex single cell profiling of chromatin accessibility by combinatorial cellular indexing. Science (New York, NY) *348*, 910-914.

D'Uva, G., Aharonov, A., Lauriola, M., Kain, D., Yahalom-Ronen, Y., Carvalho, S., Weisinger, K., Bassat, E., Rajchman, D., Yifa, O., *et al.* (2015). ERBB2 triggers mammalian heart regeneration by promoting cardiomyocyte dedifferentiation and proliferation. Nature cell biology *17*, 627-638.

Darehzereshki, A., Rubin, N., Gamba, L., Kim, J., Fraser, J., Huang, Y., Billings, J., Mohammadzadeh, R., Wood, J., Warburton, D., *et al.* (2015). Differential regenerative capacity of neonatal mouse hearts after cryoinjury. Developmental biology *399*, 91-99.

Davidson, G., Shen, J., Huang, Y.L., Su, Y., Karaulanov, E., Bartscherer, K., Hassler, C., Stannek, P., Boutros, M., and Niehrs, C. (2009). Cell cycle control of wnt receptor activation. Developmental cell *17*, 788-799.

Davis, R.L., Weintraub, H., and Lassar, A.B. (1987). Expression of a single transfected cDNA converts fibroblasts to myoblasts. Cell *51*, 987-1000.

Delgado-Olguin, P., Huang, Y., Li, X., Christodoulou, D., Seidman, C.E., Seidman, J.G., Tarakhovsky, A., and Bruneau, B.G. (2012). Epigenetic repression of cardiac progenitor gene expression by Ezh2 is required for postnatal cardiac homeostasis. Nat Genet *44*, 343-347.

Denny, S.K., Yang, D., Chuang, C.H., Brady, J.J., Lim, J.S., Gruner, B.M., Chiou, S.H., Schep, A.N., Baral, J., Hamard, C., *et al.* (2016). Nfib Promotes Metastasis through a Widespread Increase in Chromatin Accessibility. Cell *166*, 328-342.

Derrien, T., Johnson, R., Bussotti, G., Tanzer, A., Djebali, S., Tilgner, H., Guernec, G., Martin, D., Merkel, A., Knowles, D.G., *et al.* (2012). The GENCODE v7 catalog of human long noncoding RNAs: analysis of their gene structure, evolution, and expression. Genome research *22*, 1775-1789.

DeSantis, C., Ma, J., Bryan, L., and Jemal, A. (2014). Breast cancer statistics, 2013. CA Cancer J Clin *64*, 52-62.

Di Ruscio, A., Ebralidze, A.K., Benoukraf, T., Amabile, G., Goff, L.A., Terragni, J., Figueroa, M.E., De Figueiredo Pontes, L.L., Alberich-Jorda, M., Zhang, P., *et al.* (2013). DNMT1-interacting RNAs block gene-specific DNA methylation. Nature *503*, 371-376.

Di Stefano, V., Giacca, M., Capogrossi, M.C., Crescenzi, M., and Martelli, F. (2011). Knockdown of cyclin-dependent kinase inhibitors induces cardiomyocyte re-entry in the cell cycle. The Journal of biological chemistry *286*, 8644-8654.

Djebali, S., Davis, C.A., Merkel, A., Dobin, A., Lassmann, T., Mortazavi, A., Tanzer, A., Lagarde, J., Lin, W., Schlesinger, F., *et al.* (2012). Landscape of transcription in human cells. Nature *489*, 101-108.

Dobin, A., Davis, C.A., Schlesinger, F., Drenkow, J., Zaleski, C., Jha, S., Batut, P., Chaisson, M., and Gingeras, T.R. (2013). STAR: ultrafast universal RNA-seq aligner. Bioinformatics *29*, 15-21.

Drenckhahn, J.D., Schwarz, Q.P., Gray, S., Laskowski, A., Kiriazis, H., Ming, Z., Harvey, R.P., Du, X.J., Thorburn, D.R., and Cox, T.C. (2008). Compensatory growth of healthy cardiac cells in the presence of diseased cells restores tissue homeostasis during heart development. Developmental cell *15*, 521-533.

Ebelt, H., Liu, Z., Muller-Werdan, U., Werdan, K., and Braun, T. (2006). Making omelets without breaking eggs: E2F-mediated induction of cardiomyoycte cell proliferation without stimulation of apoptosis. Cell cycle (Georgetown, Tex) *5*, 2436-2439.

Ebelt, H., Zhang, Y., Kampke, A., Xu, J., Schlitt, A., Buerke, M., Muller-Werdan, U., Werdan, K., and Braun, T. (2008). E2F2 expression induces proliferation of terminally differentiated cardiomyocytes in vivo. Cardiovascular research *80*, 219-226.

Efroni, S., Duttagupta, R., Cheng, J., Dehghani, H., Hoeppner, D.J., Dash, C., Bazett-Jones, D.P., Le Grice, S., McKay, R.D.G., Buetow, K.H., *et al.* (2008). Global transcription in pluripotent embryonic stem cells. Cell stem cell *2*, 437-447.

Ehrlich, M. (2002). DNA methylation in cancer: too much, but also too little. Oncogene *21*, 5400-5413.

Ellison, G.M., Vicinanza, C., Smith, A.J., Aquila, I., Leone, A., Waring, C.D., Henning, B.J., Stirparo, G.G., Papait, R., Scarfo, M., *et al.* (2013). Adult c-kit(pos) cardiac stem cells are necessary and sufficient for functional cardiac regeneration and repair. Cell *154*, 827-842.

Engel, F.B., Hsieh, P.C., Lee, R.T., and Keating, M.T. (2006). FGF1/p38 MAP kinase inhibitor therapy induces cardiomyocyte mitosis, reduces scarring, and rescues function after myocardial infarction. Proceedings of the National Academy of Sciences of the United States of America *103*, 15546-15551.

Ennajdaoui, H., Howard, J.M., Sterne-Weiler, T., Jahanbani, F., Coyne, D.J., Uren, P.J., Dargyte, M., Katzman, S., Draper, J.M., Wallace, A., *et al.* (2016). IGF2BP3 Modulates the Interaction of Invasion-Associated Transcripts with RISC. Cell reports *15*, 1876-1883.

Eschenhagen, T., Fink, C., Remmers, U., Scholz, H., Wattchow, J., Weil, J., Zimmermann, W., Dohmen, H.H., Schafer, H., Bishopric, N., *et al.* (1997). Three-dimensional reconstitution of embryonic cardiomyocytes in a collagen matrix: a new heart muscle model system. FASEB journal : official publication of the Federation of American Societies for Experimental Biology *11*, 683-694.

Eulalio, A., Mano, M., Dal Ferro, M., Zentilin, L., Sinagra, G., Zacchigna, S., and Giacca, M. (2012). Functional screening identifies miRNAs inducing cardiac regeneration. Nature *492*, 376-381.

Evans-Anderson, H.J., Alfieri, C.M., and Yutzey, K.E. (2008). Regulation of cardiomyocyte proliferation and myocardial growth during development by FOXO transcription factors. Circulation research *102*, 686-694.

Fang, X., Poulsen, R.R., Wang-Hu, J., Shi, O., Calvo, N.S., Simmons, C.S., Rivkees, S.A., and Wendler, C.C. (2016). Knockdown of DNA methyltransferase 3a alters gene expression and inhibits function of embryonic cardiomyocytes. FASEB journal : official publication of the Federation of American Societies for Experimental Biology.

Felician, G., Collesi, C., Lusic, M., Martinelli, V., Dal Ferro, M., Zentilin, L., Zacchigna, S., and Giacca, M. (2014a). Epigenetic Modification at Notch Responsive Promoters Blunts Efficacy of Inducing Notch Pathway Reactivation After Myocardial Infarction. Circulation research.

Felician, G., Collesi, C., Lusic, M., Martinelli, V., Ferro, M.D., Zentilin, L., Zacchigna, S., and Giacca, M. (2014b). Epigenetic modification at notch responsive promoters blunts efficacy of inducing notch pathway reactivation after myocardial infarction. Circ Res *115*, 636-649.

Figueroa, M.E., Abdel-Wahab, O., Lu, C., Ward, P.S., Patel, J., Shih, A., Li, Y., Bhagwat, N., Vasanthakumar, A., Fernandez, H.F., *et al.* (2010). Leukemic IDH1 and IDH2 mutations result in a hypermethylation phenotype, disrupt TET2 function, and impair hematopoietic differentiation. Cancer cell *18*, 553-567.

Filtz, T.M., Vogel, W.K., and Leid, M. (2014). Regulation of transcription factor activity by interconnected post-translational modifications. Trends Pharmacol Sci *35*, 76-85.

Finkel, T., and Holbrook, N.J. (2000). Oxidants, oxidative stress and the biology of ageing. Nature *408*, 239-247.

Flink, I.L. (2002). Cell cycle reentry of ventricular and atrial cardiomyocytes and cells within the epicardium following amputation of the ventricular apex in the axolotl, Amblystoma mexicanum: confocal microscopic immunofluorescent image analysis of bromodeoxyuridine-labeled nuclei. Anat Embryol (Berl) *205*, 235-244.

Franco, R., Schoneveld, O., Georgakilas, A.G., and Panayiotidis, M.I. (2008). Oxidative stress, DNA methylation and carcinogenesis. Cancer letters *266*, 6-11.

Fratz, S., Hager, A., Schreiber, C., Schwaiger, M., Hess, J., and Stern, H.C. (2011). Long-term myocardial scarring after operation for anomalous left coronary artery from the pulmonary artery. Ann Thorac Surg *92*, 1761-1765.

Fujita, N., Jaye, D.L., Geigerman, C., Akyildiz, A., Mooney, M.R., Boss, J.M., and Wade, P.A. (2004). MTA3 and the Mi-2/NuRD complex regulate cell fate during B lymphocyte differentiation. Cell *119*, 75-86.

Fujita, N., Jaye, D.L., Kajita, M., Geigerman, C., Moreno, C.S., and Wade, P.A. (2003). MTA3, a Mi-2/NuRD complex subunit, regulates an invasive growth pathway in breast cancer. Cell *113*, 207-219.

Funakoshi, S., Miki, K., Takaki, T., Okubo, C., Hatani, T., Chonabayashi, K., Nishikawa, M., Takei, I., Oishi, A., Narita, M., *et al.* (2016). Enhanced engraftment, proliferation, and therapeutic potential in heart using optimized human iPSC-derived cardiomyocytes. Scientific reports *6*, 19111.

Furey, T.S. (2012). ChIP-seq and beyond: new and improved methodologies to detect and characterize protein-DNA interactions. Nature reviews Genetics *13*, 840-852.

Gao, X., and Locasale, J.W. (2016). Serine Metabolism Links Tumor Suppression to the Epigenetic Landscape. Cell Metab *24*, 777-779.

Garbern, J.C., and Lee, R.T. (2013). Cardiac stem cell therapy and the promise of heart regeneration. Cell stem cell *12*, 689-698.

Gatto, F., Nookaew, I., and Nielsen, J. (2014). Chromosome 3p loss of heterozygosity is associated with a unique metabolic network in clear cell renal carcinoma. Proceedings of the National Academy of Sciences of the United States of America *111*, E866-875.

Gaulton, K.J., Nammo, T., Pasquali, L., Simon, J.M., Giresi, P.G., Fogarty, M.P., Panhuis, T.M., Mieczkowski, P., Secchi, A., Bosco, D., *et al.* (2010). A map of open chromatin in human pancreatic islets. Nature genetics *42*, 255-259.

Gay, M.S., Dasgupta, C., Li, Y., Kanna, A., and Zhang, L. (2016). Dexamethasone Induces Cardiomyocyte Terminal Differentiation via Epigenetic Repression of Cyclin D2 Gene. J Pharmacol Exp Ther *358*, 190-198.

Gerbin, K.A., and Murry, C.E. (2015). The winding road to regenerating the human heart. Cardiovascular pathology : the official journal of the Society for Cardiovascular Pathology *24*, 133-140.

Gerstein, M.B., Kundaje, A., Hariharan, M., Landt, S.G., Yan, K.K., Cheng, C., Mu, X.J., Khurana, E., Rozowsky, J., Alexander, R., *et al.* (2012). Architecture of the human regulatory network derived from ENCODE data. Nature *489*, 91-100.

Gifford, C.A., Ziller, M.J., Gu, H., Trapnell, C., Donaghey, J., Tsankov, A., Shalek, A.K., Kelley, D.R., Shishkin, A.A., Issner, R., *et al.* (2013). Transcriptional and epigenetic dynamics during specification of human embryonic stem cells. Cell *153*, 1149-1163.

Gillette, T.G., and Hill, J.A. (2015). Readers, writers, and erasers: chromatin as the whiteboard of heart disease. Circulation research *116*, 1245-1253.

Gilsbach, R., Preissl, S., Gruning, B.A., Schnick, T., Burger, L., Benes, V., Wurch, A., Bonisch, U., Gunther, S., Backofen, R., *et al.* (2014). Dynamic DNA methylation orchestrates cardiomyocyte development, maturation and disease. Nature communications *5*, 5288.

Girard, J., Ferre, P., Pegorier, J.P., and Duee, P.H. (1992). Adaptations of glucose and fatty acid metabolism during perinatal period and suckling-weaning transition. Physiological reviews *72*, 507-562.

Gomez, N.C., Hepperla, A.J., Dumitru, R., Simon, J.M., Fang, F., and Davis, I.J. (2016). Widespread Chromatin Accessibility at Repetitive Elements Links Stem Cells with Human Cancer. Cell reports *17*, 1607-1620.

Gonzalez-Rosa, J.M., Martin, V., Peralta, M., Torres, M., and Mercader, N. (2011). Extensive scar formation and regression during heart regeneration after cryoinjury in zebrafish. Development (Cambridge, England) *138*, 1663-1674.

Gottlieb, P.D., Pierce, S.A., Sims, R.J., Yamagishi, H., Weihe, E.K., Harriss, J.V., Maika, S.D., Kuziel, W.A., King, H.L., Olson, E.N., *et al.* (2002). Bop encodes a muscle-restricted protein containing MYND and SET domains and is essential for cardiac differentiation and morphogenesis. Nature genetics *31*, 25-32.

Grote, P., Wittler, L., Hendrix, D., Koch, F., Wahrisch, S., Beisaw, A., Macura, K., Blass, G., Kellis, M., Werber, M., *et al.* (2013). The tissue-specific lncRNA Fendrr is an essential regulator of heart and body wall development in the mouse. Dev Cell *24*, 206-214.

Gruneberg, U., Neef, R., Li, X., Chan, E.H., Chalamalasetty, R.B., Nigg, E.A., and Barr, F.A. (2006). KIF14 and citron kinase act together to promote efficient cytokinesis. The Journal of cell biology *172*, 363-372.

Gurdon, J.B., Elsdale, T.R., and Fischberg, M. (1958). Sexually mature individuals of Xenopus laevis from the transplantation of single somatic nuclei. Nature *182*, 64-65.

Haas, J., Frese, K.S., Park, Y.J., Keller, A., Vogel, B., Lindroth, A.M., Weichenhan, D., Franke, J., Fischer, S., Bauer, A., *et al.* (2013). Alterations in cardiac DNA methylation in human dilated cardiomyopathy. EMBO molecular medicine *5*, 413-429.

Hagege, A.A., Carrion, C., Menasche, P., Vilquin, J.T., Duboc, D., Marolleau, J.P., Desnos, M., and Bruneval, P. (2003). Viability and differentiation of autologous skeletal myoblast grafts in ischaemic cardiomyopathy. Lancet *361*, 491-492.

Haider, S., Cordeddu, L., Robinson, E., Movassagh, M., Siggens, L., Vujic, A., Choy, M.K., Goddard, M., Lio, P., and Foo, R. (2012). The landscape of DNA repeat elements in human heart failure. Genome biology *13*, R90.

Han, P., Hang, C.T., Yang, J., and Chang, C.P. (2011). Chromatin remodeling in cardiovascular development and physiology. Circ Res *108*, 378-396.

Han, P., Li, W., Yang, J., Shang, C., Lin, C.H., Cheng, W., Hang, C.T., Cheng, H.L., Chen, C.H., Wong, J., *et al.* (2016). Epigenetic response to environmental stress: Assembly of BRG1-G9a/GLP-DNMT3 repressive chromatin complex on Myh6 promoter in pathologically stressed hearts. Biochimica et biophysica acta *1863*, 1772-1781.

Hansen, A., Eder, A., Bonstrup, M., Flato, M., Mewe, M., Schaaf, S., Aksehirlioglu, B., Schwoerer, A.P., Uebeler, J., and Eschenhagen, T. (2010). Development of a drug screening platform based on engineered heart tissue. Circulation research *107*, 35-44.

Hansen, K.D., Timp, W., Bravo, H.C., Sabunciyan, S., Langmead, B., McDonald, O.G., Wen, B., Wu, H., Liu, Y., Diep, D., *et al.* (2011). Increased methylation variation in epigenetic domains across cancer types. Nature genetics *43*, 768-775.

Hao, Z., Zhang, H., and Cowell, J. (2012). Ubiquitin-conjugating enzyme UBE2C: molecular biology, role in tumorigenesis, and potential as a biomarker. Tumour biology : the journal of the International Society for Oncodevelopmental Biology and Medicine *33*, 723-730.

Harris, R.A., Wang, T., Coarfa, C., Nagarajan, R.P., Hong, C., Downey, S.L., Johnson, B.E., Fouse, S.D., Delaney, A., Zhao, Y., *et al.* (2010). Comparison of sequencing-based methods to profile DNA methylation and identification of monoallelic epigenetic modifications. Nature biotechnology *28*, 1097-1105.

Hatzistergos, K.E., Quevedo, H., Oskouei, B.N., Hu, Q., Feigenbaum, G.S., Margitich, I.S., Mazhari, R., Boyle, A.J., Zambrano, J.P., Rodriguez, J.E., *et al.* (2010). Bone marrow mesenchymal stem cells stimulate cardiac stem cell proliferation and differentiation. Circulation research *107*, 913-922.

Haubner, B.J., Adamowicz-Brice, M., Khadayate, S., Tiefenthaler, V., Metzler, B., Aitman, T., and Penninger, J.M. (2012). Complete cardiac regeneration in a mouse model of myocardial infarction. Aging (Albany NY) *4*, 966-977.

Haubner, B.J., Schneider, J., Schweigmann, U., Schuetz, T., Dichtl, W., Velik-Salchner, C., Stein, J.I., and Penninger, J.M. (2016). Functional Recovery of a Human Neonatal Heart After Severe Myocardial Infarction. Circulation research *118*, 216-221.

He, J., Kallin, E.M., Tsukada, Y., and Zhang, Y. (2008). The H3K36 demethylase Jhdm1b/Kdm2b regulates cell proliferation and senescence through p15(Ink4b). Nature structural & molecular biology *15*, 1169-1175.

Heallen, T., Zhang, M., Wang, J., Bonilla-Claudio, M., Klysik, E., Johnson, R.L., and Martin, J.F. (2011). Hippo pathway inhibits Wnt signaling to restrain cardiomyocyte proliferation and heart size. Science (New York, NY) *332*, 458-461.

Herrington, F.D., and Nibbs, R.J. (2016). Regulation of the Adaptive Immune Response by the IkappaB Family Protein Bcl-3. Cells *5*.

Hervouet, E., Vallette, F.M., and Cartron, P.F. (2009). Dnmt3/transcription factor interactions as crucial players in targeted DNA methylation. Epigenetics : official journal of the DNA Methylation Society *4*, 487-499.

Hirt, M.N., Hansen, A., and Eschenhagen, T. (2014). Cardiac tissue engineering: state of the art. Circulation research *114*, 354-367.

Hishida, T., Eguchi, T., Osada, S., Nishizuka, M., and Imagawa, M. (2008). A novel gene, fad49, plays a crucial role in the immediate early stage of adipocyte differentiation via involvement in mitotic clonal expansion. The FEBS journal *275*, 5576-5588.

Holmstrom, K.M., and Finkel, T. (2014). Cellular mechanisms and physiological consequences of redox-dependent signalling. Nature reviews Molecular cell biology *15*, 411-421.

Hong, S., Cho, Y.W., Yu, L.R., Yu, H., Veenstra, T.D., and Ge, K. (2007). Identification of JmjC domain-containing UTX and JMJD3 as histone H3 lysine 27 demethylases. Proceedings of the National Academy of Sciences of the United States of America *104*, 18439-18444.

Hong, S.H., Rampalli, S., Lee, J.B., McNicol, J., Collins, T., Draper, J.S., and Bhatia, M. (2011). Cell fate potential of human pluripotent stem cells is encoded by histone modifications. Cell stem cell *9*, 24-36.

Hsieh, P.C., Segers, V.F., Davis, M.E., MacGillivray, C., Gannon, J., Molkentin, J.D., Robbins, J., and Lee, R.T. (2007). Evidence from a genetic fate-mapping study that stem cells refresh adult mammalian cardiomyocytes after injury. Nature medicine *13*, 970-974.

Huang, J., Perez-Burgos, L., Placek, B.J., Sengupta, R., Richter, M., Dorsey, J.A., Kubicek, S., Opravil, S., Jenuwein, T., and Berger, S.L. (2006). Repression of p53 activity by Smyd2-mediated methylation. Nature *444*, 629-632.

Huang, S., Wang, C., Yi, Y., Sun, X., Luo, M., Zhou, Z., Li, J., Cai, Y., Jiang, X., and Ke, Y. (2015). Kruppel-like factor 9 inhibits glioma cell proliferation and tumorigenicity via downregulation of miR-21. Cancer letters *356*, 547-555.

Huang, Y., Harrison, M.R., Osorio, A., Kim, J., Baugh, A., Duan, C., Sucov, H.M., and Lien, C.L. (2013). Igf Signaling is Required for Cardiomyocyte Proliferation during Zebrafish Heart Development and Regeneration. PloS one *8*, e67266.

Hughes, J.R., Bullock, S.L., and Ish-Horowicz, D. (2004). Inscuteable mRNA localization is dynein-dependent and regulates apicobasal polarity and spindle length in Drosophila neuroblasts. Current biology : CB *14*, 1950-1956.

Ieda, M., Fu, J.D., Delgado-Olguin, P., Vedantham, V., Hayashi, Y., Bruneau, B.G., and Srivastava, D. (2010). Direct reprogramming of fibroblasts into functional cardiomyocytes by defined factors. Cell *142*, 375-386.

Islas, J.F., Liu, Y., Weng, K.C., Robertson, M.J., Zhang, S., Prejusa, A., Harger, J., Tikhomirova, D., Chopra, M., Iyer, D., *et al.* (2012). Transcription factors ETS2 and MESP1 transdifferentiate human dermal fibroblasts into cardiac progenitors. Proceedings of the National Academy of Sciences of the United States of America *109*, 13016-13021.

Issa, J.P. (2014). Aging and epigenetic drift: a vicious cycle. The Journal of clinical investigation *124*, 24-29.

James, S.J., Pogribny, I.P., Pogribna, M., Miller, B.J., Jernigan, S., and Melnyk, S. (2003). Mechanisms of DNA damage, DNA hypomethylation, and tumor progression in the folate/methyl-deficient rat model of hepatocarcinogenesis. The Journal of nutrition *133*, 3740S-3747S.

Jayawardena, T.M., Egemnazarov, B., Finch, E.A., Zhang, L., Payne, J.A., Pandya, K., Zhang, Z., Rosenberg, P., Mirotsou, M., and Dzau, V.J. (2012). MicroRNA-mediated in vitro and in vivo direct reprogramming of cardiac fibroblasts to cardiomyocytes. Circ Res *110*, 1465-1473.

Jeltsch, A., and Jurkowska, R.Z. (2014). New concepts in DNA methylation. Trends in biochemical sciences *39*, 310-318.

Jeong, H.Y., Kang, W.S., Hong, M.H., Jeong, H.C., Shin, M.G., Jeong, M.H., Kim, Y.S., and Ahn, Y. (2015). 5-Azacytidine modulates interferon regulatory factor 1 in macrophages to exert a cardioprotective effect. Scientific reports *5*, 15768.

Jiang, H., Lei, R., Ding, S.W., and Zhu, S. (2014). Skewer: a fast and accurate adapter trimmer for next-generation sequencing paired-end reads. BMC bioinformatics *15*, 182.

Jjingo, D., Conley, A.B., Yi, S.V., Lunyak, V.V., and Jordan, I.K. (2012). On the presence and role of human gene-body DNA methylation. Oncotarget *3*, 462-474.

Jones, B., Su, H., Bhat, A., Lei, H., Bajko, J., Hevi, S., Baltus, G.A., Kadam, S., Zhai, H., Valdez, R., *et al.* (2008). The histone H3K79 methyltransferase Dot1L is essential for mammalian development and heterochromatin structure. PLoS genetics *4*, e1000190.

Jones, P.A. (2012). Functions of DNA methylation: islands, start sites, gene bodies and beyond. Nat Rev Genet *13*, 484-492.

Jopling, C., Sleep, E., Raya, M., Marti, M., Raya, A., and Izpisua Belmonte, J.C. (2010). Zebrafish heart regeneration occurs by cardiomyocyte dedifferentiation and proliferation. Nature *464*, 606-609.

Jung, J., Kim, T.G., Lyons, G.E., Kim, H.R., and Lee, Y. (2005). Jumonji regulates cardiomyocyte proliferation via interaction with retinoblastoma protein. J Biol Chem *280*, 30916-30923.

Kaikkonen, M.U., Spann, N.J., Heinz, S., Romanoski, C.E., Allison, K.A., Stender, J.D., Chun, H.B., Tough, D.F., Prinjha, R.K., Benner, C., *et al.* (2013). Remodeling of the enhancer landscape during macrophage activation is coupled to enhancer transcription. Molecular cell *51*, 310-325.

Kajstura, J., Gurusamy, N., Ogorek, B., Goichberg, P., Clavo-Rondon, C., Hosoda, T., D'Amario, D., Bardelli, S., Beltrami, A.P., Cesselli, D., *et al.* (2010). Myocyte turnover in the aging human heart. Circulation research *107*, 1374-1386.

Karahoca, M., and Momparler, R.L. (2013). Pharmacokinetic and pharmacodynamic analysis of 5-aza-2'-deoxycytidine (decitabine) in the design of its dose-schedule for cancer therapy. Clinical epigenetics *5*, 3.

Katzberg, A.A., Farmer, B.B., and Harris, R.A. (1977). The predominance of binucleation in isolated rat heart myocytes. The American journal of anatomy *149*, 489-499.

Keating, S.T., and El-Osta, A. (2015). Epigenetics and metabolism. Circulation research *116*, 715-736.

Kehat, I., Kenyagin-Karsenti, D., Snir, M., Segev, H., Amit, M., Gepstein, A., Livne, E., Binah, O., Itskovitz-Eldor, J., and Gepstein, L. (2001). Human embryonic stem cells can differentiate into myocytes with structural and functional properties of cardiomyocytes. The Journal of clinical investigation *108*, 407-414.

Kieffer-Kwon, K.R., Tang, Z., Mathe, E., Qian, J., Sung, M.H., Li, G., Resch, W., Baek, S., Pruett, N., Grontved, L., *et al.* (2013). Interactome maps of mouse gene regulatory domains reveal basic principles of transcriptional regulation. Cell *155*, 1507-1520.

Kikuchi, K., Holdway, J.E., Major, R.J., Blum, N., Dahn, R.D., Begemann, G., and Poss, K.D. (2011). Retinoic acid production by endocardium and epicardium is an injury response essential for zebrafish heart regeneration. Developmental cell *20*, 397-404.

Kikuchi, K., Holdway, J.E., Werdich, A.A., Anderson, R.M., Fang, Y., Egnaczyk, G.F., Evans, T., Macrae, C.A., Stainier, D.Y., and Poss, K.D. (2010). Primary contribution to zebrafish heart regeneration by gata4(+) cardiomyocytes. Nature *464*, 601-605.

Kim, H.S., Kim, D.C., Kim, H.M., Kwon, H.J., Kwon, S.J., Kang, S.J., Kim, S.C., and Choi, G.E. (2015). STAT1 deficiency redirects IFN signalling toward suppression of TLR response through a feedback activation of STAT3. Scientific reports *5*, 13414.

Kim, M., Long, T.I., Arakawa, K., Wang, R., Yu, M.C., and Laird, P.W. (2010). DNA methylation as a biomarker for cardiovascular disease risk. PloS one *5*, e9692.

Kim, Y.S., Kang, W.S., Kwon, J.S., Hong, M.H., Jeong, H.Y., Jeong, H.C., Jeong, M.H., and Ahn, Y. (2014). Protective role of 5-azacytidine on myocardial infarction is associated with modulation of macrophage phenotype and inhibition of fibrosis. Journal of cellular and molecular medicine *18*, 1018-1027.

Kimura, W., Xiao, F., Canseco, D.C., Muralidhar, S., Thet, S., Zhang, H.M., Abderrahman, Y., Chen, R., Garcia, J.A., Shelton, J.M., *et al.* (2015). Hypoxia fate mapping identifies cycling cardiomyocytes in the adult heart. Nature *523*, 226-230.

Koche, R.P., Smith, Z.D., Adli, M., Gu, H., Ku, M., Gnirke, A., Bernstein, B.E., and Meissner, A. (2011). Reprogramming factor expression initiates widespread targeted chromatin remodeling. Cell stem cell *8*, 96-105.

Koentges, C., Pfeil, K., Schnick, T., Wiese, S., Dahlbock, R., Cimolai, M.C., Meyer-Steenbuck, M., Cenkerova, K., Hoffmann, M.M., Jaeger, C., *et al.* (2015). SIRT3 deficiency impairs mitochondrial and contractile function in the heart. Basic research in cardiology *110*, 36.

Kohli, R.M., and Zhang, Y. (2013). TET enzymes, TDG and the dynamics of DNA demethylation. Nature *502*, 472-479.

Korswagen, H.C. (2006). Regulation of the Wnt/beta-catenin pathway by redox signaling. Developmental cell *10*, 687-688.

Kou, C.Y., Lau, S.L., Au, K.W., Leung, P.Y., Chim, S.S., Fung, K.P., Waye, M.M., and Tsui, S.K. (2010). Epigenetic regulation of neonatal cardiomyocytes differentiation. Biochemical and biophysical research communications *400*, 278-283.

Kubin, T., Poling, J., Kostin, S., Gajawada, P., Hein, S., Rees, W., Wietelmann, A., Tanaka, M., Lorchner, H., Schimanski, S., *et al.* (2011). Oncostatin M is a major mediator of cardiomyocyte dedifferentiation and remodeling. Cell stem cell *9*, 420-432.

Laflamme, M.A., Chen, K.Y., Naumova, A.V., Muskheli, V., Fugate, J.A., Dupras, S.K., Reinecke, H., Xu, C., Hassanipour, M., Police, S., *et al.* (2007). Cardiomyocytes derived from human embryonic stem cells in pro-survival factors enhance function of infarcted rat hearts. Nature biotechnology *25*, 1015-1024.

Laflamme, M.A., and Murry, C.E. (2011). Heart regeneration. Nature *473*, 326-335.

Lai, F., Orom, U.A., Cesaroni, M., Beringer, M., Taatjes, D.J., Blobel, G.A., and Shiekhattar, R. (2013). Activating RNAs associate with Mediator to enhance chromatin architecture and transcription. Nature *494*, 497-501.

Lander, E.S., Linton, L.M., Birren, B., Nusbaum, C., Zody, M.C., Baldwin, J., Devon, K., Dewar, K., Doyle, M., FitzHugh, W., *et al.* (2001). Initial sequencing and analysis of the human genome. Nature *409*, 860-921.

Laugwitz, K.L., Moretti, A., Caron, L., Nakano, A., and Chien, K.R. (2008). Islet1 cardiovascular progenitors: a single source for heart lineages? Development *135*, 193-205.

Laurent, L., Wong, E., Li, G., Huynh, T., Tsirigos, A., Ong, C.T., Low, H.M., Kin Sung, K.W., Rigoutsos, I., Loring, J., *et al.* (2010). Dynamic changes in the human methylome during differentiation. Genome Res *20*, 320-331.

Lederer, M., Bley, N., Schleifer, C., and Huttelmaier, S. (2014). The role of the oncofetal IGF2 mRNA-binding protein 3 (IGF2BP3) in cancer. Semin Cancer Biol *29*, 3-12.

Lee, S., Lee, J.W., and Lee, S.K. (2012). UTX, a histone H3-lysine 27 demethylase, acts as a critical switch to activate the cardiac developmental program. Dev Cell *22*, 25-37.

Leistner, D.M., Fischer-Rasokat, U., Honold, J., Seeger, F.H., Schachinger, V., Lehmann, R., Martin, H., Burck, I., Urbich, C., Dimmeler, S., *et al.* (2011). Transplantation of progenitor cells and regeneration enhancement in acute myocardial infarction (TOPCARE-AMI): final 5-year results suggest long-term safety and efficacy. Clin Res Cardiol *100*, 925-934.

Leja, M.J., Shah, D.J., and Reardon, M.J. (2011). Primary cardiac tumors. Tex Heart Inst J *38*, 261-262.

Leobon, B., Garcin, I., Menasche, P., Vilquin, J.T., Audinat, E., and Charpak, S. (2003). Myoblasts transplanted into rat infarcted myocardium are functionally isolated from their host. Proceedings of the National Academy of Sciences of the United States of America *100*, 7808-7811.

Lepilina, A., Coon, A.N., Kikuchi, K., Holdway, J.E., Roberts, R.W., Burns, C.G., and Poss, K.D. (2006). A dynamic epicardial injury response supports progenitor cell activity during zebrafish heart regeneration. Cell *127*, 607-619.

Li, B., Carey, M., and Workman, J.L. (2007). The role of chromatin during transcription. Cell *128*, 707-719.

Li, E., Bestor, T.H., and Jaenisch, R. (1992). Targeted mutation of the DNA methyltransferase gene results in embryonic lethality. Cell *69*, 915-926.

Li, F., Wang, X., Capasso, J.M., and Gerdes, A.M. (1996). Rapid transition of cardiac myocytes from hyperplasia to hypertrophy during postnatal development. Journal of molecular and cellular cardiology *28*, 1737-1746.

Li, H., and Durbin, R. (2009). Fast and accurate short read alignment with Burrows-Wheeler transform. Bioinformatics *25*, 1754-1760.

Li, M., Naqvi, N., Yahiro, E., Liu, K., Powell, P.C., Bradley, W.E., Martin, D.I., Graham, R.M., Dell'Italia, L.J., and Husain, A. (2008). c-kit is required for cardiomyocyte terminal differentiation. Circulation research *102*, 677-685.

Li, R.K., Jia, Z.Q., Weisel, R.D., Mickle, D.A., Choi, A., and Yau, T.M. (1999). Survival and function of bioengineered cardiac grafts. Circulation *100*, II63-69.

Li, W., Notani, D., Ma, Q., Tanasa, B., Nunez, E., Chen, A.Y., Merkurjev, D., Zhang, J., Ohgi, K., Song, X., *et al.* (2013). Functional roles of enhancer RNAs for oestrogen-dependent transcriptional activation. Nature *498*, 516-520.

Li, Z., Gilbert, J.A., Zhang, Y., Zhang, M., Qiu, Q., Ramanujan, K., Shavlakadze, T., Eash, J.K., Scaramozza, A., Goddeeris, M.M., *et al.* (2012). An HMGA2-IGF2BP2 axis regulates myoblast proliferation and myogenesis. Developmental cell *23*, 1176-1188.

Liao, Y., Smyth, G.K., and Shi, W. (2014). featureCounts: an efficient general purpose program for assigning sequence reads to genomic features. Bioinformatics *30*, 923-930.

Lickert, H., Takeuchi, J.K., Von Both, I., Walls, J.R., McAuliffe, F., Adamson, S.L., Henkelman, R.M., Wrana, J.L., Rossant, J., and Bruneau, B.G. (2004). Baf60c is essential for function of BAF chromatin remodelling complexes in heart development. Nature *432*, 107-112.

Lister, R., Mukamel, E.A., Nery, J.R., Urich, M., Puddifoot, C.A., Johnson, N.D., Lucero, J., Huang, Y., Dwork, A.J., Schultz, M.D., *et al.* (2013). Global epigenomic reconfiguration during mammalian brain development. Science (New York, NY) *341*, 1237905.

Lister, R., Pelizzola, M., Dowen, R.H., Hawkins, R.D., Hon, G., Tonti-Filippini, J., Nery, J.R., Lee, L., Ye, Z., Ngo, Q.M., *et al.* (2009). Human DNA methylomes at base resolution show widespread epigenomic differences. Nature *462*, 315-322.

Liu, D., Kang, J.S., and Derynck, R. (2004). TGF-beta-activated Smad3 represses MEF2-dependent transcription in myogenic differentiation. The EMBO journal *23*, 1557-1566.

Liu, H., Di Cunto, F., Imarisio, S., and Reid, L.M. (2003). Citron kinase is a cell cycle-dependent, nuclear protein required for G2/M transition of hepatocytes. The Journal of biological chemistry *278*, 2541-2548.

Locasale, J.W. (2013). Serine, glycine and one-carbon units: cancer metabolism in full circle. Nat Rev Cancer *13*, 572-583.

Lu, J., McKinsey, T.A., Nicol, R.L., and Olson, E.N. (2000). Signal-dependent activation of the MEF2 transcription factor by dissociation from histone deacetylases. Proceedings of the National Academy of Sciences of the United States of America *97*, 4070-4075.

Lu, X., Tan, C.K., Zhou, J.Q., You, M., Carastro, L.M., Downey, K.M., and So, A.G. (2002). Direct interaction of proliferating cell nuclear antigen with the small subunit of DNA polymerase delta. The Journal of biological chemistry *277*, 24340-24345.

Luczak, M.W., and Jagodzinski, P.P. (2006). The role of DNA methylation in cancer development. Folia Histochem Cytobiol *44*, 143-154.

Macaluso, M., Cinti, C., Russo, G., Russo, A., and Giordano, A. (2003). pRb2/p130-E2F4/5-HDAC1-SUV39H1-p300 and pRb2/p130-E2F4/5-HDAC1-SUV39H1-DNMT1 multimolecular complexes mediate the transcription of estrogen receptor-alpha in breast cancer. Oncogene *22*, 3511-3517.

Maddocks, O.D., Labuschagne, C.F., Adams, P.D., and Vousden, K.H. (2016). Serine Metabolism Supports the Methionine Cycle and DNA/RNA Methylation through De Novo ATP Synthesis in Cancer Cells. Mol Cell *61*, 210-221.

Mak, I.W., Evaniew, N., and Ghert, M. (2014). Lost in translation: animal models and clinical trials in cancer treatment. American journal of translational research *6*, 114-118.

Makinde, A.O., Kantor, P.F., and Lopaschuk, G.D. (1998). Maturation of fatty acid and carbohydrate metabolism in the newborn heart. Molecular and cellular biochemistry *188*, 49-56.

Makkar, R.R., Smith, R.R., Cheng, K., Malliaras, K., Thomson, L.E., Berman, D., Czer, L.S., Marban, L., Mendizabal, A., Johnston, P.V., *et al.* (2012). Intracoronary cardiosphere-derived cells for heart regeneration after myocardial infarction (CADUCEUS): a prospective, randomised phase 1 trial. Lancet *379*, 895-904.

Mao, B., Gao, Y., Bai, Y., and Yuan, Z. (2015). Hippo signaling in stress response and homeostasis maintenance. Acta biochimica et biophysica Sinica *47*, 2-9.

Martin, C.M., Meeson, A.P., Robertson, S.M., Hawke, T.J., Richardson, J.A., Bates, S., Goetsch, S.C., Gallardo, T.D., and Garry, D.J. (2004). Persistent expression of the ATP-binding cassette transporter, Abcg2, identifies cardiac SP cells in the developing and adult heart. Developmental biology *265*, 262-275.

Mathers, C.D., and Loncar, D. (2006). Projections of global mortality and burden of disease from 2002 to 2030. PLoS medicine *3*, e442.

Matz, D.G., Oberpriller, J.O., and Oberpriller, J.C. (1998). Comparison of mitosis in binucleated and mononucleated newt cardiac myocytes. The Anatomical record *251*, 245-255.

Mazhari, R., and Hare, J.M. (2007). Advances in cell-based therapy for structural heart disease. Progress in cardiovascular diseases *49*, 387-395.

Meissner, A., Mikkelsen, T.S., Gu, H., Wernig, M., Hanna, J., Sivachenko, A., Zhang, X., Bernstein, B.E., Nusbaum, C., Jaffe, D.B., *et al.* (2008). Genome-scale DNA methylation maps of pluripotent and differentiated cells. Nature *454*, 766-770.

Menasche, P., Alfieri, O., Janssens, S., McKenna, W., Reichenspurner, H., Trinquart, L., Vilquin, J.T., Marolleau, J.P., Seymour, B., Larghero, J., *et al.* (2008). The Myoblast Autologous Grafting in Ischemic Cardiomyopathy (MAGIC) trial: first randomized placebo-controlled study of myoblast transplantation. Circulation *117*, 1189-1200.

Mirotsou, M., Zhang, Z., Deb, A., Zhang, L., Gnecchi, M., Noiseux, N., Mu, H., Pachori, A., and Dzau, V. (2007). Secreted frizzled related protein 2 (Sfrp2) is the key Akt-mesenchymal stem cell-released paracrine factor mediating myocardial survival and repair. Proceedings of the National Academy of Sciences of the United States of America *104*, 1643-1648.

Mollova, M., Bersell, K., Walsh, S., Savla, J., Das, L.T., Park, S.Y., Silberstein, L.E., Dos Remedios, C.G., Graham, D., Colan, S., *et al.* (2013). Cardiomyocyte proliferation contributes to heart growth in young humans. Proceedings of the National Academy of Sciences of the United States of America *110*, 1446-1451.

Monaco, G., van Dam, S., Casal Novo Ribeiro, J.L., Larbi, A., and de Magalhaes, J.P. (2015). A comparison of human and mouse gene co-expression networks reveals conservation and divergence at the tissue, pathway and disease levels. BMC Evol Biol *15*, 259.

Montgomery, R.L., Davis, C.A., Potthoff, M.J., Haberland, M., Fielitz, J., Qi, X., Hill, J.A., Richardson, J.A., and Olson, E.N. (2007). Histone deacetylases 1 and 2 redundantly regulate cardiac morphogenesis, growth, and contractility. Genes Dev *21*, 1790-1802.

Montgomery, R.L., Potthoff, M.J., Haberland, M., Qi, X., Matsuzaki, S., Humphries, K.M., Richardson, J.A., Bassel-Duby, R., and Olson, E.N. (2008). Maintenance of cardiac energy metabolism by histone deacetylase 3 in mice. J Clin Invest *118*, 3588-3597.

Movassagh, M., Choy, M.K., Goddard, M., Bennett, M.R., Down, T.A., and Foo, R.S. (2010). Differential DNA methylation correlates with differential expression of angiogenic factors in human heart failure. PloS one *5*, e8564.

Movassagh, M., Choy, M.K., Knowles, D.A., Cordeddu, L., Haider, S., Down, T., Siggens, L., Vujic, A., Simeoni, I., Penkett, C., *et al.* (2011). Distinct epigenomic features in end-stage failing human hearts. Circulation *124*, 2411-2422.

Murry, C.E., Soonpaa, M.H., Reinecke, H., Nakajima, H., Nakajima, H.O., Rubart, M., Pasumarthi, K.B., Virag, J.I., Bartelmez, S.H., Poppa, V., *et al.* (2004). Haematopoietic stem cells do not transdifferentiate into cardiac myocytes in myocardial infarcts. Nature *428*, 664-668.

Nam, Y.J., Song, K., Luo, X., Daniel, E., Lambeth, K., West, K., Hill, J.A., DiMaio, J.M., Baker, L.A., Bassel-Duby, R., *et al.* (2013). Reprogramming of human fibroblasts toward a cardiac fate. Proceedings of the National Academy of Sciences of the United States of America *110*, 5588-5593.

Naqvi, N., Li, M., Calvert, J.W., Tejada, T., Lambert, J.P., Wu, J., Kesteven, S.H., Holman, S.R., Matsuda, T., Lovelock, J.D., *et al.* (2014). A proliferative burst during preadolescence establishes the final cardiomyocyte number. Cell *157*, 795-807.

Necsulea, A., Soumillon, M., Warnefors, M., Liechti, A., Daish, T., Zeller, U., Baker, J.C., Grutzner, F., and Kaessmann, H. (2014). The evolution of lncRNA repertoires and expression patterns in tetrapods. Nature *505*, 635-640.

Nekrasova, T., and Minden, A. (2011). PAK4 is required for regulation of the cell-cycle regulatory protein p21, and for control of cell-cycle progression. Journal of cellular biochemistry *112*, 1795-1806.

Nekrasova, T., and Minden, A. (2012). Role for p21-activated kinase PAK4 in development of the mammalian heart. Transgenic Res *21*, 797-811.

Nguyen, A.T., Xiao, B., Neppl, R.L., Kallin, E.M., Li, J., Chen, T., Wang, D.Z., Xiao, X., and Zhang, Y. (2011). DOT1L regulates dystrophin expression and is critical for cardiac function. Genes & development *25*, 263-274.

Nguyen, B.D., Abbott, K.L., Potempa, K., Kobor, M.S., Archambault, J., Greenblatt, J., Legault, P., and Omichinski, J.G. (2003). NMR structure of a complex containing the TFIIF subunit RAP74 and the RNA polymerase II carboxyl-terminal domain phosphatase FCP1. Proceedings of the National Academy of Sciences of the United States of America *100*, 5688-5693.

Niehrs, C., and Schafer, A. (2012). Active DNA demethylation by Gadd45 and DNA repair. Trends in cell biology *22*, 220-227.

Nuhrenberg, T.G., Hammann, N., Schnick, T., Preissl, S., Witten, A., Stoll, M., Gilsbach, R., Neumann, F.J., and Hein, L. (2015). Cardiac Myocyte De Novo DNA Methyltransferases 3a/3b Are Dispensable for Cardiac Function and Remodeling after Chronic Pressure Overload in Mice. PloS one *10*, e0131019.

Oberpriller, J.O., and Oberpriller, J.C. (1974). Response of the adult newt ventricle to injury. The Journal of experimental zoology *187*, 249-253.

Oh, H., Bradfute, S.B., Gallardo, T.D., Nakamura, T., Gaussin, V., Mishina, Y., Pocius, J., Michael, L.H., Behringer, R.R., Garry, D.J., *et al.* (2003). Cardiac progenitor cells from adult myocardium: homing, differentiation, and fusion after infarction. Proceedings of the National Academy of Sciences of the United States of America *100*, 12313-12318.

Ohtani, K., Zhao, C., Dobreva, G., Manavski, Y., Kluge, B., Braun, T., Rieger, M.A., Zeiher, A.M., and Dimmeler, S. (2013). Jmjd3 controls mesodermal and cardiovascular differentiation of embryonic stem cells. Circulation research *113*, 856-862.

Okano, M., Bell, D.W., Haber, D.A., and Li, E. (1999). DNA methyltransferases Dnmt3a and Dnmt3b are essential for de novo methylation and mammalian development. Cell *99*, 247-257.

Olivetti, G., Cigola, E., Maestri, R., Corradi, D., Lagrasta, C., Gambert, S.R., and Anversa, P. (1996). Aging, cardiac hypertrophy and ischemic cardiomyopathy do not affect the proportion of

mononucleated and multinucleated myocytes in the human heart. Journal of molecular and cellular cardiology *28*, 1463-1477.

Olson, E.N. (2004). A decade of discoveries in cardiac biology. Nature medicine *10*, 467-474.

Orlic, D., Kajstura, J., Chimenti, S., Jakoniuk, I., Anderson, S.M., Li, B., Pickel, J., McKay, R., Nadal-Ginard, B., Bodine, D.M., *et al.* (2001). Bone marrow cells regenerate infarcted myocardium. Nature *410*, 701-705.

Paige, S.L., Thomas, S., Stoick-Cooper, C.L., Wang, H., Maves, L., Sandstrom, R., Pabon, L., Reinecke, H., Pratt, G., Keller, G., *et al.* (2012). A temporal chromatin signature in human embryonic stem cells identifies regulators of cardiac development. Cell *151*, 221-232.

Palanichamy, J.K., Tran, T.M., Howard, J.M., Contreras, J.R., Fernando, T.R., Sterne-Weiler, T., Katzman, S., Toloue, M., Yan, W., Basso, G., *et al.* (2016). RNA-binding protein IGF2BP3 targeting of oncogenic transcripts promotes hematopoietic progenitor proliferation. The Journal of clinical investigation *126*, 1495-1511.

Palii, S.S., Van Emburgh, B.O., Sankpal, U.T., Brown, K.D., and Robertson, K.D. (2008). DNA methylation inhibitor 5-Aza-2'-deoxycytidine induces reversible genome-wide DNA damage that is distinctly influenced by DNA methyltransferases 1 and 3B. Molecular and cellular biology *28*, 752-771.

Paradis, A., Xiao, D., Zhou, J., and Zhang, L. (2014). Endothelin-1 promotes cardiomyocyte terminal differentiation in the developing heart via heightened DNA methylation. Int J Med Sci *11*, 373-380.

Pasini, D., Bracken, A.P., Hansen, J.B., Capillo, M., and Helin, K. (2007). The polycomb group protein Suz12 is required for embryonic stem cell differentiation. Molecular and cellular biology *27*, 3769-3779.

Pasumarthi, K.B., Nakajima, H., Nakajima, H.O., Soonpaa, M.H., and Field, L.J. (2005). Targeted expression of cyclin D2 results in cardiomyocyte DNA synthesis and infarct regression in transgenic mice. Circulation research *96*, 110-118.

Perez, A., Leon, A., and Lee, M.Y. (2000). Characterization of the 5'-flanking region of the gene encoding the 50 kDa subunit of human DNA polymerase delta. Biochimica et biophysica acta *1493*, 231-236.

Perin, E.C., Willerson, J.T., Pepine, C.J., Henry, T.D., Ellis, S.G., Zhao, D.X., Silva, G.V., Lai, D., Thomas, J.D., Kronenberg, M.W., *et al.* (2012). Effect of transendocardial delivery of autologous

bone marrow mononuclear cells on functional capacity, left ventricular function, and perfusion in chronic heart failure: the FOCUS-CCTRN trial. JAMA *307*, 1717-1726.

Piatkowski, T., Muhlfeld, C., Borchardt, T., and Braun, T. (2013). Reconstitution of the myocardium in regenerating newt hearts is preceded by transient deposition of extracellular matrix components. Stem cells and development *22*, 1921-1931.

Pilon, A.M., Ajay, S.S., Kumar, S.A., Steiner, L.A., Cherukuri, P.F., Wincovitch, S., Anderson, S.M., Center, N.C.S., Mullikin, J.C., Gallagher, P.G., *et al.* (2011). Genome-wide ChIP-Seq reveals a dramatic shift in the binding of the transcription factor erythroid Kruppel-like factor during erythrocyte differentiation. Blood *118*, e139-148.

Pirola, L., Balcerczyk, A., Tothill, R.W., Haviv, I., Kaspi, A., Lunke, S., Ziemann, M., Karagiannis, T., Tonna, S., Kowalczyk, A., *et al.* (2011). Genome-wide analysis distinguishes hyperglycemia regulated epigenetic signatures of primary vascular cells. Genome research *21*, 1601-1615.

Pishesha, N., Thiru, P., Shi, J., Eng, J.C., Sankaran, V.G., and Lodish, H.F. (2014). Transcriptional divergence and conservation of human and mouse erythropoiesis. Proceedings of the National Academy of Sciences of the United States of America *111*, 4103-4108.

Polo, J.M., Anderssen, E., Walsh, R.M., Schwarz, B.A., Nefzger, C.M., Lim, S.M., Borkent, M., Apostolou, E., Alaei, S., Cloutier, J., *et al.* (2012). A molecular roadmap of reprogramming somatic cells into iPS cells. Cell *151*, 1617-1632.

Porrello, E.R., D'Amore, A., Curl, C.L., Allen, A.M., Harrap, S.B., Thomas, W.G., and Delbridge, L.M. (2009). Angiotensin II type 2 receptor antagonizes angiotensin II type 1 receptor-mediated cardiomyocyte autophagy. Hypertension *53*, 1032-1040.

Porrello, E.R., Johnson, B.A., Aurora, A.B., Simpson, E., Nam, Y.J., Matkovich, S.J., Dorn, G.W., 2nd, van Rooij, E., and Olson, E.N. (2011a). MiR-15 family regulates postnatal mitotic arrest of cardiomyocytes. Circulation research *109*, 670-679.

Porrello, E.R., Mahmoud, A.I., Simpson, E., Hill, J.A., Richardson, J.A., Olson, E.N., and Sadek, H.A. (2011b). Transient regenerative potential of the neonatal mouse heart. Science *331*, 1078-1080.

Porrello, E.R., Mahmoud, A.I., Simpson, E., Johnson, B.A., Grinsfelder, D., Canseco, D., Mammen, P.P., Rothermel, B.A., Olson, E.N., and Sadek, H.A. (2013). Regulation of neonatal and adult mammalian heart regeneration by the miR-15 family. Proceedings of the National Academy of Sciences of the United States of America *110*, 187-192.

Porrello, E.R., and Olson, E.N. (2010). Building a new heart from old parts: stem cell turnover in the aging heart. Circulation research *107*, 1292-1294.

Porrello, E.R., and Olson, E.N. (2014a). A neonatal blueprint for cardiac regeneration. Stem cell research *13*, 556-570.

Porrello, E.R., and Olson, E.N. (2014b). A neonatal blueprint for cardiac regeneration. Stem Cell Res.

Poss, K.D. (2007). Getting to the heart of regeneration in zebrafish. Seminars in cell & developmental biology *18*, 36-45.

Poss, K.D., Wilson, L.G., and Keating, M.T. (2002). Heart regeneration in zebrafish. Science (New York, NY) *298*, 2188-2190.

Preissl, S., Schwaderer, M., Raulf, A., Hesse, M., Gruning, B.A., Kobele, C., Backofen, R., Fleischmann, B.K., Hein, L., and Gilsbach, R. (2015a). Deciphering the Epigenetic Code of Cardiac Myocyte Transcription. Circulation research.

Preissl, S., Schwaderer, M., Raulf, A., Hesse, M., Gruning, B.A., Kobele, C., Backofen, R., Fleischmann, B.K., Hein, L., and Gilsbach, R. (2015b). Deciphering the Epigenetic Code of Cardiac Myocyte Transcription. Circ Res *117*, 413-423.

Puente, B.N., Kimura, W., Muralidhar, S.A., Moon, J., Amatruda, J.F., Phelps, K.L., Grinsfelder, D., Rothermel, B.A., Chen, R., Garcia, J.A., *et al.* (2014). The oxygen-rich postnatal environment induces cardiomyocyte cell-cycle arrest through DNA damage response. Cell *157*, 565-579.

Quaife-Ryan, G.A., Sim, C.B., Porrello, E.R., and Hudson, J.E. (2016). Resetting the epigenome for heart regeneration. Seminars in cell & developmental biology *58*, 2-13.

Quaini, F., Urbanek, K., Beltrami, A.P., Finato, N., Beltrami, C.A., Nadal-Ginard, B., Kajstura, J., Leri, A., and Anversa, P. (2002). Chimerism of the transplanted heart. The New England journal of medicine *346*, 5-15.

Quinlan, A.R., and Hall, I.M. (2010). BEDTools: a flexible suite of utilities for comparing genomic features. Bioinformatics *26*, 841-842.

Quinn, J.J., Ilik, I.A., Qu, K., Georgiev, P., Chu, C., Akhtar, A., and Chang, H.Y. (2014). Revealing long noncoding RNA architecture and functions using domain-specific chromatin isolation by RNA purification. Nat Biotechnol *32*, 933-940.

Rada-Iglesias, A., Bajpai, R., Swigut, T., Brugmann, S.A., Flynn, R.A., and Wysocka, J. (2011). A unique chromatin signature uncovers early developmental enhancers in humans. Nature *470*, 279-283.

Ramsahoye, B.H., Biniszkiewicz, D., Lyko, F., Clark, V., Bird, A.P., and Jaenisch, R. (2000). Non-CpG methylation is prevalent in embryonic stem cells and may be mediated by DNA methyltransferase 3a. Proceedings of the National Academy of Sciences of the United States of America *97*, 5237-5242.

Rasmussen, T.L., Ma, Y., Park, C.Y., Harriss, J., Pierce, S.A., Dekker, J.D., Valenzuela, N., Srivastava, D., Schwartz, R.J., Stewart, M.D., *et al.* (2015). Smyd1 facilitates heart development by antagonizing oxidative and ER stress responses. PloS one *10*, e0121765.

Reich, M., Liefeld, T., Gould, J., Lerner, J., Tamayo, P., and Mesirov, J.P. (2006). GenePattern 2.0. Nature genetics *38*, 500-501.

Reuter, S., Soonpaa, M.H., Firulli, A.B., Chang, A.N., and Field, L.J. (2014). Recombinant neuregulin 1 does not activate cardiomyocyte DNA synthesis in normal or infarcted adult mice. PloS one *9*, e115871.

Riegler, J., Tiburcy, M., Ebert, A., Tzatzalos, E., Raaz, U., Abilez, O.J., Shen, Q., Kooreman, N.G., Neofytou, E., Chen, V.C., *et al.* (2015). Human Engineered Heart Muscles Engraft and Survive Long Term in a Rodent Myocardial Infarction Model. Circulation research *117*, 720-730.

Rinn, J.L., Kertesz, M., Wang, J.K., Squazzo, S.L., Xu, X., Brugmann, S.A., Goodnough, L.H., Helms, J.A., Farnham, P.J., Segal, E., *et al.* (2007). Functional demarcation of active and silent chromatin domains in human HOX loci by noncoding RNAs. Cell *129*, 1311-1323.

Rivenbark, A.G., Stolzenburg, S., Beltran, A.S., Yuan, X., Rots, M.G., Strahl, B.D., and Blancafort, P. (2012). Epigenetic reprogramming of cancer cells via targeted DNA methylation. Epigenetics : official journal of the DNA Methylation Society *7*, 350-360.

Roadmap Epigenomics, C., Kundaje, A., Meuleman, W., Ernst, J., Bilenky, M., Yen, A., Heravi-Moussavi, A., Kheradpour, P., Zhang, Z., Wang, J., *et al.* (2015). Integrative analysis of 111 reference human epigenomes. Nature *518*, 317-330.

Robinson, M.D., McCarthy, D.J., and Smyth, G.K. (2010). edgeR: a Bioconductor package for differential expression analysis of digital gene expression data. Bioinformatics *26*, 139-140.

Rohde, C., Zhang, Y., Reinhardt, R., and Jeltsch, A. (2010). BISMA--fast and accurate bisulfite sequencing data analysis of individual clones from unique and repetitive sequences. BMC bioinformatics *11*, 230.

Romanoski, C.E., Glass, C.K., Stunnenberg, H.G., Wilson, L., and Almouzni, G. (2015). Epigenomics: Roadmap for regulation. Nature *518*, 314-316.

Rothbart, S.B., and Strahl, B.D. (2014). Interpreting the language of histone and DNA modifications. Biochimica et biophysica acta *1839*, 627-643.

RStudio (2012). RStudio: Integrated development environment for R (Version 0.96.122) [Computer software]. . [Computer software].

Rumyantsev, P.P. (1973). Post-injury DNA synthesis, mitosis and ultrastructural reorganization of adult frog cardiac myocytes. An electron microscopic-autoradiographic study. Z Zellforsch Mikrosk Anat *139*, 431-450.

Ryall, J.G., Dell'Orso, S., Derfoul, A., Juan, A., Zare, H., Feng, X., Clermont, D., Koulnis, M., Gutierrez-Cruz, G., Fulco, M., *et al.* (2015). The NAD(+)-dependent SIRT1 deacetylase translates a metabolic switch into regulatory epigenetics in skeletal muscle stem cells. Cell Stem Cell *16*, 171-183.

San Martin, N., Cervera, A.M., Cordova, C., Covarello, D., McCreath, K.J., and Galvez, B.G. (2011). Mitochondria determine the differentiation potential of cardiac mesoangioblasts. Stem cells (Dayton, Ohio) *29*, 1064-1074.

Sartorelli, V., Huang, J., Hamamori, Y., and Kedes, L. (1997). Molecular mechanisms of myogenic coactivation by p300: direct interaction with the activation domain of MyoD and with the MADS box of MEF2C. Mol Cell Biol *17*, 1010-1026.

Schachinger, V., Assmus, B., Britten, M.B., Honold, J., Lehmann, R., Teupe, C., Abolmaali, N.D., Vogl, T.J., Hofmann, W.K., Martin, H., *et al.* (2004). Transplantation of progenitor cells and regeneration enhancement in acute myocardial infarction: final one-year results of the TOPCARE-AMI Trial. Journal of the American College of Cardiology *44*, 1690-1699.

Schachinger, V., Erbs, S., Elsasser, A., Haberbosch, W., Hambrecht, R., Holschermann, H., Yu, J., Corti, R., Mathey, D.G., Hamm, C.W., *et al.* (2006a). Intracoronary bone marrow-derived progenitor cells in acute myocardial infarction. The New England journal of medicine *355*, 1210-1221.

Schachinger, V., Erbs, S., Elsasser, A., Haberbosch, W., Hambrecht, R., Holschermann, H., Yu, J., Corti, R., Mathey, D.G., Hamm, C.W., *et al.* (2006b). Improved clinical outcome after intracoronary administration of bone-marrow-derived progenitor cells in acute myocardial infarction: final 1-year results of the REPAIR-AMI trial. European heart journal *27*, 2775-2783.

Schaeffer, D.F., Owen, D.R., Lim, H.J., Buczkowski, A.K., Chung, S.W., Scudamore, C.H., Huntsman, D.G., Ng, S.S., and Owen, D.A. (2010). Insulin-like growth factor 2 mRNA binding protein 3 (IGF2BP3) overexpression in pancreatic ductal adenocarcinoma correlates with poor survival. BMC cancer *10*, 59.

Schreiber, S.N., Emter, R., Hock, M.B., Knutti, D., Cardenas, J., Podvinec, M., Oakeley, E.J., and Kralli, A. (2004). The estrogen-related receptor alpha (ERRalpha) functions in PPARgamma coactivator 1alpha (PGC-1alpha)-induced mitochondrial biogenesis. Proceedings of the National Academy of Sciences of the United States of America *101*, 6472-6477.

Sdek, P., Zhao, P., Wang, Y., Huang, C.J., Ko, C.Y., Butler, P.C., Weiss, J.N., and Maclellan, W.R. (2011). Rb and p130 control cell cycle gene silencing to maintain the postmitotic phenotype in cardiac myocytes. The Journal of cell biology *194*, 407-423.

Seidel, M., Borczynska, A., Rozwadowska, N., and Kurpisz, M. (2009). Cell-based therapy for heart failure: skeletal myoblasts. Cell transplantation *18*, 695-707.

Sekine, H., Shimizu, T., Hobo, K., Sekiya, S., Yang, J., Yamato, M., Kurosawa, H., Kobayashi, E., and Okano, T. (2008). Endothelial cell coculture within tissue-engineered cardiomyocyte sheets enhances neovascularization and improves cardiac function of ischemic hearts. Circulation *118*, S145-152.

Sengupta, A., Kalinichenko, V.V., and Yutzey, K.E. (2013). FoxO1 and FoxM1 transcription factors have antagonistic functions in neonatal cardiomyocyte cell-cycle withdrawal and IGF1 gene regulation. Circulation research *112*, 267-277.

Senyo, S.E., Steinhauser, M.L., Pizzimenti, C.L., Yang, V.K., Cai, L., Wang, M., Wu, T.D., Guerquin-Kern, J.L., Lechene, C.P., and Lee, R.T. (2013). Mammalian heart renewal by pre-existing cardiomyocytes. Nature *493*, 433-436.

Shanks, N., Greek, R., and Greek, J. (2009). Are animal models predictive for humans? Philos Ethics Humanit Med *4*, 2.

Shapiro, S.D., Ranjan, A.K., Kawase, Y., Cheng, R.K., Kara, R.J., Bhattacharya, R., Guzman-Martinez, G., Sanz, J., Garcia, M.J., and Chaudhry, H.W. (2014). Cyclin A2 induces cardiac

regeneration after myocardial infarction through cytokinesis of adult cardiomyocytes. Science translational medicine *6*, 224ra227.

Shay, T., Jojic, V., Zuk, O., Rothamel, K., Puyraimond-Zemmour, D., Feng, T., Wakamatsu, E., Benoist, C., Koller, D., Regev, A., *et al.* (2013). Conservation and divergence in the transcriptional programs of the human and mouse immune systems. Proceedings of the National Academy of Sciences of the United States of America *110*, 2946-2951.

Shen, Z., Jiang, X., Zeng, C., Zheng, S., Luo, B., Zeng, Y., Ding, R., Jiang, H., He, Q., Guo, J., *et al.* (2013). High expression of ubiquitin-conjugating enzyme 2C (UBE2C) correlates with nasopharyngeal carcinoma progression. BMC cancer *13*, 192.

Shi, Q., and Gibson, G.E. (2007). Oxidative stress and transcriptional regulation in Alzheimer disease. Alzheimer Dis Assoc Disord *21*, 276-291.

Shiba, Y., Fernandes, S., Zhu, W.Z., Filice, D., Muskheli, V., Kim, J., Palpant, N.J., Gantz, J., Moyes, K.W., Reinecke, H., *et al.* (2012). Human ES-cell-derived cardiomyocytes electrically couple and suppress arrhythmias in injured hearts. Nature *489*, 322-325.

Shiba, Y., Filice, D., Fernandes, S., Minami, E., Dupras, S.K., Biber, B.V., Trinh, P., Hirota, Y., Gold, J.D., Viswanathan, M., *et al.* (2014). Electrical Integration of Human Embryonic Stem Cell-Derived Cardiomyocytes in a Guinea Pig Chronic Infarct Model. J Cardiovasc Pharmacol Ther *19*, 368-381.

Shikama, N., Lutz, W., Kretzschmar, R., Sauter, N., Roth, J.F., Marino, S., Wittwer, J., Scheidweiler, A., and Eckner, R. (2003). Essential function of p300 acetyltransferase activity in heart, lung and small intestine formation. The EMBO journal *22*, 5175-5185.

Shimizu, T., Sekine, H., Yang, J., Isoi, Y., Yamato, M., Kikuchi, A., Kobayashi, E., and Okano, T. (2006). Polysurgery of cell sheet grafts overcomes diffusion limits to produce thick, vascularized myocardial tissues. FASEB journal : official publication of the Federation of American Societies for Experimental Biology *20*, 708-710.

Shintani, S.A., Oyama, K., Kobirumaki-Shimozawa, F., Ohki, T., Ishiwata, S., and Fukuda, N. (2014). Sarcomere length nanometry in rat neonatal cardiomyocytes expressed with alpha-actinin-AcGFP in Z discs. J Gen Physiol *143*, 513-524.

Shiomi, Y., Masutani, C., Hanaoka, F., Kimura, H., and Tsurimoto, T. (2007). A second proliferating cell nuclear antigen loader complex, Ctf18-replication factor C, stimulates DNA polymerase eta activity. The Journal of biological chemistry *282*, 20906-20914.

Shu, F., Lv, S., Qin, Y., Ma, X., Wang, X., Peng, X., Luo, Y., Xu, B.E., Sun, X., and Wu, J. (2007). Functional characterization of human PFTK1 as a cyclin-dependent kinase. Proceedings of the National Academy of Sciences of the United States of America *104*, 9248-9253.

Shuliang, S., Lei, C., Guangwu, J., and Changjie, L. (2013). Involvement of ubiquitin-conjugating enzyme E2C in proliferation and invasion of prostate carcinoma cells. Oncol Res *21*, 121-127.

Shyh-Chang, N., Locasale, J.W., Lyssiotis, C.A., Zheng, Y., Teo, R.Y., Ratanasirintrawoot, S., Zhang, J., Onder, T., Unternaehrer, J.J., Zhu, H., *et al.* (2013). Influence of threonine metabolism on S-adenosylmethionine and histone methylation. Science *339*, 222-226.

Sim, C.B., Ziemann, M., Kaspi, A., Harikrishnan, K.N., Ooi, J., Khurana, I., Chang, L., Hudson, J.E., El-Osta, A., and Porrello, E.R. (2015). Dynamic changes in the cardiac methylome during postnatal development. FASEB journal : official publication of the Federation of American Societies for Experimental Biology *29*, 1329-1343.

Sisler, J.D., Morgan, M., Raje, V., Grande, R.C., Derecka, M., Meier, J., Cantwell, M., Szczepanek, K., Korzun, W.J., Lesnefsky, E.J., *et al.* (2015). The Signal Transducer and Activator of Transcription 1 (STAT1) Inhibits Mitochondrial Biogenesis in Liver and Fatty Acid Oxidation in Adipocytes. PloS one *10*, e0144444.

Slepak, T.I., Webster, K.A., Zang, J., Prentice, H., O'Dowd, A., Hicks, M.N., and Bishopric, N.H. (2001). Control of cardiac-specific transcription by p300 through myocyte enhancer factor-2D. The Journal of biological chemistry *276*, 7575-7585.

Smith, Z.D., and Meissner, A. (2013). DNA methylation: roles in mammalian development. Nat Rev Genet *14*, 204-220.

Sok AJ, G.A., Mamczur P, Piotrowska A, Knapik A, et al. (2014). Demethylation with 5-Aza-2'-deoxycytidine Affects Oxidative Metabolism in Human and Mouse Non-small Cell Lung Cancer Cells. J Cancer Sci Ther *6*, 036-044.

Song, K., Nam, Y.J., Luo, X., Qi, X., Tan, W., Huang, G.N., Acharya, A., Smith, C.L., Tallquist, M.D., Neilson, E.G., *et al.* (2012). Heart repair by reprogramming non-myocytes with cardiac transcription factors. Nature *485*, 599-604.

Song, L., Zhang, Z., Grasfeder, L.L., Boyle, A.P., Giresi, P.G., Lee, B.K., Sheffield, N.C., Graf, S., Huss, M., Keefe, D., *et al.* (2011). Open chromatin defined by DNaseI and FAIRE identifies regulatory elements that shape cell-type identity. Genome research *21*, 1757-1767.

Soonpaa, M.H., and Field, L.J. (1997). Assessment of cardiomyocyte DNA synthesis in normal and injured adult mouse hearts. Am J Physiol *272*, H220-226.

Soonpaa, M.H., Kim, K.K., Pajak, L., Franklin, M., and Field, L.J. (1996). Cardiomyocyte DNA synthesis and binucleation during murine development. Am J Physiol *271*, H2183-2189.

Soonpaa, M.H., Koh, G.Y., Pajak, L., Jing, S., Wang, H., Franklin, M.T., Kim, K.K., and Field, L.J. (1997). Cyclin D1 overexpression promotes cardiomyocyte DNA synthesis and multinucleation in transgenic mice. The Journal of clinical investigation *99*, 2644-2654.

Stefanovic, S., and Christoffels, V.M. (2015). GATA-dependent transcriptional and epigenetic control of cardiac lineage specification and differentiation. Cellular and molecular life sciences : CMLS *72*, 3871-3881.

Stergachis, A.B., Neph, S., Reynolds, A., Humbert, R., Miller, B., Paige, S.L., Vernot, B., Cheng, J.B., Thurman, R.E., Sandstrom, R., *et al.* (2013). Developmental fate and cellular maturity encoded in human regulatory DNA landscapes. Cell *154*, 888-903.

Stevens, K.R., Kreutziger, K.L., Dupras, S.K., Korte, F.S., Regnier, M., Muskheli, V., Nourse, M.B., Bendixen, K., Reinecke, H., and Murry, C.E. (2009). Physiological function and transplantation of scaffold-free and vascularized human cardiac muscle tissue. Proceedings of the National Academy of Sciences of the United States of America *106*, 16568-16573.

Stevens, M., Cheng, J.B., Li, D., Xie, M., Hong, C., Maire, C.L., Ligon, K.L., Hirst, M., Marra, M.A., Costello, J.F., *et al.* (2013). Estimating absolute methylation levels at single-CpG resolution from methylation enrichment and restriction enzyme sequencing methods. Genome research *23*, 1541-1553.

Strungs, E.G., Ongstad, E.L., O'Quinn, M.P., Palatinus, J.A., Jourdan, L.J., and Gourdie, R.G. (2013). Cryoinjury models of the adult and neonatal mouse heart for studies of scarring and regeneration. Methods in molecular biology (Clifton, NJ) *1037*, 343-353.

Sturzu, A.C., Rajarajan, K., Passer, D., Plonowska, K., Riley, A., Tan, T.C., Sharma, A., Xu, A.F., Engels, M.C., Feistritzer, R., *et al.* (2015). Fetal Mammalian Heart Generates a Robust Compensatory Response to Cell Loss. Circulation *132*, 109-121.

Subramanian, A., Tamayo, P., Mootha, V.K., Mukherjee, S., Ebert, B.L., Gillette, M.A., Paulovich, A., Pomeroy, S.L., Golub, T.R., Lander, E.S., *et al.* (2005). Gene set enrichment analysis: a knowledge-based approach for interpreting genome-wide expression profiles. Proceedings of the National Academy of Sciences of the United States of America *102*, 15545-15550.

Sultana, N., Zhang, L., Yan, J., Chen, J., Cai, W., Razzaque, S., Jeong, D., Sheng, W., Bu, L., Xu, M., *et al.* (2015). Resident c-kit(+) cells in the heart are not cardiac stem cells. Nature communications *6*, 8701.

Sun, X., Chuang, J.C., Kanchwala, M., Wu, L., Celen, C., Li, L., Liang, H., Zhang, S., Maples, T., Nguyen, L.H., *et al.* (2016). Suppression of the SWI/SNF Component Arid1a Promotes Mammalian Regeneration. Cell stem cell *18*, 456-466.

Sundaresan, N.R., Gupta, M., Kim, G., Rajamohan, S.B., Isbatan, A., and Gupta, M.P. (2009). Sirt3 blocks the cardiac hypertrophic response by augmenting Foxo3a-dependent antioxidant defense mechanisms in mice. The Journal of clinical investigation *119*, 2758-2771.

Sundaresan, N.R., Vasudevan, P., Zhong, L., Kim, G., Samant, S., Parekh, V., Pillai, V.B., Ravindra, P.V., Gupta, M., Jeevanandam, V., *et al.* (2012). The sirtuin SIRT6 blocks IGF-Akt signaling and development of cardiac hypertrophy by targeting c-Jun. Nature medicine *18*, 1643-1650.

Suzuki, M.M., and Bird, A. (2008). DNA methylation landscapes: provocative insights from epigenomics. Nature reviews Genetics *9*, 465-476.

Takaya, T., Kawamura, T., Morimoto, T., Ono, K., Kita, T., Shimatsu, A., and Hasegawa, K. (2008). Identification of p300-targeted acetylated residues in GATA4 during hypertrophic responses in cardiac myocytes. The Journal of biological chemistry *283*, 9828-9835.

Takeuchi, T., Kojima, M., Nakajima, K., and Kondo, S. (1999). jumonji gene is essential for the neurulation and cardiac development of mouse embryos with a C3H/He background. Mechanisms of development *86*, 29-38.

Tallini, Y.N., Greene, K.S., Craven, M., Spealman, A., Breitbach, M., Smith, J., Fisher, P.J., Steffey, M., Hesse, M., Doran, R.M., *et al.* (2009). c-kit expression identifies cardiovascular precursors in the neonatal heart. Proceedings of the National Academy of Sciences of the United States of America *106*, 1808-1813.

Tan, X., Rotllant, J., Li, H., De Deyne, P., and Du, S.J. (2006). SmyD1, a histone methyltransferase, is required for myofibril organization and muscle contraction in zebrafish embryos. Proceedings of the National Academy of Sciences of the United States of America *103*, 2713-2718.

Thillainadesan, G., Chitilian, J.M., Isovic, M., Ablack, J.N., Mymryk, J.S., Tini, M., and Torchia, J. (2012). TGF-beta-dependent active demethylation and expression of the p15ink4b tumor suppressor are impaired by the ZNF217/CoREST complex. Molecular cell *46*, 636-649.

Thomson, M., Liu, S.J., Zou, L.N., Smith, Z., Meissner, A., and Ramanathan, S. (2011). Pluripotency factors in embryonic stem cells regulate differentiation into germ layers. Cell *145*, 875-889.

Thurman, R.E., Rynes, E., Humbert, R., Vierstra, J., Maurano, M.T., Haugen, E., Sheffield, N.C., Stergachis, A.B., Wang, H., Vernot, B., *et al.* (2012). The accessible chromatin landscape of the human genome. Nature *489*, 75-82.

Tian, H.P., Lun, S.M., Huang, H.J., He, R., Kong, P.Z., Wang, Q.S., Li, X.Q., and Feng, Y.M. (2015). DNA Methylation Affects the SP1-regulated Transcription of FOXF2 in Breast Cancer Cells. The Journal of biological chemistry *290*, 19173-19183.

Tian, Y., Lei, L., and Minden, A. (2011). A key role for Pak4 in proliferation and differentiation of neural progenitor cells. Developmental biology *353*, 206-216.

Tousoulis, D., Briasoulis, A., Antoniades, C., Stefanadi, E., and Stefanadis, C. (2008). Heart regeneration: what cells to use and how? Current opinion in pharmacology *8*, 211-218.

Toyoda, M., Shirato, H., Nakajima, K., Kojima, M., Takahashi, M., Kubota, M., Suzuki-Migishima, R., Motegi, Y., Yokoyama, M., and Takeuchi, T. (2003). jumonji downregulates cardiac cell proliferation by repressing cyclin D1 expression. Developmental cell *5*, 85-97.

Traverse, J.H., Henry, T.D., Pepine, C.J., Willerson, J.T., Zhao, D.X., Ellis, S.G., Forder, J.R., Anderson, R.D., Hatzopoulos, A.K., Penn, M.S., *et al.* (2012). Effect of the use and timing of bone marrow mononuclear cell delivery on left ventricular function after acute myocardial infarction: the TIME randomized trial. JAMA *308*, 2380-2389.

Traverse, J.H., Henry, T.D., Vaughan, D.E., Ellis, S.G., Pepine, C.J., Willerson, J.T., Zhao, D.X., Simpson, L.M., Penn, M.S., Byrne, B.J., *et al.* (2010). LateTIME: a phase-II, randomized, double-blinded, placebo-controlled, pilot trial evaluating the safety and effect of administration of bone marrow mononuclear cells 2 to 3 weeks after acute myocardial infarction. Tex Heart Inst J *37*, 412-420.

Trivedi, C.M., Lu, M.M., Wang, Q., and Epstein, J.A. (2008). Transgenic overexpression of Hdac3 in the heart produces increased postnatal cardiac myocyte proliferation but does not induce hypertrophy. The Journal of biological chemistry *283*, 26484-26489.

Trivedi, C.M., Zhu, W., Wang, Q., Jia, C., Kee, H.J., Li, L., Hannenhalli, S., and Epstein, J.A. (2010). Hopx and Hdac2 interact to modulate Gata4 acetylation and embryonic cardiac myocyte proliferation. Dev Cell *19*, 450-459.

Tsankov, A.M., Gu, H., Akopian, V., Ziller, M.J., Donaghey, J., Amit, I., Gnirke, A., and Meissner, A. (2015). Transcription factor binding dynamics during human ES cell differentiation. Nature *518*, 344-349.

Tulloch, N.L., and Murry, C.E. (2013). Trends in cardiovascular engineering: organizing the human heart. Trends in cardiovascular medicine *23*, 282-286.

Tulloch, N.L., Muskheli, V., Razumova, M.V., Korte, F.S., Regnier, M., Hauch, K.D., Pabon, L., Reinecke, H., and Murry, C.E. (2011). Growth of engineered human myocardium with mechanical loading and vascular coculture. Circulation research *109*, 47-59.

Tyagi, S., Chabes, A.L., Wysocka, J., and Herr, W. (2007). E2F activation of S phase promoters via association with HCF-1 and the MLL family of histone H3K4 methyltransferases. Molecular cell *27*, 107-119.

Udali, S., Guarini, P., Moruzzi, S., Choi, S.W., and Friso, S. (2013). Cardiovascular epigenetics: from DNA methylation to microRNAs. Molecular aspects of medicine *34*, 883-901.

Uosaki, H., Cahan, P., Lee, D.I., Wang, S., Miyamoto, M., Fernandez, L., Kass, D.A., and Kwon, C. (2015). Transcriptional Landscape of Cardiomyocyte Maturation. Cell reports *13*, 1705-1716.

Uygur, A., and Lee, R.T. (2016). Mechanisms of Cardiac Regeneration. Developmental cell *36*, 362-374.

Vakhrusheva, O., Smolka, C., Gajawada, P., Kostin, S., Boettger, T., Kubin, T., Braun, T., and Bober, E. (2008). Sirt7 increases stress resistance of cardiomyocytes and prevents apoptosis and inflammatory cardiomyopathy in mice. Circulation research *102*, 703-710.

van Amerongen, M.J., Diehl, F., Novoyatleva, T., Patra, C., and Engel, F.B. (2010). E2F4 is required for cardiomyocyte proliferation. Cardiovascular research *86*, 92-102.

van Berlo, J.H., Kanisicak, O., Maillet, M., Vagnozzi, R.J., Karch, J., Lin, S.C., Middleton, R.C., Marban, E., and Molkentin, J.D. (2014). c-kit+ cells minimally contribute cardiomyocytes to the heart. Nature *509*, 337-341.

van Ree, J.H., Jeganathan, K.B., Malureanu, L., and van Deursen, J.M. (2010). Overexpression of the E2 ubiquitin-conjugating enzyme UbcH10 causes chromosome missegregation and tumor formation. The Journal of cell biology *188*, 83-100.

Veerman, C.C., Kosmidis, G., Mummery, C.L., Casini, S., Verkerk, A.O., and Bellin, M. (2015). Immaturity of human stem-cell-derived cardiomyocytes in culture: fatal flaw or soluble problem? Stem cells and development *24*, 1035-1052.

von Gise, A., Lin, Z., Schlegelmilch, K., Honor, L.B., Pan, G.M., Buck, J.N., Ma, Q., Ishiwata, T., Zhou, B., Camargo, F.D., *et al.* (2012). YAP1, the nuclear target of Hippo signaling, stimulates heart growth through cardiomyocyte proliferation but not hypertrophy. Proceedings of the National Academy of Sciences of the United States of America *109*, 2394-2399.

Wamstad, J.A., Alexander, J.M., Truty, R.M., Shrikumar, A., Li, F., Eilertson, K.E., Ding, H., Wylie, J.N., Pico, A.R., Capra, J.A., *et al.* (2012). Dynamic and coordinated epigenetic regulation of developmental transitions in the cardiac lineage. Cell *151*, 206-220.

Wang, J., Alexander, P., Wu, L., Hammer, R., Cleaver, O., and McKnight, S.L. (2009). Dependence of mouse embryonic stem cells on threonine catabolism. Science *325*, 435-439.

Wang, J., Greene, S.B., Bonilla-Claudio, M., Tao, Y., Zhang, J., Bai, Y., Huang, Z., Black, B.L., Wang, F., and Martin, J.F. (2010). Bmp signaling regulates myocardial differentiation from cardiac progenitors through a MicroRNA-mediated mechanism. Developmental cell *19*, 903-912.

Wang, J., Panakova, D., Kikuchi, K., Holdway, J.E., Gemberling, M., Burris, J.S., Singh, S.P., Dickson, A.L., Lin, Y.F., Sabeh, M.K., *et al.* (2011). The regenerative capacity of zebrafish reverses cardiac failure caused by genetic cardiomyocyte depletion. Development (Cambridge, England) *138*, 3421-3430.

Wang, L., Zhao, Y., Bao, X., Zhu, X., Kwok, Y.K., Sun, K., Chen, X., Huang, Y., Jauch, R., Esteban, M.A., *et al.* (2015). LncRNA Dum interacts with Dnmts to regulate Dppa2 expression during myogenic differentiation and muscle regeneration. Cell Res *25*, 335-350.

Watson, C.J., Collier, P., Tea, I., Neary, R., Watson, J.A., Robinson, C., Phelan, D., Ledwidge, M.T., McDonald, K.M., McCann, A., *et al.* (2013). Hypoxia-induced epigenetic modifications are associated with cardiac tissue fibrosis and the development of a myofibroblast-like phenotype. Human molecular genetics.

Welstead, G.G., Creyghton, M.P., Bilodeau, S., Cheng, A.W., Markoulaki, S., Young, R.A., and Jaenisch, R. (2012). X-linked H3K27me3 demethylase Utx is required for embryonic development in a sex-specific manner. Proceedings of the National Academy of Sciences of the United States of America *109*, 13004-13009.

Wen, S.L., Zhang, F., and Feng, S. (2013). Decreased copy number of mitochondrial DNA: A potential diagnostic criterion for gastric cancer. Oncol Lett *6*, 1098-1102.

Witman, N., Murtuza, B., Davis, B., Arner, A., and Morrison, J.I. (2011). Recapitulation of developmental cardiogenesis governs the morphological and functional regeneration of adult newt hearts following injury. Developmental biology *354*, 67-76.

Wohrle, S., Wallmen, B., and Hecht, A. (2007). Differential control of Wnt target genes involves epigenetic mechanisms and selective promoter occupancy by T-cell factors. Mol Cell Biol *27*, 8164-8177.

Wollert, K.C., Meyer, G.P., Lotz, J., Ringes-Lichtenberg, S., Lippolt, P., Breidenbach, C., Fichtner, S., Korte, T., Hornig, B., Messinger, D., *et al.* (2004). Intracoronary autologous bone-marrow cell transfer after myocardial infarction: the BOOST randomised controlled clinical trial. Lancet *364*, 141-148.

Woo, Y.J., Panlilio, C.M., Cheng, R.K., Liao, G.P., Atluri, P., Hsu, V.M., Cohen, J.E., and Chaudhry, H.W. (2006). Therapeutic delivery of cyclin A2 induces myocardial regeneration and enhances cardiac function in ischemic heart failure. Circulation *114*, I206-213.

World Health Organization. (2011). Global status report on noncommunicable diseases 2010 (Geneva: World Health Organization).

Wu, H., and Zhang, Y. (2014). Reversing DNA methylation: mechanisms, genomics, and biological functions. Cell *156*, 45-68.

Wu, J., Anczukow, O., Krainer, A.R., Zhang, M.Q., and Zhang, C. (2013). OLego: fast and sensitive mapping of spliced mRNA-Seq reads using small seeds. Nucleic acids research *41*, 5149-5163.

Xiao, D., Dasgupta, C., Chen, M., Zhang, K., Buchholz, J., Xu, Z., and Zhang, L. (2013). Inhibition of DNA methylation reverses norepinephrine-induced cardiac hypertrophy in rats. Cardiovascular research.

Xiao, D., Dasgupta, C., Chen, M., Zhang, K., Buchholz, J., Xu, Z., and Zhang, L. (2014). Inhibition of DNA methylation reverses norepinephrine-induced cardiac hypertrophy in rats. Cardiovascular research *101*, 373-382.

Xin, M., Kim, Y., Sutherland, L.B., Murakami, M., Qi, X., McAnally, J., Porrello, E.R., Mahmoud, A.I., Tan, W., Shelton, J.M., *et al.* (2013a). Hippo pathway effector Yap promotes cardiac regeneration. Proceedings of the National Academy of Sciences of the United States of America *110*, 13839-13844.

Xin, M., Olson, E.N., and Bassel-Duby, R. (2013b). Mending broken hearts: cardiac development as a basis for adult heart regeneration and repair. Nature reviews Molecular cell biology *14*, 529-541.

Yang, K.C., Yamada, K.A., Patel, A.Y., Topkara, V.K., George, I., Cheema, F.H., Ewald, G.A., Mann, D.L., and Nerbonne, J.M. (2014a). Deep RNA sequencing reveals dynamic regulation of myocardial noncoding RNAs in failing human heart and remodeling with mechanical circulatory support. Circulation *129*, 1009-1021.

Yang, X., Pabon, L., and Murry, C.E. (2014b). Engineering adolescence: maturation of human pluripotent stem cell-derived cardiomyocytes. Circulation research *114*, 511-523.

Yao, T.P., Oh, S.P., Fuchs, M., Zhou, N.D., Ch'ng, L.E., Newsome, D., Bronson, R.T., Li, E., Livingston, D.M., and Eckner, R. (1998). Gene dosage-dependent embryonic development and proliferation defects in mice lacking the transcriptional integrator p300. Cell *93*, 361-372.

Yasumi, M., Sakisaka, T., Hoshino, T., Kimura, T., Sakamoto, Y., Yamanaka, T., Ohno, S., and Takai, Y. (2005). Direct binding of Lgl2 to LGN during mitosis and its requirement for normal cell division. The Journal of biological chemistry *280*, 6761-6765.

Zaret, K.S., and Carroll, J.S. (2011). Pioneer transcription factors: establishing competence for gene expression. Genes Dev *25*, 2227-2241.

Zerbe, L.K., and Kuchta, R.D. (2002). The p58 subunit of human DNA primase is important for primer initiation, elongation, and counting. Biochemistry *41*, 4891-4900.

Zhang, C.L., McKinsey, T.A., Chang, S., Antos, C.L., Hill, J.A., and Olson, E.N. (2002). Class II histone deacetylases act as signal-responsive repressors of cardiac hypertrophy. Cell *110*, 479-488.

Zhang, J., Wilson, G.F., Soerens, A.G., Koonce, C.H., Yu, J., Palecek, S.P., Thomson, J.A., and Kamp, T.J. (2009). Functional cardiomyocytes derived from human induced pluripotent stem cells. Circulation research *104*, e30-41.

Zhang, M., Chen, M., Kim, J.R., Zhou, J., Jones, R.E., Tune, J.D., Kassab, G.S., Metzger, D., Ahlfeld, S., Conway, S.J., *et al.* (2011). SWI/SNF complexes containing Brahma or Brahma-related gene 1 play distinct roles in smooth muscle development. Molecular and cellular biology *31*, 2618-2631.

Zhang, Y., Baranovskiy, A.G., Tahirov, T.H., and Pavlov, Y.I. (2014). The C-terminal domain of the DNA polymerase catalytic subunit regulates the primase and polymerase activities of the human DNA polymerase alpha-primase complex. The Journal of biological chemistry *289*, 22021-22034.

Zhang, Y., Liu, T., Meyer, C.A., Eeckhoute, J., Johnson, D.S., Bernstein, B.E., Nusbaum, C., Myers, R.M., Brown, M., Li, W., *et al.* (2008). Model-based analysis of ChIP-Seq (MACS). Genome biology *9*, R137.

Zhang, Y., Zhong, J.F., Qiu, H., MacLellan, W.R., Marban, E., and Wang, C. (2015). Epigenomic Reprogramming of Adult Cardiomyocyte-Derived Cardiac Progenitor Cells. Scientific reports *5*, 17686.

Zhong, R., Ge, X., Chu, T., Teng, J., Yan, B., Pei, J., Jiang, L., Zhong, H., and Han, B. (2016). Lentivirus-mediated knockdown of CTDP1 inhibits lung cancer cell growth in vitro. J Cancer Res Clin Oncol *142*, 723-732.

Zhou, B., Ma, Q., Rajagopal, S., Wu, S.M., Domian, I., Rivera-Feliciano, J., Jiang, D., von Gise, A., Ikeda, S., Chien, K.R., *et al.* (2008). Epicardial progenitors contribute to the cardiomyocyte lineage in the developing heart. Nature *454*, 109-113.

Zhou, P., He, A., and Pu, W.T. (2012). Regulation of GATA4 transcriptional activity in cardiovascular development and disease. Current topics in developmental biology *100*, 143-169.

Zhou, X.Q., Huang, S.Y., Zhang, D.S., Zhang, S.Z., Li, W.G., Chen, Z.W., and Wu, H.W. (2015). Effects of 5-aza-2'deoxycytidine on RECK gene expression and tumor invasion in salivary adenoid cystic carcinoma. Brazilian journal of medical and biological research = Revista brasileira de pesquisas medicas e biologicas / Sociedade Brasileira de Biofisica [et al] *48*, 254-260.

Zhu, J., Adli, M., Zou, J.Y., Verstappen, G., Coyne, M., Zhang, X., Durham, T., Miri, M., Deshpande, V., De Jager, P.L., *et al.* (2013). Genome-wide chromatin state transitions associated with developmental and environmental cues. Cell *152*, 642-654.

Ziech, D., Franco, R., Pappa, A., and Panayiotidis, M.I. (2011). Reactive oxygen species (ROS)--induced genetic and epigenetic alterations in human carcinogenesis. Mutat Res *711*, 167-173.

Zimmermann, W.H., Melnychenko, I., Wasmeier, G., Didie, M., Naito, H., Nixdorff, U., Hess, A., Budinsky, L., Brune, K., Michaelis, B., *et al.* (2006). Engineered heart tissue grafts improve systolic and diastolic function in infarcted rat hearts. Nature medicine *12*, 452-458.